

Using PMU and PQ monitor for voltage sag extended-characterization

– Master Thesis work by Peiyuan Chen–

May, 2006



Institutionen för Energi och Miljö
International masters program in Electric Power Engineering
CHALMERS TEKNISKA HÖGSKOLA
Göteborg, Sverige, 2006
Examinator: Jaap Daalder

Abstract

Modern industrial processes are sensitive to power quality problems, due to the use of power electronic equipment in the power systems. For example, rolling mills are sensitive to voltage disturbances, due to the use of converter drive systems, which trip due to voltage sags. Voltage sag (dip) is one of the most severe power quality problems. The root cause of voltage sag is a short circuit in the power system, e.g., due to lightning. The consequence of voltage sag may be that expensive power electronic devices are damaged, and the industrial products are scrapped. In order to evaluate the impact of different voltage sags and accompanying economic losses on the industrial processes, a detailed study of characterization of voltage sags is needed.

In this thesis, different methods for the characterization of voltage sags in the single-phase events and three-phase events are studied. The indices for characterizing voltage sags are discussed in terms of voltage magnitude, sag duration, and phase-angle jump, for both the single-phase events and the three-phase events. For the latter case, the characteristic voltage, the ABC classification and the symmetrical component classification are also analyzed.

Theoretical, simulation and experimental studies have been done to compare the results from different indices, based on four generic configurations constructed in the analog network. The simulation tool is PSCAD/EMTDC. The simulation results have shown accordance with the theoretical and experimental results with an acceptable error. It also has been shown in the three-phase events that the results of the minimum retained voltage and the magnitude of the characteristic voltage are identical for the sag type A and E, but not for the sag type B and C. The results also indicate that for the ideal sag type A, B, C and E, the phase-angle jump of the characteristic voltage is equal to that of the symmetrical phase voltage. However, this equivalence will not be valid if there is asymmetry of the other two phases with respect to the symmetrical phase.

The effect of induction machine on voltage sags in terms of sag magnitude, phase-angle jump, and jump of the transmission angle is discussed intensively. The voltage data recorded by phasor measurement unit (PMU) and power quality monitor (PQ monitor) are analyzed and compared. The results of the voltage magnitude recorded by PMU are in accordance with those recorded by PQ monitor. However, the results of phase-angle jump are not in accordance with each other, due to the low sampling frequency of PMU. Finally, the voltages sag types are summarized according to the ABC classification and the symmetrical component classification. However, the algorithm of the latter classification may lead to erroneous results due to the impact of the load condition.

Acknowledgments

This master's thesis work has been carried out at the Department of Energy and Environment, Division of Electric Power Engineering at Chalmers University of Technology, Gothenburg, Sweden.

I would like to thank my supervisor, Mr. Roberto Chouhy Leborgne, for his instruction, inspiration and unconditional help, both during and after the thesis work. I would also like to thank Dr. Gabriel Olguin for his co-supervision at the beginning of the thesis work at Chalmers.

I would like to thank my examiner, Prof. Jaap Daalder, for reading my thesis and giving some helpful advice.

I would also like to express my gratitude to Mr. Massimo Bongiorno, for his generous help in the Power System Lab as well as his 'magic box'.

Special thanks are given to the STINT organization in Sweden, for its financial support during this wonderful and fruitful international master's program.

Finally, I would like to thank all of my five interesting flat mates for their enjoyable company and wonderful European student life in Frölunda.

Table of Contents

ABSTRACT	II
ACKNOWLEDGMENTS.....	IV
TABLE OF CONTENTS	VI
1 INTRODUCTION	1
1.1 POWER QUALITY	1
1.2 VOLTAGE SAG AND VOLTAGE DIP	1
1.3 THE PROJECT	2
2 THEORETICAL BACKGROUND	3
2.1 VOLTAGE SAGS CHARACTERIZATION	3
2.1.1 <i>Single-phase events</i>	3
2.1.2 <i>Three-phase events</i>	6
3 ANALOG NETWORK MODEL.....	13
3.1 DESCRIPTION OF THE ANALOG NETWORK MODEL	13
3.1.1 <i>The line model</i>	13
3.1.2 <i>Load models</i>	13
3.2 NETWORK CONFIGURATIONS	14
4 RESULTS	16
4.1 MAGNITUDE.....	24
4.1.1 <i>Modeling and algorithm</i>	24
4.1.2 <i>The retained voltage versus the characteristic voltage</i>	25
4.1.3 <i>The effect of induction machine load</i>	26
4.1.4 <i>PMU versus PQ monitor</i>	34
4.2 PHASE-ANGLE JUMP	37
4.2.1 <i>Modeling and algorithm</i>	37
4.2.2 <i>Phase voltage versus the characteristic voltage</i>	38
4.2.3 <i>The effect of induction machine load</i>	39
4.2.4 <i>PMU versus PQ monitor</i>	40
4.3 VOLTAGE SAG TYPE	40
5 CONCLUSIONS.....	42
5.1 SUMMARY	42
5.2 CONCLUSIONS	42
REFERENCES	45
APPENDIX A: SIMULATION CONFIGURATIONS IN PSCAD	46

APPENDIX B: THE CHARACTERISTIC VOLTAGE AND PN FACTOR.....	46
APPENDIX C: RESULTS SUMMARIZED IN THE CHAPTER 4	46
C.1 ANALYTICAL ESTIMATION OF VOLTAGE SAGS	46
C.2 SIMULATIONS USING PSCAD.....	46
C.3 MEASUREMENTS ON THE ANALOG NETWORK MODEL.....	46

1 Introduction

1.1 Power quality

It is not until the recent fifteen years that power quality issues are becoming the focus of both the industries and the research institutes, although the quality of power exists as early as it comes into being. In 1993, Jane Clemmensen of the Electric Power Research Institute (EPRI) estimated that the U.S. national cost of power-related problems reaches \$26 billion per year. Primen of EPRI, in 2001, raised this figure to \$119 billion per year based on the cost of power interruption and power quality (LaCommare, 2004). The enormous cost draws utility and industrial company's great attention to the quality of power. Additionally, modern equipment, especially electronic and power electronic equipment, is very sensitive to voltage disturbances. Many reasons may finally lead the engineers' attention to the power quality issue.

Naturally, the following questions arise. What is power quality? What kind of indices can be used to quantify power quality? There are more questions to be addressed related power quality, but these two are the most basic and intractable ones. The Institute of Electrical and Electronics Engineers (IEEE) defines power quality as "the concept of powering and grounding electronic equipment in a manner that is suitable to the operation of that equipment and compatible with the premise wiring system and other connected equipment" (IEEE Std 1100, 1999). The definition is focused on electronic equipment, and the interaction between the equipment and the system it is connected to. It doesn't quantify power quality by any parameters. The International Electrotechnical Commission (IEC) defines power quality as "the characteristics of the electricity at a given point on an electrical system, evaluated against a set of reference technical parameters" (IEC 61000-4-30, 2001). IEC also notes that these parameters might, in some cases, relate to the compatibility between electricity supplied on a network and the loads connected to that network. This definition is focused on the parameters which may be measured or calculated at a certain point. It doesn't specify what these parameters are; only indicating that they might relate to the compatibility between power supply and loads. Regarding the vagueness and uncertainty of what power quality really is, more studies need to be dedicated in order to make it clear, not only for the research interests but for the tremendous economic effect.

1.2 Voltage sag and voltage dip

IEEE standard 1346 (IEEE Std 1346, 1998) defines sag as "a decrease in rms voltage or current at the power frequency for durations of 0.5 cycle to 1min. Typical values are 0.1 to 0.9 pu." This definition specifies two important parameters for voltage sag: rms voltage and duration. The standard also notes that to give a numerical value to a sag, the recommended usage is "a sag to 20%", which means that the line voltage is

reduced down to 20% of the normal value, not reduced by 20%. The standard treats voltage dip in the same way as voltage sag.

IEC standard 61000-4-30 (IEC 61000-4-30, 2001) defines voltage dip as “a temporary reduction of the voltage at a point in the electrical system below a threshold”. The standard notes that dips are described by duration and retained voltage. It also notes that if, during a voltage dip the voltage falls below an interruption threshold, the event is sometimes considered to be both a dip and an interruption. The latter note indicates that when counting the number of dips, interruption should also be included. Additionally, IEC standard 61000-2-8 (IEC 61000-2-8, 2002) states that “voltage sag is an alternative name for the phenomenon of voltage dip”.

In this project, voltage sag and voltage dip are used as synonym of each other, both referring to the residual voltage of an event. Deeper discussion on voltage sag or voltage dip will be presented in Chapter 2.

1.3 The project

This master’s thesis work will discuss about the characterization of voltage sags. Firstly, two kinds of classification, the ABC classification and the symmetrical component classification, will be discussed for the characterization of voltage sags. Secondly, four typical configurations of power system networks will be constructed and analyzed based on theoretical estimation, PSCAD simulation and real measurement. The analysis will be carried out on the results of four types of faults (three-phase-to-ground faults, single-phase-to-ground faults, double-phase faults and double-phase-to-ground faults). All the results will be analyzed and discussed in detail regarding the magnitude, the phase-angle jump and the voltage dip type. Thirdly, the effect of induction machine on the bus voltages during voltage sags will be discussed as well. Finally, the voltage data recorded by phasor measurement unit (PMU) and power quality monitor (PQ monitor) will be analyzed and compared.

2 Theoretical Background

2.1 Voltage sags characterization

2.1.1 Single-phase events

As discussed in section 1.2, both IEEE and IEC standards of voltage sag indicate that it is a phenomenon of reduction of the voltage, which can be graphically explained in Fig. 2.1 in the form of instantaneous voltage versus time. This particular event of a single-phase voltage sag is caused by a short-circuit fault in a 50 Hz system. We can see that the voltage amplitude during the fault is reduced to about 60% of the pre-fault value for about five cycles. Voltage sag may happen due to other reasons, such as overloading and motor starting, which will give another profile. We will mainly talk about voltage sag due to short-circuit fault in this thesis. However, the indices for characterizing voltage sag described in this thesis can certainly be applied to sags due to other reasons. For single-phase events, three main indices, magnitude, duration and phase-angle jump, will be introduced to characterize voltage sag.

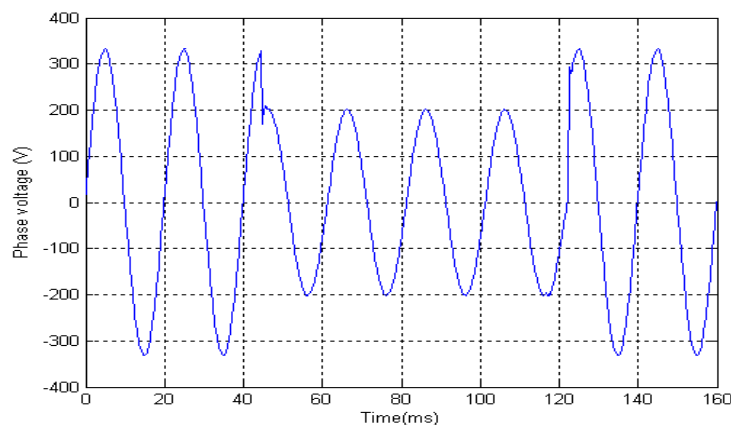


Fig. 2.1 Voltage sag due to a fault

- **Magnitude and duration**

The magnitude of a voltage sag can be determined in a number of ways. The most popular way to obtain a sag magnitude is to use rms voltage. There may be other alternatives, i.e., fundamental rms voltage, peak voltage. As long as the voltage is pure sinusoidal, these three options will give the same results, although in most situations this is not the case. In this thesis, the fundamental rms voltage will be adopted to describe sag magnitude. The fundamental component of a voltage as a function of time may be calculated as,

$$\overline{U}_{fund} = \frac{2}{T} \int_{t-T}^t u(\tau) e^{j\omega_0 \tau} d\tau \quad (2.1)$$

The fundamental voltage is calculated for each cycle. The advantage of using fundamental voltage is that phase-angle jump can be obtained at the same time, which

will be discussed in the following section. Therefore, the fundamental rms voltage can be expressed as,

$$U_{rms} = \frac{U_{fund}}{\sqrt{2}} \quad (2.2)$$

Using this algorithm, the corresponding fundamental rms voltage of the Fig. 2.1 is shown in Fig 2.2. There are several terminologies to name the magnitude of the sag voltage, such as sag magnitude, remaining voltage, residual voltage and retained voltage. All of them are referring to the same thing of a voltage sag, the real voltage left during an event, not the drop of it. As from section 1.2, we see that IEC use the term of “retained voltage” to characterize the magnitude of a voltage sag. IEC also defines that retained voltage is the minimum value of the rms voltage recorded during a voltage dip or interruption (IEC 61000-4-30, 2001). Therefore, we are going to use the terminology of retained voltage in the thesis as well. The corresponding retained voltage of the voltage sag in Fig. 2.1 is shown in Fig. 2.2. It is about 142 V in this case.

We can also see that there are two oscillating periods in the fundamental rms voltage profile. Rms voltage or fundamental rms voltage is calculated cycle by cycle. When taking one cycle data of a voltage sag event, it may happen that in this particular cycle, some data are from the pre-fault voltage and the rest are from the during-fault voltage. These cycles do not repeat as the “pure” pre-fault voltage or the “pure” during-fault voltage does, and exist only for their own particular instants. They appear in rms voltages in the oscillating period, which is referred to as the transition period. Therefore, for this instantaneous feature of the values during the transition period, it would be inappropriate to take them to characterize a voltage sag event. In other words, rms values during the transition period are not considered for the index of retained voltage.

The duration of a voltage sag is the time between the rms voltage (downwardly) crossing the sag starting threshold and the rms voltage (upwardly) crossing the sag ending threshold (IEEE Std P1564, 2004). The duration of the voltage sag in Fig. 2.1 is shown in Fig. 2.2 as well.

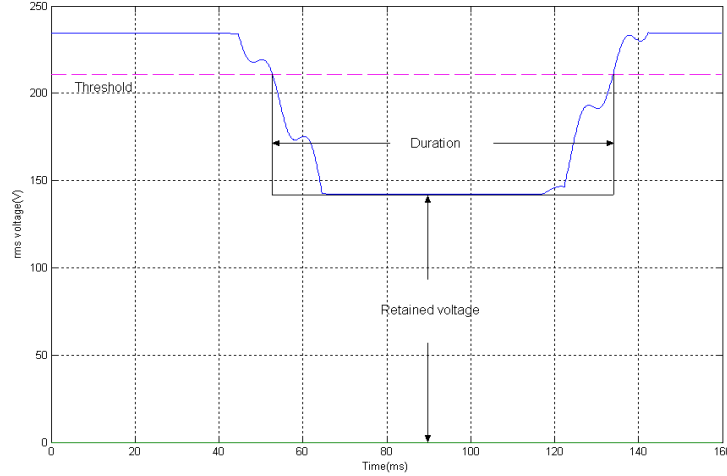


Fig. 2.2 Fundamental rms voltage for the voltage sag shown in Fig. 2.1

● Phase-angle jump

A short-circuit fault in power systems causes a change in voltage at a certain point, not only in magnitude but also in phase angle. However, both IEEE and IEC standards have not yet provided a unique definition of the change in phase angle. In some references, the change in phase angle is referred to as the phase-angle jump associated with the voltage sag (Bollen, 2000 a). The phase-angle jump manifests itself as a shift in zero crossing of the instantaneous voltage (Bollen, 2000 a). In order to have an intuitive idea of what phase-angle jump means, a virtual voltage sag event with retained voltage of 50% and phase-angle jump of -45 degrees are made and shown in Fig. 2.3. The zero crossing of the during-fault voltage lags that of the pre-fault voltage by 2.5 ms, which is 45 degrees in angle in a 50 Hz system. The minus sign indicates that the phase angle of the voltage decreases due to the fault.

There are several mathematical ways to obtain the equation for phase-angle jump. One of them is to use the argument of fundamental voltage shown in equation (2.1). If we take the angle of pre-fault voltage as the reference phase angle, phase-angle jump may be expressed as,

$$\Delta\phi = \arg(\overline{U_{dur,fund}}) - \arg(\overline{U_{pre,fund}}) \quad (2.3)$$

where $\Delta\phi$ is the phase-angle jump, $U_{dur,fund}$ is the during-fault fundamental rms voltage, $U_{pre,fund}$ is the pre-fault fundamental rms voltage. $\Delta\phi$ is restricted between -180 degrees and 180 degrees. Therefore, equation (2.3) can be expressed as,

$$\Delta\phi = \arg\left(\frac{\overline{U_{dur,fund}}}{\overline{U_{pre,fund}}}\right) \quad (2.4)$$

Using the algorithm in equation (2.4), the corresponding phase-angle jump of the voltage sag event in Fig. 2.1 can be shown in Fig. 2.4. The one with the maximum absolute value is chosen for the index of phase-angle jump in single-phase event. It is -25.2 degrees in this case. Note that phase-angle jump could also be positive, which means that the phase angle increases during the fault. Therefore, phase-angle jump is

not necessarily the minimum value of the profile, but can be the maximum one. The values at the transition periods should not be considered due to the same reason explained for the retained voltage index estimation.

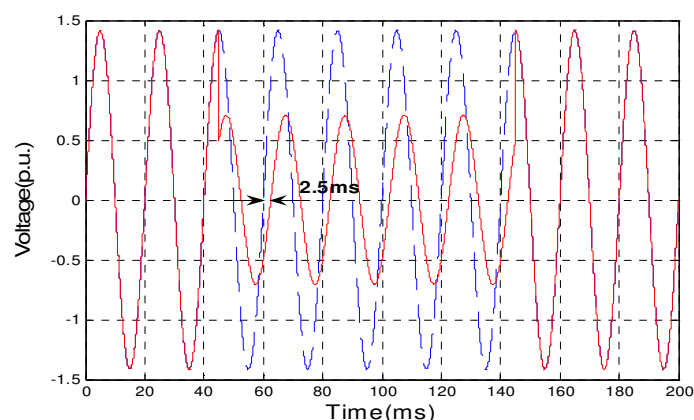


Fig. 2.3 Voltage sag with retained voltage of 50% and phase-angle jump of -45 degrees

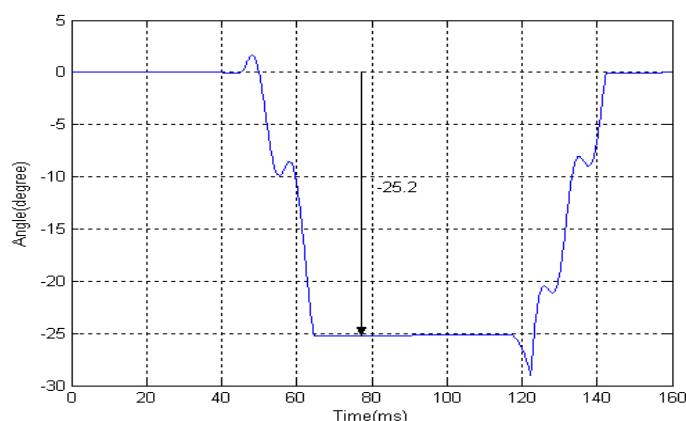


Fig. 2.4 Phase-angle jump for the voltage sag shown in Fig. 2.1

2.1.2 Three-phase events

● Magnitude

IEEE and IEC have no standard definition of indices of magnitude for three-phase events. Therefore, in the published literatures, the sag magnitude for three-phase events may be represented by the most severe phase (Olguin, 2005), the characteristic voltage (Bollen, 2000 a), or the symmetrical components of the three-phase voltage (Macken, 2004), etc. Each way of characterizing three-phase events by magnitude has its own advantage in the specific fields. As stated above, there is still no common agreement on which one is preferable to use as an index of the magnitude for three-phase voltage sags. In this thesis, two ways of interpreting magnitude for three-phase events will be employed. They are the minimum retained voltage and the magnitude of the characteristic voltage.

A. The minimum retained voltage

The minimum retained voltage originates from the retained voltage for single-phase event. The idea is to apply the definition of the retained voltage to three individual phase voltages in the three-phase events. The minimum retained voltage is just to choose the minimum value of these three retained voltages obtained during the three-phase events. This way of charactering three-phase sag magnitude will be used in Chapter 4 and 5, and compared with the characteristic voltage, which will be discussed in the next paragraph.

B. The characteristic voltage

The characteristic voltage is introduced by Zhang (1999). The absolute value of the characteristic voltage is used to represent the three-phase sag magnitude index. But in the following equations, we will show the complex form of the characteristic voltage \bar{U} instead. Characteristic voltage is defined based on the symmetrical components of the phase voltages. Another parameter related with characteristic voltage will be introduced as well, which is the so-called positive-negative factor \bar{F} .

For the three-phase-to-ground fault, the characteristic voltage and the PN factor are expressed as,

$$\bar{U} = \bar{F} = \bar{U}_1 \quad (2.5)$$

where \bar{U}_1 is the positive-sequence voltage at PCC during faults.

For the single-phase-to-ground fault, the characteristic voltage and the PN factor are expressed as,

$$\bar{U} = \bar{U}_1 + \bar{U}_2 \quad (2.6)$$

$$\bar{F} = \bar{U}_1 - \bar{U}_2 \quad (2.7)$$

where \bar{U}_2 is the negative-sequence voltage at PCC during faults.

For the double-phase and double-phase-to-ground faults, the characteristic voltage and the PN factor are both expressed as,

$$\bar{U} = \bar{U}_1 - \bar{U}_2 \quad (2.8)$$

$$\bar{F} = \bar{U}_1 + \bar{U}_2 \quad (2.9)$$

Refer to Appendix B for more explanation of the characteristic voltage and PN factor.

● **Duration**

There are mainly three factors that affect the result of duration for three-phase voltage sags. One is the choice of the threshold. Two others, which are more controversial, are the starting instant and the ending instant of a voltage sag for three-phase event.

Therefore, the duration of a three-phase event can be calculated based on the phase with the lowest magnitude of the three phases, the longest one of the three durations of the three phases, etc. In this thesis, we choose to define the duration of the three-phase voltage sags as “a voltage sag starts when the rms voltage of one or more channels is below the dip-starting threshold, typically between 85% and 95% of the nominal voltage, and ends when the rms voltage on all measured channels is equal to or above the dip-ending threshold”(IEC 61000-4-30, 2002). Graphically, this definition of the duration is shown in Fig. 2.5 below.

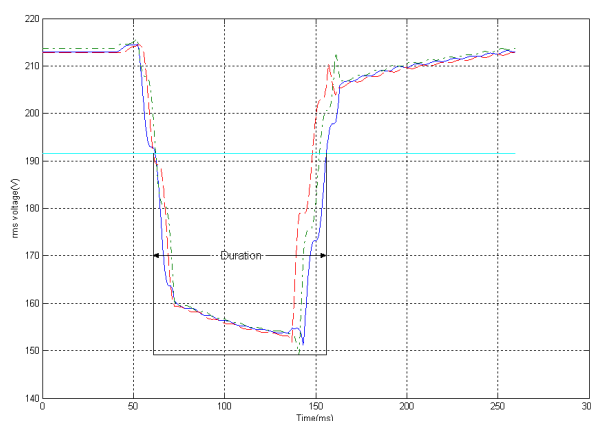


Fig. 2.5 Duration of three-phase unbalanced voltage sags

● Phase-angle jump

Corresponding to the definitions of magnitude, the index of phase-angle jump of three-phase voltage sags can also have two alternatives. One is called the maximum phase-angle jump, which is simply to apply the definition of phase-angle jump in single-phase event to all the three phases and choose the maximum value. Another alternative is to choose the phase angle of the characteristic voltage. Both definitions will be used and compared to obtain the phase-angle jump in Chapter 4.

● The ABC classification

There are a number of other proposals for the classifications of three-phase voltage sags. One of the most common classifications is the ABC method, which is introduced by Bollen (2000). The ABC classification includes seven types of three-phase voltage sags. It concerns the voltage sags experienced by the end-user equipment, where the voltage level is in general lower than the one at which faults happen. This phenomenon requires the consideration of the propagation of voltage sags through transformers. The effect of different types of transformers is briefly summarized below (Bollen, 2000). Although transformers can be of different winding connections and clock numbers, the effect of them can be grouped into three categories.

1. Transformers that do not change anything to the phase voltages, e.g., Yyn connected transformer. The phase voltages in p.u. at both sides of the transformers are equal to each other.
2. Transformers that block the zero-sequence voltage, e.g., Yny, Yy and Dd

connected transformers. After crossing this kind of transformers, voltages at the secondary side will have no zero-sequence component. In mathematical way, this kind of transformation can be expressed in the following matrix form.

$$T_1 = \frac{1}{3} \begin{bmatrix} 2 & -1 & -1 \\ -1 & 2 & -1 \\ -1 & -1 & 2 \end{bmatrix} \quad (2.10)$$

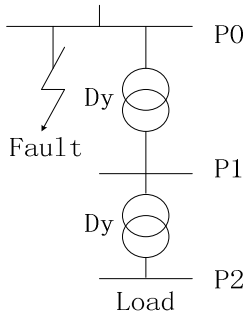
3. Transformers that swap line and phase voltages, e.g., Dy, Yd connected transformers. After crossing this kind of transformers, each secondary-side phase voltage will be equal to the corresponding primary-side phase-to-phase voltage in p.u. value. This kind of transformation can also be expressed in the matrix form.

$$T_2 = \frac{j}{\sqrt{3}} \begin{bmatrix} 0 & 1 & -1 \\ -1 & 0 & 1 \\ 1 & -1 & 0 \end{bmatrix} \quad (2.11)$$

Note that $T_2^2=T_1$, $T_1^2=T_2$, $T_2T_1=T_2$, which mean that the combination of different transformers will not result in another kind of transformation. Here, the star-connected three-phase loads are assumed. Compared with star-connected three-phase loads, delta-connected three-phase loads will experience the same phase voltages after the transformation in equation (2.11). These three types of transformers combined with the four shunt faults will result in mainly seven types of voltage sags, *A*, *B*, *C*, *D*, *E*, *F* and *G*, which is the so-called ABC classification. This combination process is presented in Table 2.1, whereas the equation forms and the phasor forms of these seven types are shown in Table 2.2. It is necessary to point out that among the seven types, only type *B* and type *E* contain zero-sequence component, which is rarely transferred to the terminals of end-user equipment. In other words, for most cases, end-user equipment will experience only five types of voltage sags, which are type *A*, *C*, *D*, *F* and *G*. The seven types of the ABC classification are based on the assumption that positive- and negative-sequence impedances are identical. All the phase voltages here are with respect to the neutral point (of the end-user equipment). Load currents, before, during, and after the fault, are neglected.

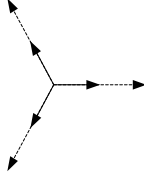
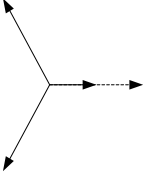
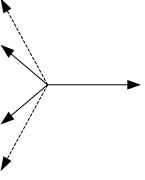
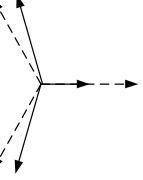
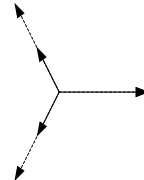
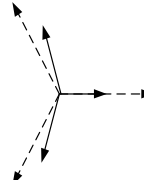
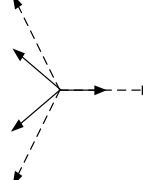
As shown in Table 2.2, the ABC classification is a very intuitive method to understand the possible types of voltage sags the end-user equipment is going to experience. Hence, the ABC classification is useful to test the equipment tolerance of voltage sags, i.e., grid-connected power-electronic converters (Sannino, 2005). There are also drawbacks of this classification. One is that the ABC classification is only simulation-based, and originates from ideal voltage sag equations in Table 2.2. Because of its intuitive feature, it is not easy to extract dip type from measured voltage waveforms by the ABC classification.

Table 2.1 Propagation of voltage sags through transformers

Propagation of voltage sags	Type	3PG	1PG	2P	2PG
	P0	A	B	C	E
	P1	A	C	D	F
	P2	A	D	C	G

Note: 3PG: Three-phase-to-ground fault, 1PG: Single-phase-to-ground fault, 2P: Double-phase fault, 2PG: Double-phase-to-ground fault

Table 2.2 Seven types of three-phase voltage sags according to the ABC classification

Type	A	B	C	D
Voltages	$\bar{U}_a = \bar{U}$ $\bar{U}_b = -\frac{1}{2}\bar{U} - j\frac{\sqrt{3}}{2}\bar{U}$ $\bar{U}_c = -\frac{1}{2}\bar{U} + j\frac{\sqrt{3}}{2}\bar{U}$	$\bar{U}_a = \bar{U}^\#$ $\bar{U}_b = -\frac{1}{2}\bar{U} - j\frac{\sqrt{3}}{2}\bar{U}$ $\bar{U}_c = -\frac{1}{2}\bar{U} + j\frac{\sqrt{3}}{2}\bar{U}$	$\bar{U}_a = 1$ $\bar{U}_b = -\frac{1}{2} - j\frac{\sqrt{3}}{2}$ $\bar{U}_c = -\frac{1}{2} + j\frac{\sqrt{3}}{2}$	$\bar{U}_a = \bar{U}$ $\bar{U}_b = -\frac{1}{2}\bar{U} - j\frac{\sqrt{3}}{2}\bar{U}$ $\bar{U}_c = -\frac{1}{2}\bar{U} + j\frac{\sqrt{3}}{2}\bar{U}$
Phasors				
Type	E		F	G
Voltages	$\bar{U}_a = 1$ $\bar{U}_b = -\frac{1}{2}\bar{U} - j\frac{\sqrt{3}}{2}\bar{U}$ $\bar{U}_c = -\frac{1}{2}\bar{U} + j\frac{\sqrt{3}}{2}\bar{U}$		$\bar{U}_a = \bar{U}$ $\bar{U}_b = -\frac{1}{2}\bar{U} - j(\frac{\sqrt{3}}{3} + \frac{\sqrt{3}}{6}\bar{U})$ $\bar{U}_c = -\frac{1}{2}\bar{U} + j(\frac{\sqrt{3}}{3} + \frac{\sqrt{3}}{6}\bar{U})$	$\bar{U}_a = \frac{2}{3} + \frac{1}{3}\bar{U}$ $\bar{U}_b = -(\frac{1}{3} + \frac{1}{6}\bar{U}) - j\frac{\sqrt{3}}{2}\bar{U}$ $\bar{U}_c = -(\frac{1}{3} + \frac{1}{6}\bar{U}) + j\frac{\sqrt{3}}{2}\bar{U}$
Phasors				

Note: \bar{U} is the characteristic voltage, a complex value, $\bar{U}^\#$ (in type B) is equal to $\frac{3}{2}\bar{U} - \frac{1}{2}$

● **The symmetrical component classification**

Aiming at extracting sag types from the measured voltage waveforms, a generalized

ABC classification is proposed in (Bollen, 2000 b), which is later called the symmetrical component algorithm or the symmetrical component classification. This generalization is achieved by introducing a second characteristic, the so-called PN factor \overline{F} . As a result, under the condition of the symmetrical component classification, positive- and negative- sequence impedances no longer have to be equal. The seven types A , B , C , D , E , F and G in the ABC classification are classified into two more general types C and D in the symmetrical component classification, which are further subdivided into C_a , C_b , C_c , D_a , D_b , and D_c , to include the symmetrical phase. The type C and D in the symmetrical component classification are slightly different from those in the ABC classification. For the general, the symmetrical component classification distinguishes the positive- and the negative-sequence impedance, and includes PN factor, \overline{F} . For example, for sag type C_a , the equation is expressed as,

$$\begin{aligned}\overline{U}_a &= \overline{F} \\ \overline{U}_b &= -\frac{1}{2}\overline{F} - j\frac{\sqrt{3}}{2}\overline{U} \\ \overline{U}_c &= -\frac{1}{2}\overline{F} + j\frac{\sqrt{3}}{2}\overline{U}\end{aligned}\quad (2.12)$$

and for sag type D_a , the equation is expressed as,

$$\begin{aligned}\overline{U}_a &= \overline{U} \\ \overline{U}_b &= -\frac{1}{2}\overline{U} - j\frac{\sqrt{3}}{2}\overline{F} \\ \overline{U}_c &= -\frac{1}{2}\overline{U} + j\frac{\sqrt{3}}{2}\overline{F}\end{aligned}\quad (2.13)$$

As presented in (Bollen, 2003 a), the six phasors of the symmetrical component method are shown in Fig. 2.6.

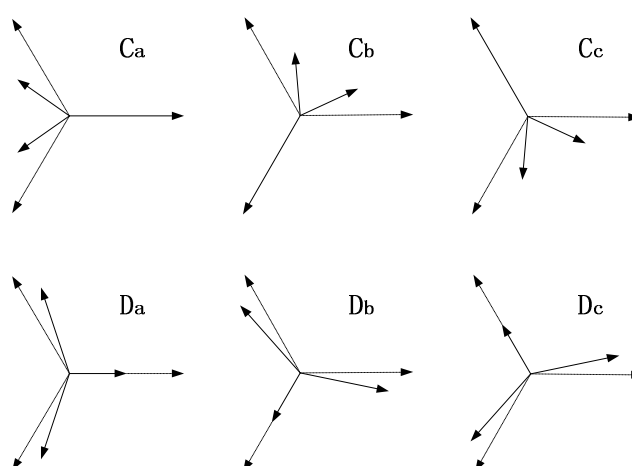


Fig. 2.6 Six types of three-phase unbalanced voltage sags according to the symmetrical component classification

As are shown in Appendix B the definition of the characteristic voltage \overline{U} and the positive-negative factor \overline{F} , as well as the discussion in (Bollen, 2003 b), it can be

concluded that the positive-sequence voltages for all the six sag types in Fig. 2.17 are the same, and can be expressed as,

$$\bar{U}_1 = \frac{1}{2}(\bar{F} + \bar{U}) \quad (2.14)$$

where \bar{U}_1 is the positive-sequence voltage. The negative-sequence voltages \bar{U}_2 , however the same in magnitude, are different in argument for the six different sag types. The expressions of the negative-sequence voltages are shown in Table 2.3.

As analyzed in (Bollen, 2003 a), if we assume that $\bar{F} = 1$, the angle between the drop in the positive-sequence voltage and the negative-sequence voltage is an integer multiple of 60 degrees, which indicates that for different sag types, the values of this angle are different. Mathematically, we can introduce an index T , which is expressed as,

$$T = \frac{1}{60^\circ} \times \arg\left(\frac{\bar{U}_2}{1 - \bar{U}_1}\right) \quad (2.15)$$

where the value of the argument should be ranged between 0 and 360 degree; T is rounded into the nearest integer. Also note that \bar{U}_1 and \bar{U}_2 are in per unit value with respect to the pre-fault voltage at PCC or monitoring point. For different negative-sequence voltages or sag types, different values of T are calculated in Table 2.3. The value of T is directly related to each sag type. The foremost objective of the symmetrical component classification, to extract sag type from the measured voltage waveforms, is finally achieved through the index T .

Table 2.3 Six types of three-phase unbalanced voltage sags according to the symmetrical classification.

Type	C_a	C_b	C_c	D_a	D_b	D_c
\bar{U}_2	$\frac{1}{2}(\bar{F} - \bar{U})$	$\frac{1}{2}a(\bar{F} - \bar{U})$	$\frac{1}{2}a^2(\bar{F} - \bar{U})$	$-\frac{1}{2}(\bar{F} - \bar{U})$	$-\frac{1}{2}a(\bar{F} - \bar{U})$	$-\frac{1}{2}a^2(\bar{F} - \bar{U})$
T	0	2	4	3	5	1

Note: $a = e^{j120^\circ}$.

3 Analog network model

3.1 Description of the analog network model

The analog network model (the power system model) is a three-phase model of a 400 kV transmission system and consists of power plant model, transmission line model, two transformer models with on-load tap changers as well as dynamic loads. As only the transmission line model and the dynamic loads are going to be used during the actual measurement, other two models will not be introduced here. The entire model operates at 400 V and the rated generator power is 75 kVA. Consequently, the voltage scale of the model is 1:1000. The power scale is 1:18,800 due to the impedance scale of the line model. The power system model can also be supplied by the common three-phase grid voltage (400V, line-to-line).

3.1.1 The line model

The line model consists of six identical π -sections, each corresponding to 150 km of a 400 kV line. The sections can be connected arbitrarily in series or parallel.

Data for a π -section are as follows.

$$R_1 = 50.0 \text{ m}\Omega$$

$$L_1 = 2.05 \text{ mH}$$

$$C_1 = 46.0 \text{ }\mu\text{F}$$

$$\bar{Z} = R_1 + j\omega L_1 = 50.0 + j644 \text{ m}\Omega$$

$$\bar{Z}_c = -j/(\omega C_1) = -j69.2 \text{ }\Omega$$

The capacitors are only connected to the ground at the location where PQ monitor and PMU are installed during the actual measurement. The reason is that the neutral point of the PQ monitor and PMU need to be grounded in order to measure the phase-to-ground voltages. However, in the analytical estimation and the simulation, the connected capacitors at PCC or monitoring point will be neglected.

3.1.2 Load models

The industrial part of the load is modeled as a 30 kW induction motor. During the actual measurement, the induction motor is running under no load condition.

Data for the induction machine (delta-connected) are as follows.

$$\text{Rated line voltage } U_{\text{rated}} = 380 \text{ V}$$

$$\text{Rated phase current } I_{\text{rated}} = 62 \text{ A}$$

$$\text{Power factor } \cos\varphi = 0.81$$

$$\text{Rated rotation speed } n_{\text{rated}} = 1450 \text{ rpm}$$

In addition, there are two three-phase resistive loads with rated line voltage of 400 V and rated power of 9 kW.

3.2 Network configurations

In order to measure actual voltage sags in a real network, four typical configurations are constructed and tested in the Power System Lab. Different types of voltage sags are obtained as a consequence of the faults performed at the analog model in the lab.

The first typical configuration shown in Fig.3.1 is named as “Basic circuit”. It represents a distribution feeder. The faults happen at the end of the feeder and the voltage sags are measured at the point of common coupling. The voltage source is solidly grounded. Each impedance corresponds to one section of the line model discussed in section 3.1.

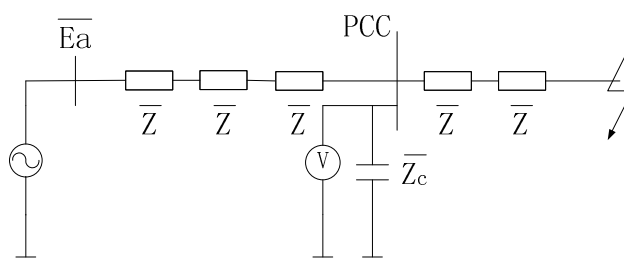


Fig. 3.1 Basic circuit

The second typical configuration, called “Voltage-divider circuit”, is shown in Fig. 3.2. This Voltage-divider circuit under no load condition is similar to Basic circuit in Fig. 3.1. The measurement is also done when the voltage-divider circuit is loaded with induction machine. The effect of induction machine on the PCC bus will be investigated when different types of fault occur at the other feeder.

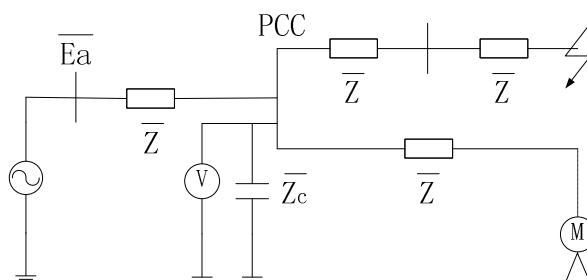


Fig. 3.2 Voltage-divider circuit

The third configuration, which is called “Fault-load circuit” and shown in Fig. 3.3, is constructed to model the parallel lines in the transmission system. Two identical three-phase resistive loads are connected at the monitoring point (MP). The aim is to analyze what will happen at the load side, e.g., load voltage, if fault happens directly at the load side. It is also intended to investigate the effect of induction machine on the monitoring point. Load conditions with and without induction machine are both tested in the analog network model.

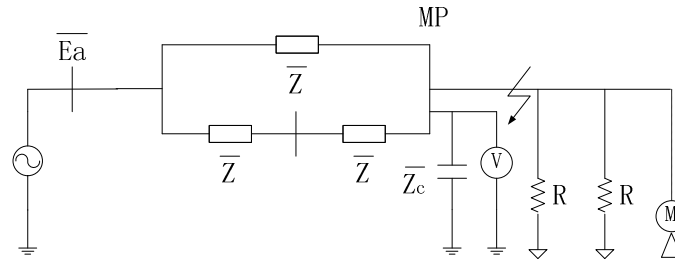


Fig. 3.3 Fault-load circuit

The last studied configuration, which is called “Fault-line circuit”, shown in Fig. 3.4, are both to analyze the voltages at the source side (MP1) and the load side (MP2) of the parallel transmission lines when faults occur at one of the parallel lines. The effect of induction machine during faults on both sides will be investigated as well. Load conditions with and without induction machine are both tested in the analog network model.

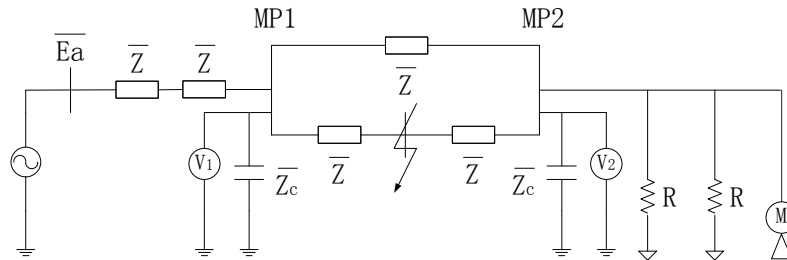
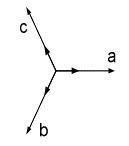
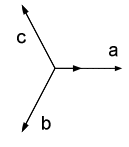
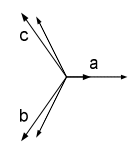
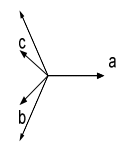
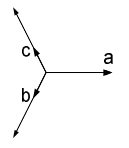
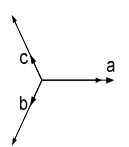


Fig. 3.4 Fault-line circuit

4 Results

Analytical (theoretical), simulation, and experimental results of the four circuits shown in section 3.2 are obtained and processed. Due to the large amount of the information, all the calculations, simulations, and measurements are shown in the Appendix C. The results from the four different circuits are summarized from Table 4.1 to Table 4.9. The indices of magnitude, phase-angle jump and sag type are analyzed according to all the results obtained.

Table 4.1 Results of three-phase voltage sags from “Basic Circuit”

		Phasors	U_r (V)	$\Delta\phi$ (deg)	$ \bar{U} $ (V)	$\arg(\bar{U})$ (deg)	$ \bar{F} $ (V)	Sag Type	
								ABC	T
3PG	Theor.		92.0	0	92.0	0	92.0	A	0(Ca)
	Simul.	see above	92.0	0	92.0	0	92.0	A	0(Ca)
	Exper.	see above	93.4	0.3	93.5	0.3	93.5	A	2(Cb)
1PG	Theor.		92.0	0	138	0	230	B	3(Da)
	Simul.	see above	92.0	0	138	0	230	B	3(Da)
	Exper.		93.5	-9.6	170	-0.5	238	B	3(Da)
2P	Theor.		140	-25.3	92.0	0	230	C	0(Ca)
	Simul.	see above	140	-25.3	92.0	0	230	C	0(Ca)
	Exper.	see above	142	-25.2	96.0	-0.1	232	C	0(Ca)
2PG	Theor.		92.0	0	92.0	0	184	E	0(Ca)
	Simul.	see above	92.0	0	92.0	0	184	E	0(Ca)
	Exper.		93.5	0.1	94.7	0.1	211	E	0(Ca)

Note: 3PG: Three-phase-to-ground fault, 1PG: Single-phase-to-ground fault, 2P: Double-phase fault, 2PG: Double-phase-to-ground fault, Theor.: Theoretical (analytical) value, Simul.: Simulation value, Exper.: Experimental value, U_r : Minimum retained voltage. $\Delta\phi$: Maximum phase-angle jump, U : Characteristic voltage

Table 4.2 Results of three-phase voltage sags from “Voltage-divider circuit”
No load condition

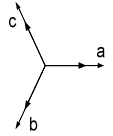
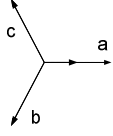
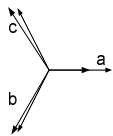
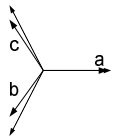
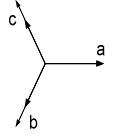
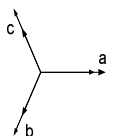
		Phasors	U_r (V)	$\Delta\phi$ (deg)	$ \bar{U} $ (V)	$\arg(\bar{U})$ (deg)	$ \bar{F} $ (V)	Sag Type	
								ABC	T
3PG	Theor.		153	0	153	0	153	A	0(Ca)
	Simul.	see above	153	0	153	0	153	A	0(Ca)
	Exper.	see above	154	-0.4	155	-0.9	154	A	2(Cb)
1PG	Theor.		153	0	178	0	230	B	3(Da)
	Simul.	see above	153	0	179	0	230	B	3(Da)
	Exper.		154	7.8	199	2.4	232	B	3(Da)
2P	Theor.		176	-10.9	154	0	230	C	0(Ca)
	Simul.	see above	176	-10.9	153	0	230	C	0(Ca)
	Exper.	see above	177	-11.0	154	0.4	233	C	0(Ca)
2PG	Theor.		153	0	153	0	205	E	0(Ca)
	Simul.	see above	153	0	153	0	204	E	0(Ca)
	Exper.		154	1.2	155	2.0	220	E	0(Ca)

Table 4.3 Results of three-phase voltage sags from “Voltage-divider circuit”**Load: Induction machine**

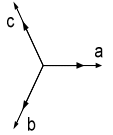
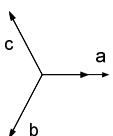
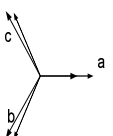
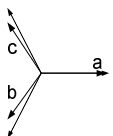
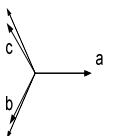
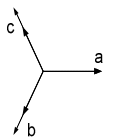
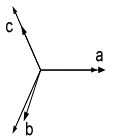
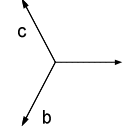
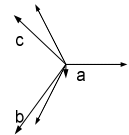
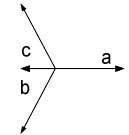
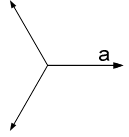
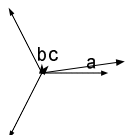
		Phasors	U_r (V)	$\Delta\phi$ (deg)	$ \bar{U} $ (V)	$\arg(\bar{U})$ (deg)	$ \bar{F} $ (V)	Sag Type	
								ABC	T
3PG	Simul.		155	-1.1	155	-1.1	155	A	0(Ca)
	Exper.	see above	154	1.4	153	1.6	153	A	3(Da)
1PG	Simul..		155	-2.1	181	0.4	217	B	3(Da)
	Exper.		149	-7.4	192	-0.2	215	B	3(Da)
2P	Simul.		174	-8.5	159	0.6	215	C	0(Ca)
	Exper.		172	10.0	154	2.9	216	C	0(Ca)
2PG	Simul.		155	-2.2	158	-0.4	196	E	0(Ca)
	Exper.		153	4.5	155	2.1	206	E	0(Ca)

Table 4.4 Results of three-phase voltage sags from “Fault-load circuit”
Two resistive loads

		Phasors	U_r (V)	$\Delta\phi$ (deg)	$ \bar{U} $ (V)	$\arg(\bar{U})$ (deg)	$ \bar{F} $ (V)	Sag Type	
								ABC	T
3PG	Theor.	\$	0	\$	0	\$	0	A	0(Ca)
	Simul.	\$	0	\$	0	\$	0	A	0(Ca)
	Exper.	\$	1.63	\$	1.76	\$	1.76	A	1(Dc)
1PG	Theor.		0	\$	76.6	1.9	229	B	3(Da)
	Simul.	see above	0	\$	77.0	1.9	229	B	3(Da)
	Exper.		26.3	-88.4	128	2.1	217	B	3(Da)
2P	Theor.		115	-60.2	0.408	\$	229	C	0(Ca)
	Simul.	see above	114	-60.0	0	\$	229	C	0(Ca)
	Exper.	see above	108	61.0	1.35	-112.4	217	C	0(Ca)
2PG	Theor.		0	\$	0	\$	153	E	0(Ca)
	Simul.	see above	0	\$	0	\$	153	E	0(Ca)
	Exper.		18.0	-147.5	1.4	-80.3	179	E	0(Ca)

Note: \$: NOT applicable under this condition.

Table 4.5 Results of three-phase voltage sags from “Fault-load circuit”
Two resistive loads and induction machine loaded

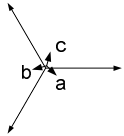
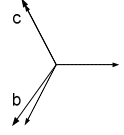
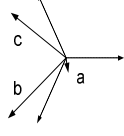
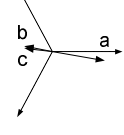
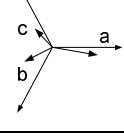
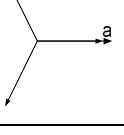
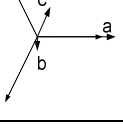
		Phasors	U_r (V)	$\Delta\phi$ (deg)	$ \bar{U} $ (V)	$\arg(\bar{U})$ (deg)	$ \bar{F} $ (V)	Sag Type	
								ABC	T
3PG	Simul.	\$	0	\$	0	\$	0	A	0(Ca)
	Exper.		40.8	-48.0	40.6	-46.3	40.6	A	5(Db)
1PG	Simul..		0	\$	86.7	2.6	204	B	3(Da)
	Exper.		31.9	-72.1	144	-2.5	168	B	3(Da)
2P	Simul.		88.5	-70.3	0	\$	206	C	0(Ca)
	Exper.		89.5	-32.1	92.8	-17.4	143	C	0(Ca)
2PG	Simul.		0	\$	0	\$	129	E	0(Ca)
	Exper.		29.8	-55.3	67.1	-11.6	125	E	0(Ca)

Table 4.6 Results of three-phase voltage sags at MP2 from “Fault-line circuit”**Two resistive loads**

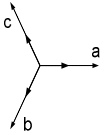
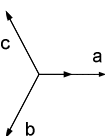
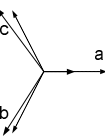
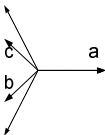
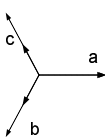
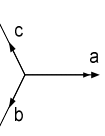
		Phasors	U_r (V)	$\Delta\phi$ (deg)	$ \bar{U} $ (V)	$\arg(\bar{U})$ (deg)	$ \bar{F} $ (V)	Sag Type	
								ABC	T
3PG	Theor.		115	0.7	115	0.7	115	A	4(Cc)
	Simul.	see above	115	0.7	115	0.7	115	A	4(Cc)
	Exper.	see above	112	1.7	113	1.5	113	A	3(Da)
1PG	Theor.		115	2.8	154	2.6	229	B	3(Da)
	Simul.	see above	114	0.3	153	0.5	229	B	3(Da)
	Exper.		111	11	182	2.5	233	B	3(Da)
2P	Theor.		149	21.3	115	3.5	229	C	0(Ca)
	Simul.	see above	151	19.4	115	0.7	229	C	0(Ca)
	Exper.	see above	149	22.7	113	4.1	233	C	0(Ca)
2PG	Theor.		114	3.2	115	3.5	191	E	0(Ca)
	Simul.	see above	113	0.5	115	0.7	191	E	0(Ca)
	Exper.		111	2.3	113	2.4	214	E	0(Ca)

Table 4.7 Results of three-phase voltage sags at MP2 from “Fault-line circuit”
Two resistive loads and induction machine loaded

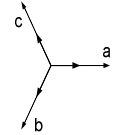
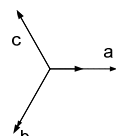
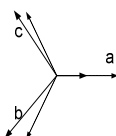
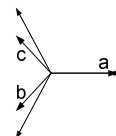
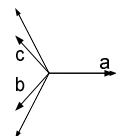
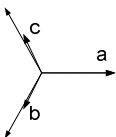
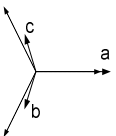
		Phasors	U_r (V)	$\Delta\phi$ (deg)	$ \bar{U} $ (V)	$\arg(\bar{U})$ (deg)	$ \bar{F} $ (V)	Sag Type	
								ABC	T
3PG	Simul.		119	-3.5	119	-3.5	119	A	4(Cc)
	Exper.	see above	115	-4.1	115	-3.8	115	A	1(Dc)
1PG	Simul.		122	-3.9	162	0.9	214	B	3(Da)
	Exper.		113	-13.8	184	-2.0	212	B	2(Ca)
2P	Simul.		150	-14.4	129	1.7	210	C	0(Ca)
	Exper.		146	-13.4	130	1.1	203	C	0(Ca)
2PG	Simul.		118	-5.8	126	-1.1	181	E	0(Ca)
	Exper.		116	9.4	127	2.1	189	E	0(Ca)

Table 4.8 PMU measurements at MP1 and MP2 from “Fault-line circuit”**Two resistive loads**

		U_{MP1}	$\Delta\phi_{MP1}$	U_{MP2}	$\Delta\phi_{MP2}$	$\Delta\phi_{MP21}$
		(V)	(deg)	(V)	(deg)	(deg)
3PG	Theor.	230	0	115	0.7	0.7
	Simul.	230	0	115	0.7	0.7
	Exper.	222	4.4	110	4.4	0.1
1PG	Theor.	230	0	191	1.9	1.9
	Simul.	230	0	191	0.2	0.2
	Exper.	227	2.5	197	2.8	0.2
2P	Theor.	230	0	172	2.1	2.1
	Simul.	230	0	172	0.2	0.2
	Exper.	225	3.0	169	2.7	-0.3
2PG	Theor.	230	0	153	2.5	2.5
	Simul.	230	0	153	0.4	0.4
	Exper.	224	1.7	160	1.7	0.1

Note: U_{MP1} : minimum positive-sequence voltage at MP1, U_{MP21} : minimum positive-sequence voltage at MP1, $\Delta\phi_{MP1}$: maximum phase-angle jump of positive-sequence voltage at MP1, $\Delta\phi_{MP21}$: maximum phase-angle jump of positive-sequence voltage at MP2, $\Delta\phi_{MP21}$: maximum jump of the phase-angle difference (transmission angle) between the positive-sequence voltage at MP2 and MP1

Table 4.9 PMU measurements at MP1 and MP2 from “Fault-line circuit”**Two resistive loads and induction machine loaded**

		U_{MP1}	$\Delta\phi_{MP1}$	U_{MP2}	$\Delta\phi_{MP2}$	$\Delta\phi_{MP21}$
		(V)	(deg)	(V)	(deg)	(deg)
3PG	Simul.	230	0	119	-3.4	-3.4
	Exper.	222	3.9	113	1.8	-3.9
1PG	Simul.	230	0	188	-0.1	-0.1
	Exper.	227	-0.2	190	-0.3	-0.1
2P	Simul.	230	0	170	-1.6	-1.6
	Exper.	225	1.8	164	-1.4	-2.6
2PG	Simul.	230	0	154	-2.0	-2.0
	Exper.	225	1.5	156	-1.9	-2.0

4.1 Magnitude

In this section, four aspects of the results from Table 4.1 to Table 4.9, in terms of the retained voltage U_r , the magnitude of the characteristic voltage $|\bar{U}|$, and the PN factor $|\bar{F}|$, will be discussed in detail.

4.1.1 Modeling and algorithm

The first aspect is the comparison among theoretical, simulation, and experimental results. According to the tables shown above, the theoretical and the simulation values of U_r , $|\bar{U}|$ and $|\bar{F}|$ are very similar to each other, respectively. The relative error between theoretical values and simulation values is less than 2% in all the cases shown in Table 4.1, 4.2, 4.4, 4.6 and 4.8. For most cases in Table 4.1 to 4.3 and Table 4.6 to 4.9, the relative error between simulation values and experimental values of U_r , $|\bar{U}|$ and $|\bar{F}|$ are within 5%, except for the cases listed again in Table 4.10 below.

Table 4.10 Relative error between simulation and experimental results (in magnitude) $\delta > 5\%$

Table	Fault type	Index	Simul. (V)	Exper. (V)	δ (%)
4.1	1PG	$ \bar{U} $	138	170	18.8
4.1	2PG	$ \bar{F} $	184	211	12.8
4.2	1PG	$ \bar{U} $	179	199	10.1
4.2	2PG	$ \bar{F} $	204	220	7.3
4.3	1PG	$ \bar{U} $	181	192	5.7
4.6	2PG	$ \bar{F} $	191	214	10.7
4.7	1PG	$ \bar{U} $	162	184	12.0
4.7	1PG	U_r	122	113	8.0
4.9	3PG	U_{MP2}	119	113	5.3

Note: δ is relative error, calculated by $\left| \frac{Exper. - Simul.}{Exper.} \right| \times 100$

Large errors ($\delta > 5\%$) occur mostly in two cases. One is the magnitude of the characteristic voltage $|\bar{U}|$ during the single-phase-to-ground fault, and another is the magnitude of the PN factor $|\bar{F}|$ during the double-phase-to-ground fault, which are

both equal to the sum of positive-sequence voltage and negative-sequence voltage ($\bar{U}_1 + \bar{U}_2$, or $\bar{U}_a - \bar{U}_0$). This phenomenon is reasonable and understandable. As in the actual measurement, the zero-sequence impedance of the power line is different from (usually larger than) the positive- and negative-sequence impedance of it. However, in PSCAD/EMTDC simulation, the three sequence impedances of the power line are assumed to be equal, and all represented by a concentrated resistor with an inductor. During the single-phase-to-ground fault and the double-phase-to-ground fault, there are zero-sequence currents flowing in the circuits; whereas during the three-phase-to-ground fault and the double-phase fault, there are not. This is the reason why the large error happens between the simulation and experimental results shown in Table 4.10.

The error would be reduced if the line model with a proper value of zero-sequence impedance is adopted. For the data in Table 4.4 and 4.5, most of the simulation values are equal to zero, because the monitoring point is directly connected to the fault point. However, the experimental results have certain values which are not zero. This is due to the voltage contribution of induction motors during voltage sags, and will be discussed later.

4.1.2 The retained voltage versus the characteristic voltage

The second aspect is about the comparison between the two indices, the retained voltage and the characteristic voltage, in order to characterize the sag magnitude during three-phase events. Both Table 4.8 and 4.9 (recorded by PMU) will not be considered here due to the reason that there are only positive-sequence voltages. According to the data in Table 4.1, 4.2, 4.3, 4.6 and 4.7, for the three-phase-to-ground and double-phase-to-ground faults, the values of the retained voltage U_r and the magnitude of the characteristic voltage $|\bar{U}|$ are very similar, and the relative difference are all within 2%, with an exception in Table 4.7 for the double-phase-to-ground fault, which has a difference of 6.3% for simulation results and 8.7% for experimental results. The three-phase-to-ground fault is a balanced fault, and only positive-sequence parameters exist in the circuit. Therefore, according to the definitions of U_r and $|\bar{U}|$, the results should be identical. Although double-phase-to-ground fault is an unbalanced fault, the two faulted phases have zero or “around-zero” phase-angle jumps. Therefore, the two faulted phase have similar magnitudes with 120 degrees apart. According to the explanation in Appendix B, we know that $|\bar{U}|$ in the double-phase-to-ground fault is equal to the line voltage between the two faulted phases in p.u. value, which is the same as the faulted phase voltage or the retained voltage in p.u. value. Therefore, U_r and $|\bar{U}|$ are identical during double-phase-to-ground fault. However, as mentioned above, an exception happens in Table 4.7. In this case, due to the configuration of the “Fault-line circuit”, there are phase-angle jumps of 9.4 degrees and -7.9 degrees during the double-phase-to-ground fault for faulted phase b and c, respectively. Therefore, $|\bar{U}|$ is no longer equal to, but larger than the faulted phase voltage under the phase-angle jumps.

For the single-phase-to-ground fault, $|\bar{U}|$ is defined as the sum of positive-sequence voltage and negative-sequence voltage ($\bar{U}_1 + \bar{U}_2$, or $\bar{U}_a - \bar{U}_0$). However, U_r is just the magnitude of the fault phase voltage (\bar{U}_a). Therefore, $|\bar{U}|$ is larger than U_r due to the reason that the angle difference between zero-sequence voltage and a-phase voltage is around 180 degrees for single-phase-to-ground fault. For the double-phase fault, although $|\bar{U}|$ is still equal to the line voltage between the two faulted phases in p.u. value, it no longer equals to the faulted phase voltage or the retained voltage in p.u. value, because there are significant phase-angle jumps of the two faulted phases. Under the phase-angle jumps of double-phase fault, $|\bar{U}|$ should be smaller than U_r as shown in Table 4.1, 4.2, 4.3, 4.6 and 4.7.

4.1.3 The effect of induction machine load

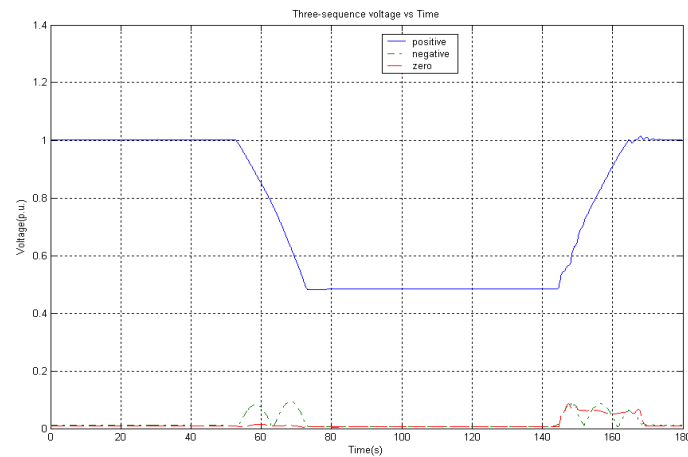
The third aspect is about the effect of the induction machine on voltage magnitude at PCC or monitoring point during and after the faults. For consistency, “Fault-line circuit” will be used as an example here as well. Moreover, “Voltage-divider circuit” and “Fault-load circuit” will give the similar results. The analysis will be performed based on the sequence components of the phase voltages. The concerning point in “Fault-line circuit” is at the monitoring point 2 (MP2), where the induction machine and the two resistive loads are connected. As in the actual measurement, the voltage source is not ideal, which can be considered as an ideal voltage source behind source impedance. As a result, the pre-fault voltage at MP2 will be different for the two different load conditions. Therefore, in order to be comparable, per unit sequence voltages with respect to their pre-fault voltages will be used for both cases.

● Three-phase-to-ground fault

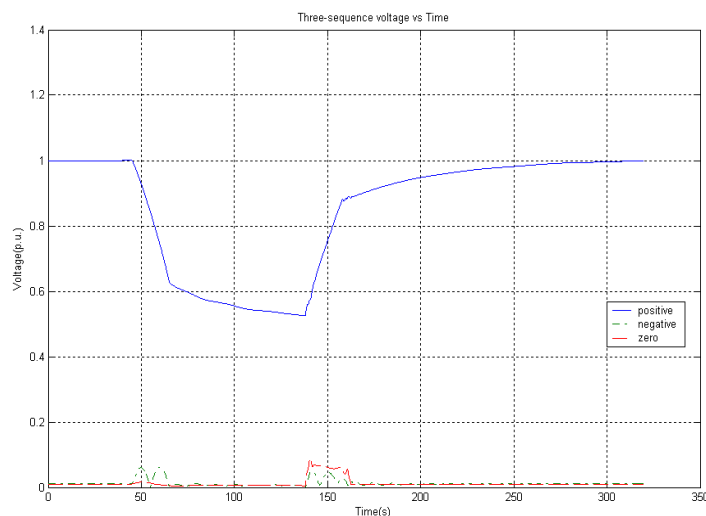
For the balanced faults, there will be no negative- and zero-sequence components in the phase voltages at MP2, which can also be seen in Fig. 4.1. Both the three-sequence voltages under the two resistive loads condition and the two resistive loads with induction motor condition are shown in Fig. 4.1 (a) and (b), respectively. As shown in Fig. 4.1 (a), the positive-sequence voltage decreases to 0.48 and remains almost constant during the fault. Whereas in Fig. 4.1 (b), the positive sequence voltage decreases to 0.63 p.u. when the fault occurs, and decays slowly to 0.52 p.u. when the fault is cleared. Therefore, during the fault, induction machine contributes to the fault and keeps up the positive-sequence voltage at the load point (MP2). This is because when the fault occurs, the voltage at the load point decreases. However, the mutual air-gap flux of the induction machine will not change suddenly due to the hysteresis. As a result, the induction machine works in the generator mode and keeps up certain amount of the positive-sequence voltage at the load point. Although it keeps up certain amount of voltage, the flux decays at a time constant while the mechanical load (torque) remains stably unchanged (here, only shaft inertia and mechanical damping). In order to balance the supply power (torque) and the demand power (torque), the rotor shaft has to sacrifice its kinetic energy and serves as a part of the supply power for a certain short time. Therefore, the rotor slows down and the slip increases. The positive-sequence impedance of the machine will decrease and become

more inductive. As a result, the motor will draw a larger current with a smaller power factor, which brings down the positive-sequence voltage at MP2. The decay of the flux and the slow down of the rotor explain the decay of the voltage under the load condition with induction machine during the fault as shown in Fig. 4.1 (b).

From Fig. 4.1 (a), it is observed that the positive-sequence voltage recovers immediately to 1 p.u. after the fault is cleared. However, in Fig. 4.1 (b), the positive-sequence voltage recovers slowly after the fault is cleared. This is the so-called post-fault voltage sag. The post-fault voltage sag lasts about 8 cycles as shown in Fig. 4.1 (b). As soon as the voltage at the load point recovers, the flux in the mutual air-gap will build up again with a time constant. This is to a certain extent, similar to the starting of an induction machine. Therefore, there will be an inrush current, which slows down the voltage recovery. After that, as the mechanical load will remain unchanged at the moment, in order to balance the supply and the demand power, the rotor will reaccelerate and store part of the supply power as kinetic energy. The inrush current explains the post-fault voltage sag shown in Fig. 4.1 (b).



(a) Two resistive loads



(b) Two resistive loads with induction machine

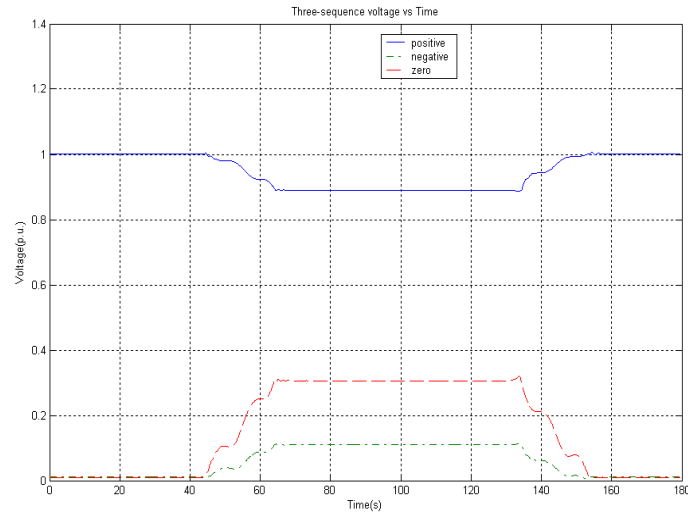
Fig. 4.1 Three-sequence voltages at MP2 (Three-phase-to-ground fault)

● Single-phase-to-ground fault

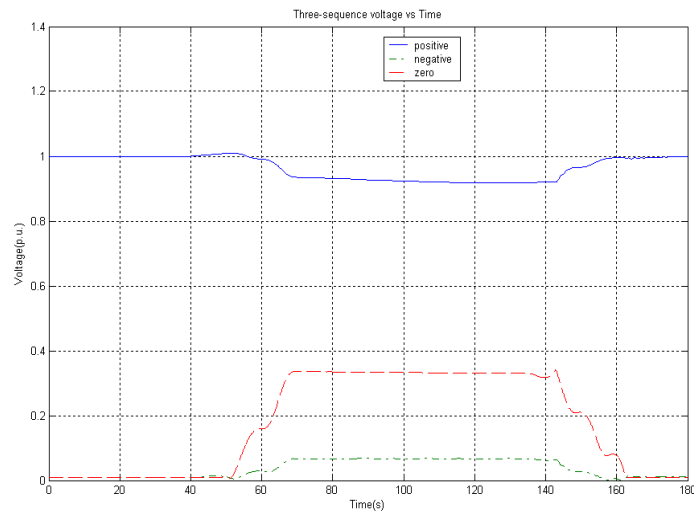
For the single-phase-to-ground fault, the three-sequence voltages at the load point (MP2) of two different load conditions are shown in Fig. 4.2 (a) and (b), respectively. According to Fig. 4.2 (a), the positive-sequence voltage decreases to 0.89 p.u. during the fault, whereas in Fig. 4.2 (b), it decreases to 0.94 p.u. after fault initiation and decays to 0.92 p.u. at the end of the fault. After the fault is cleared, the positive-sequence voltage in Fig. 4.2 (a) recovers immediately, whereas post-fault voltage sag occurs in Fig. 4.2 (b). All the phenomena of the positive-sequence voltage comply with the one described for the three-phase-to-ground fault. The explanation of the phenomena is also similar to the one for three-phase-to-ground fault.

The negative-sequence voltage only exists during the fault and remains constant in both cases shown in Fig. 4.2 (a) and (b). However, the values of the negative-sequence voltage are 0.11 p.u. in Fig. 4.2 (a) and 0.07 p.u. in Fig. 4.2 (b). If the rotor rotates in the same direction as that of the positive-sequence air-gap flux with a slip of s , the slip between the negative-sequence air-gap flux and the rotor will be $(2-s)$. Therefore, the equivalent negative-sequence rotor resistance ($R_r/(2-s)$) is much smaller than the equivalent positive-sequence one (R_r/s), since the slip s is usually much smaller than 1. However, for the resistive loads, the negative-sequence resistance is the same as the positive-sequence resistance. Assume two identical negative-sequence voltage sources supplying an induction machine and resistive loads (provided both the machine and the resistors have the same absolute positive-sequence impedance) through static impedance, respectively. As the negative-sequence impedance of the machine is much smaller than that of the resistive load, the negative-sequence current of the machine will be higher and cause more voltage drop. As a result, the negative-sequence voltage at the load terminal will be lower for the induction machine than for the resistive load. This explains why the negative-sequence voltage value in Fig 4.2 (b) is lower than the one in Fig. 4.2 (a). As the slip s is so small that, the negative-sequence impedance of the motor ($R_r/(2-s)$) can be considered to be independent of the slip, i.e. $R_r/2$. The impact of the deceleration or acceleration of the rotor (small change of s) will be little on the negative-sequence voltage. Therefore, the negative-sequence voltage remains almost constant as well under the load condition of the induction machine.

As the induction machine is not grounded, it takes no zero-sequence currents. In another word, the induction machine has infinite large zero-sequence impedance. Therefore, theoretically, zero-sequence voltages under the two load conditions are the same. The zero-sequence voltages in single-phase-to-ground fault are 0.31 p.u. and 0.33 p.u. in Fig. 4.2 (a) and (b), respectively. The error of 0.02 p.u. is acceptable due to the actual measuring environment.



(a) Two resistive loads

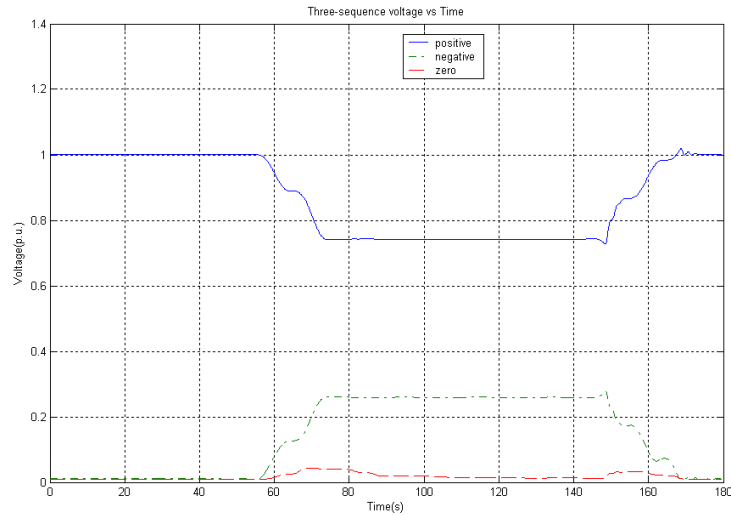


(b) Two resistive loads with induction machine

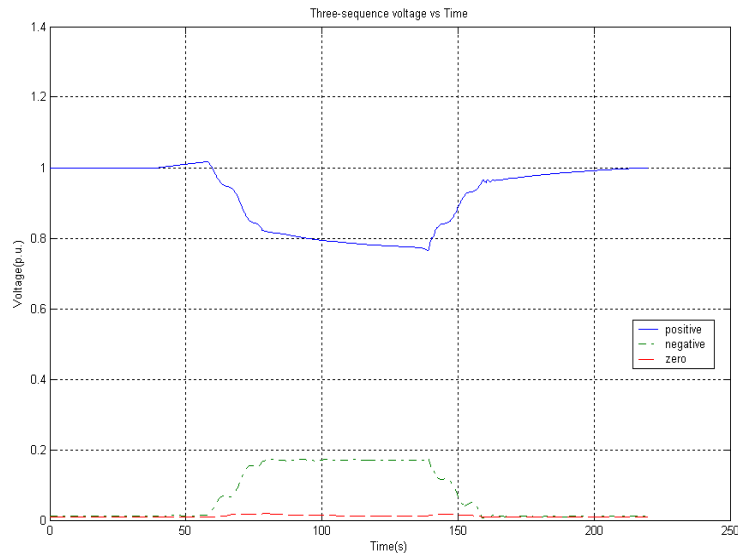
Fig. 4.2 Three-sequence voltages at MP2 (Single-phase-to-ground fault)

● Double-phase fault

The three-sequence voltages of the double-phase fault under the two load conditions are shown in Fig. 4.3 (a) and (b). The positive-sequence voltage decreases to 0.74 p.u. during the fault in Fig. 4.3 (a), whereas it decreases to 0.82 p.u. after fault initiation and decays to 0.77 p.u. at the end of the fault in Fig. 4.3 (b). After the fault is cleared, the positive-sequence voltage in Fig. 4.3 (a) recovers immediately, whereas post-fault voltage sag occurs in Fig. 4.3 (b). The negative-sequence voltage is 0.26 p.u. in Fig. 4.3 (a) and 0.17 p.u. in Fig. 4.3 (b). There is no zero-sequence voltage in double-phase fault. All the phenomena in the double-phase fault are similar to those in the single-phase-to-ground fault and can all be explained by the same reasons.



(a) Two resistive loads

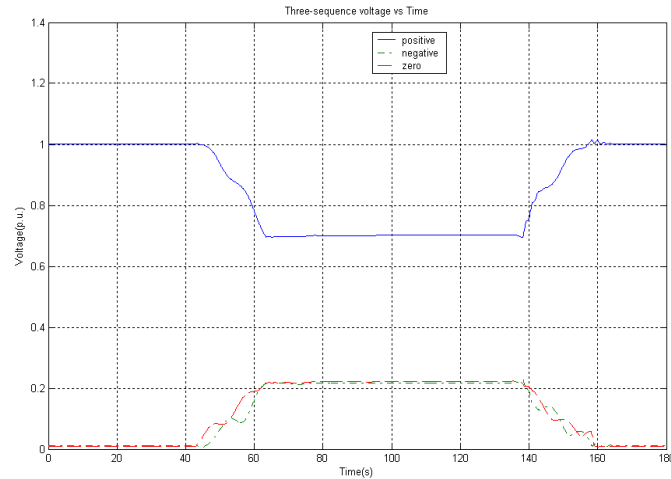


(b) Two resistive loads with induction machine

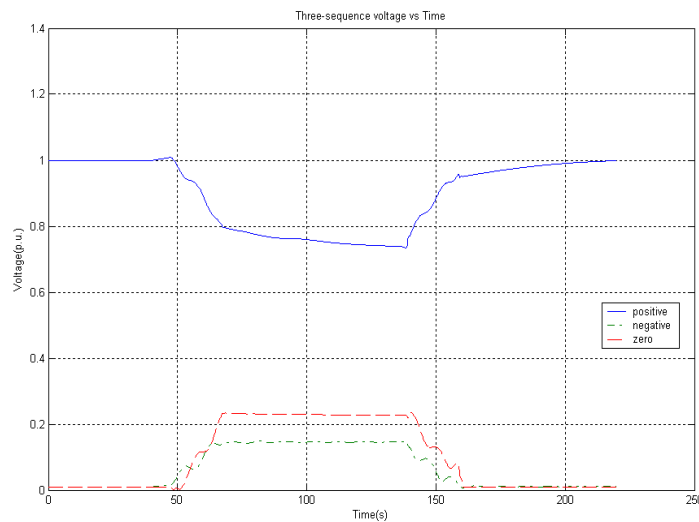
Fig. 4.3 Three-sequence voltages at MP2 (Double-phase fault)

● Double-phase-to-ground fault

The three-sequence voltages of the double-phase-to-ground fault under the two load conditions are shown in Fig. 4.4 (a) and (b). The positive-sequence voltage decreases to 0.70 p.u. during the fault in Fig. 4.4 (a), whereas it decreases to 0.80 p.u. after fault initiation and decays to 0.74 p.u. at the end of the fault in Fig. 4.4 (b). After the fault is cleared, the positive-sequence voltage in Fig. 4.4 (a) recovers immediately, whereas the post-fault voltage sag occurs in Fig. 4.4 (b). The negative-sequence voltage is 0.22 p.u. in Fig. 4.4 (a) and 0.15 p.u. in Fig. 4.4 (b). The zero-sequence voltage is 0.22 p.u. in Fig. 4.4 (a) and 0.23 p.u. in Fig. 4.4 (b). The error of 0.01 is acceptable due to the actual measuring environment. All the phenomena in the double-phase-to-ground fault are similar to those in the single-phase-to-ground fault and can all be explained by the same reasons.



(a) Two resistive loads



(b) Two resistive loads with induction machine

Fig. 4.4 Three-sequence components at MP2 (Double-phase-to-ground fault)

Without showing more figures, three-sequence voltage values at the sag starting and ending instants in both simulation and experimental results will be summarized in Table 4.11, 4.12 and 4.13 for 'Voltage-divider circuit', 'Fault-load circuit' and 'Fault-line' circuit, respectively. The values are all shown in per unit with respect to the pre-fault voltage at PCC or monitoring point.

Table 4.11 Sequence voltages at sag starting and ending instants from “Voltage-divider circuit”

	Load	Positive		Negative		Zero	
		NO	IM	NO	IM	NO	IM
3PG	Simul.	0.67	0.74->0.70	0	0	0	0
	Exper.	0.67	0.75->0.72	0	0.01	0	0.01
1PG	Simul.	0.89	0.92->0.90	0.11	0.08	0.11	0.12
	Exper.	0.93	0.96->0.95	0.07	0.05	0.19	0.20
2P	Simul.	0.83	0.87->0.85	0.17	0.13	0	0
	Exper.	0.83	0.89->0.87	0.17	0.13	0.01	0.01
2PG	Simul.	0.78	0.83->0.80	0.11	0.09	0.11	0.11
	Exper.	0.81	0.87->0.85	0.14	0.11	0.14	0.14

Note: NO: No load condition, Positive: Positive-sequence voltages at PCC or monitoring point during sags, IM: Induction machine loaded, A->B: sequence voltages at sag starting-> sequence voltages at sag ending, A: One value means A and B are the same

As shown in Table 4.11, for both the experimental and simulation results, it is observed that the induction machine keeps up the positive-sequence voltages and damps the negative-sequence voltages during the faults, that the zero-sequence voltages are the same under the two load conditions. Although not shown in figures, there are post-fault sags in both the simulation and experiment results under the load condition of induction machine. Taking into account of the assumptions in the simulation, i.e. ideal three-phase voltage source and three-sequence transmission line impedance identical, the results obtained from the simulation and the experiment can be considered coherent. The model of the induction machine in PSCAD/EMTDC is good enough to simulate its behavior during voltage sags on the ‘Voltage-divider circuit’.

Table 4.12 Sequence voltages at sag starting and ending instants from “Fault-load circuit”

	Load	Positive		Negative		Zero	
		2R	2R_IM	2R	2R_IM	2R	2R_IM
3PG	Simul.	0	0	0	0	0	0
	Exper.	0.01	0.54->0.23	0	0	0	0
1PG	Simul.	0.67	0.70->0.65	0.33	0.27	0.33	0.39
	Exper.	0.79	0.93->0.88	0.21	0.07	0.60	0.76
2P	Simul.	0.50	0.49->0.40	0.50	<u>0.49->0.40</u>	0	0
	Exper.	0.50	0.78->0.61	0.50	0.20	0.02	0.02
2PG	Simul.	0.33	0.36->0.29	0.33	<u>0.36->0.29</u>	0.33	<u>0.36->0.29</u>
	Exper.	0.42	0.73->0.54	0.42	0.17	0.44	0.47

Note: 2R: Two resistive loads, 2R_IM: Two resistive loads with Induction machine loaded.

From the experimental results of the “Fault-load circuit” shown in Table 4.12, it is clearly observed that the induction machine keeps up the positive-sequence voltage

significantly even during a three-phase-to-ground fault at the load terminal (boldfaced data); the negative-sequence voltage is damped very much under the induction machine load condition; the zero-sequence voltages are almost the same under two load conditions, except the one at single-phase-to-ground fault, which has a large difference of 16% (bold-italic data). More experiments need to be done to further verify and confirm this large difference in the zero-sequence voltage, as theoretically induction machine should not influence the zero-sequence component.

From the simulation results, we could also see that the positive-sequence voltages decay and the negative-sequence voltages damp during the faults, that the zero-sequence voltages are almost the same under the two load conditions. However, the induction machine keeps up the positive-sequence voltages. In some cases (underlined data), the negative-sequence voltages and zero-sequence voltage vary during the faults. These results show the variance between the simulation and the actual experiment in the induction machine behavior when the faults occur at the induction machine terminal. This variance may happen due to two reasons. One is that there is fault impedance between the induction machine terminal and the common ground in the actual experiment. The other one is the model of the induction machine in PSCAD/EMTDC, which still needs improving. More parameters, such as the sub-transient and transient impedance, need to be specified in order to simulate the dynamic behavior of the induction machine more accurately during the faults at its terminal.

Table 4.13 Sequence voltages at sag starting and ending instants from “Fault-line circuit”

	<i>Load</i>	Positive		Negative		Zero	
		<i>2R</i>	<i>2R_IM</i>	<i>2R</i>	<i>2R_IM</i>	<i>2R</i>	<i>2R_IM</i>
3PG	Simul.	0.50	0.61->0.54	0	0	0	0
	Experi.	0.48	0.63->0.52	0	0	0	0
1PG	Simul.	0.83	0.88->0.85	0.17	0.12	0.17	0.18
	Experi.	0.89	0.94->0.92	0.11	0.07	0.31	0.33
2P	Simul.	0.75	0.81->0.76	0.25	0.18	0	0
	Experi.	0.74	0.82->0.77	0.26	0.17	0	0
2PG	Simul.	0.67	0.75->0.69	0.17	0.12	0.17	0.17
	Experi.	0.70	0.80->0.74	0.22	0.15	0.22	0.23

The simulation results show a similar performance of positive-, negative- and zero-sequence voltages during voltage sags as expected. The simulation results are coherent with the experimental results quite well at three-phase-to-ground and double-phase fault, which indicate a good modeling of the induction machine in PSCAD/EMTDC. The relative large errors occur at single-phase-to-ground and double-phase-to-ground fault may attribute to the assumption that the three-sequence transmission line impedances are identical in PSCAD/EMTDC.

4.1.4 PMU versus PQ monitor

The last aspect is to compare the different results of the voltage magnitude recorded by PMU and PQ monitor. The comparison here is different from the one in section 4.1.1. In this section, we are going to compare two different monitoring equipments, which monitor at the same bus at the same time in the same circuit; whereas in section 4.1.1, we compared the results by different modeling strategies. The analysis will be focused on MP2 with the “Fault-line circuit” only. In order to compare with the PMU measurements, the positive-sequence voltages obtained from the PQ monitor measurements are shown in Fig. 4.5 - 4.12.

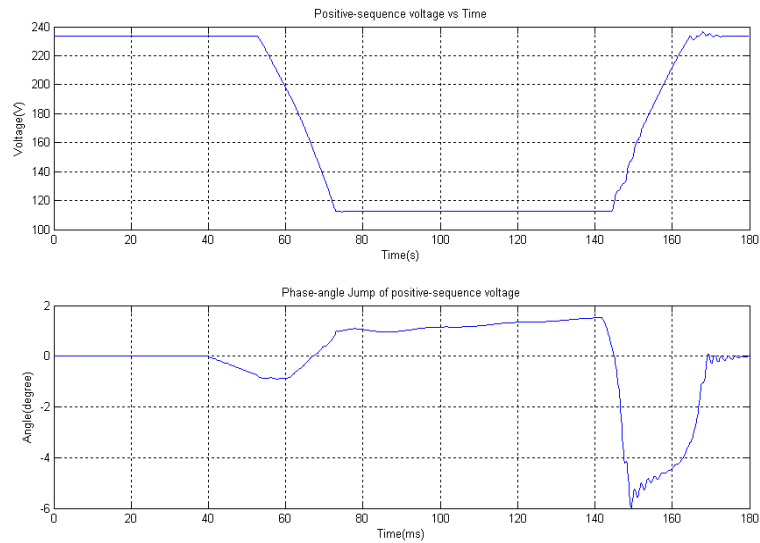


Fig. 4.5 Positive-sequence voltage for 3PG fault (PQ monitor, resistive loads)

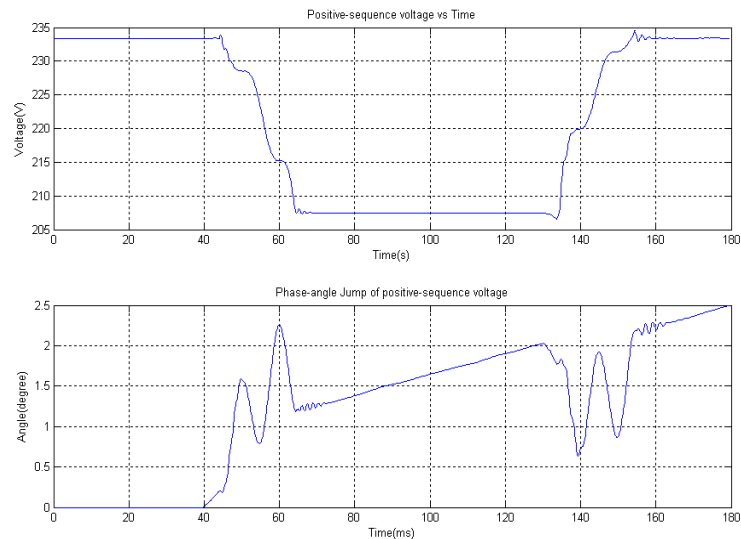


Fig. 4.6 Positive-sequence voltage for 1PG fault (PQ monitor, resistive loads)

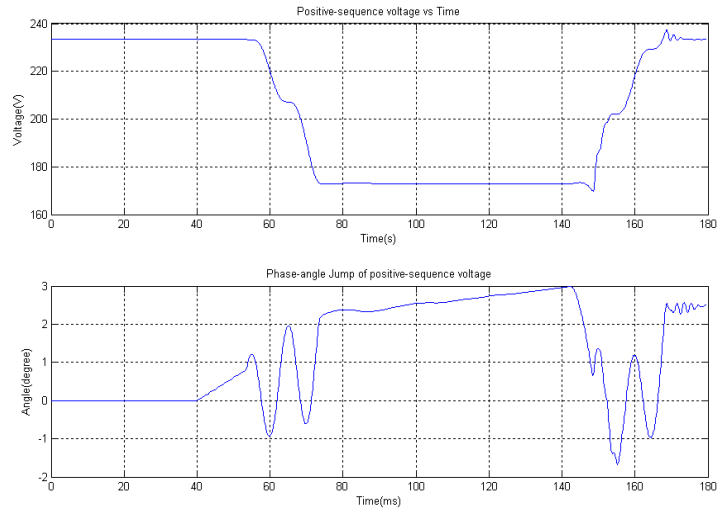


Fig. 4.7 Positive-sequence voltage for 2P fault (PQ monitor, resistive loads)

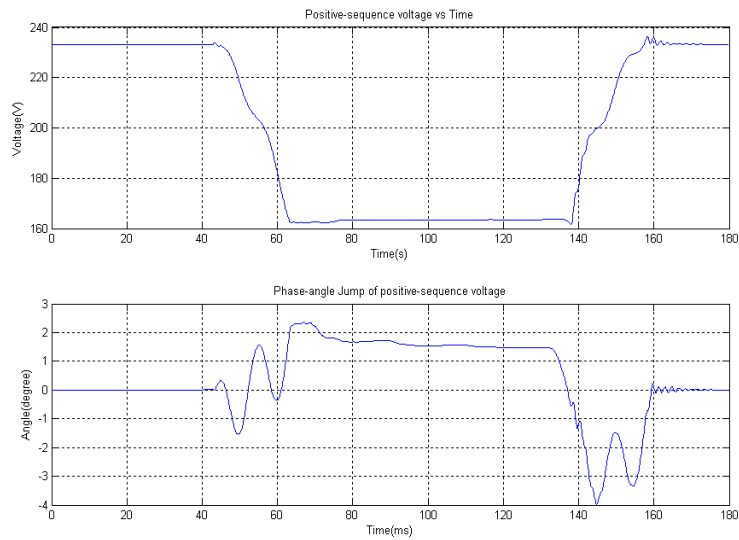


Fig. 4.8 Positive-sequence voltage for 2PG fault (PQ monitor, resistive loads)

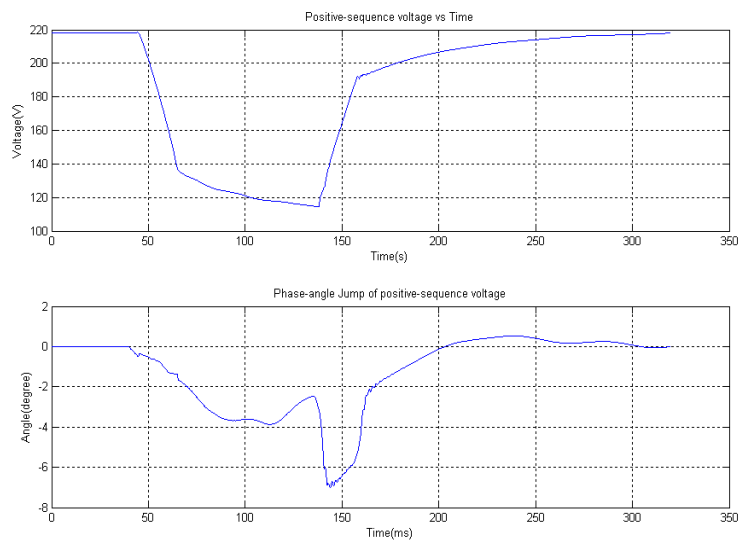


Fig. 4.9 Positive-sequence voltage for 3PG fault (PQ monitor, resistive loads & IM)

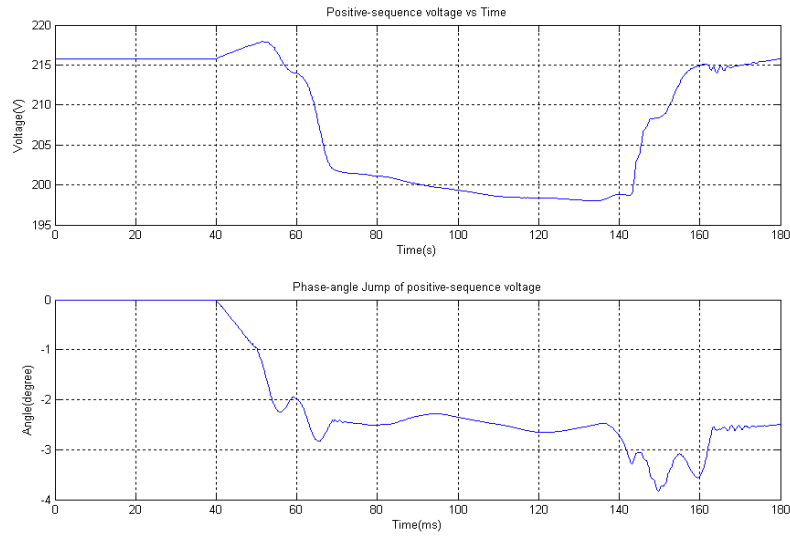


Fig. 4.10 Positive-sequence voltage for 1PG fault (PQ monitor, resistive loads & IM)

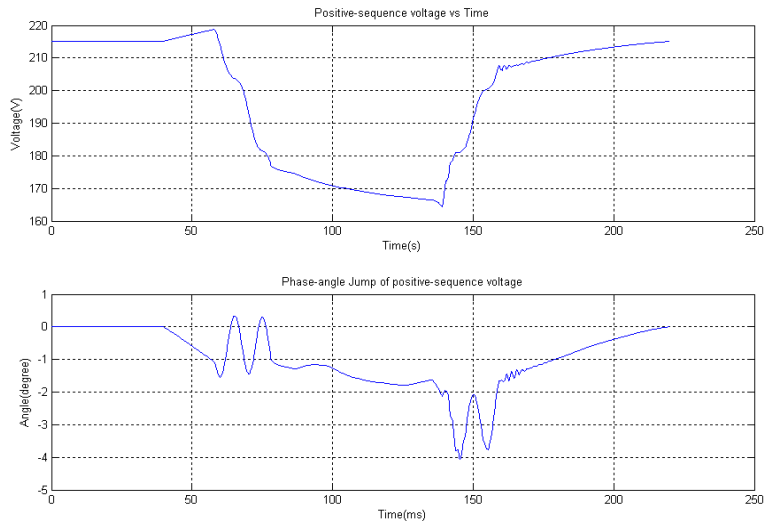


Fig. 4.11 Positive-sequence voltage for 2P fault (PQ monitor, resistive loads & IM)

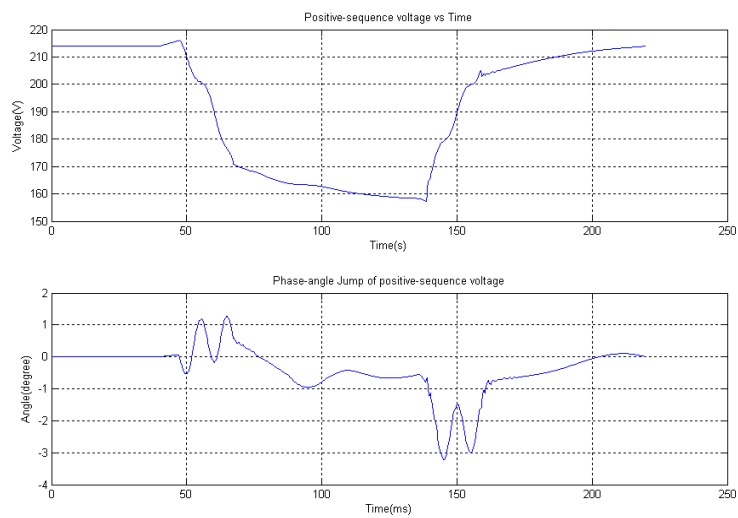


Fig. 4.12 Positive-sequence voltage for 2PG fault (PQ monitor, resistive loads & IM)

As PMU records phasor at the frequency of once per cycle, the data obtained by PMU may not be adequate to use in power quality monitoring compared with PQ monitor, which has a sampling frequency of 7.2 kHz (144 samples per cycle) or even more. In order to investigate the feasibility of PMU used as power quality monitoring equipment, the results from PMU and PQ monitor need to be compared.

According to the PMU results shown in section C.3 in the Appendix C and the PQ monitor results from Fig. 4.5 to 4.12, the magnitude of positive-sequence voltages at MP2 in the “Fault-line circuit” are summarized in Table 4.14. From the results of magnitude in Table 4.14, we can see that the positive-sequence voltages obtained by PMU comply with the ones obtained by PQ monitor, and the relative errors are all within 5%. Therefore, PMU gives relatively accurate results in the information of “the minimum positive-sequence voltage magnitude” for the characterization of sag events if an error of 5% in the positive-sequence voltage is accepted.

Table 4.14 Positive-sequence voltages at MP2 recorded by PMU and PQ monitor (Experiment)

	<i>Load</i>	Magnitude (V)		Phase angle (deg)	
		<i>2R</i>	<i>2R_IM</i>	<i>2R</i>	<i>2R_IM</i>
3PG	PMU	110	113	4.4	1.8
	PQM	113	114	1.5	-3.9
1PG	PMU	197	190	2.8	-0.3
	PQM	207	198	2.0	-2.7
2P	PMU	169	164	2.7	-1.4
	PQM	173	164	3.0	-1.8
2PG	PMU	160	156	1.7	-1.9
	PQM	163	157	1.7	-1.0

4.2 Phase-angle jump

4.2.1 Modeling and algorithm

This section is to compare theoretical, simulation, and experimental results in terms of phase-angle jump. The maximum phase-angle jump is determined by its maximum angle variation. The three values of the maximum phase-angle jump under the same event may not be obtained from the same phase. Therefore, the errors among theoretical, simulation, and experimental results will be calculated using absolute value of the maximum phase-angle jump.

According to the results shown in Table 4.1, 4.2, 4.3, 4.6, 4.7, 4.8, and 4.9, the errors of the maximum phase-angle jump of phase voltages between theoretical and simulation values are all within 5 degrees. However, the errors between simulation

and experimental values have some exceptions, which are listed in Table 4.15. From Table 4.15, we could see that the large errors happen exclusively at single-phase-to-ground faults. The explanation is the same as in section 4.1.1. In simulation, the zero-sequence impedance and positive-sequence impedance of the transmission line are identical. The errors can be reduced if the transmission line model with a proper value of the zero-sequence impedance is used. The errors of the maximum phase-angle jump of the characteristic voltages are all within 5 degrees between the theoretical and simulation values, as well as between the simulation and experimental values. The data of phase-angle jump in Table 4.4 and 4.5 will not be analyzed, as for some cases, they are not applicable.

Table 4.15 Error between simulation and experimental results
(in phase-angle jump) $\sigma > 5$ degree

Table	Fault type	Simulation (deg)	Experimental (deg)	σ (deg)
4.1	1PG	0	-9.6	9.6
4.2	1PG	0	7.8	7.8
4.3	1PG	-2.1	-7.4	5.3
4.6	1PG	0.3	11	10.7
4.7	1PG	-3.9	-13.8	9.9

Note: $\sigma = ||Exper.|-|Simul.||$

4.2.2 Phase voltage versus the characteristic voltage

This section is going to analyze the difference between phase-angle jumps obtained from phase voltage and characteristic voltage. As shown in Table 4.1, 4.2, 4.3, 4.6 and 4.7, for three-phase-to-ground fault, the phase-angle jumps obtained from phase voltage and characteristic voltage are in accordance with each other. Because for the balanced fault there are only positive-sequence voltages in the system, thus, the characteristic voltage is the symmetrical phase voltage (phase a in this thesis).

For the unbalanced faults, however, the accordance will not always hold. For the single-phase-to-ground fault and the double-phase-to-ground fault under the condition of two resistive loads, as shown in Table 4.1, 4.2, 4.6, the phase-angle jumps obtained from phase voltage and characteristic voltage are still in accordance with each other in both theoretical and simulation results. However, they differ from each other in the experimental results and under the load condition with induction machine.

As explained in the Appendix B, according to the equation B.4 and B.5, the phase angle of the characteristic voltage will be equal to that of the symmetrical phase if the two healthy phases in the single-phase-to-ground fault (or the two faulted phases in both double-phase and double-phase-to-ground fault) are symmetrical with respect to the axis where the third phase (the symmetrical phase) lies on. Therefore, the phase-angle jump of the characteristic voltage should be equal to the phase-angle

jump of the symmetrical phase. During the single-phase-to-ground fault and double-phase-to-ground fault, the three phase voltages remain 120 degrees apart from each other. Therefore, the maximum phase-angle jump of the phase voltages is the phase-angle jump of the symmetrical phase. Consequently, the phase-angle jump of the characteristic voltage equals the maximum phase-angle jump of the phase voltages under the resistive load conditions, both in the theoretical and simulation results.

The difference occurs in the experimental results, because the phase-angle jump of the characteristic voltage deviates from the phase-angle jump of the symmetrical phase, due to the realistic asymmetry of the two healthy phases in the single-phase-to-ground fault (or two faulted phase in double-phase-to-ground fault). The difference that occurs under the load condition of induction machine has the same justification.

However, the maximum phase-angle jump of the phase voltages will not be necessarily the phase-angle jump of the symmetrical phase, in the double-phase fault. In this case, the maximum phase-angle jump of the phase voltages will be at one of the faulted phases. As the phase-angle jump of the characteristic voltage is normally equal to the phase-angle jump of the symmetrical phase, which is the non-faulted phase and usually much smaller than the phase-angle jump of the faulted phase during double-phase fault, there is a large difference between the two definitions of phase-angle jump.

4.2.3 The effect of induction machine load

This section is going to investigate the effect of the induction machine load on the phase-angle jump at MP1, MP2, and especially the jump of phase angle difference (transmission angle) between MP1 and MP2 due to voltage sags in the “Fault-line circuit”. The interests on the jump of transmission angle rely on its direct relation with active power flow. As power flow calculation is performed with the positive-sequence components in the circuit, the discussion in this section will be carried out based on the results from PMU in Table 4.8 and 4.9.

As shown in Table 4.8, the phase-angle jumps at MP2 are all positive, which indicate the increase of phase angle under the condition of the two resistive loads; whereas they are all negative in Table 4.9, except the one from experimental results at 3PG, which indicate the decrease of phase angle under the load condition with induction machine. Therefore, the induction machine causes a phase-angle jump of the positive-sequence voltage at MP2. Actually the exceptional case in Table 4.9 of positive value at MP2 for 3PG fault can be understood as the phase angle at MP1 increases even more. The measured phase-angle jump at MP1 is due to the source impedance, which was neglected during the theoretical calculations and simulations. Therefore, it will be more suitable if we look at the jumps of transmission angle instead, in order to study the effect of induction machine on phase-angle jump.

As we know, the active power flow through the transmission line is proportional to

the sine value of the transmission angle, the change of it during a voltage sag will be of great concern. During the simulation and the experiment, the change (or jump) of the transmission angle $\Delta\phi_{MP21}$ in the “Fault-line circuit” under the two load conditions are shown in Table 4.8 and 4.9 (boldfaced data). If we assume that the voltage magnitudes at MP1 and MP2 remain the same during faults as the ones before faults (although not the case in the “Fault-line circuit” here), positive value of $\Delta\phi_{MP21}$ corresponds to the decrease of active power flow from MP1 to MP2; whereas negative value corresponds to the increase of active power flow from MP1 to MP2. As a matter of fact, the jumps of transmission angle are all negative in Table 4.9 with induction machine loaded, but all positive in Table 4.8 with an exceptional case of the experimental result for 2P fault. Therefore, neglecting the exception, the results indicate that the effect of the induction machine on the jump of transmission angle tends to increase the active power flow from the source side to the load side. The induction machine behaves “active” during the voltage sags compared with the resistive loads.

4.2.4 PMU versus PQ monitor

The last aspect is to investigate the difference of phase-angle jumps recorded by PMU and PQ monitor. As shown in Table 4.14, the largest difference between PMU (1.8 degree) and PQ monitor (-3.9 degree) is 5.7 degree. The smallest difference between PMU (1.7 degree) and PQ monitor (1.7 degree) is 0. The time resolution of PMU is so low that the maximum value can happen in between two measured lower values. The low frequency of PMU limits its application in power quality monitoring and voltage sag characterization. However, if the time resolution of PMU can be increased, it is considered to be a good alternative of PQ monitor in power quality monitoring.

4.3 Voltage sag type

The voltage sag type in this thesis is mainly determined by the ABC classification method and the symmetrical component algorithm. As shown in the tables of Chapter 4 and Appendix C, the sag type based on ABC classification is determined by three phase voltage phasors. Although the three phasors do not comply exactly with the phasors shown in Table 2.2, it is possible to identify the actual phasor diagrams and classify them into right sag types, as shown in Table 4.1 - 4.9. The ABC classification method, although very intuitive, can not be easily implemented in the way of computational algorithm.

The alternative is the symmetrical component algorithm. The calculated T index, shown in Appendix C, gives accurate results of sag type according to Table 2.3, but an exception. The exception happens at MP2 for the “Fault-line circuit” during the single-phase-to-ground fault under the condition of two resistive loads with the induction machine. As discussed in section 4.2.3, the induction machine will cause a phase-angle jump on the positive-sequence voltage at MP2. Moreover, the induction machine will also cause a shift of phase angle of the negative-sequence voltage

compared with the results under the two resistive loads condition (Bollen, 2003 a). Therefore, the symmetrical component algorithm may give an erroneous result of the sag type if the load causes an additional phase-angle jump.

5 Conclusions

5.1 Summary

Voltage sag (dip) is one of the most severe power quality issues. In the beginning of the thesis, the definitions of voltage sag (dip) from IEEE and IEC standards were introduced. Both standards agree that voltage sag (dip) is a decrease in voltage below a certain threshold and refers to the residual voltage, not the drop of the voltage. After that, the characterization of voltage sags was presented based on the work done by previous researchers. For the single-phase event, a characterization based on the retained voltage, duration and phase-angle jump was presented. For the three-phase event, both balanced and unbalanced, a similar characterization was presented. However, the magnitude (phase-angle jump) index was extended to the minimum retained voltage (maximum phase-angle jump) of the three voltage phasors as well as the magnitude (phase-angle jump) of the characteristic voltage. Subsequently, the ABC classification method and the symmetrical component method were presented for the further classification of the voltage sag types for the three-phase events.

The methods for the characterization of voltage sags were applied to the four generic circuits, which were implemented in the analog network lab. For comparison, the same circuits were simulated using PSCAD/EMTDC. The simulation required the modeling of a three-phase voltage source, transmission lines, two resistive loads, and an induction machine. At the same time, the analytical estimation was performed as well to predict the results from simulation and experiment. Finally, an analysis based on the indices of magnitude, phase-angle jump, and voltage sag type was carried out in detail. The voltage sag magnitude and phase-angle jump were analyzed under four perspectives. Firstly, a comparison among analytical, simulation and experimental results was executed to study the accuracy of the simulation modeling. Secondly, a comparison between voltage phasors and characteristic voltage was performed to determine the difference between the two methods of characterization. Thirdly, the investigation of the load effect of induction machine during voltage sags were carried out. Finally, the comparison of the voltage results from PMU and PQ monitor were studied to demonstrate the possibility of PMU used as a power quality monitoring equipment.

5.2 Conclusions

The comparisons performed in section 4.1.1 and 4.2.1, between theoretical, simulation and experimental results have shown that the transmission line model and the induction machine model constructed in PSCAD/EMTDC are suitable to simulate voltage sags within an acceptable accuracy. The accuracy can be increased if the transmission line model is implemented with an accurate value of the zero-sequence impedance.

From the analysis in section 4.1.2, it can be concluded that the minimum retained voltage and the magnitude of the characteristic voltage are identical for sag type A and E. However, they greatly differ for the sag type B and C. For the sag type A, the two definitions are in fact the same. For the sag type E, the identity is due to the reason that, in p.u. value, the magnitude of the characteristic voltage is equal to the line voltage of the two-faulted phase, which is also equal to the single-faulted phase voltage or the minimum retained voltage. For the sag type B, the magnitude of the characteristic voltage is the retained voltage minus corresponding zero-sequence voltage. For the sag type C, the difference occurs due to the phase-angle jump of the two faulted phases.

The analysis of phase-angle jump in section 4.2.2 has shown that for the ideal sag type A, B, C and E, the phase-angle jump of the characteristic voltage is equal to that of the symmetrical phase voltage. For the ideal sag type A, B and E, or a symmetrical rotation of the three phasors, the maximum phase-angle jump of the three phasors is equal to the phase-angle jump of the symmetrical phase voltage, which is the same as the phase-angle jump of the characteristic voltage. For the sag type C, the maximum phase-angle jump usually occurs at the two faulted phases and normally it is larger than the phase-angle jump of the characteristic voltage. If any asymmetry with respect to the symmetrical phase axis happens to the two faulted phases or the two healthy phases of the sag type A, B and E, the phase-angle jumps of the characteristic voltage and the symmetrical phase voltage will greatly differ.

From the analysis in section 4.1.3, it can be concluded that the induction machine keeps up the positive-sequence voltages and damps the negative-sequence voltages at PCC or the monitoring point during the faults. The positive-sequence voltages decay during the voltage sags, whereas the negative-sequence voltages remain constant. However, the induction machine will not affect the zero-sequence voltage at PCC or the monitoring point. The induction machine slows down the recovery of the voltages (i.e. faulted-phase voltages, the positive-sequence voltages) when the fault is cleared. This is the so-called “post-fault sags”. The model of the induction machine in PSCAD/EMTDC is further demonstrated to be good enough to simulate its behavior during voltage sags. However, the model needs improving when the faults happen directly at the terminal of the induction machine.

The analysis in section 4.2.3 has shown the effect of the induction machine on the phase-angle in two aspects. Firstly, the induction machine causes an additional phase-angle jump at the load terminal during voltage sags compared with the static resistive loads. Secondly, the effect of the induction machine in comparison to the static loads on the jump of transmission angle during voltage sags indicates an increase of the active power flow from the source side to the load side.

The analysis of PMU and PQ monitor in terms of the magnitude of the positive-sequence voltage has shown that, they are in accordance with each other, and

the relative errors are within 5%. PMU gives relatively accurate results in the information of “the minimum positive-sequence voltage magnitude” for the characterization of sag events. From the analysis in section 4.2.4, however, there is a difference of the phase-angle jump measured by PMU and PQ monitor, as the time resolution of PMU is relatively low. This drawback of PMU will limit its application in power quality monitoring and voltage sag characterization.

The ABC classification method is very intuitive, and is difficult to implement as a computational algorithm. The phasor diagrams shown in the tables in chapter 4 are quite distorted compared with the ideal phasor diagrams shown in Table 2.2. The symmetrical component algorithm, however, gives very accurate results of sag types in almost all the cases. The exception is due to the effect of the induction machine on the voltage. This kind of loads affects the phase-angle jump provoking errors in the implementation of the symmetrical component algorithm. The algorithm can be improved according to Bollen (2003,a). However, the effect of the induction machine on phase-angle jump of the PN factor needs to be known in advance.

References

- [1] Bollen, M.H.J. (2000 a). *Understanding Power Quality Problems: Voltage Sags and Interruptions*. IEEE Press series on power engineering, New York, 2000.
- [2] Bollen, M.H.J.; Styvaktakis, E. (2000 b). Characterization of Three-phase Unbalanced Dips (as easy as one-two-three?). *IEEE Power Eng. Soc. Summer Meeting*, Vol. 2, Seattle, WA, USA, July 16-20, 2000, pp.899-90C.
- [3] Bollen, M.H.J. (2003 a). Algorithms for Characterizing Measured Three-phase Unbalanced Voltage Dips. *IEEE Transactions on Power Delivery*, Vol. 18, No. 3, July 2003.
- [4] Bollen, M.H.J.; Zhang L. D. (2003 b). Different Methods for Classification of Three-phase Unbalanced Voltage Dips due to Faults. *Electric Power Systems Research* 66 (2003) 59-69.
- [5] Grainger, John J.; Stevenson, William D. (1994). *Power System Analysis*. McGraw-Hill, ISBN 0-07-061293-5. New York, 199C.
- [6] IEC 61000-2-8 (2002). *Electromagnetic Compatibility (EMC). Part 2-8: Environment-Voltage Dips and Short Interruptions on Public Electric Power Supply Systems with Statistical Measurement Results* [draft, 22-02-2002]. International Electrotechnical Commission.
- [7] IEC 61000-4-30 (2001). *Electromagnetic Compatibility (EMC). Part 4-30: Testing and Measurement Techniques-Power Quality Measurement Methods*
- [8] IEEE Std 1100 (1999). *Recommended Practice for Powering and Grounding Electronic Equipment*. [Revision of IEEE Std 1100-1992].
- [9] IEEE Std 1346 (1998). *IEEE Recommended Practice for Evaluating Electric Power System Compatibility with Electronic Process Equipment*.
- [10] IEEE Std P1564 (2004). Draft 6, *Recommended Practice for the Establishment of Voltage Sag Indices*.
- [11] LaCommare, K. H.; Eto, J. H. (2004). *Understanding the Cost of Power Interruptions to U.S. Electricity Consumers*. Energy Analysis Department, Ernest Orlando Lawrence Berkeley National Laboratory, University of California Berkeley. Berkeley, California, U.S..
- [12] Macken, K.J.P; Bollen, M.H.J.; Belmans, R.J.M. (2004). Mitigation of Voltage Dips Through Distributed Generation Systems. *IEEE Transaction on Industry Applications*, Vol. 40, No. 6, November/December, 2004.
- [13] Olguin, G. (2005). *Voltage Dip (Sag) Estimation in Power Systems based on Stochastic Assessment and Optimal Monitoring*. Doctor of Philosophy dissertation. Department of Energy and Environment, Division of Electric Power Engineering, Chalmers University of Technology, Gothenburg, Sweden.
- [14] Sannino, A.; Bollen, M.H.J.; Svensson, J. (2005). Voltage Tolerance Testing of Three-phase Voltage Source Converters. *IEEE Transaction on Power Delivery*, Vol. 20, No. 2, April 2005.
- [15] Zhang, L.D. (1999). *Three-Phase Unbalance of Voltage Dips*. Licentiate, Chalmers University of Technology, Gothenburg, Sweden, 1999.

Appendix A: Simulation configurations in PSCAD**Appendix B: The characteristic voltage and PN Factor****Appendix C: Results summarized in the Chapter 4*****C.1 Analytical estimation of voltage sags******C.2 Simulations using PSCAD******C.3 Measurements on the analog network model***

Appendix A: Simulation configurations in PSCAD

The simulation configurations modeled using PSCAD are shown in the following figures from Fig. A.1 to Fig. A.9.

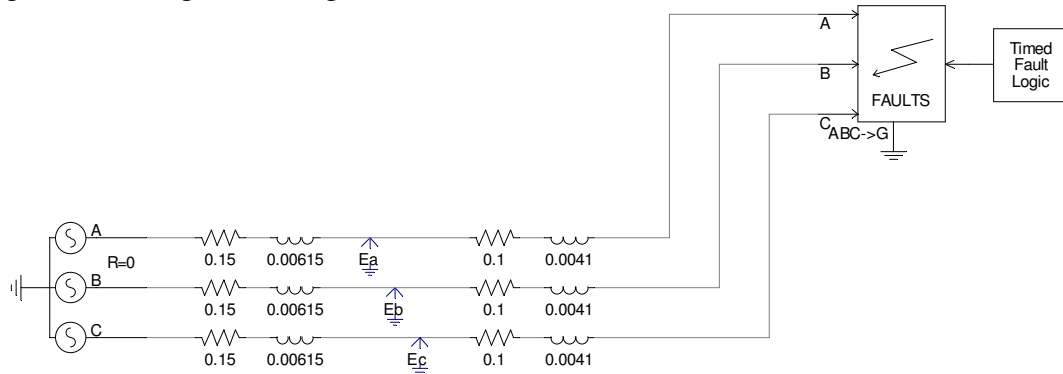


Fig. A.1 Basic circuit in PSCAD

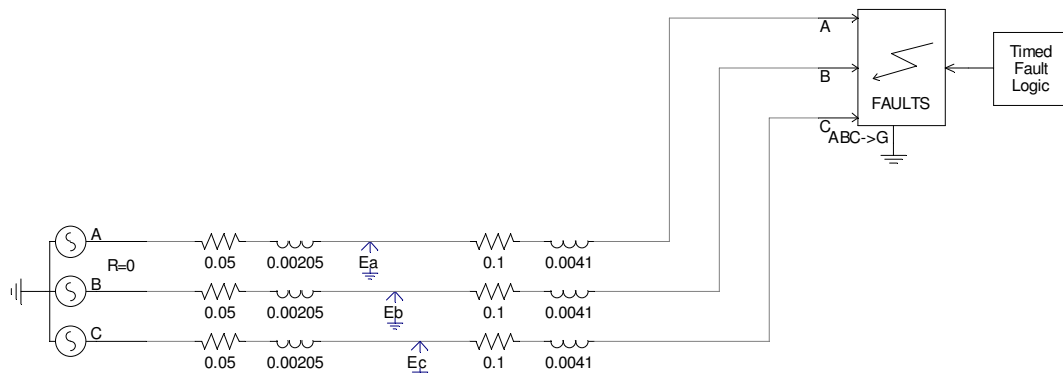


Fig. A.2 Voltage-divider circuit with no load in PSCAD

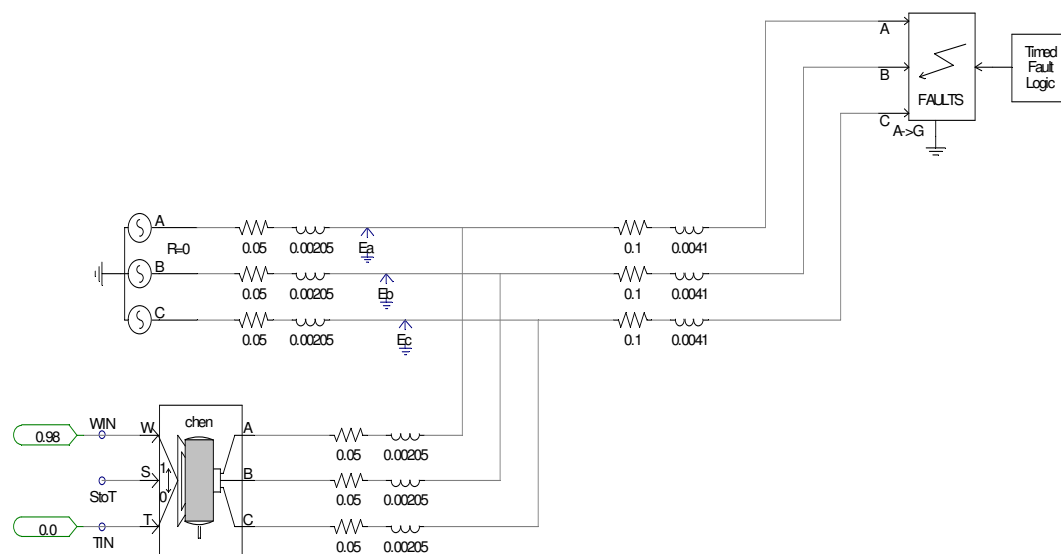


Fig. A.3 Voltage-divider circuit with Induction Machine in PSCAD

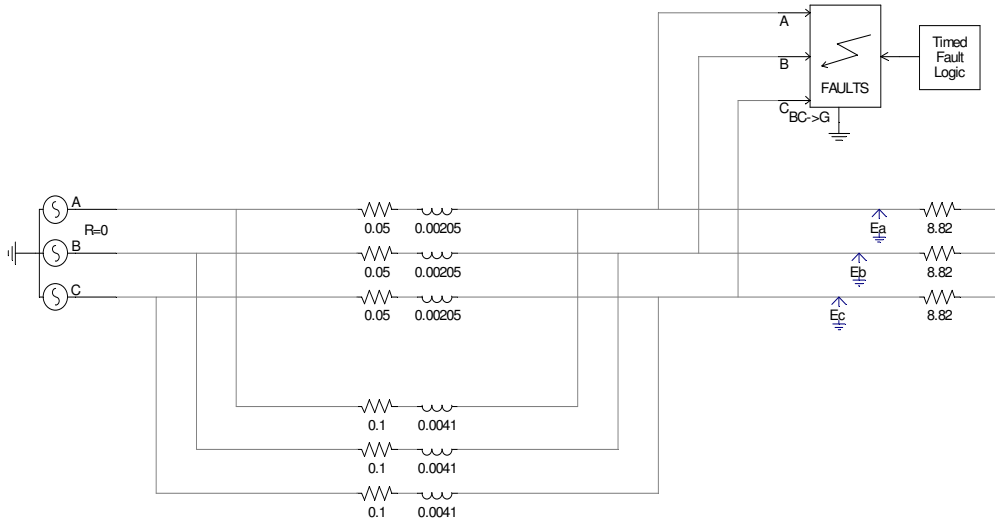


Fig. A.4 Fault-load circuit with Two Resistive loads in PSCAD

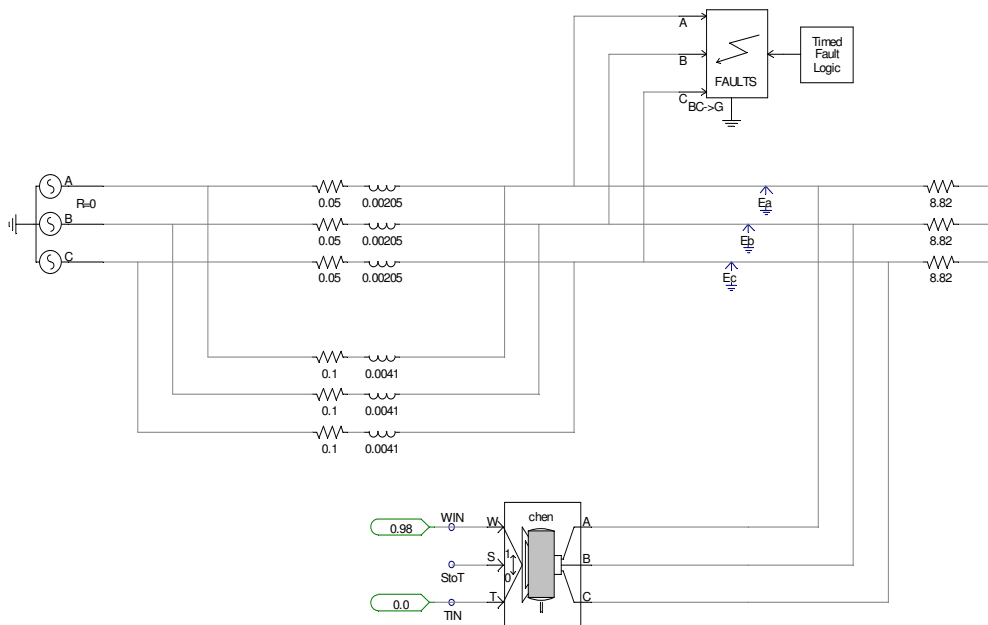


Fig. A.5 Fault-load circuit with Two Resistive loads and Induction Machine in PSCAD

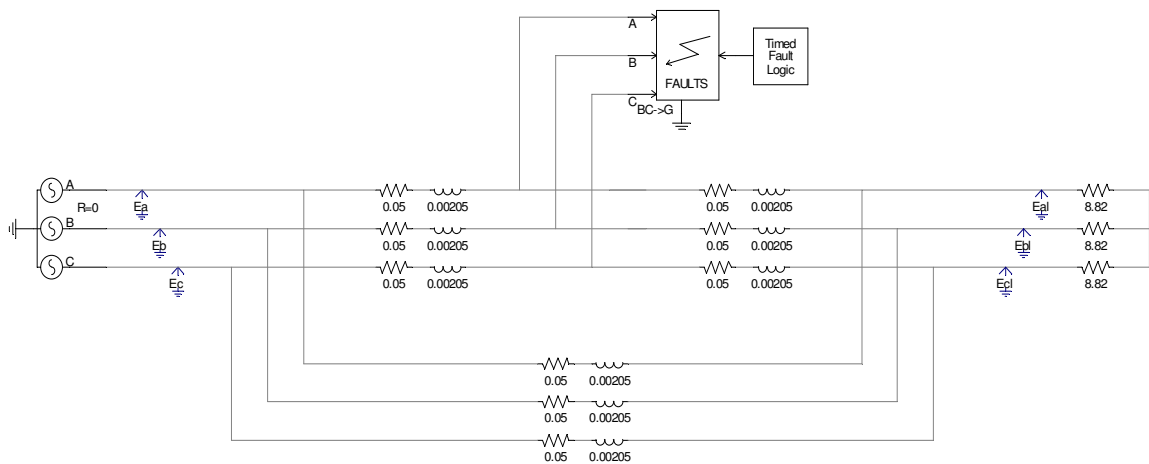


Fig. A.6 Fault-line circuit 1 with Two Resistive loads in PSCAD

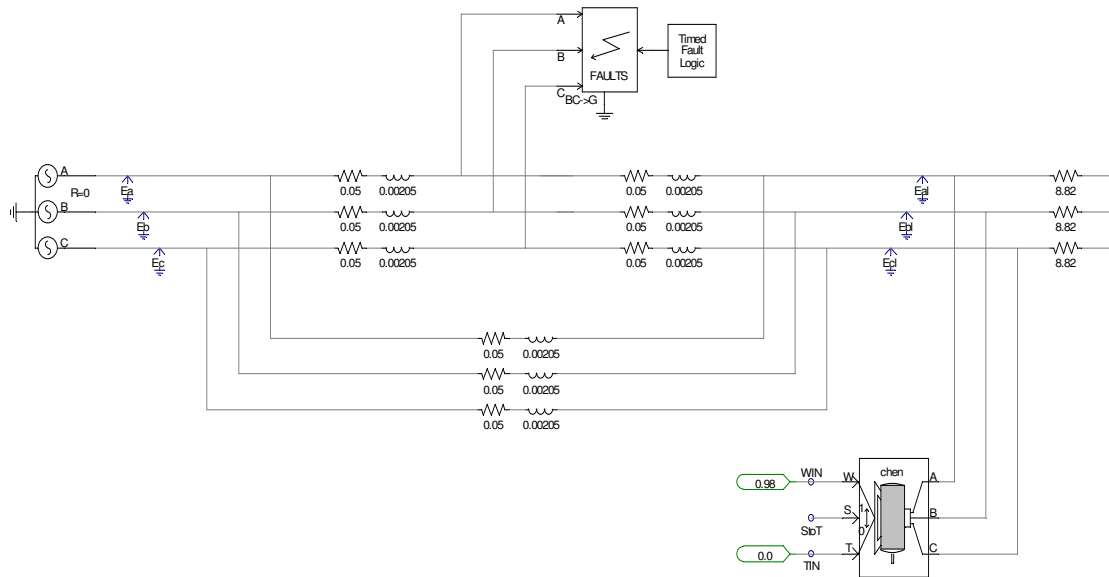


Fig. A.7 Fault-line circuit 1 with Two Resistive loads and Induction Machine in PSCAD

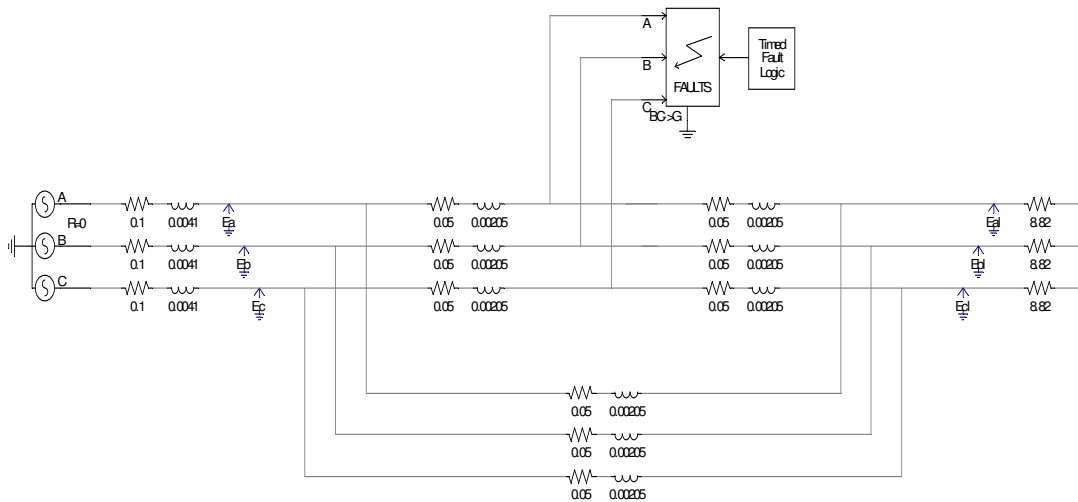


Fig. A.8 Fault-line circuit 2 with Two Resistive loads in PSCAD

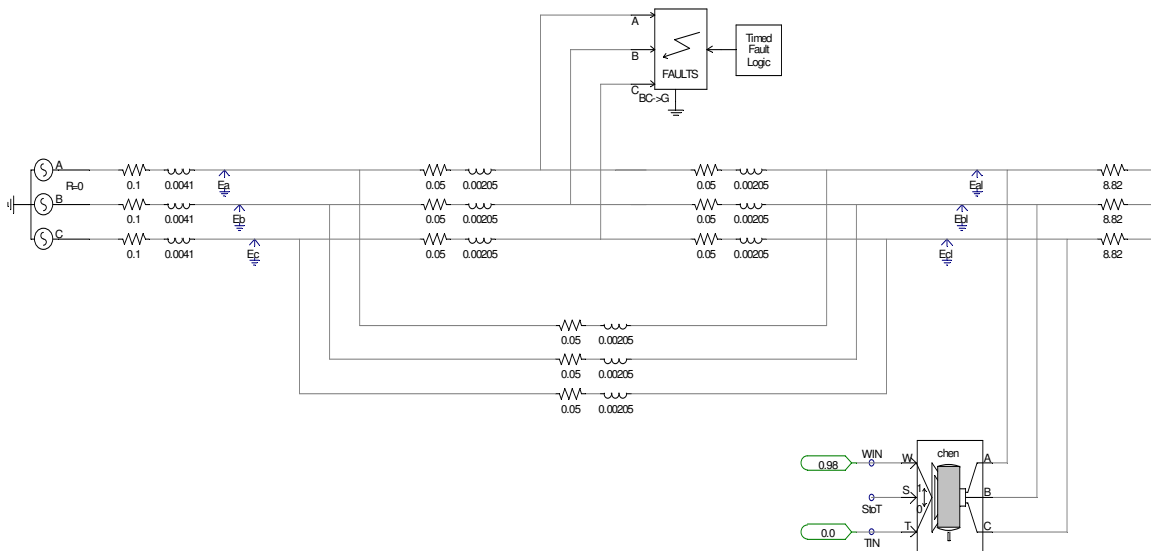


Fig. A.9 Fault-line circuit 2 with Two Resistive loads and Induction Machine in PSCAD

Appendix B: The characteristic voltage and PN Factor

Let's recall the equations of the three-sequence voltages during the fault at PCC in section 2.2 and the typical voltage divider model in Fig. 2.6, which is shown below again in Fig. B.1

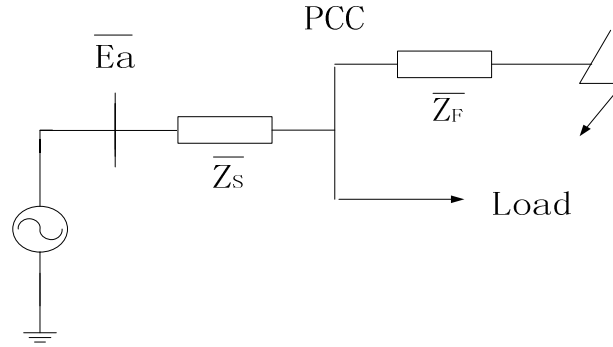


Fig. B.1 Typical voltage divider model

● Three-phase-to-ground fault

For three-phase-to-ground fault, both characteristic voltage \bar{U} and positive-negative factor (PN factor) \bar{F} are defined as the remaining complex voltage or positive-sequence voltage \bar{U}_1 at PCC. Therefore, for the typical voltage divider model shown in Fig B.1, characteristic voltage \bar{U} and PN factor \bar{F} can be expressed as,

$$\bar{U} = \bar{F} = \frac{\bar{Z}_{F1}}{\bar{Z}_{S1} + \bar{Z}_{F1}} \cdot \bar{E}_a \quad (\text{B.1})$$

Therefore, there is no difference between characteristic voltage and remaining complex voltage at PCC for three-phase-to-ground fault. Here we use remaining complex voltage instead of retained voltage, because the latter does not give the complex value, but absolute one.

For unbalanced faults, we will first present two quantities \bar{U}_Σ and \bar{U}_Δ , which are defined as,

$$\bar{U}_\Sigma = \bar{U}_1 + \bar{U}_2 \quad (\text{B.2})$$

$$\bar{U}_\Delta = \bar{U}_1 - \bar{U}_2 \quad (\text{B.3})$$

According to the sequence voltage equations, we can also see these two quantities in

another form,

$$\overline{U}_\Sigma = \overline{U}_a - \overline{U}_0 = \frac{2\overline{U}_a - (\overline{U}_b + \overline{U}_c)}{3} \quad (\text{B.4})$$

$$\overline{U}_\Delta = j \frac{\overline{U}_b - \overline{U}_c}{\sqrt{3}} \quad (\text{B.5})$$

Equation (B.4) and (B.5) would be helpful for us to understand what the characteristic voltage represents in different types of faults later on.

● Single-phase-to-ground fault

For single-phase-to-ground fault, according to its fault sequence equations, \overline{U}_Σ and \overline{U}_Δ can be expressed as,

$$\overline{U}_\Sigma = \frac{\overline{Z}_{S0} + (\overline{Z}_{F1} + \overline{Z}_{F2} + \overline{Z}_{F0})}{(\overline{Z}_{S1} + \overline{Z}_{S2} + \overline{Z}_{S0}) + (\overline{Z}_{F1} + \overline{Z}_{F2} + \overline{Z}_{F0})} \cdot \overline{E}_a \quad (\text{B.6})$$

$$\overline{U}_\Delta = \frac{(2\overline{Z}_{S2} + \overline{Z}_{S0}) + (\overline{Z}_{F1} + \overline{Z}_{F2} + \overline{Z}_{F0})}{(\overline{Z}_{S1} + \overline{Z}_{S2} + \overline{Z}_{S0}) + (\overline{Z}_{F1} + \overline{Z}_{F2} + \overline{Z}_{F0})} \cdot \overline{E}_a \quad (\text{B.7})$$

Here, \overline{U}_Σ is defined as characteristic voltage \overline{U} for single-phase-to-ground fault.

\overline{U}_Δ is termed as PN factor \overline{F} .

Characteristic voltage \overline{U} in equation (B.6) can be expressed in a simplified form,

$$\overline{U} = \frac{1}{1 + \frac{\overline{Z}_{S\Sigma} - \overline{Z}_{S0}}{\overline{Z}_{F\Sigma} + \overline{Z}_{S0}}} \cdot \overline{E}_a \quad (\text{B.8})$$

where,

$$\overline{Z}_{S\Sigma} = \overline{Z}_{S1} + \overline{Z}_{S2} + \overline{Z}_{S0} \quad (\text{B.9})$$

$$\overline{Z}_{F\Sigma} = \overline{Z}_{F1} + \overline{Z}_{F2} + \overline{Z}_{F0} \quad (\text{B.10})$$

According to equation (B.4), characteristic voltage represents the fault-phase-to-ground voltage with zero-sequence component removed for single-phase-to-ground fault. This feature of characteristic voltage can also be understood in equation (B.8).

As for non-rotating electrical component, positive-sequence impedance of the component is normally equal to negative-sequence impedance of it. Thus, if we

assume that,

$$\overline{Z}_{S1} = \overline{Z}_{S2} \quad (\text{B.11})$$

$$\overline{Z}_{F1} = \overline{Z}_{F2} \quad (\text{B.12})$$

PN factor in equation (B.7) can be simplified as,

$$F = \overline{E}_a \quad (\text{B.13})$$

Equation (B.13) shows that PN factor is equal to unity (pre-fault voltage at the fault location). It tells nothing about the during-fault information. This can also be understood through equation (B.5) that, PN factor is proportional to the phase-to-phase voltage of the two non-fault phases in single-phase-ground fault.

● Double-phase fault

For double-phase fault, according to its fault sequence equations, \overline{U}_Σ and \overline{U}_Δ can be expressed as,

$$\overline{U}_\Sigma = \frac{2\overline{Z}_{S2} + (\overline{Z}_{F1} + \overline{Z}_{F2})}{(\overline{Z}_{S1} + \overline{Z}_{S2}) + (\overline{Z}_{F1} + \overline{Z}_{F2})} \cdot \overline{E}_a \quad (\text{B.14})$$

$$\overline{U}_\Delta = \frac{\overline{Z}_{F1} + \overline{Z}_{F2}}{(\overline{Z}_{S1} + \overline{Z}_{S2}) + (\overline{Z}_{F1} + \overline{Z}_{F2})} \cdot \overline{E}_a \quad (\text{B.15})$$

Here, \overline{U}_Δ is defined as characteristic voltage \overline{U} for double-phase fault. \overline{U}_Σ is defined as PN factor \overline{F} .

Characteristic voltage \overline{U} in equation (B.15) can be expressed in a simplified form,

$$\overline{U} = \frac{1}{1 + \frac{\overline{Z}_{S\Sigma} - \overline{Z}_{S0}}{\overline{Z}_{F\Sigma} - \overline{Z}_{F0}}} \cdot \overline{E}_a \quad (\text{B.16})$$

According to equation (B.5), \overline{U} represents the phase-to-phase voltage of the two fault phases in double-phase fault. The factor $\sqrt{3}$ in equation (B.5) can be considered to change the base of the pu values, so that the normal operating voltage remains at 100%. The factor j , which is a 90° rotation, can be considered to keep the axis of symmetry of \overline{U}_Δ in the direction of real axis. As \overline{U}_Δ is a “normalized” phase-to-phase voltage, \overline{U} is a zero-sequence component free voltage as well in

double-phase fault. This feature of \bar{U} can also be apprehended in equation (B.16).

With the assumption in equation (B.11), the PN factor \bar{F} in equation (B.14) can also be simplified as,

$$\bar{F} = \bar{E}_a \quad (\text{B.17})$$

PN factor still tells nothing about the fault information during double-phase fault.

● Double-phase-to-ground fault

For double-phase-to-ground fault, according to its fault sequence equations, \bar{U}_Σ and \bar{U}_Δ can be expressed as,

$$\bar{U}_\Sigma = \frac{\bar{Z}_{F1} \cdot [(\bar{Z}_{S2} + \bar{Z}_{F2}) + (\bar{Z}_{S0} + \bar{Z}_{F0})] + (2\bar{Z}_{S2} + \bar{Z}_{F2}) \cdot (\bar{Z}_{S0} + \bar{Z}_{F0})}{D} \cdot \bar{E}_a \quad (\text{B.18})$$

$$\bar{U}_\Delta = \frac{\bar{Z}_{F1} \cdot [(\bar{Z}_{S2} + \bar{Z}_{F2}) + (\bar{Z}_{S0} + \bar{Z}_{F0})] + \bar{Z}_{F2} \cdot (\bar{Z}_{S0} + \bar{Z}_{F0})}{D} \cdot \bar{E}_a \quad (\text{B.19})$$

Here, \bar{U}_Δ is defined as characteristic voltage \bar{U} for double-phase-to-ground fault.

\bar{U}_Σ is defined as PN factor \bar{F} .

Characteristic voltage \bar{U} in equation (B.18) can also be expressed in a simplified form,

$$\bar{U} = \frac{1}{\frac{\bar{Z}_{S1} \cdot \bar{Z}_2}{\bar{Z}_0} + (\bar{Z}_{S\Sigma} - \bar{Z}_{S0})} \cdot \bar{E}_a \quad (\text{B.20})$$

$$1 + \frac{\frac{\bar{Z}_{F1} \cdot \bar{Z}_2}{\bar{Z}_0} + (\bar{Z}_{F\Sigma} - \bar{Z}_{F0})}{\bar{Z}_0}$$

where, \bar{Z}_2 and \bar{Z}_0 are the negative- and zero-sequence Thevenin's equivalent impedance seen from the fault location.

$$\bar{Z}_2 = \bar{Z}_{S2} + \bar{Z}_{F2} \quad (\text{B.21})$$

$$\bar{Z}_0 = \bar{Z}_{S0} + \bar{Z}_{F0} \quad (\text{B.22})$$

According to equation (B.5), \bar{U} in double-phase-to-ground fault has a similar

physical meaning as it in double-phase fault. Compare the equation (B.20) and (B.16) for \overline{U} , we can see that equation (B.16) of double-phase fault is a special case of equation (B.20) with the infinite zero-sequence impedance \overline{Z}_0 .

With the assumption in equation (B.11), the PN factor \overline{F} in equation (B.18) can also be simplified as,

$$\overline{F} = \left(1 - \frac{\overline{Z}_{s1} \cdot \overline{Z}_2}{D}\right) \cdot \overline{E}_a \quad (\text{B.23})$$

In double-phase-to-ground fault, PN factor \overline{F} is less than unity.

Appendix C: Results summarized in the Chapter 4

C.1 Analytical estimation of voltage sags

C.1.1 Basic circuit

The configuration of “Basic circuit” is shown in Fig. 3.1. Three-phase-to-ground fault, single-phase-to-ground fault, double-phase fault and double-phase-to-ground fault are tested in the lab model. The parameters of line impedance \bar{Z} , source impedance \bar{Z}_S and feeder impedance \bar{Z}_F are as follows. Assume no fault impedance.

$$\bar{Z} = 0.050 + j0.644 = 0.646 \angle 85.6^\circ \Omega$$

$$\bar{Z}_S = 3\bar{Z} = 0.150 + j1.93 = 1.94 \angle 85.6^\circ \Omega$$

$$\bar{Z}_F = 2\bar{Z} = 0.10 + j1.29 = 1.29 \angle 85.6^\circ \Omega$$

Three-phase source voltages are as follows.

$$\bar{E}_a = 230 \angle 0^\circ V, \quad \bar{E}_b = 230 \angle -120^\circ V, \quad \bar{E}_c = 230 \angle 120^\circ V$$

Phase A is the default phase for symmetrical component calculation.

- **Three-phase-to-ground fault**

As three-phase-to-ground fault is a balanced fault, both one-phase method and symmetrical component method can be used to calculate the retained voltage and phase-angle jump at PCC during the fault.

$$\bar{U}_{PCC} = \frac{\bar{Z}_F}{\bar{Z}_S + \bar{Z}_F} \cdot \bar{E}_a = \frac{2\bar{Z}}{3\bar{Z} + 2\bar{Z}} \cdot 230 \angle 0^\circ = 92.0 \angle 0^\circ V$$

Pre-fault voltage at PCC is equal to \bar{E}_a . Phase-angle jump in this thesis is defined as the difference between the during-fault phase angle and the pre-fault phase angle at the monitoring point.

Therefore, the three-phase retained voltages at PCC are,

$$U_a = U_b = U_c = 92.0V$$

The phase-angle jumps at PCC are,

$$\Delta\phi_a = 0 - 0 = 0$$

$$\Delta\phi_b = -120^\circ - (-120^\circ) = 0$$

$$\Delta\phi_c = 120^\circ - 120^\circ = 0$$

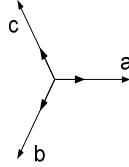
The magnitudes of characteristic voltage and PN factor at PCC are,

$$U = 92.0V, F = 92.0V$$

The phase-angle jump of characteristic voltage at PCC is,

$$\Delta\phi = 0$$

The phasor diagram of the three phase voltages is,



Thus, according to Table 2.2, it is classified as sag type A.

According to equation (45), the sag index T is,

$$T = \frac{1}{60^\circ} \times \arg\left(\frac{0}{230\angle 0 - 92\angle 0}\right) = 0$$

Thus, according to Table 2.3, it is classified as sag type Ca.

● Single-phase-to-ground fault

According to the sequence network connection of single-phase-to-ground fault, sequence parameters are derived as follows. Assume that zero-sequence impedance of the line model is the same as the positive- and negative-sequence impedance.

The sequence source impedances are,

$$\overline{Z}_{S1} = \overline{Z}_{S2} = \overline{Z}_{S0} = \overline{Z}_S = 1.94\angle 85.6^\circ \Omega$$

The sequence feeder impedances are,

$$\overline{Z}_{F1} = \overline{Z}_{F2} = \overline{Z}_{F0} = \overline{Z}_F = 1.29\angle 85.6^\circ \Omega$$

The sequence impedances are,

$$\overline{Z}_1 = \overline{Z}_2 = \overline{Z}_0 = \overline{Z}_S + \overline{Z}_F = 5\overline{Z} = 3.23\angle 85.6^\circ \Omega$$

The sequence fault currents are,

$$\overline{I}_1 = \overline{I}_2 = \overline{I}_0 = \frac{\overline{E}_1}{\overline{Z}_1 + \overline{Z}_2 + \overline{Z}_0} = \frac{230\angle 0}{3 \cdot 3.23\angle 85.6^\circ} = 23.7\angle -85.6^\circ \text{ A}$$

The sequence voltages at PCC are,

$$\overline{U}_1 = \overline{E}_1 - \overline{Z}_{S1} \cdot \overline{I}_1 = 230 - 1.94\angle 85.6^\circ \cdot 23.7\angle -85.6^\circ = 184\angle 0V$$

$$\overline{U}_2 = -\overline{Z}_{S2} \cdot \overline{I}_2 = -1.94\angle 85.6^\circ \cdot 23.7\angle -85.6^\circ = -46.0\angle 0V$$

$$\overline{U}_0 = -\overline{Z}_{S0} \cdot \overline{I}_0 = -1.94\angle 85.6^\circ \cdot 23.7\angle -85.6^\circ = -46.0\angle 0V$$

As a result, the phase voltages at PCC are,

$$\begin{bmatrix} \overline{U}_a \\ \overline{U}_b \\ \overline{U}_c \end{bmatrix} = T \begin{bmatrix} \overline{U}_0 \\ \overline{U}_1 \\ \overline{U}_2 \end{bmatrix} = \begin{bmatrix} 1 & 1 & 1 \\ 1 & a^2 & a \\ 1 & a & a^2 \end{bmatrix} \begin{bmatrix} -46.0\angle 0 \\ 184\angle 0 \\ -46.0\angle 0 \end{bmatrix} = \begin{bmatrix} 92.0\angle 0 \\ 230\angle -120^\circ \\ 230\angle 120^\circ \end{bmatrix}$$

Therefore, the three-phase retained voltages at PCC are,

$$U_a = 92.0V, \quad U_b = U_c = 230V$$

The phase-angle jumps at PCC are,

$$\Delta\phi_a = 0 - 0 = 0$$

$$\Delta\phi_b = -120^\circ - (-120^\circ) = 0$$

$$\Delta\phi_c = 120^\circ - 120^\circ = 0$$

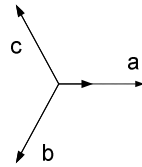
The magnitudes of characteristic voltage and PN factor at PCC are,

$$U = 138.0V, \quad F = 230V$$

The phase-angle jump of characteristic voltage at PCC is,

$$\Delta\phi = 0$$

The phasor diagram of the three phase voltages is,



The sag index T is,

$$T = \frac{1}{60^\circ} \times \arg\left(\frac{-46.0\angle 0}{230\angle 0 - 184\angle 0}\right) = 3$$

Thus, according to Table 2.3, it is classified as sag type Da.

● Double-phase fault

As double-phase fault is an ungrounded fault, there is no path for zero-sequence current during the fault. Therefore, only positive- and negative-sequence networks are considered during calculation.

According to the sequence network connection of double-phase fault, the sequence fault currents are,

$$\overline{I}_1 = -\overline{I}_2 = \frac{\overline{E}_1}{\overline{Z}_1 + \overline{Z}_2} = \frac{230\angle 0}{2 \cdot 3.23\angle 85.6^\circ} = 35.6\angle -85.6^\circ A$$

$$\overline{I}_0 = 0$$

The sequence voltages at PCC are,

$$\overline{U}_1 = \overline{E}_1 - \overline{Z}_{s1} \cdot \overline{I}_1 = 230 - 1.94 \angle 85.6^\circ \cdot 35.6 \angle -85.6^\circ = 161 \angle 0^\circ$$

$$\overline{U}_2 = -\overline{Z}_{s2} \cdot \overline{I}_2 = -1.94 \angle 85.6^\circ \cdot (-35.6 \angle -85.6^\circ) = 69.0 \angle 0^\circ$$

$$\overline{U}_0 = 0$$

As a result, the phase voltages at PCC are,

$$\begin{bmatrix} \overline{U}_a \\ \overline{U}_b \\ \overline{U}_c \end{bmatrix} = T \begin{bmatrix} \overline{U}_0 \\ \overline{U}_1 \\ \overline{U}_2 \end{bmatrix} = \begin{bmatrix} 1 & 1 & 1 \\ 1 & a^2 & a \\ 1 & a & a^2 \end{bmatrix} \begin{bmatrix} 0 \\ 161 \angle 0^\circ \\ 69.0 \angle 0^\circ \end{bmatrix} = \begin{bmatrix} 230 \angle 0^\circ \\ 140 \angle -145.3^\circ \\ 140 \angle 145.3^\circ \end{bmatrix}$$

Therefore, the three-phase retained voltages at PCC are,

$$U_a = 230V, \quad U_b = U_c = 140V$$

The phase-angle jumps at PCC are,

$$\Delta\phi_a = 0 - 0 = 0$$

$$\Delta\phi_b = -145.3^\circ - (-120^\circ) = -25.3^\circ$$

$$\Delta\phi_c = 145.3^\circ - 120^\circ = 25.3^\circ$$

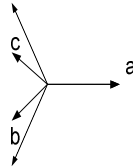
The magnitudes of characteristic voltage and PN factor at PCC are,

$$U = 92.0V, \quad F = 230V$$

The phase-angle jump of characteristic voltage at PCC is,

$$\Delta\phi = 0$$

The phasor diagram of the three phase voltages is,



Thus, according to Table 2.2, it is classified as sag type C.

The sag index T is,

$$T = \frac{1}{60^\circ} \times \arg\left(\frac{69.0 \angle 0^\circ}{230 \angle 0^\circ - 161 \angle 0^\circ}\right) = 0$$

Thus, according to Table 2.3, it is classified as sag type Ca.

● Double-phase-to-ground fault

Assume zero-sequence source impedance and feeder impedance being the same as the positive- and negative-sequence source impedance and feeder impedance, respectively.

According to the sequence network connection of double-phase-to-ground fault, the sequence fault currents are,

$$\bar{I}_1 = \frac{\bar{E}_1}{\bar{Z}_1 + \bar{Z}_2 \parallel \bar{Z}_0} = \frac{230\angle 0}{3.23\angle 85.6^\circ + 0.5 \cdot 3.23\angle 85.6^\circ} = 47.5\angle -85.6^\circ \text{ A}$$

$$\bar{I}_2 = \bar{I}_0 = -\frac{1}{2} \cdot \bar{I}_1 = -23.7\angle -85.6^\circ \text{ A}$$

The sequence voltages at PCC are,

$$\bar{U}_1 = \bar{E}_1 - \bar{Z}_{s1} \cdot \bar{I}_1 = 230\angle 0 - 1.94\angle 85.6^\circ \cdot 47.5\angle -85.6^\circ = 138\angle 0 \text{ V}$$

$$\bar{U}_2 = -\bar{Z}_{s2} \cdot \bar{I}_2 = -1.94\angle 85.6^\circ \cdot (-23.7\angle -85.6^\circ) = 46.0\angle 0 \text{ V}$$

$$\bar{U}_0 = -\bar{Z}_{s0} \cdot \bar{I}_0 = -1.93\angle 85.6^\circ \cdot (-23.7\angle -85.6^\circ) = 46.0\angle 0 \text{ V}$$

As a result, the phase voltages at PCC are,

$$\begin{bmatrix} \bar{U}_a \\ \bar{U}_b \\ \bar{U}_c \end{bmatrix} = T \begin{bmatrix} \bar{U}_0 \\ \bar{U}_1 \\ \bar{U}_2 \end{bmatrix} = \begin{bmatrix} 1 & 1 & 1 \\ 1 & a^2 & a \\ 1 & a & a^2 \end{bmatrix} \begin{bmatrix} 46.0\angle 0 \\ 138\angle 0 \\ 46.0\angle 0 \end{bmatrix} = \begin{bmatrix} 230\angle 0 \\ 92\angle -120^\circ \\ 92\angle 120^\circ \end{bmatrix}$$

Therefore, the three-phase retained voltages at PCC are,

$$U_a = 230 \text{ V}, \quad U_b = U_c = 92.0 \text{ V}$$

The phase-angle jumps at PCC are,

$$\Delta\phi_a = 0 - 0 = 0$$

$$\Delta\phi_b = -120^\circ - (-120^\circ) = 0$$

$$\Delta\phi_c = 120^\circ - 120^\circ = 0$$

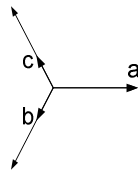
The magnitudes of characteristic voltage and PN factor at PCC are,

$$U = 92.0 \text{ V}, \quad F = 184 \text{ V}$$

The phase-angle jump of characteristic voltage at PCC is,

$$\Delta\phi = 0$$

The phasor diagram of the three phase voltages is,



Thus, according to Table 2.2, it is classified as sag type E.

The sag index T is,

$$T = \frac{1}{60^\circ} \times \arg\left(\frac{46.0\angle 0}{230\angle 0 - 138\angle 0}\right) = 0$$

Thus, according to Table 2.3, it is classified as sag type Ca.

C.1.2 Voltage-divider circuit

The configuration of “Voltage-divider circuit” is shown in Fig. 3.2. The difference between voltage-divider circuit and basic circuit is that the former one is loaded with induction machine. However, when estimating fault and short circuit in power system, only the case without load is analyzed. Therefore, these two circuits are similar to each other in terms of analytical estimation. Source impedance \overline{Z}_S and feeder impedance \overline{Z}_F are as follows. Assume no fault impedance.

$$\overline{Z}_S = \overline{Z} = 0.646\angle 85.6^\circ \Omega$$

$$\overline{Z}_F = 2\overline{Z} = 1.29\angle 85.6^\circ \Omega$$

The three-phase source voltages are as follows.

$$\overline{E}_a = 230\angle 0^\circ V, \quad \overline{E}_b = 230\angle -120^\circ V, \quad \overline{E}_c = 230\angle 120^\circ V$$

Phase A is again chosen as the default phase for symmetrical component calculation.

● Three-phase-to-ground fault

Similar to the basic circuit, the phase voltage (phase A) at PCC during three-phase-to-ground fault is as follows.

$$\overline{U}_{PCC} = \frac{\overline{Z}_F}{\overline{Z}_S + \overline{Z}_F} \cdot \overline{E}_a = \frac{2\overline{Z}}{\overline{Z} + 2\overline{Z}} \cdot 230\angle 0 = 153\angle 0V$$

Therefore, the three-phase retained voltages at PCC are,

$$U_a = U_b = U_c = 153V$$

The phase-angle jumps at PCC are,

$$\Delta\phi_a = 0 - 0 = 0$$

$$\Delta\phi_b = -120^\circ - (-120^\circ) = 0$$

$$\Delta\phi_c = 120^\circ - 120^\circ = 0$$

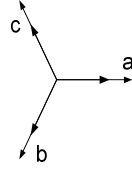
The magnitudes of characteristic voltage and PN factor at PCC are,

$$U = 153V, \quad F = 153V$$

The phase-angle jump of characteristic voltage at PCC is,

$$\Delta\phi = 0$$

The phasor diagram of the three phase voltages is,



Thus, according to Table 2.2, it is classified as sag type A.

According to equation (45), the sag index T is,

$$T = \frac{1}{60^0} \times \arg\left(\frac{0}{230\angle 0 - 153\angle 0}\right) = 0$$

Thus, according to Table 2.3, it is classified as sag type Ca.

● Single-phase-to-ground fault

Assume that zero-sequence impedance of the line model is the same as the positive- and negative-sequence impedance.

The sequence source impedances are,

$$\overline{Z}_{S1} = \overline{Z}_{S2} = \overline{Z}_{S0} = \overline{Z}_S = 0.646\angle 85.6^0 \Omega$$

The sequence feeder impedances are,

$$\overline{Z}_{F1} = \overline{Z}_{F2} = \overline{Z}_{F0} = \overline{Z}_F = 1.29\angle 85.6^0 \Omega$$

The sequence impedances are,

$$\overline{Z}_1 = \overline{Z}_2 = \overline{Z}_0 = \overline{Z}_S + \overline{Z}_F = 3\overline{Z} = 1.94\angle 85.6^0 \Omega$$

According to the sequence network connection of single-phase-to-ground fault, the sequence fault currents are,

$$\overline{I}_1 = \overline{I}_2 = \overline{I}_0 = \frac{\overline{E}_1}{\overline{Z}_1 + \overline{Z}_2 + \overline{Z}_0} = \frac{230\angle 0}{3 \cdot 1.94\angle 85.6^0} = 39.6\angle -85.6^0 \text{ A}$$

The sequence voltages at PCC are,

$$\overline{U}_1 = \overline{E}_1 - \overline{Z}_{S1} \cdot \overline{I}_1 = 230\angle 0 - 1.94\angle 85.6^0 \cdot 39.6\angle -85.6^0 = 204\angle 0 \text{ V}$$

$$\overline{U}_2 = -\overline{Z}_{S2} \cdot \overline{I}_2 = -1.94\angle 85.6^0 \cdot 39.6\angle -85.6^0 = -25.6\angle 0 \text{ V}$$

$$\overline{U}_0 = -\overline{Z}_{S0} \cdot \overline{I}_0 = -0.646\angle 85.6^0 \cdot 39.6\angle -85.6^0 = -25.6\angle 0 \text{ V}$$

As a result, the phase voltages at PCC are,

$$\begin{bmatrix} \overline{U}_a \\ \overline{U}_b \\ \overline{U}_c \end{bmatrix} = T \begin{bmatrix} \overline{U}_0 \\ \overline{U}_1 \\ \overline{U}_2 \end{bmatrix} = \begin{bmatrix} 1 & 1 & 1 \\ 1 & a^2 & a \\ 1 & a & a^2 \end{bmatrix} \begin{bmatrix} -25.6\angle 0 \\ 204\angle 0 \\ -25.6\angle 0 \end{bmatrix} = \begin{bmatrix} 153\angle 0 \\ 230\angle -120^0 \\ 230\angle 120^0 \end{bmatrix}$$

Therefore, the three-phase retained voltages at PCC are,

$$U_a = 153V, U_b = U_c = 230V$$

The phase-angle jumps at PCC are,

$$\Delta\phi_a = 0 - 0 = 0$$

$$\Delta\phi_b = -120^\circ - (-120^\circ) = 0$$

$$\Delta\phi_c = 120^\circ - 120^\circ = 0$$

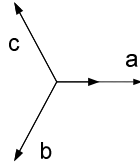
The magnitudes of characteristic voltage and PN factor at PCC are,

$$U = 178.4V, F = 230V$$

The phase-angle jump of characteristic voltage at PCC is,

$$\Delta\phi = 0$$

The phasor diagram of the three phase voltages is,



The sag index T is,

$$T = \frac{1}{60^\circ} \times \arg\left(\frac{-25.6\angle 0}{230\angle 0 - 204\angle 0}\right) = 3$$

Thus, according to Table 2.3, it is classified as sag type Da.

● Double-phase fault

According to the sequence network connection of double-phase fault, the sequence fault currents are,

$$\bar{I}_1 = -\bar{I}_2 = \frac{\bar{E}_1}{\bar{Z}_1 + \bar{Z}_2} = \frac{230\angle 0}{2 \cdot 1.94\angle 85.6^\circ} = 59.4\angle -85.6^\circ A$$

$$\bar{I}_0 = 0$$

The sequence voltages at PCC are,

$$\bar{U}_1 = \bar{E}_1 - \bar{Z}_{s1} \cdot \bar{I}_1 = 230\angle 0 - 0.646\angle 85.6^\circ \cdot 59.4\angle -85.6^\circ = 192\angle 0V$$

$$\bar{U}_2 = -\bar{Z}_{s2} \cdot \bar{I}_2 = -0.646\angle 85.6^\circ \cdot (-59.4\angle -85.6^\circ) = 38.3\angle 0V$$

$$\bar{U}_0 = 0$$

As a result, the phase voltages at PCC are,

$$\begin{bmatrix} \overline{U_a} \\ \overline{U_b} \\ \overline{U_c} \end{bmatrix} = T \begin{bmatrix} \overline{U_0} \\ \overline{U_1} \\ \overline{U_2} \end{bmatrix} = \begin{bmatrix} 1 & 1 & 1 \\ 1 & a^2 & a \\ 1 & a & a^2 \end{bmatrix} \begin{bmatrix} 0 \\ 192\angle 0 \\ 38.3\angle 0 \end{bmatrix} = \begin{bmatrix} 230\angle 0 \\ 176\angle -130.9^\circ \\ 176\angle 130.9^\circ \end{bmatrix}$$

Therefore, the three-phase retained voltages at PCC are,

$$U_a = 230V, \quad U_b = U_c = 176V$$

The phase-angle jumps at PCC are,

$$\Delta\phi_a = 0 - 0 = 0$$

$$\Delta\phi_b = -130.9^\circ - (-120^\circ) = -10.9^\circ$$

$$\Delta\phi_c = 130.9^\circ - 120^\circ = 10.9^\circ$$

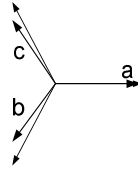
The magnitudes of characteristic voltage and PN factor at PCC are,

$$U = 153.7V, \quad F = 230V$$

The phase-angle jump of characteristic voltage at PCC is,

$$\Delta\phi = 0$$

The phasor diagram of the three phase voltages is,



Thus, according to Table 2.2, it is classified as sag type C.

The sag index T is,

$$T = \frac{1}{60^\circ} \times \arg\left(\frac{38.3\angle 0}{230\angle 0 - 192\angle 0}\right) = 0$$

Thus, according to Table 2.3, it is classified as sag type Ca.

● Double-phase-to-ground fault

According to the sequence network connection of double-phase-to-ground fault, the sequence fault currents are,

$$\overline{I_1} = \frac{\overline{E_1}}{\overline{Z_1} + \overline{Z_2} // \overline{Z_0}} = \frac{230\angle 0}{1.94\angle 85.6^\circ + 0.5 \cdot 1.94\angle 85.6^\circ} = 79.1\angle -85.6^\circ A$$

$$\overline{I_2} = \overline{I_0} = -\frac{1}{2} \cdot \overline{I_1} = -39.6\angle -85.6^\circ A$$

The sequence voltages at PCC are,

$$\overline{U_1} = \overline{E_1} - \overline{Z_{s1}} \cdot \overline{I_1} = 230\angle 0 - 0.646\angle 85.6^\circ \cdot 79.1\angle -85.6^\circ = 179\angle 0V$$

$$\overline{U}_2 = -\overline{Z}_{s2} \cdot \overline{I}_2 = -0.646 \angle 85.6^\circ \cdot (-39.6 \angle -85.6^\circ) = 25.6 \angle 0^\circ V$$

$$\overline{U}_0 = -\overline{Z}_{s0} \cdot \overline{I}_0 = -0.646 \angle 85.6^\circ \cdot (-39.6 \angle -85.6^\circ) = 25.6 \angle 0^\circ V$$

As a result, the phase voltages at PCC are,

$$\begin{bmatrix} \overline{U}_a \\ \overline{U}_b \\ \overline{U}_c \end{bmatrix} = T \begin{bmatrix} \overline{U}_0 \\ \overline{U}_1 \\ \overline{U}_2 \end{bmatrix} = \begin{bmatrix} 1 & 1 & 1 \\ 1 & a^2 & a \\ 1 & a & a^2 \end{bmatrix} \begin{bmatrix} 25.6 \angle 0^\circ \\ 179 \angle 0^\circ \\ 25.6 \angle 0^\circ \end{bmatrix} = \begin{bmatrix} 230 \angle 0^\circ \\ 153 \angle -120^\circ \\ 153 \angle 120^\circ \end{bmatrix}$$

Therefore, the three-phase retained voltages at PCC are,

$$U_a = 230V, \quad U_b = U_c = 153V$$

The phase-angle jumps at PCC are,

$$\Delta\phi_a = 0 - 0 = 0$$

$$\Delta\phi_b = -120^\circ - (-120^\circ) = 0$$

$$\Delta\phi_c = 120^\circ - 120^\circ = 0$$

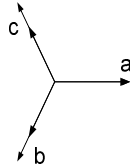
The magnitudes of characteristic voltage and PN factor at PCC are,

$$U = 153.4V, \quad F = 204.6V$$

The phase-angle jump of characteristic voltage at PCC is,

$$\Delta\phi = 0$$

The phasor diagram of the three phase voltages is,



Thus, according to Table 2.2, it is classified as sag type E.

The sag index T is,

$$T = \frac{1}{60^\circ} \times \arg\left(\frac{25.6 \angle 0^\circ}{230 \angle 0^\circ - 179 \angle 0^\circ}\right) = 0$$

Thus, according to Table 2.3, it is classified as sag type Ca.

C.1.3 Fault-load circuit

The configuration of ‘‘Fault-load circuit’’ is shown in Fig. 3.3. Fault happens directly at the supplying point of the loads, where the PQ monitor is located. In theoretical estimation, only the case with two three-phase resistive loads is analyzed. Both resistive loads are ungrounded. Resistance per phase and source impedance is as follows.

$$R = 17.6\Omega$$

$$\overline{Z}_S = \overline{Z} // 2\overline{Z} = 0.430\angle 85.6^\circ \Omega$$

The three-phase source voltages are as follows.

$$\overline{E}_a = 230\angle 0^\circ V, \quad \overline{E}_b = 230\angle -120^\circ V, \quad \overline{E}_c = 230\angle 120^\circ V$$

Phase A is the default phase for symmetrical component calculation.

According to the configuration of the 'Fault-load circuit', the pre-fault voltage of phase A at MP is,

$$\overline{U}_{PCC,pre} = \frac{\overline{E}_a}{\overline{Z} // 2\overline{Z} + R/2} \cdot \frac{R}{2} = 229\angle -2.8^\circ V$$

As the pre-fault system is symmetrical, thus, the pre-fault characteristic voltage at MP is the same as the phase A voltage, which is

$$\overline{U}_{pre} = \overline{U}_{PCC,pre} = 229\angle -2.8^\circ V$$

● Three-phase-to-ground fault

As the three-phase-to-ground fault happens at the same location as the monitoring point (MP), the phase voltage (phase A) at MP during fault should be equal to zero.

$$\overline{U}_{PCC} = 0$$

Therefore, the three-phase retained voltages at MP are,

$$U_a = U_b = U_c = 0$$

There is no definition of phase angle for a zero voltage. Thus, the phase-angle jump is not applicable in this case.

The magnitudes of characteristic voltage and PN factor at MP are,

$$U = U_1 = 0, \quad F = U_1 = 0$$

The phase-angle jump of characteristic voltage at MP is not applicable.

There is no phasor diagram of the three phase voltages.

Thus, according to Table 2.2, it can be classified as any sag type, i.e. sag type A.

According to equation (45), the sag index T is,

$$T = \frac{1}{60^\circ} \times \arg\left(\frac{0}{229\angle -2.8^\circ - 0}\right) = 0$$

Thus, according to Table 2.3, it is classified as sag type Ca.

● **Single-phase-to-ground fault**

Again assume that zero-sequence impedance of the line model is the same as the positive- and negative-sequence impedance.

Seen from the fault point, the Thevenin's equivalent impedance of positive-sequence network is,

$$\bar{Z}_1 = \bar{Z}_s // \frac{R}{2} = 0.430 \angle 85.56^\circ // 8.80 = 0.428 \angle 82.8^\circ \Omega$$

The Thevenin's equivalent impedance of negative-sequence network is,

$$\bar{Z}_2 = \bar{Z}_1 = 0.428 \angle 82.8^\circ \Omega$$

The Thevenin's equivalent impedance of zero-sequence network is,

$$\bar{Z}_0 = \bar{Z}_s = 0.430 \angle 85.6^\circ \Omega$$

According to the sequence network connection of single-phase-to-ground fault, sequence current can be calculated as,

$$\bar{I}_1 = \bar{I}_2 = \bar{I}_0 = \frac{\bar{E}_1}{\bar{Z}_1 + \bar{Z}_2 + \bar{Z}_0} = \frac{229 \angle -2.8^\circ}{2 \cdot (0.428 \angle 82.8^\circ) + 0.430 \angle 85.6^\circ} = 178 \angle -86.5^\circ \text{ A}$$

The sequence voltages at MP are,

$$\bar{U}_1 = \bar{E}_1 - \bar{Z}_1 \cdot \bar{I}_1 = 153 \angle -2.3^\circ \text{ V}$$

$$\bar{U}_2 = -\bar{Z}_2 \cdot \bar{I}_2 = 76.2 \angle 176.3^\circ \text{ V}$$

$$\bar{U}_0 = -\bar{Z}_0 \cdot \bar{I}_0 = 76.6 \angle 179.1^\circ \text{ V}$$

As a result, the phase voltages at MP are,

$$\begin{bmatrix} \bar{U}_a \\ \bar{U}_b \\ \bar{U}_c \end{bmatrix} = T \begin{bmatrix} \bar{U}_0 \\ \bar{U}_1 \\ \bar{U}_2 \end{bmatrix} = \begin{bmatrix} 1 & 1 & 1 \\ 1 & a^2 & a \\ 1 & a & a^2 \end{bmatrix} \begin{bmatrix} 76.6 \angle 179.1^\circ \\ 153 \angle -2.3^\circ \\ 76.2 \angle 176.3^\circ \end{bmatrix} = \begin{bmatrix} 0 \\ 232 \angle -122.4^\circ \\ 226 \angle 117.7^\circ \end{bmatrix}$$

Therefore, the three-phase retained voltages at MP are,

$$U_a = 0, \quad U_b = 232 \text{ V}, \quad U_c = 226 \text{ V}$$

The phase-angle jumps at MP are,

$$\Delta\phi_a \text{ (Not applicable)}$$

$$\Delta\phi_b = -122.4^\circ - (-122.8^\circ) = 0.4^\circ$$

$$\Delta\phi_c = 117.7^\circ - 117.2^\circ = 0.5^\circ$$

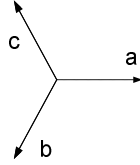
The magnitudes of characteristic voltage and PN factor at MP are,

$$U = |\overline{U}_1 + \overline{U}_2| = 76.6V, \quad F = |\overline{U}_1 - \overline{U}_2| = 229V$$

The phase-angle jump of characteristic voltage at MP is,

$$\Delta\phi = -0.9^\circ - (-2.8^\circ) = 1.9^\circ$$

The phasor diagram of the three phase voltages is,



Thus, according to Table 2.2, it is classified as sag type B.

According to equation (45), the sag index T is,

$$T = \frac{1}{60^\circ} \times \arg\left(\frac{76.2 \angle 176.3^\circ}{229 \angle -2.8^\circ - 153 \angle -2.3^\circ}\right) = 3$$

Thus, according to Table 2.3, it is classified as sag type Da.

● Double-phase fault

According to the sequence network connection of double-phase fault, the sequence fault currents are,

$$\overline{I}_1 = -\overline{I}_2 = \frac{\overline{E}_1}{\overline{Z}_1 + \overline{Z}_2} = \frac{229 \angle -2.8}{2 \cdot 0.428 \angle 82.8^\circ} = 268 \angle -85.6^\circ \text{ A}$$

$$\overline{I}_0 = 0$$

The sequence voltages at MP are,

$$\overline{U}_1 = \overline{E}_1 - \overline{Z}_1 \cdot \overline{I}_1 = 229 \angle -2.8^\circ - 0.428 \angle 82.8^\circ \cdot 268 \angle -85.6^\circ = 114 \angle -2.8^\circ \text{ V}$$

$$\overline{U}_2 = -\overline{Z}_2 \cdot \overline{I}_2 = -0.428 \angle 82.8^\circ \cdot (-268 \angle -85.6^\circ) = 115 \angle -2.8^\circ \text{ V}$$

$$\overline{U}_0 = 0$$

As a result, the phase voltages at MP are,

$$\begin{bmatrix} \overline{U}_a \\ \overline{U}_b \\ \overline{U}_c \end{bmatrix} = T \begin{bmatrix} \overline{U}_0 \\ \overline{U}_1 \\ \overline{U}_2 \end{bmatrix} = \begin{bmatrix} 1 & 1 & 1 \\ 1 & a^2 & a \\ 1 & a & a^2 \end{bmatrix} \begin{bmatrix} 0 \\ 114 \angle -2.8^\circ \\ 115 \angle -2.8^\circ \end{bmatrix} = \begin{bmatrix} 229 \angle -2.8^\circ \\ 115 \angle 177.0^\circ \\ 115 \angle 177.4^\circ \end{bmatrix}$$

Therefore, the three-phase retained voltages at MP are,

$$U_a = 229V, \quad U_b = U_c = 115V$$

Phase-angle jumps at PCC are,

$$\Delta\phi_a = -2.8^\circ - (-2.8^\circ) = 0$$

$$\Delta\phi_b = 177.0^\circ - (-122.8^\circ) - 360^\circ = -60.2^\circ$$

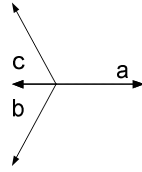
$$\Delta\phi_c = 177.4^\circ - 117.2^\circ = 60.2^\circ$$

The magnitudes of characteristic voltage and PN factor at MP are,

$$U = |\overline{U}_1 - \overline{U}_2| = 0.408V, \quad F = |\overline{U}_1 + \overline{U}_2| = 229V$$

The phase-angle jump of characteristic voltage at MP is not applicable.

The phasor diagram of the three phase voltages is,



Thus, according to Table 2.2, it is classified as sag type C.

The sag index T is,

$$T = \frac{1}{60^\circ} \times \arg\left(\frac{115\angle -2.8^\circ}{229\angle -2.8^\circ - 114\angle -2.8^\circ}\right) = 0$$

Thus, according to Table 2.3, it is classified as sag type Ca.

● Double-phase-to-ground fault

According to the sequence network connection of double-phase-to-ground fault, the sequence fault currents are,

$$\overline{I}_1 = \frac{\overline{E}_1}{\overline{Z}_1 + \overline{Z}_2 // \overline{Z}_0} = \frac{229\angle -2.8^\circ}{0.428\angle 82.8^\circ + 0.215\angle 84.2^\circ} = 356\angle -86.1^\circ A$$

$$\overline{I}_2 = -\frac{\overline{Z}_0}{\overline{Z}_2 + \overline{Z}_0} \cdot \overline{I}_1 = -\frac{0.430\angle 85.6^\circ}{0.428\angle 82.8^\circ + 0.430\angle 85.6^\circ} \cdot 356\angle -86.1^\circ = 178\angle 95.3^\circ A$$

$$\overline{I}_0 = -\overline{I}_1 - \overline{I}_2 = -356\angle -86.1^\circ - 178\angle 95.3^\circ = 178\angle 92.5^\circ A$$

The sequence voltages at MP are,

$$\overline{U}_1 = \overline{U}_2 = \overline{U}_0 = \overline{E}_1 - \overline{Z}_1 \cdot \overline{I}_1 = 229\angle -2.8^\circ - 0.428\angle 82.8^\circ \cdot 356\angle -86.1^\circ = 76.6\angle -1.8^\circ V$$

As a result, the phase voltages at MP are,

$$\begin{bmatrix} \overline{U_a} \\ \overline{U_b} \\ \overline{U_c} \end{bmatrix} = T \begin{bmatrix} \overline{U_0} \\ \overline{U_1} \\ \overline{U_2} \end{bmatrix} = \begin{bmatrix} 1 & 1 & 1 \\ 1 & a^2 & a \\ 1 & a & a^2 \end{bmatrix} \begin{bmatrix} 76.6 \angle -1.8^\circ \\ 76.6 \angle -1.8^\circ \\ 76.6 \angle -1.8^\circ \end{bmatrix} = \begin{bmatrix} 230 \angle -1.8^\circ \\ 0 \\ 0 \end{bmatrix}$$

Therefore, the three-phase retained voltages at MP are,

$$U_a = 230V, \quad U_b = U_c = 0$$

The phase-angle jumps at MP are,

$$\Delta\phi_a = -1.8^\circ - (-2.8^\circ) = 1.0^\circ$$

$$\Delta\phi_b \text{ (Not applicable)}$$

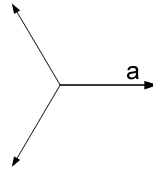
$$\Delta\phi_c \text{ (Not applicable)}$$

The magnitudes of characteristic voltage and PN factor at MP are,

$$U = |\overline{U_1} - \overline{U_2}| = 0V, \quad F = |\overline{U_1} + \overline{U_2}| = 153V$$

The phase-angle jump of characteristic voltage at MP is not applicable.

The phasor diagram of the three phase voltages is,



Thus, according to Table 2.2, it is classified as sag type E.

The sag index T is,

$$T = \frac{1}{60^\circ} \times \arg\left(\frac{76.6 \angle -1.8^\circ}{229 \angle -2.8^\circ - 76.6 \angle -1.8^\circ}\right) = 0.03 \cong 0$$

Thus, according to Table 2.3, it is classified as sag type Ca.

C1.4 Fault-line circuit

The configuration of “**Fault-line circuit**” is shown in Fig. 3.4. Fault happens at the middle of one of the parallel lines. In this case, two locations are monitored as shown in Fig. 3.4. In this section, only the case with two resistive loads is analyzed as well. Resistance per phase is as follows.

$$R = 17.6\Omega$$

The line impedance is as follows.

$$\overline{Z} = 0.050 + j0.644 = 0.646 \angle 85.6^\circ \Omega$$

The three-phase source voltages are as follows.

$$\overline{E}_a = 230\angle 0^\circ V, \quad \overline{E}_b = 230\angle -120^\circ V, \quad \overline{E}_c = 230\angle 120^\circ V$$

Phase A is the default phase for symmetrical component calculation.

As the monitoring point 1 is directly connected to the terminal of the voltage source (assumed ideal in analytical calculation), for different kinds of shunt faults at the transmission line, the voltages at MP1 will be always equal to source voltages. Therefore, for either kind of the four shunt faults, the voltage at MP 1 is always,

$$\overline{U}_{PCC1} = \overline{E}_a = 230\angle 0V$$

The three-phase retained voltages at MP 1 are always,

$$U_a = U_b = U_c = 230V$$

The phase-angle jumps at MP 1 are always,

$$\Delta\phi_a = 0 - 0 = 0$$

$$\Delta\phi_b = -120^\circ - (-120^\circ) = 0$$

$$\Delta\phi_c = 120^\circ - 120^\circ = 0$$

The magnitudes of characteristic voltage and PN factor at MP1 are always,

$$U = 230V, \quad F = 230V$$

The phase-angle jump of characteristic voltage at MP1 is always,

$$\Delta\phi = 0$$

For the following calculations, only voltages at MP2 will be presented. According to the configuration of the 'Fault-line circuit', the pre-fault voltage of phase A at MP2 is,

$$\overline{U}_{PCC2,pre} = \frac{\overline{E}_a}{\overline{Z} // 2\overline{Z} + R/2} \cdot \frac{R}{2} = 229\angle -2.8^\circ V$$

As the pre-fault system is symmetrical, thus, the pre-fault characteristic voltage at MP2 is the same as the phase A voltage, which is

$$\overline{U}_{pre} = \overline{U}_{PCC2,pre} = 229\angle -2.8^\circ V$$

The pre-fault voltage of phase A at the fault location is,

$$\overline{E}_1 = \frac{\overline{E}_a}{2\overline{Z}/3 + R/2} \cdot (\overline{Z}/3 + R/2) = 229\angle -1.4^\circ V$$

● Three-phase-to-ground fault

According to the delta-wye transformation of the 'Fault-line circuit', the total impedance of the circuit equates to,

$$\overline{Z}_t = \frac{\overline{Z}}{3} + \left(\frac{\overline{Z}}{3} // \left(\frac{\overline{Z}}{3} + \frac{R}{2} \right) \right) = 0.430\angle 84.9^\circ \Omega$$

As a result, the voltage at MP2 is,

$$\overline{U}_{PCC2} = \frac{\overline{Z}_t - \overline{Z}/3}{\overline{Z}_t} \cdot \overline{E}_a \cdot \frac{R/2}{\overline{Z}/3 + R/2} = 115 \angle -2.1^\circ \text{V}$$

Therefore, the three-phase retained voltages at MP2 are,

$$U_a = U_b = U_c = 115 \text{V}$$

The phase-angle jumps at MP2 are,

$$\Delta\phi_a = -2.1^\circ - (-2.8^\circ) = 0.7^\circ$$

$$\Delta\phi_b = -122.1^\circ - (-122.8^\circ) = 0.7^\circ$$

$$\Delta\phi_c = 117.9^\circ - 117.2^\circ = 0.7^\circ$$

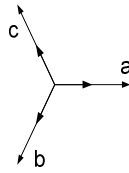
The magnitudes of characteristic voltage and PN factor at MP2 are,

$$U = U_1 = 115 \text{V}, \quad F = U_1 = 115 \text{V}$$

The phase-angle jump of characteristic voltage at MP2 is,

$$\Delta\phi = -2.1^\circ - (-2.8^\circ) = 0.7^\circ$$

The phasor diagram of the three phase voltages is,



Thus, according to Table 2.2, it is classified as sag type A.

According to equation (45), the sag index T is,

$$T = \frac{1}{60^\circ} \times \arg\left(\frac{0}{229 \angle -2.8^\circ - 115 \angle -2.1^\circ}\right) = 0$$

Thus, according to Table 2.3, it is classified as sag type Ca.

● Single-phase-to-ground fault

Assume that zero-sequence impedance of the line model is the same as the positive- and negative-sequence impedance of it.

Seen from the fault point, the Thevenin's equivalent impedance of positive-sequence network can be calculated as,

$$\overline{Z}_1 = \frac{\overline{Z}}{3} // \left(\frac{R}{2} + \frac{\overline{Z}}{3}\right) + \frac{\overline{Z}}{3} = 0.430 \angle 84.9^\circ \Omega$$

The Thevenin's equivalent impedance of negative-sequence network is,

$$\overline{Z}_2 = \overline{Z}_1 = 0.430 \angle 84.9^\circ \Omega$$

The Thevenin's equivalent impedance of zero-sequence network can be calculated as,

$$\bar{Z}_0 = (\bar{Z} // (\bar{Z} + \bar{Z})) = 0.431 \angle 85.6^\circ \Omega$$

According to the sequence network connection of single-phase-to-ground fault, the sequence current can be calculated as,

$$\bar{I}_1 = \bar{I}_2 = \bar{I}_0 = \frac{\bar{E}_1}{\bar{Z}_1 + \bar{Z}_2 + \bar{Z}_0} = \frac{229 \angle -1.4^\circ}{2 \cdot (0.430 \angle 84.9^\circ) + 0.431 \angle 85.6^\circ} = 177 \angle -86.5^\circ \text{ A}$$

The sequence voltages at MP 2 are,

$$\bar{U}_1 = \bar{E}_1 - (\bar{Z}_1 - \frac{\bar{Z}}{3}) \cdot \bar{I}_1 \cdot \frac{R/2}{R/2 + \bar{Z}/3} = 191 \angle -0.9^\circ \text{ V}$$

$$\bar{U}_2 = -(\bar{Z}_2 - \frac{\bar{Z}}{3}) \cdot \bar{I}_2 \cdot \frac{R/2}{R/2 + \bar{Z}/3} = 38.0 \angle 176.3^\circ \text{ V}$$

$$\bar{U}_0 = -\frac{2}{3} \bar{Z} \cdot \bar{I}_0 \cdot \frac{1}{2} = 38.2 \angle -179.1^\circ \text{ V}$$

As a result, the phase voltages at MP 2 are,

$$\begin{bmatrix} \bar{U}_{a2} \\ \bar{U}_{b2} \\ \bar{U}_{c2} \end{bmatrix} = T \begin{bmatrix} \bar{U}_0 \\ \bar{U}_1 \\ \bar{U}_2 \end{bmatrix} = \begin{bmatrix} 1 & 1 & 1 \\ 1 & a^2 & a \\ 1 & a & a^2 \end{bmatrix} \begin{bmatrix} 38.2 \angle -179.1^\circ \\ 191 \angle -0.9^\circ \\ 38.0 \angle 176.3^\circ \end{bmatrix} = \begin{bmatrix} 115 \angle 0 \\ 231 \angle -121.2^\circ \\ 228 \angle 118.9^\circ \end{bmatrix}$$

Therefore, the three-phase retained voltages at MP 2 are,

$$U_a = 115 \text{ V}, U_b = 231 \text{ V}, U_c = 228 \text{ V}$$

The phase-angle jumps at MP 2 are,

$$\Delta\phi_a = 0 - (-2.8^\circ) = 2.8^\circ$$

$$\Delta\phi_b = -121.2^\circ - (-122.8^\circ) = 1.6^\circ$$

$$\Delta\phi_c = 118.9^\circ - 117.2^\circ = 1.7^\circ$$

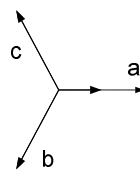
The magnitudes of characteristic voltage and PN factor at MP2 are,

$$U = |\bar{U}_1 + \bar{U}_2| = 153 \text{ V}, F = |\bar{U}_1 - \bar{U}_2| = 229 \text{ V}$$

The phase-angle jump of characteristic voltage at MP2 is,

$$\Delta\phi = -0.2^\circ - (-2.8^\circ) = 2.6^\circ$$

The phasor diagram of the three phase voltages is,



Note that the small phase-angle jumps in the phasor diagram cannot be identified clearly although they actually exist. Thus, according to Table 2.2, it is classified as sag type B.

The sag index T is,

$$T = \frac{1}{60^0} \times \arg\left(\frac{38.0 \angle 176.3^0}{229 \angle -2.8^0 - 191 \angle -0.9^0}\right) = 3.14 \cong 3$$

Thus, according to Table 2.3, it is classified as sag type Da.

● Double-phase fault

According to the sequence network connection of double-phase fault, the sequence fault currents are,

$$\bar{I}_1 = -\bar{I}_2 = \frac{\bar{E}_1}{\bar{Z}_1 + \bar{Z}_2} = \frac{229 \angle -1.4^0}{2 \cdot 0.430 \angle 84.9} = 266 \angle -86.3^0 \text{ A}$$

$$\bar{I}_0 = 0$$

The sequence voltages at MP 2 are,

$$\bar{U}_1 = \bar{E}_1 - (\bar{Z}_1 - \frac{\bar{Z}}{3}) \cdot \bar{I}_1 \cdot \frac{R/2}{R/2 + \bar{Z}/3} = 172 \angle -0.7^0 \text{ V}$$

$$\bar{U}_2 = -(\bar{Z}_2 - \frac{\bar{Z}}{3}) \cdot \bar{I}_2 \cdot \frac{R/2}{R/2 + \bar{Z}/3} = 57.0 \angle -3.5^0 \text{ V}$$

$$\bar{U}_0 = 0$$

As a result, the phase voltages at MP 2 are,

$$\begin{bmatrix} \bar{U}_{a2} \\ \bar{U}_{b2} \\ \bar{U}_{c2} \end{bmatrix} = T \begin{bmatrix} \bar{U}_0 \\ \bar{U}_1 \\ \bar{U}_2 \end{bmatrix} = \begin{bmatrix} 1 & 1 & 1 \\ 1 & a^2 & a \\ 1 & a & a^2 \end{bmatrix} \begin{bmatrix} 0 \\ 172 \angle -0.7^0 \\ 57.0 \angle -3.5^0 \end{bmatrix} = \begin{bmatrix} 229 \angle -1.4^0 \\ 149 \angle -139.5^0 \\ 154 \angle 138.5^0 \end{bmatrix}$$

Therefore, the three-phase retained voltages at MP 2 are,

$$U_a = 229 \text{ V}, U_b = 149 \text{ V}, U_c = 154 \text{ V}$$

The phase-angle jumps at MP 2 are,

$$\Delta\phi_a = -1.4^0 - (-2.8^0) = 1.4^0$$

$$\Delta\phi_b = -139.5^0 - (-122.8^0) = -16.7^0$$

$$\Delta\phi_c = 138.5^0 - 117.2^0 = 21.3^0$$

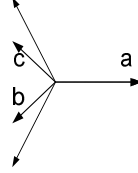
The magnitudes of characteristic voltage and PN factor at MP2 are,

$$U = |\overline{U}_1 - \overline{U}_2| = 115V, \quad F = |\overline{U}_1 + \overline{U}_2| = 229V$$

The phase-angle jump of characteristic voltage at MP2 is,

$$\Delta\phi = 0.7^\circ - (-2.8^\circ) = 3.5^\circ$$

The phasor diagram of the three phase voltages is,



Thus, according to Table 2.2, it is classified as sag type C.

The sag index T is,

$$T = \frac{1}{60^\circ} \times \arg\left(\frac{57.0\angle -3.5^\circ}{229\angle -2.8^\circ - 172\angle -0.7^\circ}\right) = 0.09 \cong 0$$

Thus, according to Table 2.3, it is classified as sag type Ca.

● Double-phase-to-ground fault

According to the sequence network connection of double-phase-to-ground fault, the sequence fault currents are,

$$\overline{I}_1 = \frac{\overline{E}_1}{\overline{Z}_1 + \overline{Z}_2 // \overline{Z}_0} = \frac{229\angle -1.4^\circ}{0.430\angle 84.9^\circ + 0.430\angle 84.9^\circ // 0.431\angle 85.6^\circ} = 354\angle -86.4^\circ \text{ A}$$

$$\overline{I}_2 = -\frac{\overline{Z}_0}{\overline{Z}_2 + \overline{Z}_0} \cdot \overline{I}_1 = -\frac{0.431\angle 85.6^\circ}{0.430\angle 84.9^\circ + 0.431\angle 85.6^\circ} \cdot 354\angle -86.4^\circ = 177\angle 93.9^\circ \text{ A}$$

$$\overline{I}_0 = -\overline{I}_1 - \overline{I}_2 = -356\angle -85.0^\circ - 178\angle 95.3^\circ = 177\angle 93.3^\circ \text{ A}$$

The sequence voltages at MP 2 are,

$$\overline{U}_1 = \overline{E}_1 - (\overline{Z}_1 - \frac{\overline{Z}}{3}) \cdot \overline{I}_1 \cdot \frac{R/2}{R/2 + \overline{Z}/3} = 153\angle -0.3^\circ \text{ V}$$

$$\overline{U}_2 = -(\overline{Z}_2 - \frac{\overline{Z}}{3}) \cdot \overline{I}_2 \cdot \frac{R/2}{R/2 + \overline{Z}/3} = 37.9\angle -3.3^\circ \text{ V}$$

$$\overline{U}_0 = -\frac{2}{3}\overline{Z} \cdot \overline{I}_0 \cdot \frac{1}{2} = 38.1\angle -1.1^\circ \text{ V}$$

As a result, the phase voltages at MP 2 are,

$$\begin{bmatrix} \overline{U}_{a2} \\ \overline{U}_{b2} \\ \overline{U}_{c2} \end{bmatrix} = T \begin{bmatrix} \overline{U}_0 \\ \overline{U}_1 \\ \overline{U}_2 \end{bmatrix} = \begin{bmatrix} 1 & 1 & 1 \\ 1 & a^2 & a \\ 1 & a & a^2 \end{bmatrix} \begin{bmatrix} 38.1\angle -1.1^\circ \\ 153\angle -0.3^\circ \\ 37.9\angle -3.3^\circ \end{bmatrix} = \begin{bmatrix} 229\angle -0.9^\circ \\ 114\angle -119.6^\circ \\ 117\angle 120.2^\circ \end{bmatrix}$$

Therefore, the three-phase retained voltages at MP 2 are,

$$U_a = 229V, U_b = 114V, U_c = 117V$$

The phase-angle jumps at MP 2 are,

$$\Delta\phi_a = -0.9^\circ - (-2.8^\circ) = 1.9^\circ$$

$$\Delta\phi_b = -119.6^\circ - (-122.8^\circ) = 3.2^\circ$$

$$\Delta\phi_c = 120.2^\circ - 117.2^\circ = 3.0^\circ$$

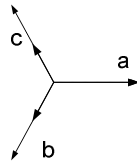
The magnitudes of characteristic voltage and PN factor at MP2 are,

$$U = |\overline{U}_1 - \overline{U}_2| = 115V, F = |\overline{U}_1 + \overline{U}_2| = 191V$$

The phase-angle jump of characteristic voltage at MP2 is,

$$\Delta\phi = 0.7^\circ - (-2.8^\circ) = 3.5^\circ$$

The phasor diagram of the three phase voltages is,



Thus, according to Table 2.2, it is classified as sag type E.

The sag index T is,

$$T = \frac{1}{60^\circ} \times \arg\left(\frac{37.9 \angle -3.3^\circ}{229 \angle -2.8^\circ - 153 \angle -0.3^\circ}\right) = 0.08 \cong 0$$

Thus, according to Table 2.3, it is classified as sag type Ca.

C.2 Simulations using PSCAD

For further understanding the effect of unbalanced faults on the power system, simulation of faults in the previous analyzed circuits are implemented individually. There are a number of simulation tools available, for example, SIMULINK, PSPICE, ATP, EMTP, PSCAD/EMTDC, etc. Therefore, we can use any of them to simulate different kind of faults in the power system. In this thesis, PSCAD/EMTDC is adopted for the simulation of faults in the four pre-defined circuits. The configurations constructed in PSCAD are shown in Appendix A.

The three-phase voltages at corresponding PCC buses are measured and recorded, for basic circuit, voltage-divider circuit, open-line circuit and fault-line circuit, respectively. The voltage data are transferred and processed using MATLAB algorithm. Fundamental rms voltages and phase-angle jumps for different circuits from the simulation are plotted and shown in the following figures.

The ideal three-phase voltage source is chosen in the simulation, because the source impedance is relatively small compared with the transmission line impedance. As the monitoring point 1 is, in Fault-line circuit, directly connected to the terminal of the voltage source, for different kinds of shunt faults at the transmission line, the voltages at MP1 will be always equal to source voltages. Therefore, for any kind of the four shunt faults, the phase voltage as well as positive-sequence voltage at MP 1 is always,

$$\overline{U_{PCC1}} = \overline{E_a} = 230\angle 0V$$

The three-phase retained voltages at MP 1 are always,

$$U_a = U_b = U_c = 230V$$

The phase-angle jumps at MP 1 are always,

$$\Delta\phi_a = 0 - 0 = 0$$

$$\Delta\phi_b = -120^\circ - (-120^\circ) = 0$$

$$\Delta\phi_c = 120^\circ - 120^\circ = 0$$

The magnitudes of characteristic voltage and PN factor at MP1 are always,

$$U = 230V, F = 230V$$

The phase-angle jump of characteristic voltage at MP1 is always,

$$\Delta\phi = 0$$

For the following data processing, only voltages at MP2 will be shown.

C.2.1 Basic circuit

- Three-phase-to-ground fault

As shown in Fig.C.1, the three-phase retained voltages at PCC are,

$$U_a = 92.0V , U_b = 92.0V , U_c = 92.0V$$

The phase-angle jumps at PCC are,

$$\Delta\phi_a = 0 , \Delta\phi_b = 0 , \Delta\phi_c = 0$$

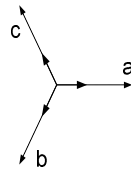
The magnitudes of characteristic voltage and PN factor at PCC are,

$$U = 92.0V , F = 92.0V$$

The phase-angle jump of characteristic voltage at PCC is,

$$\Delta\phi = 0$$

The phasor diagram of the three phase voltages is,



Thus, according to Table 2.2, it is classified as sag type A.

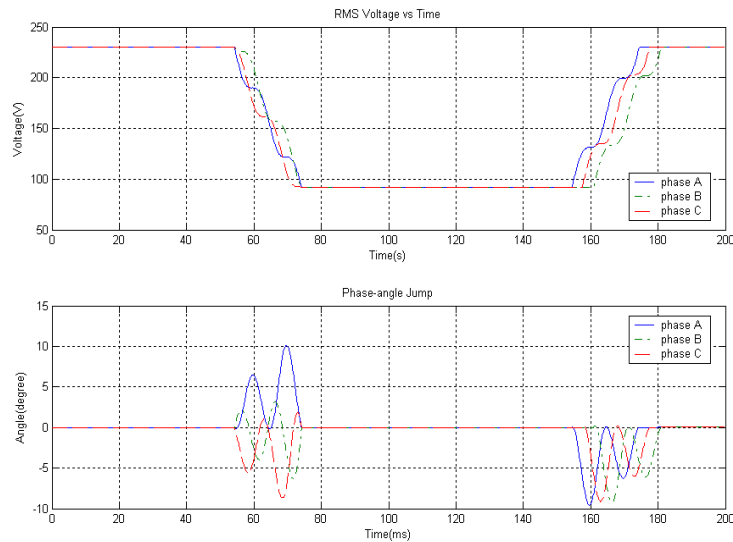
The sequence voltages calculated from the three phasors at PCC are,

$$\overline{U}_1 = 92\angle 0V , \overline{U}_2 = 0$$

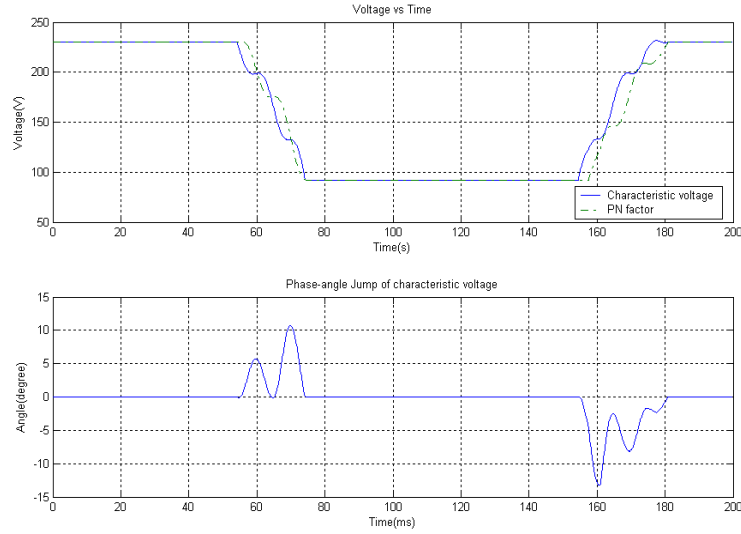
According to equation (45), the sag index T is,

$$T = \frac{1}{60^0} \times \arg\left(\frac{0}{230\angle 0 - 92\angle 0}\right) = 0$$

Thus, according to Table 2.3, it is classified as sag type Ca.



(a) Three-phase voltages



(b) Characteristic voltage and PN factor

Fig. C.1 Three-phase-to-ground fault (basic circuit, simulation)

- **Single-phase-to-ground fault**

As shown in Fig.C.2, the three-phase retained voltages at PCC are,

$$U_a = 92.0V, U_b = 230V, U_c = 230V$$

The phase-angle jumps at PCC are,

$$\Delta\phi_a = 0, \Delta\phi_b = 0, \Delta\phi_c = 0$$

The magnitudes of characteristic voltage and PN factor at PCC are,

$$U = 138V, F = 230V$$

The phase-angle jump of characteristic voltage at PCC is,

$$\Delta\phi = 0$$

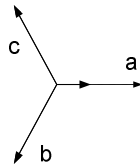
The magnitudes of characteristic voltage and PN factor at PCC are,

$$U = 138.0V, F = 230V$$

The phase-angle jump of characteristic voltage at PCC is,

$$\Delta\phi = 0$$

The phasor diagram of the three phase voltages is,



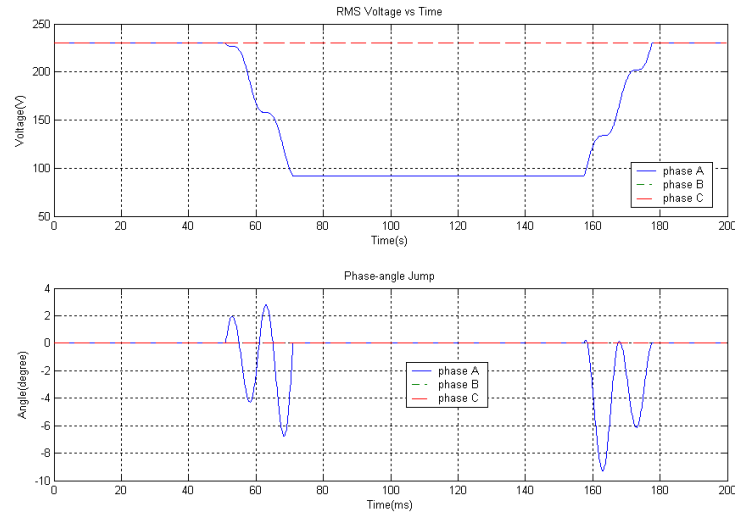
The sequence voltages calculated from the three phasors at PCC are,

$$\overline{U}_1 = 184\angle 0V, \overline{U}_2 = -46.0\angle 0V$$

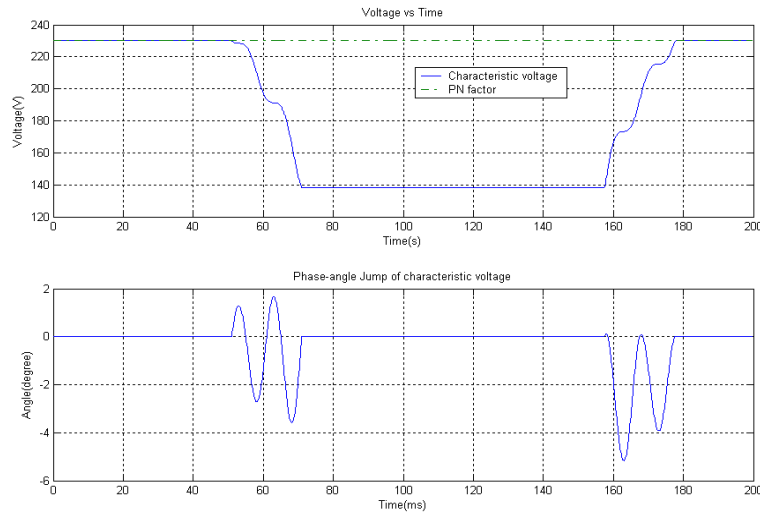
The sag index T is,

$$T = \frac{1}{60^0} \times \arg\left(\frac{-46.0\angle 0}{230\angle 0 - 184\angle 0}\right) = 3$$

Thus, according to Table 2.3, it is classified as sag type Da.



(a) Three-phase voltages



(b) Characteristic voltage and PN factor

Fig. C.2 Single-phase-to-ground fault (basic circuit, simulation)

● Double-phase fault

As shown in Fig.C.3, the three-phase retained voltages at PCC are,

$$U_a = 230V, U_b = 140V, U_c = 140V$$

The phase-angle jumps at PCC are,

$$\Delta\phi_a = 0, \Delta\phi_b = -25.3^0, \Delta\phi_c = 25.3^0$$

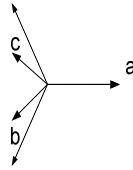
The magnitudes of characteristic voltage and PN factor at PCC are,

$$U = 92V, F = 230V$$

The phase-angle jump of characteristic voltage at PCC is,

$$\Delta\phi = 0$$

The phasor diagram of the three phase voltages is,



Thus, according to Table 2.2, it is classified as sag type C.

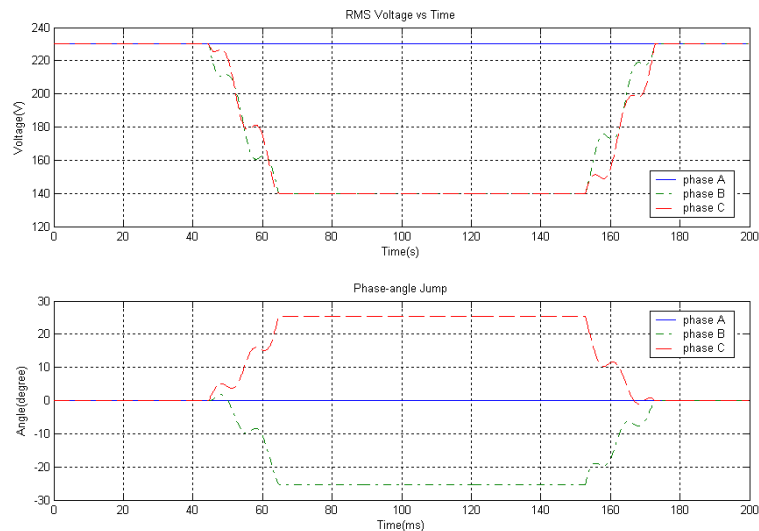
The sequence voltages calculated from the three phasors at PCC are,

$$\overline{U}_1 = 161\angle 0V, \quad \overline{U}_2 = 69.0\angle 0V$$

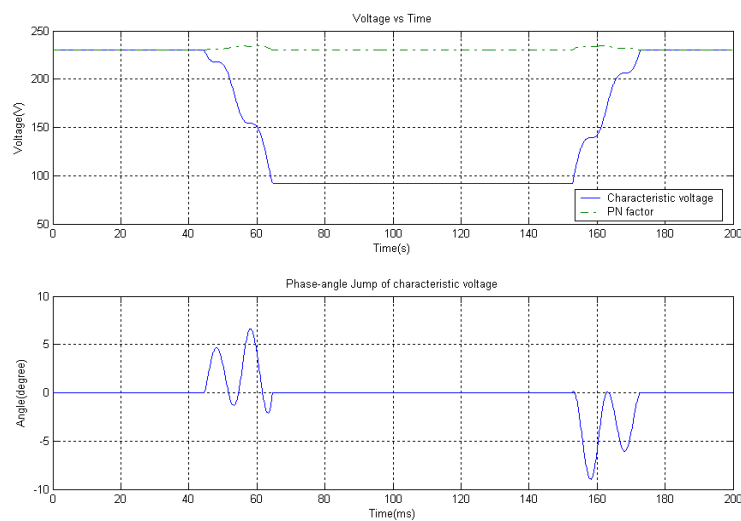
The sag index T is,

$$T = \frac{1}{60^0} \times \arg\left(\frac{69.0\angle 0}{230\angle 0 - 161\angle 0}\right) = 0$$

Thus, according to Table 2.3, it is classified as sag type Ca.



(a) Three-phase voltages



(b) Characteristic voltage and PN factor

Fig. C.3 Double-phase fault (basic circuit, simulation)

● **Double-phase-to-ground fault**

As shown in Fig.C.4, the three-phase retained voltages at PCC are,

$$U_a = 230V, U_b = 92.0V, U_c = 92.0V$$

The phase-angle jumps at PCC are,

$$\Delta\phi_a = 0, \Delta\phi_b = 0, \Delta\phi_c = 0$$

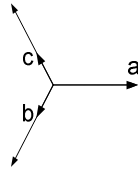
The magnitudes of characteristic voltage and PN factor at PCC are,

$$U = 92.0V, F = 184V$$

The phase-angle jump of characteristic voltage at PCC is,

$$\Delta\phi = 0$$

The phasor diagram of the three phase voltages is,



Thus, according to Table 2.2, it is classified as sag type E.

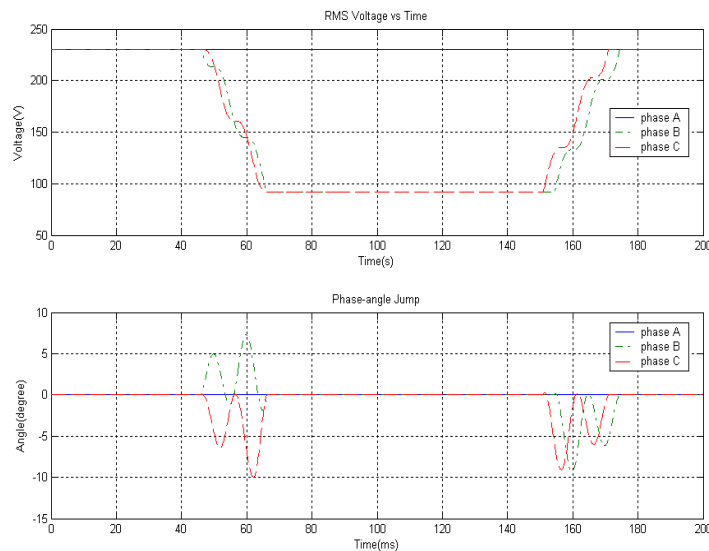
The sequence voltages calculated from the three phasors at PCC are,

$$\overline{U}_1 = 138\angle 0V, \overline{U}_2 = 46.0\angle 0V$$

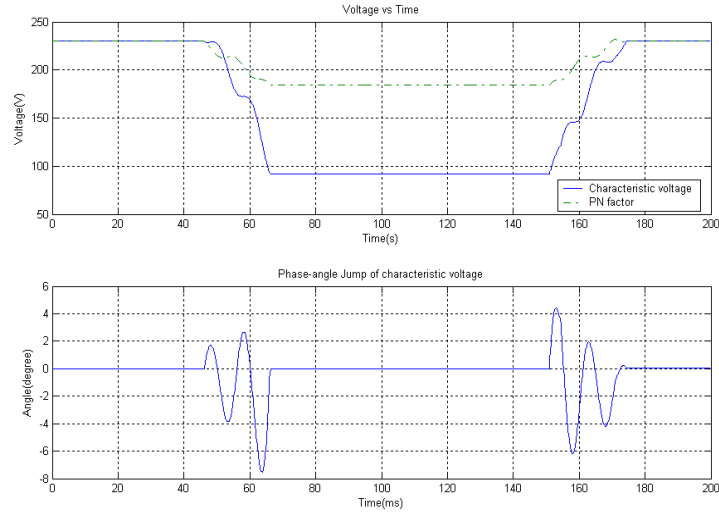
The sag index T is,

$$T = \frac{1}{60^0} \times \arg\left(\frac{46.0\angle 0}{230\angle 0 - 138\angle 0}\right) = 0$$

Thus, according to Table 2.3, it is classified as sag type Ca.



(a) Three-phase voltages



(b) Characteristic voltage and PN factor

Fig. C.4 Double-phase-to-ground fault (basic circuit, simulation)

C.2.2 Voltage-divider circuit

✧ NO LOAD CONDITION

● Three-phase-to-ground fault

As shown in Fig.C.5, the three-phase retained voltages at PCC are,

$$U_a = 153V, U_b = 153V, U_c = 153V$$

The phase-angle jumps at PCC are,

$$\Delta\phi_a = 0, \Delta\phi_b = 0, \Delta\phi_c = 0$$

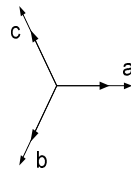
The magnitudes of characteristic voltage and PN factor at PCC are,

$$U = 153V, F = 153V$$

The phase-angle jump of characteristic voltage at PCC is,

$$\Delta\phi = 0$$

The phasor diagram of the three phase voltages is,



Thus, according to Table 2.2, it is classified as sag type A.

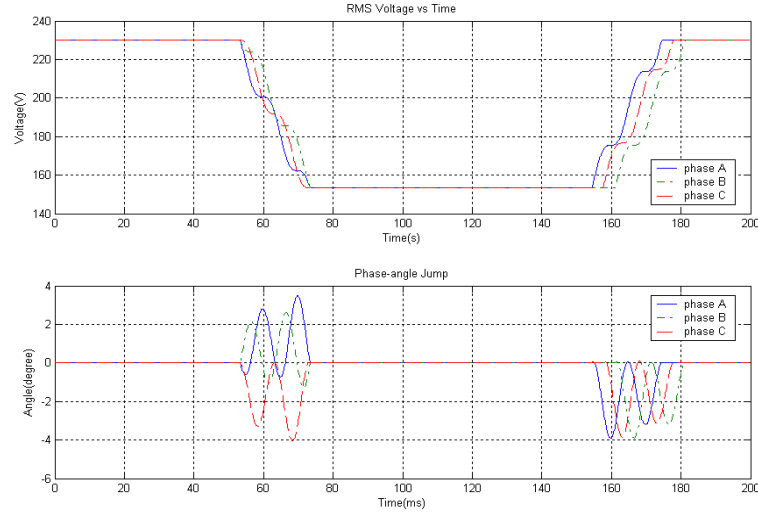
The sequence voltages calculated from the three phasors at PCC are,

$$\overline{U_1} = 153\angle 0V, \overline{U_2} = 0$$

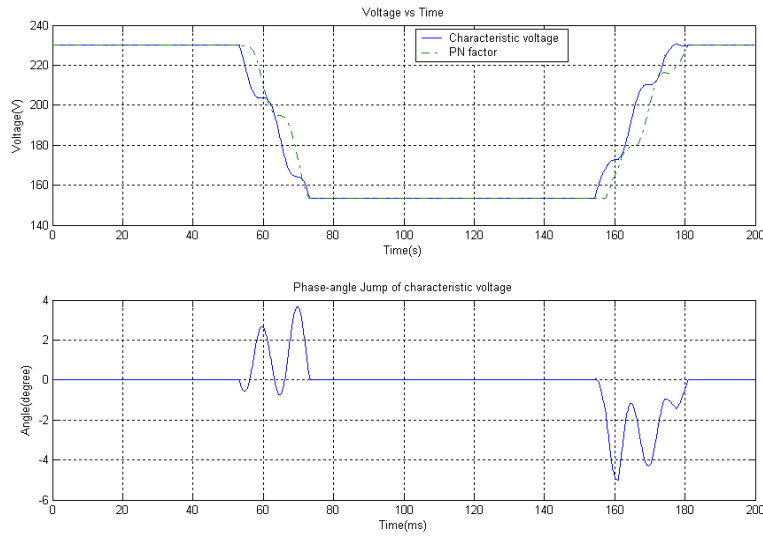
According to equation (45), the sag index T is,

$$T = \frac{1}{60^0} \times \arg\left(\frac{0}{230\angle 0 - 153\angle 0}\right) = 0$$

Thus, according to Table 2.3, it is classified as sag type Ca.



(a) Three-phase voltages



(b) Characteristic voltage and PN factor

Fig. C.5 Three-phase-to-ground fault (voltage-divider, simulation)

● Single-phase-to-ground fault

As shown in Fig.C.6, the three-phase retained voltages at PCC are,

$$U_a = 153V, U_b = 230V, U_c = 230V$$

The phase-angle jumps at PCC are,

$$\Delta\phi_a = 0, \Delta\phi_b = 0, \Delta\phi_c = 0$$

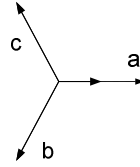
The magnitudes of characteristic voltage and PN factor at PCC are,

$$U = 179V, F = 230V$$

The phase-angle jump of characteristic voltage at PCC is,

$$\Delta\phi = 0$$

The phasor diagram of the three phase voltages is,



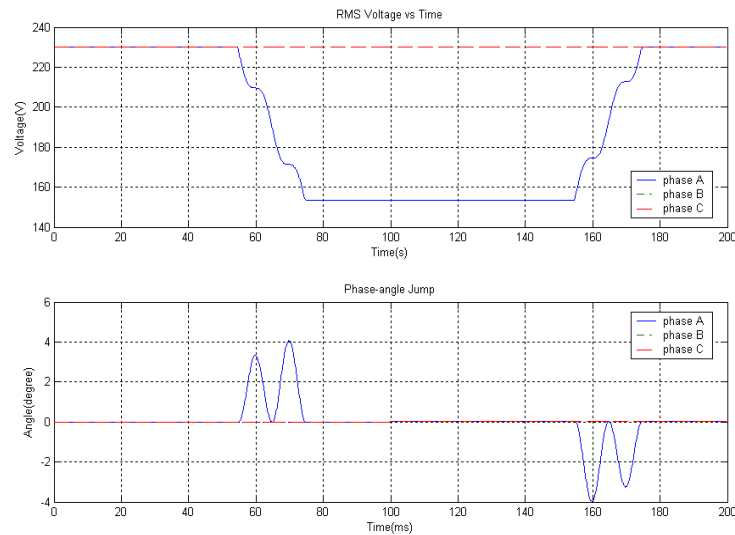
The sequence voltages calculated from the three phasors at PCC are,

$$\overline{U}_1 = -25.6\angle 0V, \quad \overline{U}_2 = 204\angle 0V$$

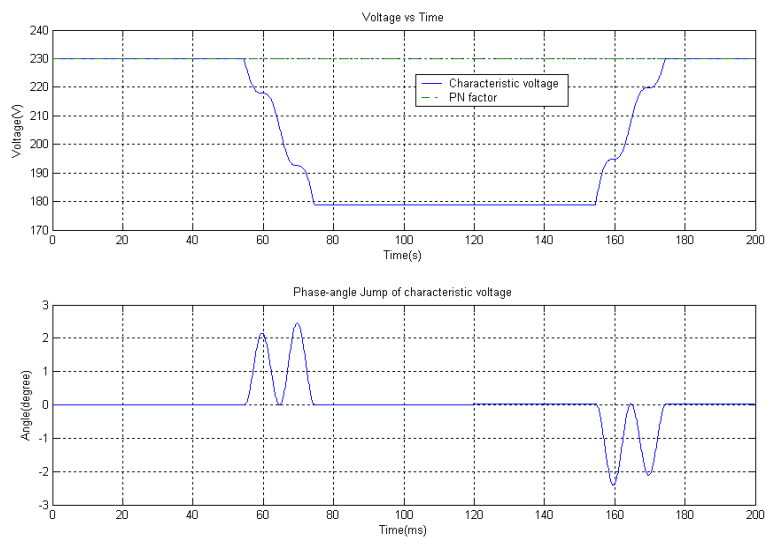
The sag index T is,

$$T = \frac{1}{60^\circ} \times \arg\left(\frac{204\angle 0}{230\angle 0 + 25.6\angle 0}\right) = 3$$

Thus, according to Table 2.3, it is classified as sag type Da.



(a) Three-phase voltages



(b) Characteristic voltage and PN factor

Fig. C.6 Single-phase-to-ground fault (voltage-divider, simulation)

● **Double-phase fault**

As shown in Fig.C.7, the three-phase retained voltages at PCC are,

$$U_a = 230V, U_b = 176V, U_c = 176V$$

The phase-angle jumps at PCC are,

$$\Delta\phi_a = 0, \Delta\phi_b = -10.9^\circ, \Delta\phi_c = 10.9^\circ$$

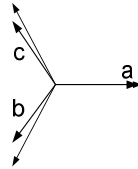
The magnitudes of characteristic voltage and PN factor at PCC are,

$$U = 153V, F = 230V$$

The phase-angle jump of characteristic voltage at PCC is,

$$\Delta\phi = 0$$

The phasor diagram of the three phase voltages is,



Thus, according to Table 2.2, it is classified as sag type C.

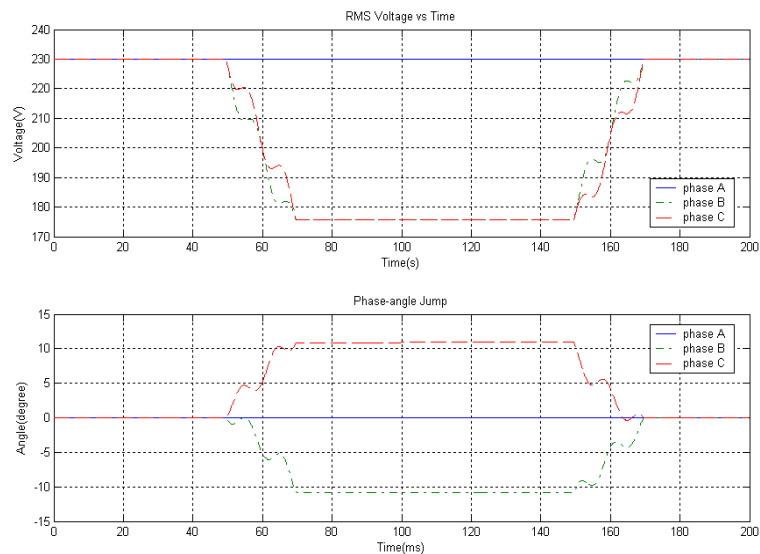
The sequence voltages calculated from the three phasors at PCC are,

$$\bar{U}_1 = 192\angle 0V, \bar{U}_2 = 38.3\angle 0V$$

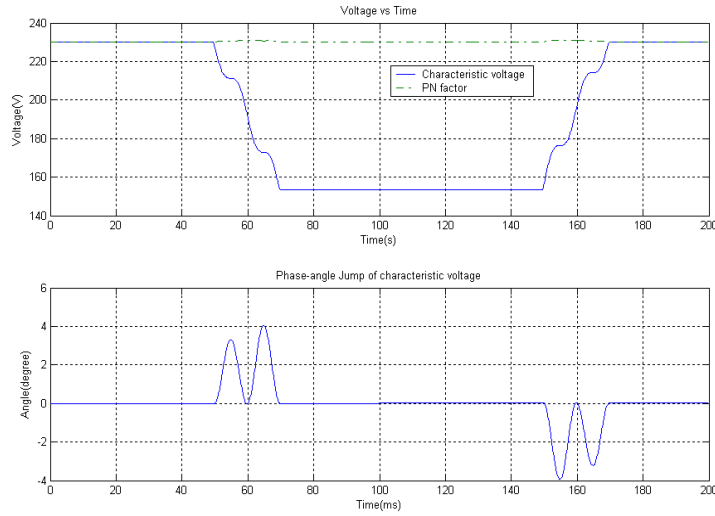
The sag index T is,

$$T = \frac{1}{60^\circ} \times \arg\left(\frac{38.3\angle 0}{230\angle 0 - 192\angle 0}\right) = 0$$

Thus, according to Table 2.3, it is classified as sag type Ca.



(a) Three-phase voltages



(b) Characteristic voltage and PN factor

Fig. C.7 Double-phase fault (voltage-divider, simulation)

- **Double-phase-to-ground fault**

As shown in Fig.C.8, the three-phase retained voltages at PCC are,

$$U_a = 230V, U_b = 153V, U_c = 153V$$

The phase-angle jumps at PCC are,

$$\Delta\phi_a = 0, \Delta\phi_b = 0, \Delta\phi_c = 0$$

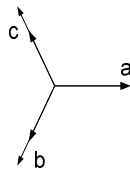
The magnitudes of characteristic voltage and PN factor at PCC are,

$$U = 153V, F = 204V$$

The phase-angle jump of characteristic voltage at PCC is,

$$\Delta\phi = 0$$

The phasor diagram of the three phase voltages is,



Thus, according to Table 2.2, it is classified as sag type E.

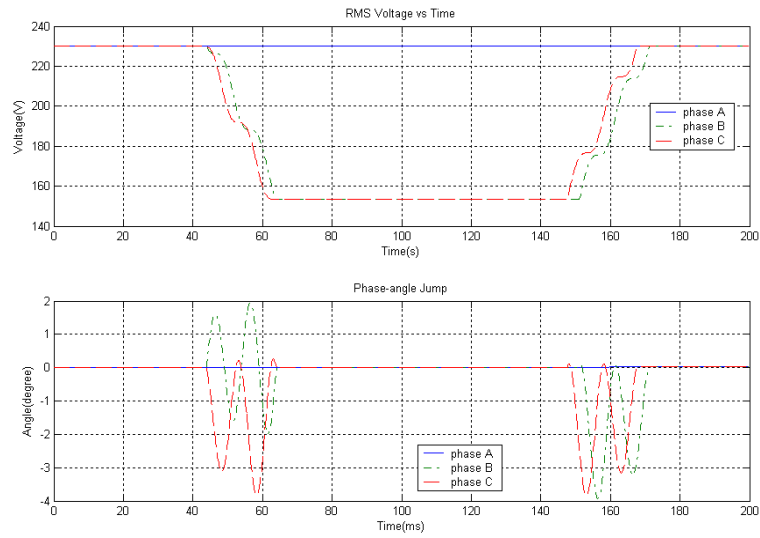
The sequence voltages calculated from the three phasors at PCC are,

$$\overline{U}_1 = 179\angle 0V, \overline{U}_2 = 25.6\angle 0V$$

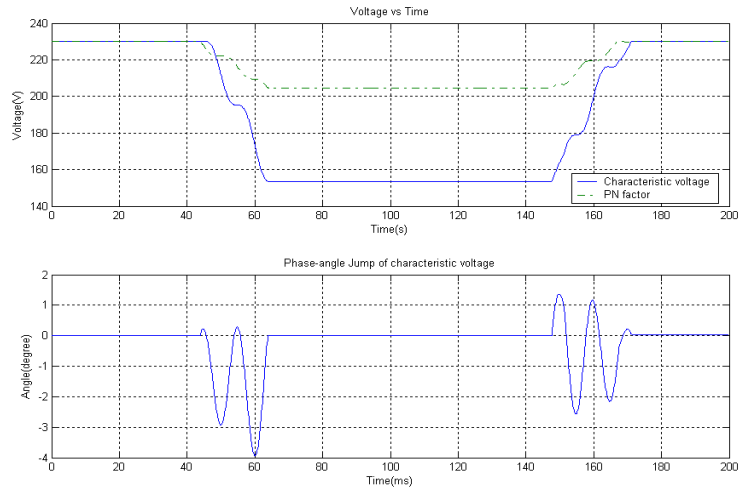
The sag index T is,

$$T = \frac{1}{60^0} \times \arg\left(\frac{25.6\angle 0}{230\angle 0 - 179\angle 0}\right) = 0$$

Thus, according to Table 2.3, it is classified as sag type Ca.



(a) Three-phase voltages



(b) Characteristic voltage and PN factor

Fig. C.8 Double-phase-to-ground fault (voltage-divider, simulation)

✧ LOAD: INDUCTION MACHINE

● Three-phase-to-ground fault

As shown in Fig.C.9, the three-phase retained voltages at PCC are,

$$U_a = 155V, U_b = 155V, U_c = 155V$$

The phase-angle jumps at PCC are,

$$\Delta\phi_a = -1.1^\circ, \Delta\phi_b = -1.1^\circ, \Delta\phi_c = -1.1^\circ$$

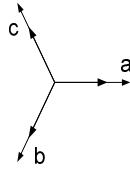
The magnitudes of characteristic voltage and PN factor at PCC are,

$$U = 155V, F = 155V$$

The phase-angle jump of characteristic voltage at PCC is,

$$\Delta\phi = -1.1^\circ$$

The phasor diagram of the three phase voltages is,



Thus, according to Table 2.2, it is classified as sag type A.

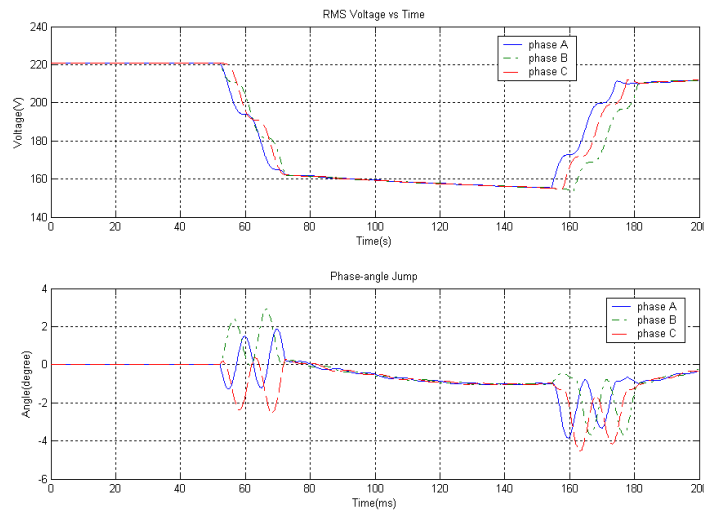
The sequence voltages calculated from the three phasors at PCC are,

$$\overline{U}_1 = 155\angle 0V, \quad \overline{U}_2 = 0$$

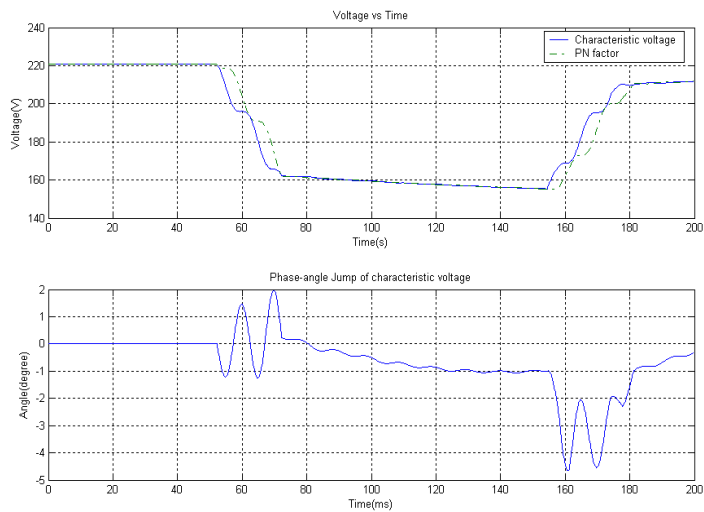
If we assume the pre-fault voltage at PCC is $220\angle 0V$, according to equation (45), the sag index T is,

$$T = \frac{1}{60^\circ} \times \arg\left(\frac{0}{220\angle 0 - 155\angle 0}\right) = 0$$

Thus, according to Table 2.3, it is classified as sag type Ca.



(a) Three-phase voltages



(b) Characteristic voltage and PN factor

Fig. C.9 Three-phase-to-ground fault (voltage-divider with IM, simulation)

● **Single-phase-to-ground fault**

As shown in Fig.C.10, the three-phase retained voltages at PCC are,

$$U_a = 155V, U_b = 225V, U_c = 224V$$

The phase-angle jumps at PCC are,

$$\Delta\phi_a = 0.4^\circ, \Delta\phi_b = -2.1^\circ, \Delta\phi_c = 1.7^\circ$$

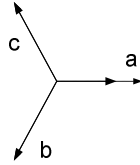
The magnitudes of characteristic voltage and PN factor at PCC are,

$$U = 181V, F = 217V$$

The phase-angle jump of characteristic voltage at PCC is,

$$\Delta\phi = 0.4^\circ$$

The phasor diagram of the three phase voltages is,



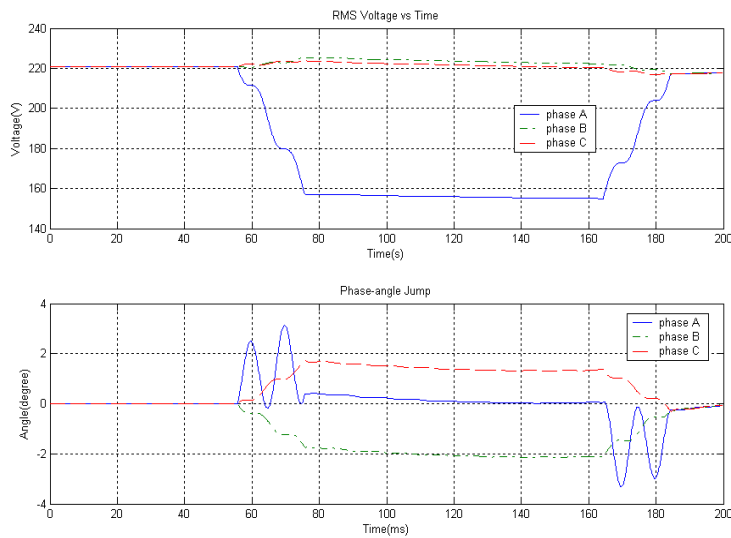
The sequence voltages calculated from the three phasors at PCC are,

$$\overline{U}_1 = 201\angle 0^\circ V, \overline{U}_2 = 18.8\angle 177.3^\circ V$$

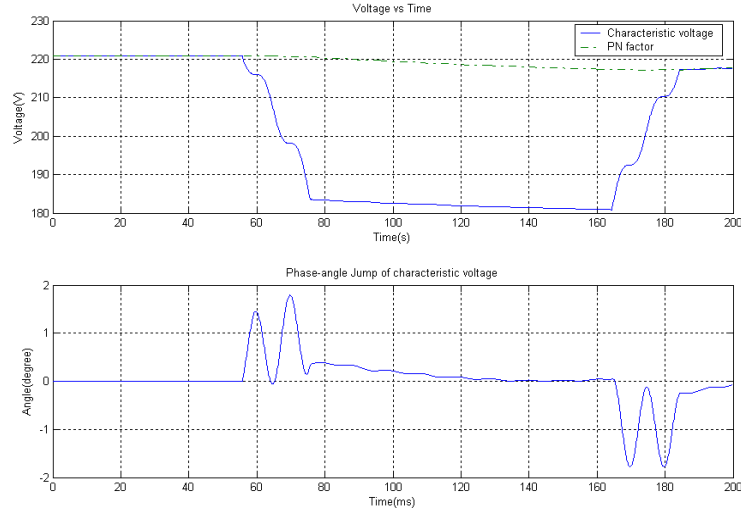
The sag index T is,

$$T = \frac{1}{60^\circ} \times \arg\left(\frac{18.8\angle 177.3^\circ}{220\angle 0^\circ - 201\angle 0^\circ}\right) = 2.95 \cong 3$$

Thus, according to Table 2.3, it is classified as sag type Da.



(a) Three-phase voltages



(b) Characteristic voltage and PN factor

Fig. C.10 Single-phase-to-ground fault (voltage-divider with IM, simulation)

● Double-phase fault

As shown in Fig.C.11, the three-phase retained voltages at PCC are,

$$U_a = 215V, U_b = 174V, U_c = 176V$$

The phase-angle jumps at PCC are,

$$\Delta\phi_a = -1.0^\circ, \Delta\phi_b = -8.5^\circ, \Delta\phi_c = 8.3^\circ$$

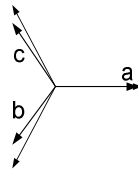
The magnitudes of characteristic voltage and PN factor at PCC are,

$$U = 159V, F = 215V$$

The phase-angle jump of characteristic voltage at PCC is,

$$\Delta\phi = 0.6^\circ$$

The phasor diagram of the three phase voltages is,



Thus, according to Table 2.2, it is classified as sag type C.

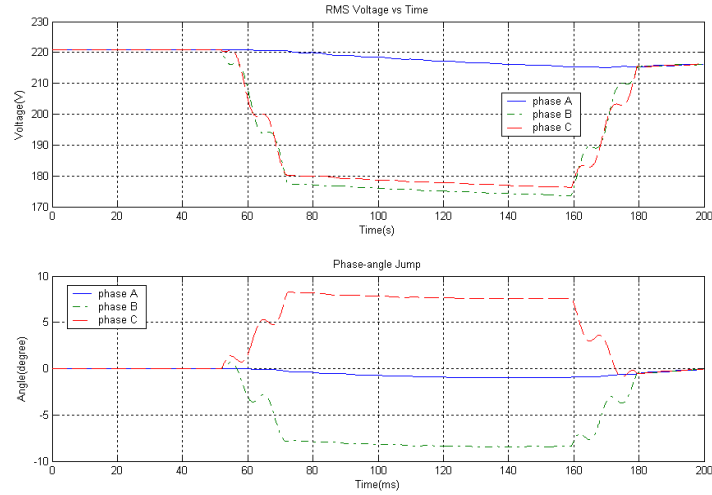
The sequence voltages calculated from the three phasors at PCC are,

$$\overline{U}_1 = 187 \angle -0.4^\circ V, \overline{U}_2 = 28.8 \angle -3.6^\circ V$$

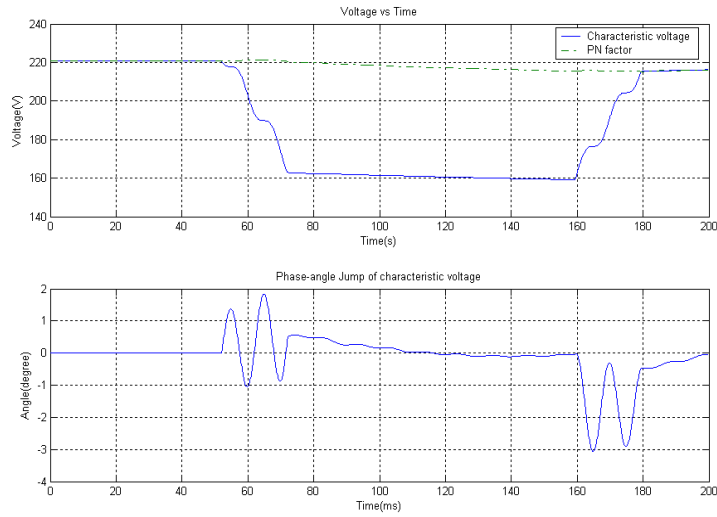
The sag index T is,

$$T = \frac{1}{60^\circ} \times \arg\left(\frac{28.8 \angle -3.6^\circ}{220 \angle 0^\circ - 187 \angle -0.4^\circ}\right) = 0.1 \cong 0$$

Thus, according to Table 2.3, it is classified as sag type Ca.



(a) Three-phase voltages



(b) Characteristic voltage and PN factor

Fig. C.11 Double-phase fault (voltage-divider with IM, simulation)

- **Double-phase-to-ground fault**

As shown in Fig.C.12, the three-phase retained voltages at PCC are,

$$U_a = 228V, U_b = 155V, U_c = 156V$$

The phase-angle jumps at PCC are,

$$\Delta\phi_a = -1.0^{\circ}, \Delta\phi_b = 2.0^{\circ}, \Delta\phi_c = -2.2^{\circ}$$

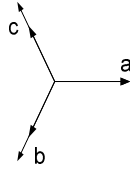
The magnitudes of characteristic voltage and PN factor at PCC are,

$$U = 158V, F = 196V$$

The phase-angle jump of characteristic voltage at PCC is,

$$\Delta\phi = -0.4^{\circ}$$

The phasor diagram of the three phase voltages is,



Thus, according to Table 2.2, it is classified as sag type E.

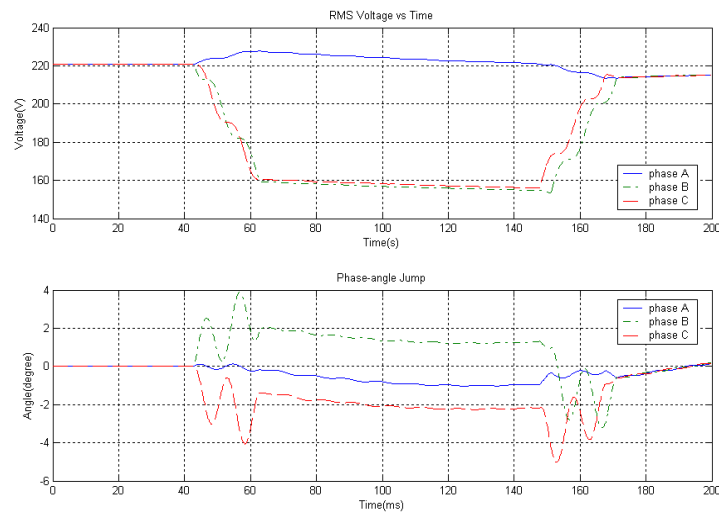
The sequence voltages calculated from the three phasors at PCC are,

$$\overline{U}_1 = 180 \angle -0.5^\circ V, \quad \overline{U}_2 = 21.0 \angle -4.1^\circ V$$

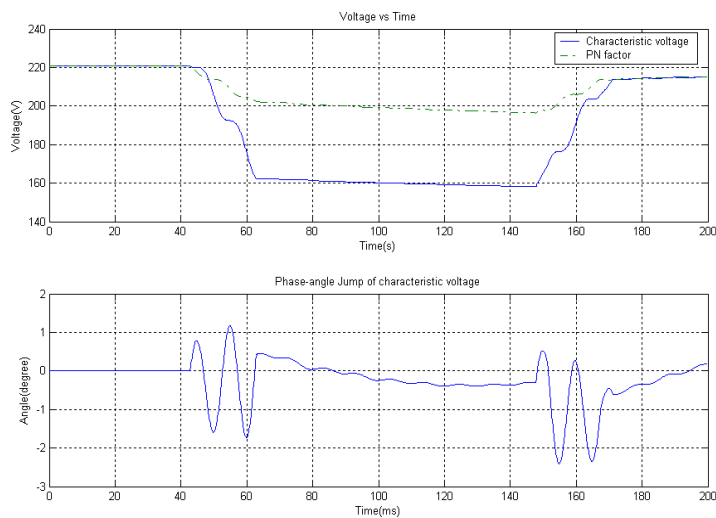
The sag index T is,

$$T = \frac{1}{60^\circ} \times \arg\left(\frac{21.0 \angle -4.1^\circ}{220 \angle 0 - 180 \angle -0.5^\circ}\right) = 0.1 \cong 0$$

Thus, according to Table 2.3, it is classified as sag type Ca.



(a) Three-phase voltages



(b) Characteristic voltage and PN factor

Fig. C.12 Double-phase-to-ground fault (voltage-divider with IM, simulation)

C.2.3 Fault-load circuit

◇ TWO RESISTIVE LOADS

● Three-phase-to-ground fault

As shown in Fig.C.13, the three-phase retained voltages at MP are,

$$U_a = 0, U_b = 0, U_c = 0$$

The phase-angle jumps at MP are not applicable.

The magnitudes of characteristic voltage and PN factor at MP are,

$$U = 0, F = 0$$

The phase-angle jump of characteristic voltage at MP is not applicable,

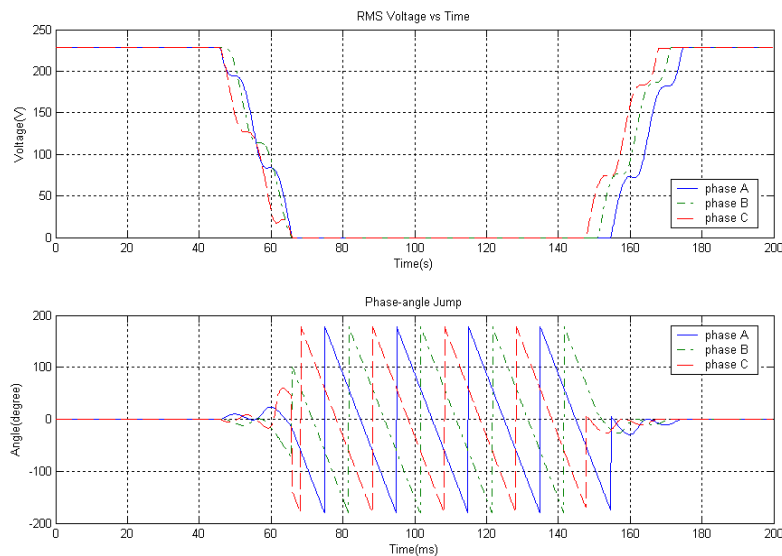
There is no phasor diagram of the three phase voltages.

Thus, according to Table 2.2, it can be classified as any sag type, i.e. sag type A.

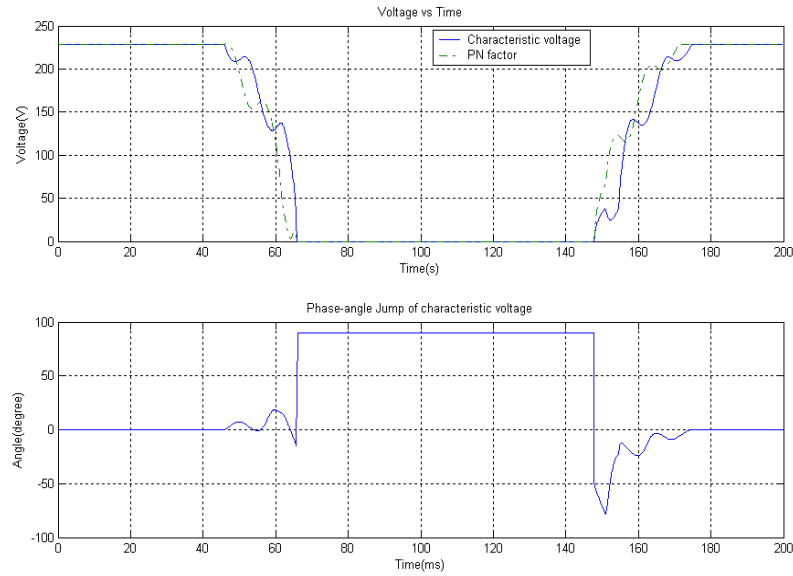
If assume the pre-fault voltage at MP2 to be $229\angle 0V$, according to equation (45), the sag index T is,

$$T = \frac{1}{60^0} \times \arg\left(\frac{0}{229\angle 0 - 0}\right) = 0$$

Thus, according to Table 2.3, it is classified as sag type Ca.



(a) Three-phase voltages



(b) Characteristic voltage and PN factor

Fig. C.13 Three-phase-to-ground fault (fault-load with two resistive loads, simulation)

- **Single-phase-to-ground fault**

As shown in Fig.C.14, the three-phase retained voltages at MP are,

$$U_a = 0, \quad U_b = 232V, \quad U_c = 226V$$

The phase-angle jumps at MP are,

$$\Delta\phi_a \text{ (Not applicable)}, \quad \Delta\phi_b = 0.4^{\circ}, \quad \Delta\phi_c = 0.6^{\circ}$$

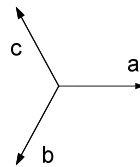
The magnitudes of characteristic voltage and PN factor at MP are,

$$U = 77V, \quad F = 229V$$

The phase-angle jump of characteristic voltage at MP is,

$$\Delta\phi = 1.9^{\circ}$$

The phasor diagram of the three phase voltages is,



Thus, according to Table 2.2, it is classified as sag type B.

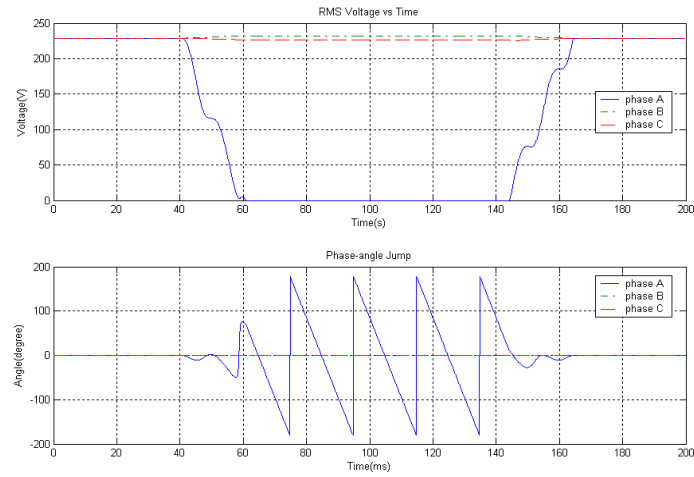
The sequence voltages calculated from the three phasors at MP2 are,

$$\overline{U_1} = 153\angle -2.3^{\circ}V, \quad \overline{U_2} = 76.1\angle 176.4^{\circ}V$$

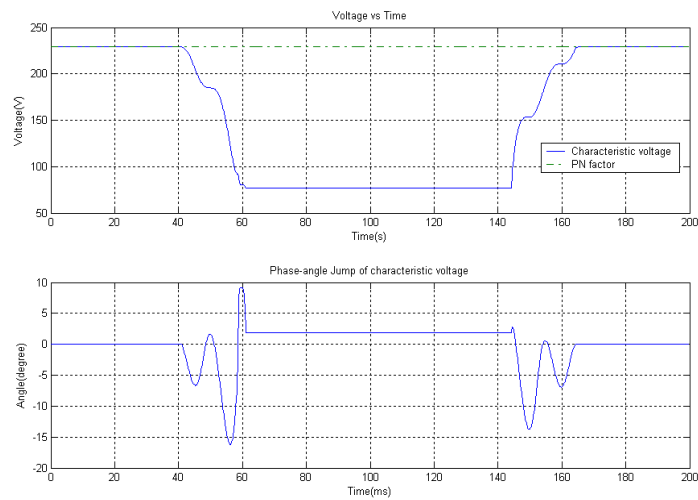
The sag index T is,

$$T = \frac{1}{60^{\circ}} \times \arg\left(\frac{76.1\angle 176.4^{\circ}}{229\angle 0 - 153\angle -2.3^{\circ}}\right) = 2.9 \cong 3$$

Thus, according to Table 2.3, it is classified as sag type Da.



(a) Three-phase voltages



(b) Characteristic voltage and PN factor

Fig. C.14 Single-phase-to-ground fault (fault-load with two resistive loads, simulation)

● Double-phase fault

As shown in Fig.C.15, the three-phase retained voltages at MP are,

$$U_a = 229V, U_b = 114V, U_c = 114V$$

The phase-angle jumps at MP are,

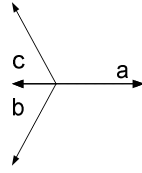
$$\Delta\phi_a = 0, \Delta\phi_b = -60^0, \Delta\phi_c = 60^0$$

The magnitudes of characteristic voltage and PN factor at MP are,

$$U = 0, F = 229V$$

The phase-angle jump of characteristic voltage at MP is not applicable.

The phasor diagram of the three phase voltages is,



Thus, according to Table 2.2, it is classified as sag type C.

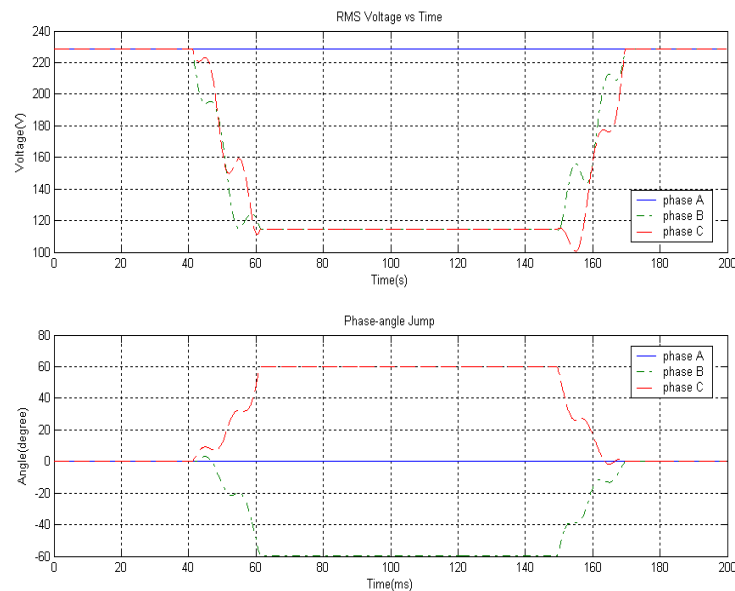
The sequence voltages calculated from the three phasors at MP2 are,

$$\overline{U}_1 = 114 \angle -1.8^\circ V, \quad \overline{U}_2 = 114 \angle -1.8^\circ V$$

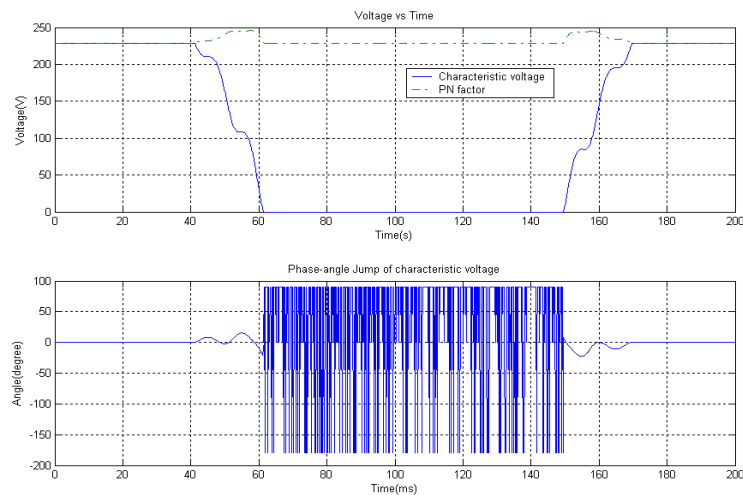
The sag index T is,

$$T = \frac{1}{60^\circ} \times \arg\left(\frac{114 \angle -1.8^\circ}{229 \angle 0^\circ - 114 \angle -1.8^\circ}\right) = 0.1 \cong 0$$

Thus, according to Table 2.3, it is classified as sag type Ca.



(a) Three-phase voltages



(b) Characteristic voltage and PN factor

Fig. C.15 Double-phase fault (fault-load with two resistive loads, simulation)

● **Double-phase-to-ground fault**

As shown in Fig.C.16, the three-phase retained voltages at MP are,

$$U_a = 229V, U_b = 0, U_c = 0$$

The phase-angle jumps at MP are,

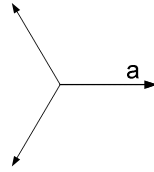
$$\Delta\phi_a = 0.9^\circ, \Delta\phi_b \text{ (Not applicable)}, \Delta\phi_c \text{ (Not applicable)}$$

The magnitudes of characteristic voltage and PN factor at MP are,

$$U = 0, F = 153V$$

The phase-angle jump of characteristic voltage at MP is not applicable.

The phasor diagram of the three phase voltages is,



Thus, according to Table 2.2, it is classified as sag type E.

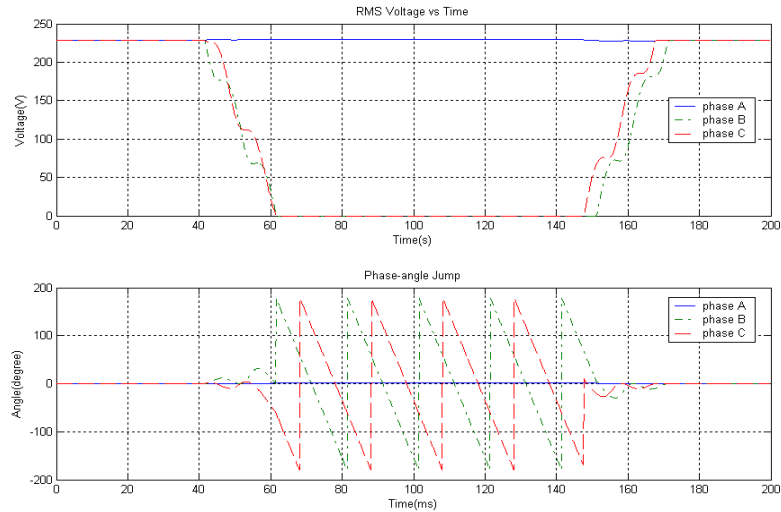
The sequence voltages calculated from the three phasors at MP2 are,

$$\overline{U}_1 = 76.3\angle -1.9^\circ V, \overline{U}_2 = 76.3\angle -1.9^\circ V$$

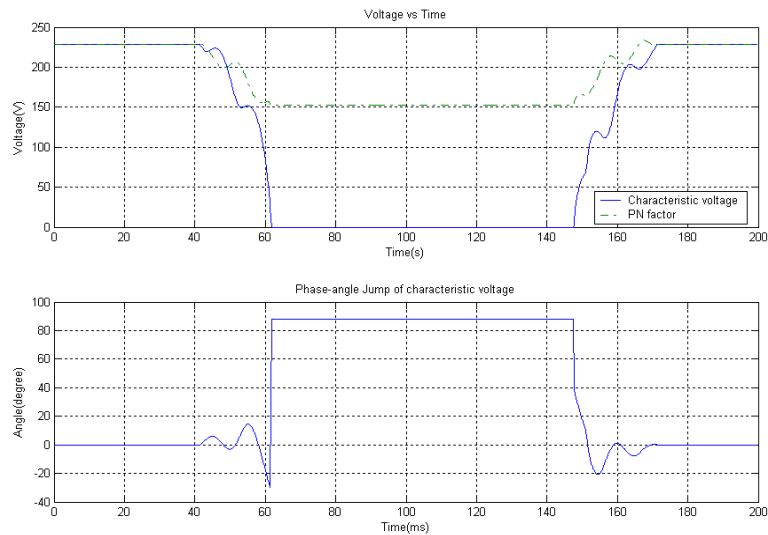
The sag index T is,

$$T = \frac{1}{60^\circ} \times \arg\left(\frac{76.3\angle -1.9^\circ}{229\angle 0 - 76.3\angle -1.9^\circ}\right) = 0.05 \cong 0$$

Thus, according to Table 2.3, it is classified as sag type Ca.



(a) Three-phase voltages



(b) Characteristic voltage and PN factor

Fig. C.16 Double-phase-to-ground fault (fault-load with two resistive loads, simulation)

◇ TWO RESISTIVE LOADS AND INDUCTION MACHINE(IM) LOADED

● Three-phase-to-ground fault

As shown in Fig.C.17, the three-phase retained voltages at MP are,

$$U_a = 0, U_b = 0, U_c = 0$$

The phase-angle jumps at MP are not applicable.

The magnitudes of characteristic voltage and PN factor at MP are,

$$U = 0, F = 0$$

The phase-angle jump of characteristic voltage at MP is not applicable.

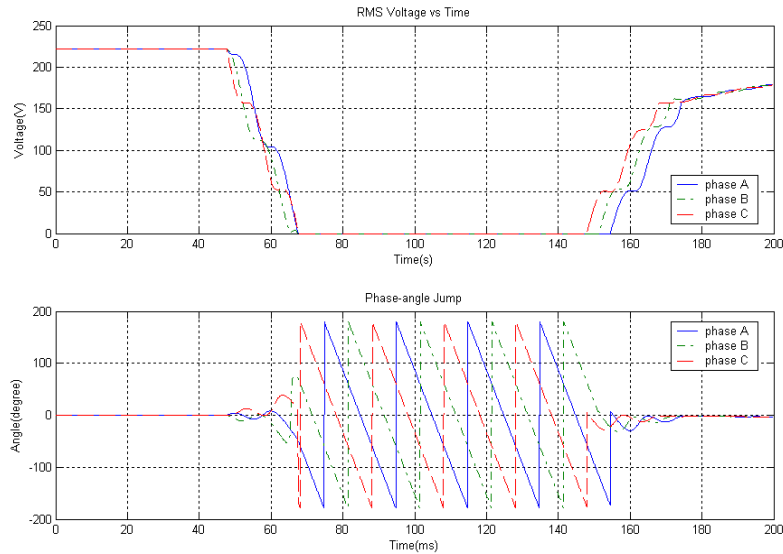
There is no phasor diagram of the three phase voltages.

Thus, according to Table 2.2, it can be classified as any sag type, i.e. sag type A.

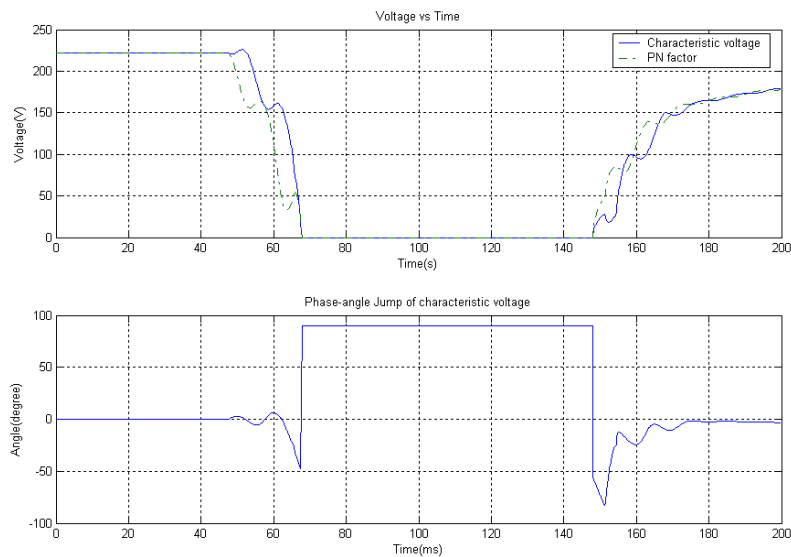
If assume the pre-fault voltage at MP2 to be $222\angle 0V$, according to equation (45), the sag index T is,

$$T = \frac{1}{60^0} \times \arg\left(\frac{0}{222\angle 0 - 0}\right) = 0$$

Thus, according to Table 2.3, it is classified as sag type Ca.



(a) Three-phase voltages



(b) Characteristic voltage and PN factor

Fig. C.17 Three-phase-to-ground fault (fault-load with two resistive loads and IM, simulation)

● Single-phase-to-ground fault

As shown in Fig.C.18, the three-phase retained voltages at MP are,

$$U_a = 0, U_b = 246V, U_c = 227V$$

The phase-angle jumps at MP are,

$$\Delta\phi_a \text{ (Not applicable), } \Delta\phi_b = -9.4^\circ, \Delta\phi_c = 3.3^\circ$$

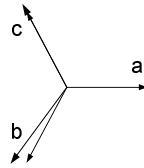
The magnitudes of characteristic voltage and PN factor at MP are,

$$U = 86.7V, F = 204V$$

The phase-angle jump of characteristic voltage at MP is,

$$\Delta\phi = 2.6^\circ$$

The phasor diagram of the three phase voltages is,



Thus, according to Table 2.2, it is classified as sag type B.

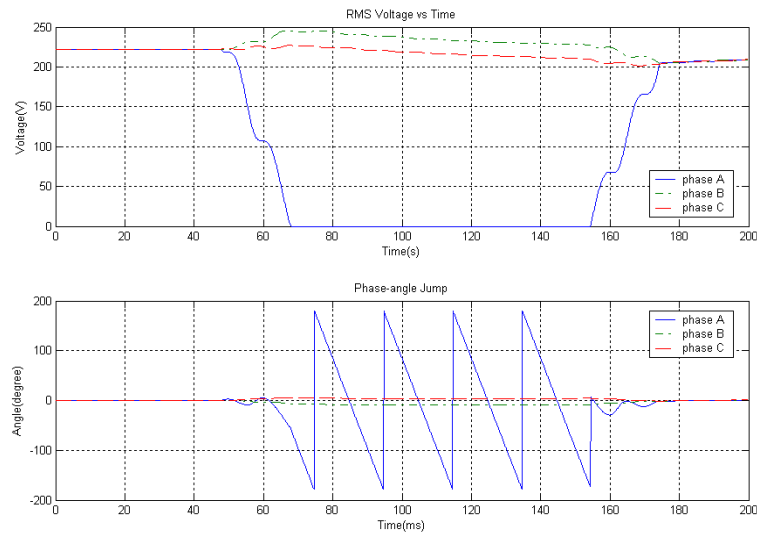
The sequence voltages calculated from the three phasors at MP2 are,

$$\overline{U}_1 = 157\angle -6.1^\circ V, \overline{U}_2 = 63.5\angle 168.9^\circ V$$

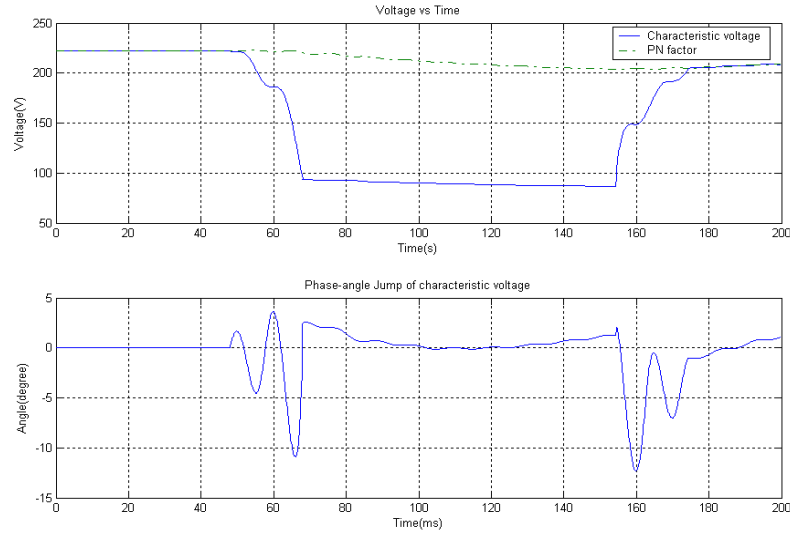
The sag index T is,

$$T = \frac{1}{60^\circ} \times \arg\left(\frac{63.5\angle 168.9^\circ}{222\angle 0 - 157\angle -6.1^\circ}\right) = 2.58 \cong 3$$

Thus, according to Table 2.3, it is classified as sag type Da.



(a) Three-phase voltages



(b) Characteristic voltage and PN factor

Fig. C.18 Single-phase-to-ground fault (fault-load with two resistive loads and IM, simulation)

- **Double-phase fault**

As shown in Fig.C.19, the three-phase retained voltages at MP are,

$$U_a = 178V, U_b = 88.5V, U_c = 88.5V$$

The phase-angle jumps at MP are,

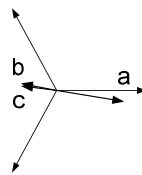
$$\Delta\phi_a = -10.4^\circ, \Delta\phi_b = -70.3^\circ, \Delta\phi_c = 57.0^\circ$$

The magnitudes of characteristic voltage and PN factor at MP are,

$$U = 0, F = 206V$$

The phase-angle jump of characteristic voltage at MP is not applicable.

The phasor diagram of the three phase voltages is,



Thus, according to Table 2.2, it is classified as sag type C.

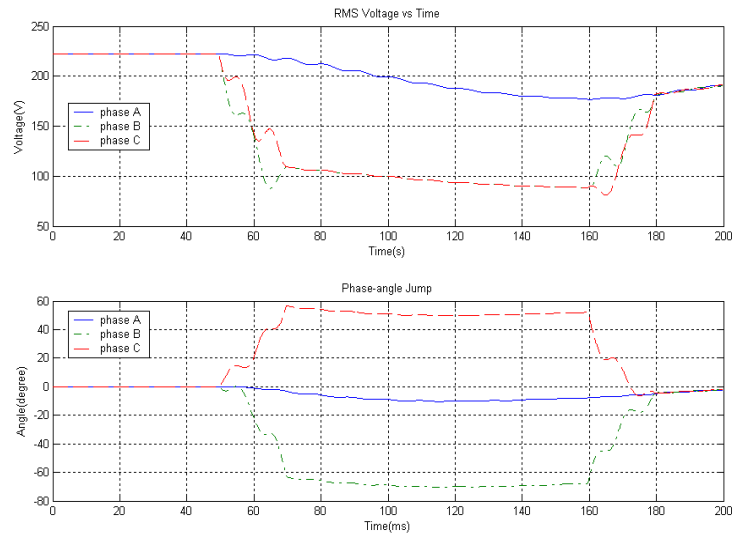
The sequence voltages calculated from the three phasors at MP2 are,

$$\overline{U}_1 = 85.5\angle -12.0^\circ V, \overline{U}_2 = 92.0\angle -11.9^\circ V$$

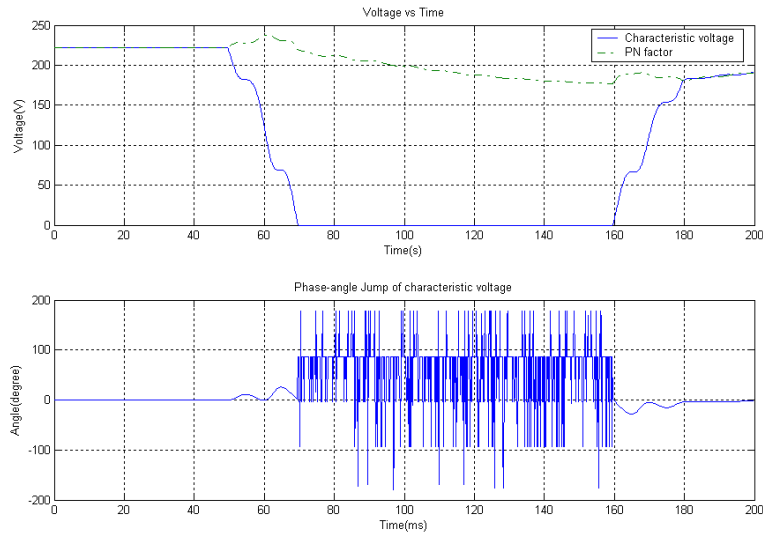
The sag index T is,

$$T = \frac{1}{60^\circ} \times \arg\left(\frac{92.0\angle -11.9^\circ}{222\angle 0^\circ - 85.5\angle -12.0^\circ}\right) = 0.32 \cong 0$$

Thus, according to Table 2.3, it is classified as sag type Ca.



(a) Three-phase voltages



(b) Characteristic voltage and PN factor

Fig. C.19 Double-phase fault (fault-load with two resistive loads and IM, simulation)

● Double-phase-to-ground fault

As shown in Fig.C.20, the three-phase retained voltages at MP are,

$$U_a = 242V, \quad U_b = 0, \quad U_c = 0$$

The phase-angle jumps at MP are,

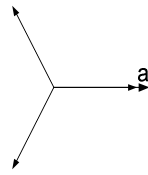
$$\Delta\phi_a = -9.1^\circ, \quad \Delta\phi_b \text{ (Not applicable)}, \quad \Delta\phi_c \text{ (Not applicable)}$$

The magnitudes of characteristic voltage and PN factor at MP are,

$$U = 0, \quad F = 129V$$

The phase-angle jump of characteristic voltage at MP is not applicable.

The phasor diagram of the three phase voltages is,



Thus, according to Table 2.2, it is classified as sag type E.

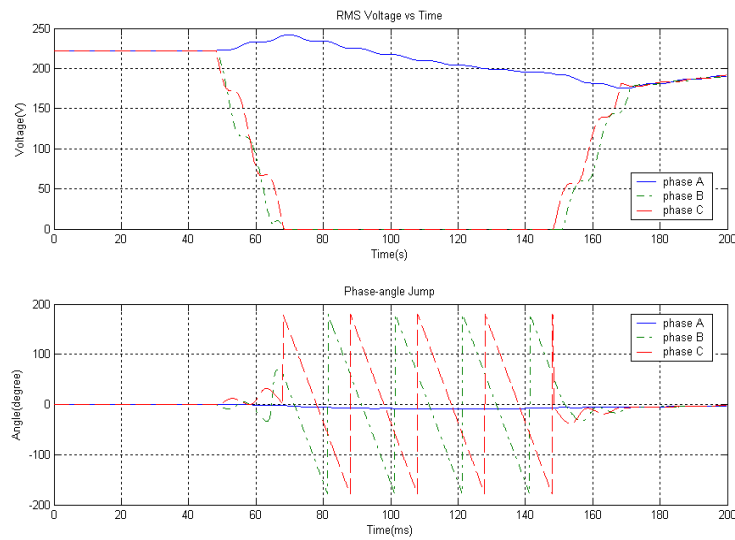
The sequence voltages calculated from the three phasors at MP2 are,

$$\overline{U}_1 = 80.7 \angle -11.9^\circ \text{V}, \quad \overline{U}_2 = 80.7 \angle -11.9^\circ \text{V}$$

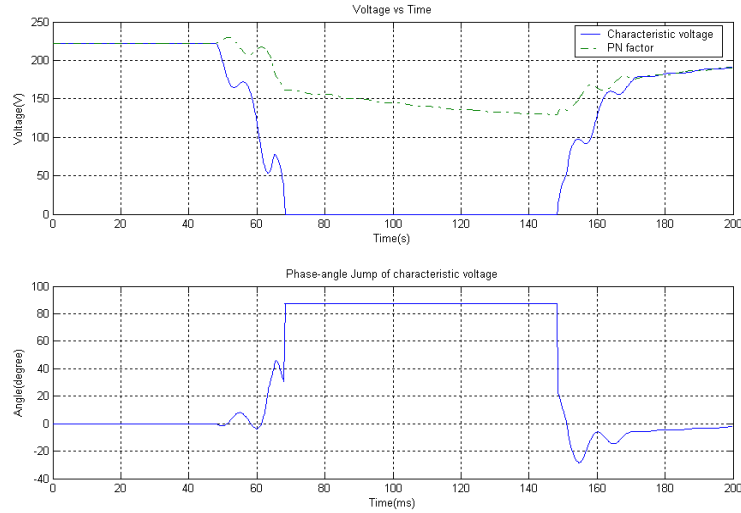
The sag index T is,

$$T = \frac{1}{60^\circ} \times \arg\left(\frac{80.7 \angle -11.9^\circ}{222 \angle 0^\circ - 80.7 \angle -11.9^\circ}\right) = 0.31 \cong 0$$

Thus, according to Table 2.3, it is classified as sag type Ca.



(a) Three-phase voltages



(b) Characteristic voltage and PN factor

Fig. C.19 Double-phase-to-ground fault (fault-load with two resistive loads and IM, simulation)

C.2.4 Fault-line circuit

✧ TWO RESISTIVE LOADS

● Three-phase-to-ground fault

As shown in Fig.4.1, the three-phase retained voltages at monitoring point 2 (MP2) are,

$$U_a = 115V, U_b = 115V, U_c = 115V$$

The phase-angle jumps at MP2 are,

$$\Delta\phi_a = 0.7^\circ, \Delta\phi_b = 0.7^\circ, \Delta\phi_c = 0.7^\circ$$

The magnitudes of characteristic voltage and PN factor at MP2 are,

$$U = 115V, F = 115V$$

The phase-angle jump of characteristic voltage at MP2 is,

$$\Delta\phi = 0.7^\circ$$

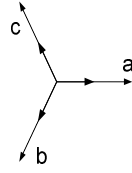
The magnitudes of positive-sequence voltage at MP2 is,

$$U_{MP2} = 115V$$

The phase-angle jump of positive-sequence voltage at MP2 is,

$$\Delta\phi_{MP2} = 0.7^\circ$$

The phasor diagram of the three phase voltages is,



Thus, according to Table 2.2, it is classified as sag type A.

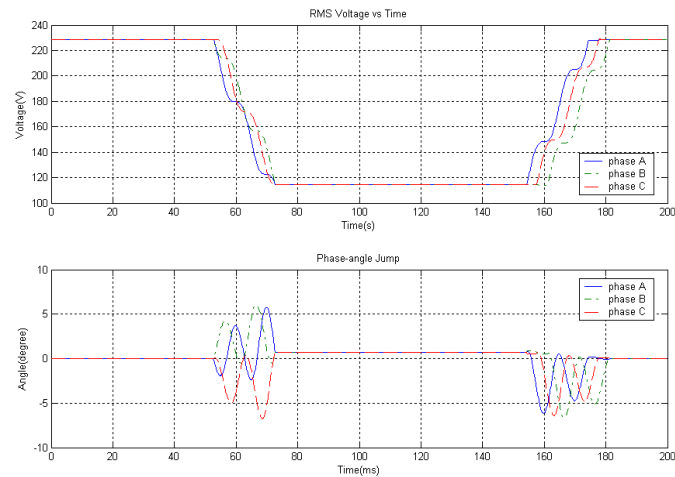
If assume the pre-fault voltage at MP2 to be $229\angle 0^\circ V$, the sequence voltages calculated from the three phasors at MP2 are,

$$\overline{U}_1 = 115\angle 0.7^\circ V, \quad \overline{U}_2 = 0$$

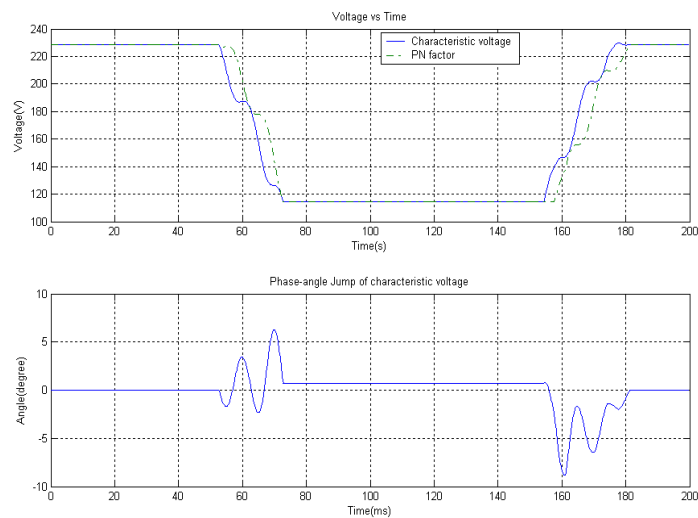
The sag index T is,

$$T = \frac{1}{60^\circ} \times \arg\left(\frac{0}{229\angle 0^\circ - 115\angle 0.7^\circ}\right) = 0$$

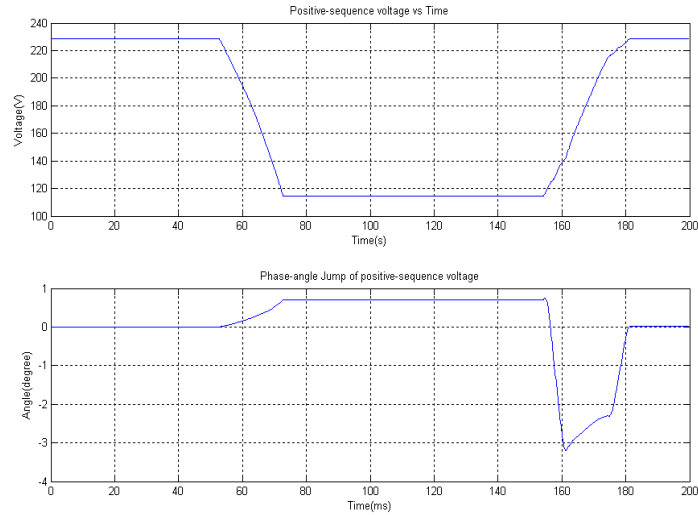
Thus, according to Table 2.3, it is classified as sag type Ca.



(a) Three-phase voltages



(b) Characteristic voltage and PN factor



(c) Positive-sequence voltage

Fig. 4.1 Three-phase-to-ground fault (MP2, fault-line with two resistive loads, simulation)

● **Single-phase-to-ground fault**

As shown in Fig.4.2, the three-phase retained voltages at MP2 are,

$$U_a = 114V, U_b = 231V, U_c = 227V$$

The phase-angle jumps at MP2 are,

$$\Delta\phi_a = 0, \Delta\phi_b = 0.2^\circ, \Delta\phi_c = 0.3^\circ$$

The magnitudes of characteristic voltage and PN factor at MP2 are,

$$U = 153V, F = 229V$$

The phase-angle jump of characteristic voltage at MP2 is,

$$\Delta\phi = 0.5^\circ$$

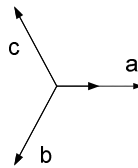
The magnitudes of positive-sequence voltage at MP2 is,

$$U_{MP2} = 191V$$

The phase-angle jump of positive-sequence voltage at MP2 is,

$$\Delta\phi_{MP2} = 0.2^\circ$$

The phasor diagram of the three phase voltages is,



Thus, according to Table 2.2, it is classified as sag type B.

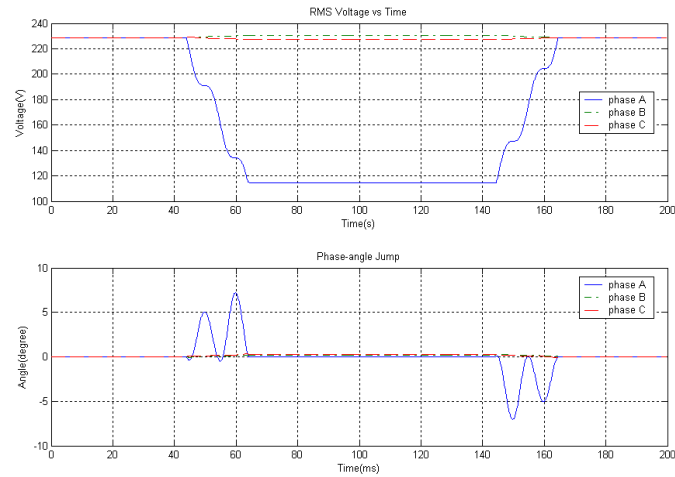
The sequence voltages calculated from the three phasors at MP2 are,

$$\overline{U}_1 = 191\angle 0.2^\circ V, \quad \overline{U}_2 = 38.2\angle 178.8^\circ V$$

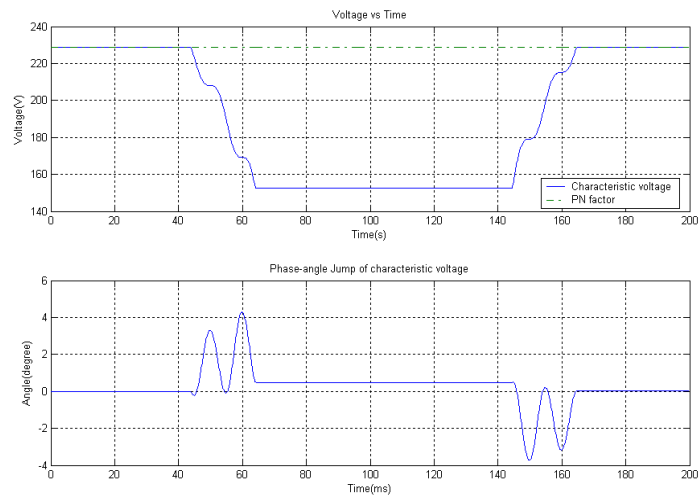
The sag index T is,

$$T = \frac{1}{60^\circ} \times \arg\left(\frac{38.2\angle 178.8^\circ}{229\angle 0 - 191\angle 0.2^\circ}\right) = 3.00 \approx 3$$

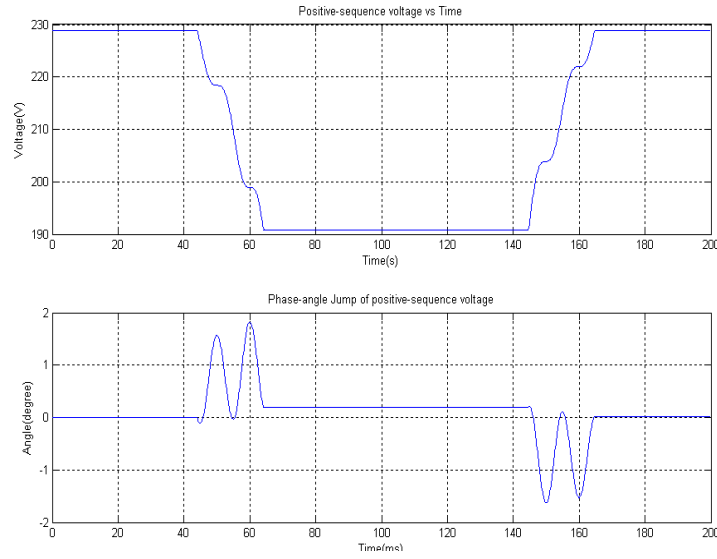
Thus, according to Table 2.3, it is classified as sag type Da.



(a) Three-phase voltages



(b) Characteristic voltage and PN factor



(c) Positive-sequence voltage

Fig. 4.2 Single-phase-to-ground fault (MP2, fault-line with two resistive loads, simulation)

- **Double-phase fault**

As shown in Fig.4.3, the three-phase retained voltages at MP2 are,

$$U_a = 229V, U_b = 151V, U_c = 152V$$

The phase-angle jumps at MP2 are,

$$\Delta\phi_a = 0, \Delta\phi_b = -18.8^\circ, \Delta\phi_c = 19.4^\circ$$

The magnitudes of characteristic voltage and PN factor at MP2 are,

$$U = 115V, F = 229V$$

The phase-angle jump of characteristic voltage at MP2 is,

$$\Delta\phi = 0.7^\circ$$

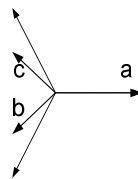
The magnitudes of positive-sequence voltage at MP2 is,

$$U_{MP2} = 172V$$

The phase-angle jump of positive-sequence voltage at MP2 is,

$$\Delta\phi_{MP2} = 0.2^\circ$$

The phasor diagram of the three phase voltages is,



Thus, according to Table 2.2, it is classified as sag type C.

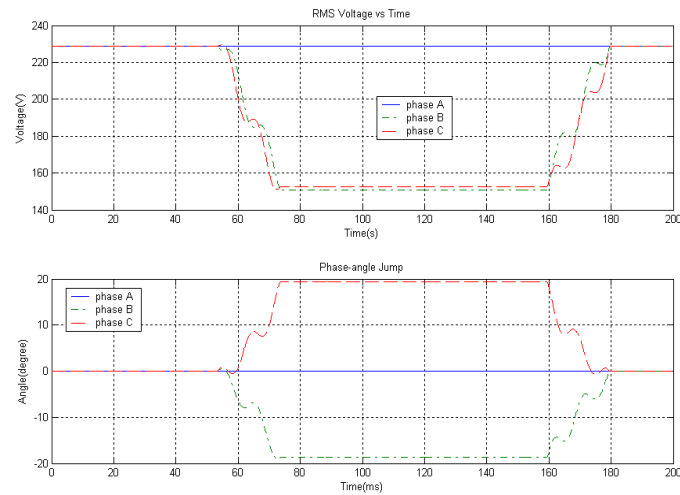
The sequence voltages calculated from the three phasors at MP2 are,

$$\overline{U}_1 = 172 \angle 0.2^\circ V, \quad \overline{U}_2 = 57.2 \angle -0.4^\circ V$$

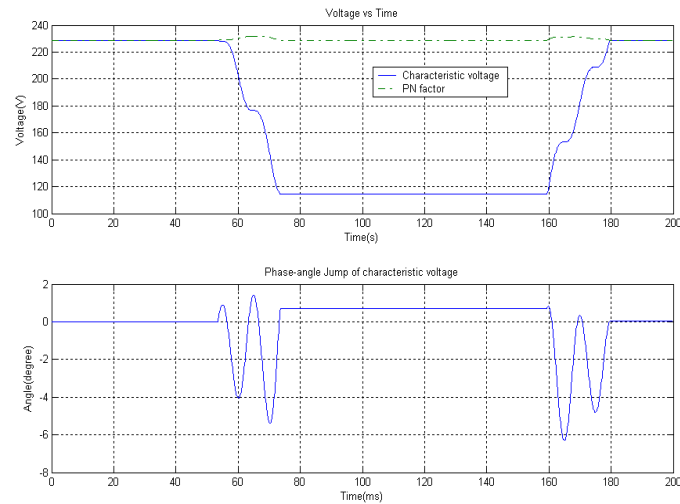
The sag index T is,

$$T = \frac{1}{60^\circ} \times \arg\left(\frac{57.2 \angle -0.4^\circ}{229 \angle 0 - 172 \angle 0.2^\circ}\right) = 0$$

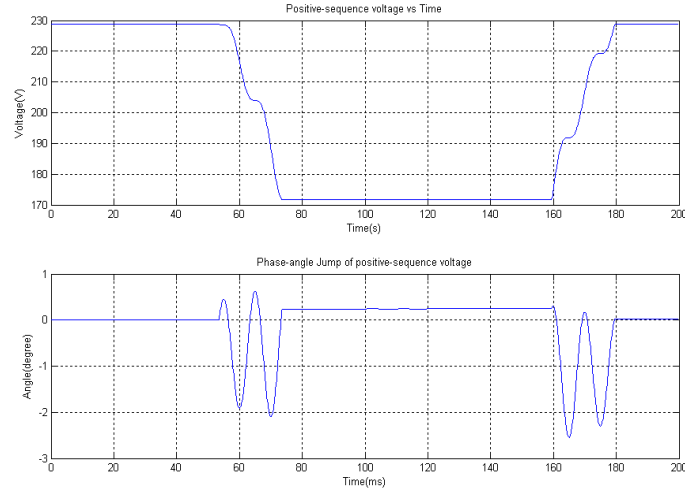
Thus, according to Table 2.3, it is classified as sag type Ca.



(a) Three-phase voltages



(b) Characteristic voltage and PN factor



(c) Positive-sequence voltage

Fig. 4.3 Double-phase fault (MP2, fault-line with two resistive loads, simulation)

● **Double-phase-to-ground fault**

As shown in Fig.4.4, the three-phase retained voltages at MP2 are,

$$U_a = 229V, U_b = 113V, U_c = 116V$$

The phase-angle jumps at MP2 are,

$$\Delta\phi_a = 0.5^\circ, \Delta\phi_b = 0.4^\circ, \Delta\phi_c = 0.3^\circ$$

The magnitudes of characteristic voltage and PN factor at MP2 are,

$$U = 115V, F = 191V$$

The phase-angle jump of characteristic voltage at MP2 is,

$$\Delta\phi = 0.7^\circ$$

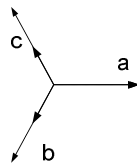
The magnitudes of positive-sequence voltage at MP2 is,

$$U_{MP2} = 153V$$

The phase-angle jump of positive-sequence voltage at MP2 is,

$$\Delta\phi_{MP2} = 0.4^\circ$$

The phasor diagram of the three phase voltages is,



Thus, according to Table 2.2, it is classified as sag type E.

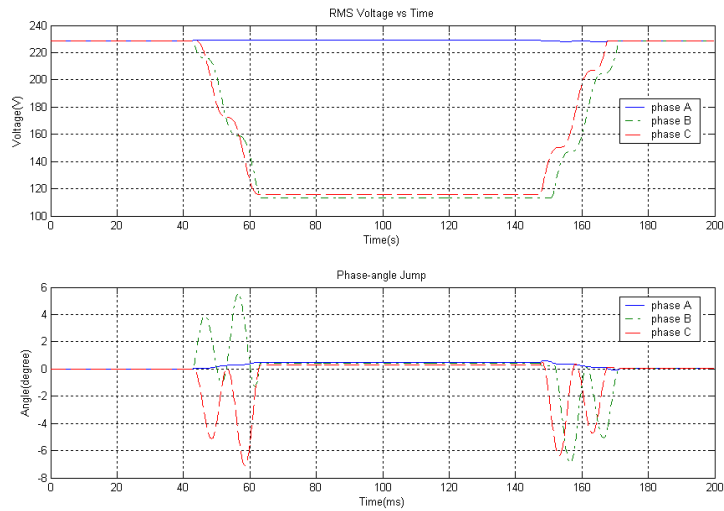
The sequence voltages calculated from the three phasors at MP2 are,

$$\overline{U_1} = 172\angle 0.2^\circ V, \overline{U_2} = 38.1\angle -0.7^\circ V$$

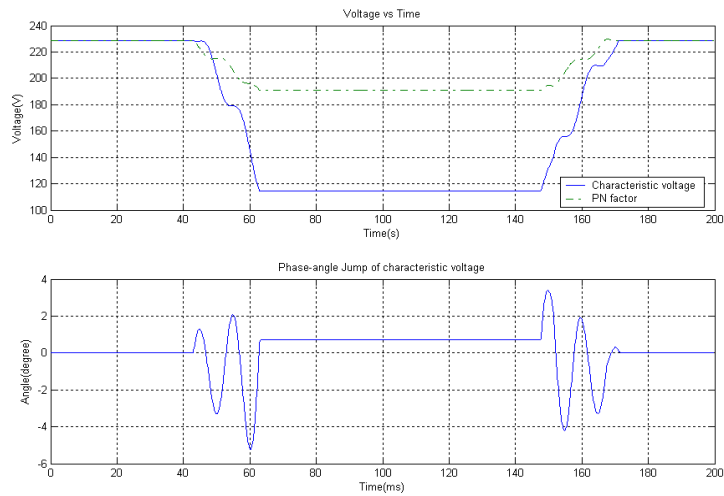
The sag index T is,

$$T = \frac{1}{60^0} \times \arg\left(\frac{38.1 \angle -0.7^0}{229 \angle 0 - 172 \angle 0.2^0}\right) = 0$$

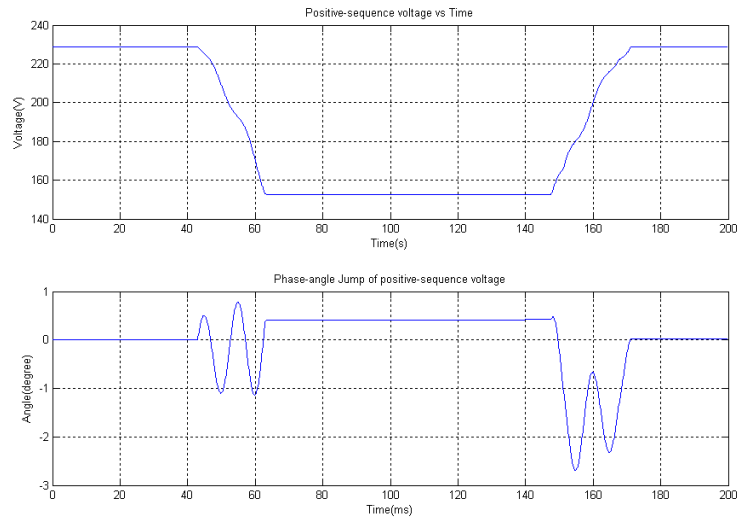
Thus, according to Table 2.3, it is classified as sag type Ca.



(a) Three-phase voltages



(b) Characteristic voltage and PN factor



(c) Positive-sequence voltage

Fig. 4.4 Double-phase-to-ground fault (MP2, fault-line with two resistive loads, simulation)

◇ **TWO RESISTIVE LOADS AND INDUCTION MACHINE(IM)**

● **Three-phase-to-ground fault**

As shown in Fig.4.5, the three-phase retained voltages at MP2 are,

$$U_a = 119V, U_b = 119V, U_c = 119V$$

The phase-angle jumps at MP2 are,

$$\Delta\phi_a = -3.5^\circ, \Delta\phi_b = -3.5^\circ, \Delta\phi_c = -3.5^\circ$$

The magnitudes of characteristic voltage and PN factor at MP2 are,

$$U = 119V, F = 119V$$

The phase-angle jump of characteristic voltage at MP2 is,

$$\Delta\phi = -3.5^\circ$$

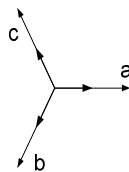
The magnitudes of positive-sequence voltage at MP2 is,

$$U_{MP2} = 119V$$

The phase-angle jump of positive-sequence voltage at MP2 is,

$$\Delta\phi_{MP2} = -3.4^\circ$$

The phasor diagram of the three phase voltages is,



Thus, according to Table 2.2, it is classified as sag type A. It has to be pointed out that

the magnitude and the phase angle of each phasor shown above normally don't happen at the same time. In another word, the phasor shown above don't really exist in any instant, but a combination of the worst magnitude and the worst phase-angle jump in that phase. This interpolation of phasors will overestimate the severity of the voltage sag experienced by loads.

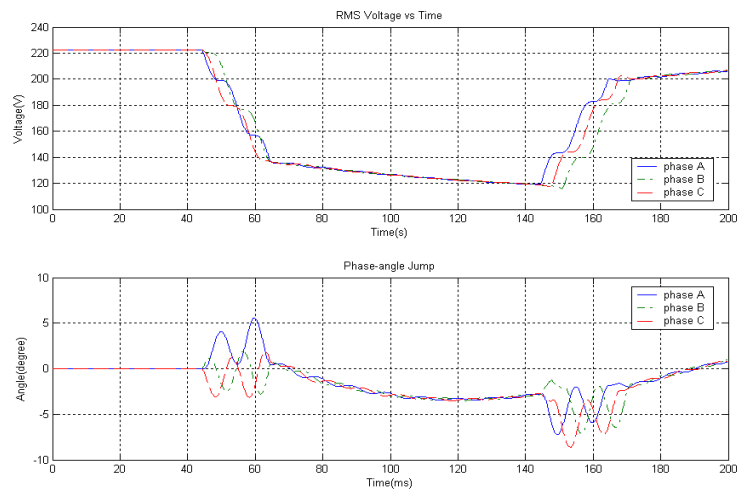
If we assume the pre-fault voltage at MP2 is $222\angle 0V$, the sequence voltages calculated from the three phasors at MP2 are,

$$\overline{U}_1 = 119\angle -3.5^\circ V, \quad \overline{U}_2 = 0$$

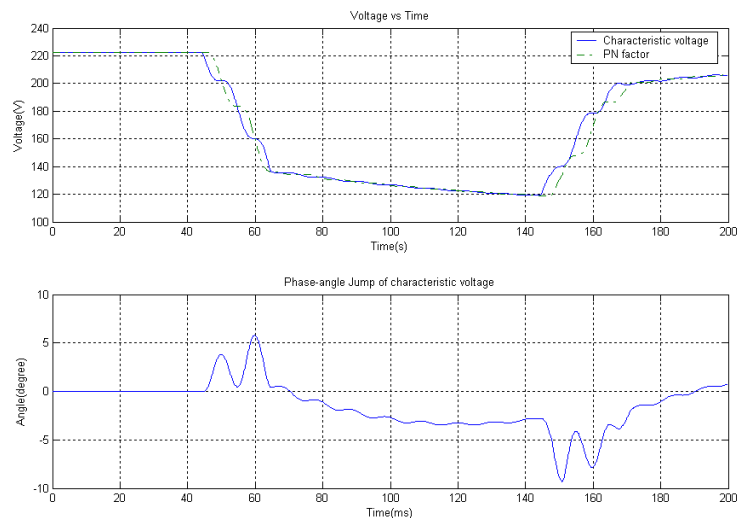
The sag index T is,

$$T = \frac{1}{60^\circ} \times \arg\left(\frac{0}{222\angle 0 - 119\angle -3.5^\circ}\right) = 0$$

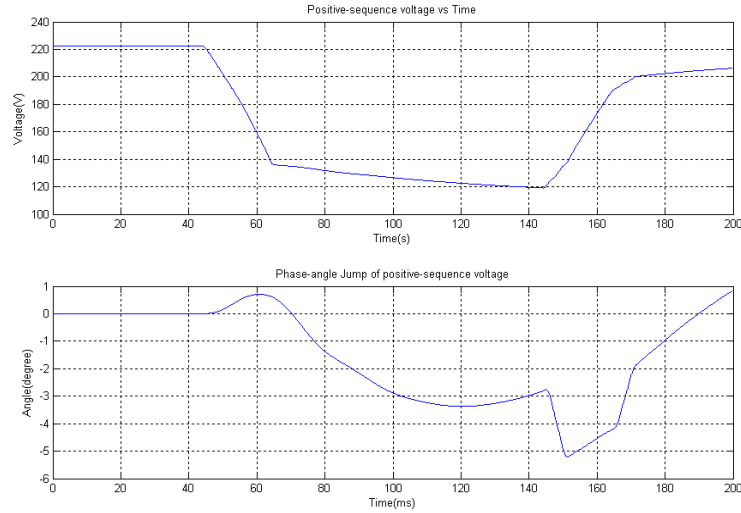
Thus, according to Table 2.3, it is classified as sag type Ca.



(a) Three-phase voltages



(b) Characteristic voltage and PN factor



(c) Positive-sequence voltage

Fig. 4.5 Three-phase-to-ground fault (MP2, fault-line with two resistive loads and IM, simulation)

● **Single-phase-to-ground fault**

As shown in Fig.4.6, the three-phase retained voltages at MP2 are,

$$U_a = 122V, U_b = 232V, U_c = 225V$$

The phase-angle jumps at MP2 are,

$$\Delta\phi_a = -0.6^\circ, \Delta\phi_b = -3.9^\circ, \Delta\phi_c = 2.6^\circ$$

The magnitudes of characteristic voltage and PN factor at MP2 are,

$$U = 162V, F = 214V$$

The phase-angle jump of characteristic voltage at MP2 is,

$$\Delta\phi = 0.9^\circ$$

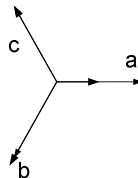
The magnitudes of positive-sequence voltage at MP2 is,

$$U_{MP2} = 188V$$

The phase-angle jump of positive-sequence voltage at MP2 is,

$$\Delta\phi_{MP2} = -0.1^\circ$$

The phasor diagram of the three phase voltages is,



Thus, according to Table 2.2, it is classified as sag type B.

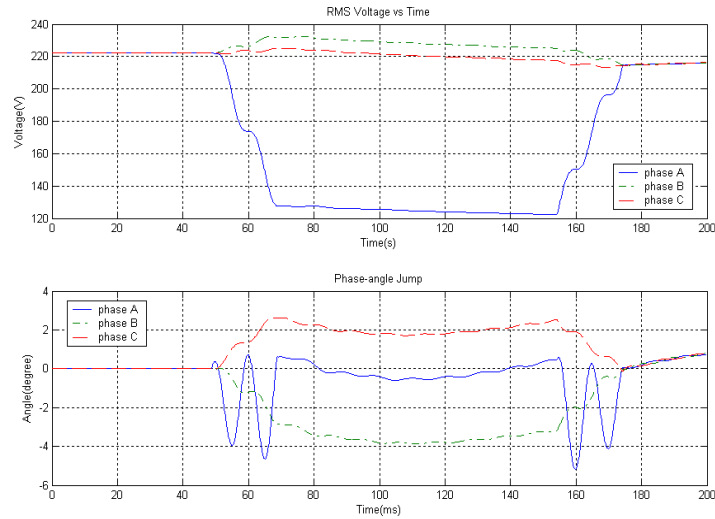
The sequence voltages calculated from the three phasors at MP2 are,

$$\overline{U}_1 = 193 \angle -0.7^\circ V, \overline{U}_2 = 28.0 \angle 175.0^\circ V$$

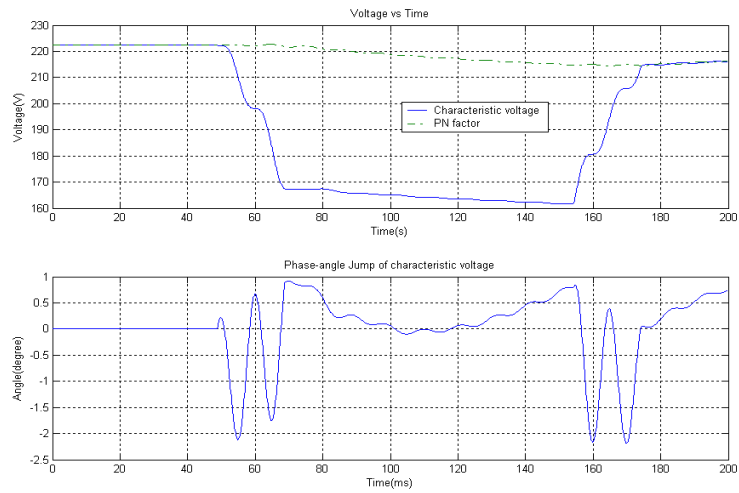
The sag index T is,

$$T = \frac{1}{60^0} \times \arg\left(\frac{28.0 \angle 175.0^0}{222 \angle 0 - 193 \angle -0.7^0}\right) = 2.86 \cong 3$$

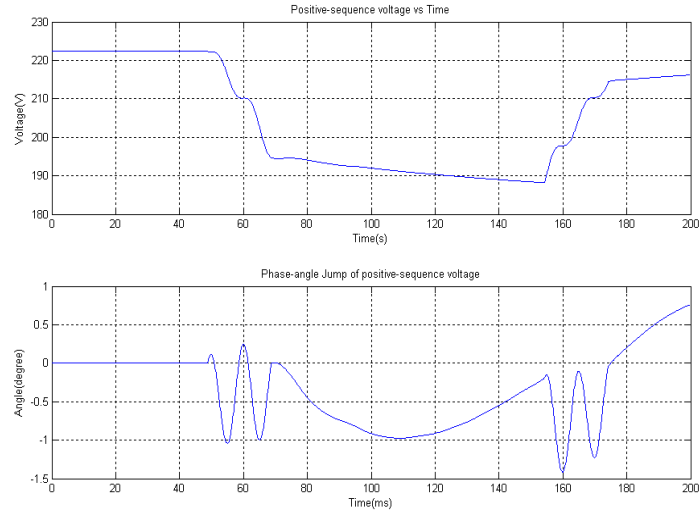
Thus, according to Table 2.3, it is classified as sag type Da.



(a) Three-phase voltages



(b) Characteristic voltage and PN factor



(c) Positive-sequence voltage

Fig. 4.6 Single-phase-to-ground fault (MP2, fault-line with two resistive loads and IM, simulation)

- **Double-phase fault**

As shown in Fig.4.7, the three-phase retained voltages at MP2 are,

$$U_a = 210V, U_b = 150V, U_c = 158V$$

The phase-angle jumps at MP2 are,

$$\Delta\phi_a = -2.6^\circ, \Delta\phi_b = -14.4^\circ, \Delta\phi_c = 13.8^\circ$$

The magnitudes of characteristic voltage and PN factor at MP2 are,

$$U = 129V, F = 210V$$

The phase-angle jump of characteristic voltage at MP2 is,

$$\Delta\phi = 1.7^\circ$$

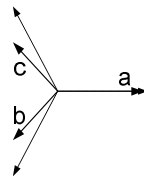
The magnitudes of positive-sequence voltage at MP2 is,

$$U_{MP2} = 170V$$

The phase-angle jump of positive-sequence voltage at MP2 is,

$$\Delta\phi_{MP2} = -1.6^\circ$$

The phasor diagram of the three phase voltages is,



Thus, according to Table 2.2, it is classified as sag type C.

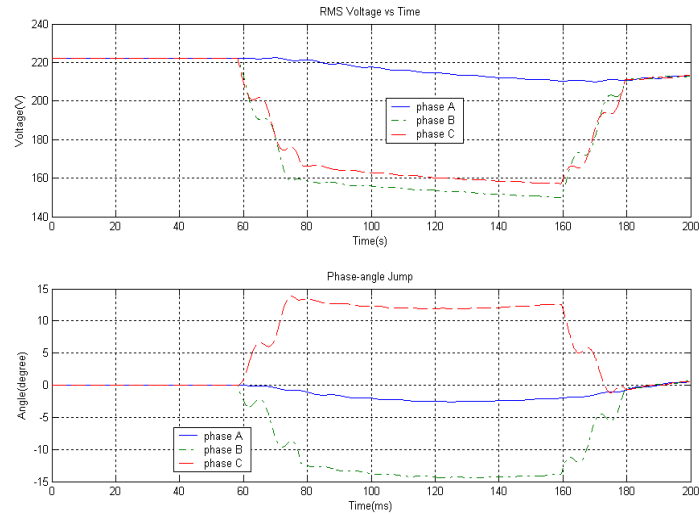
The sequence voltages calculated from the three phasors at MP2 are,

$$\overline{U}_1 = 170\angle -1.0^\circ V, \overline{U}_2 = 42.2\angle -7.6^\circ V$$

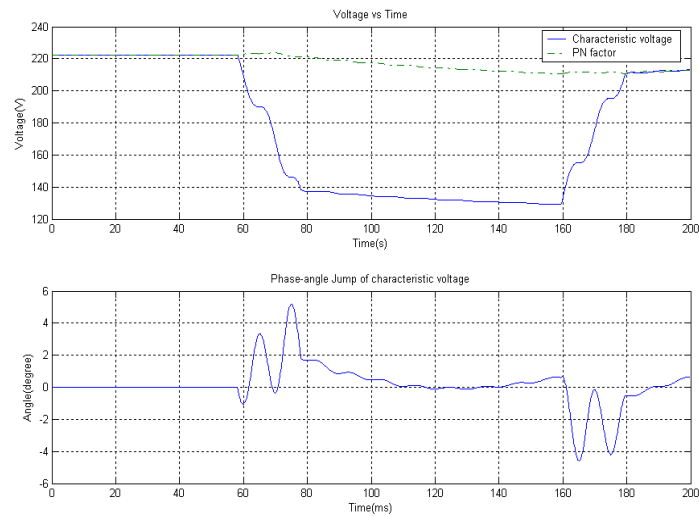
The sag index T is,

$$T = \frac{1}{60^0} \times \arg\left(\frac{42.2 \angle -7.6^0}{222 \angle 0 - 170 \angle -1.0^0}\right) = 0.18 \cong 0$$

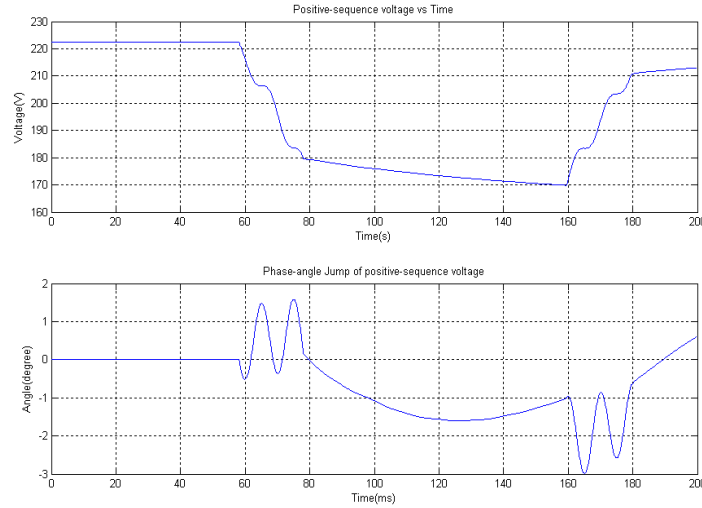
Thus, according to Table 2.3, it is classified as sag type Ca.



(a) Three-phase voltages



(b) Characteristic voltage and PN factor



(c) Positive-sequence voltage

Fig. 4.7 Double-phase fault (MP2, fault-line with two resistive loads and IM, simulation)

● **Double-phase-to-ground fault**

As shown in Fig.4.8, the three-phase retained voltages at MP2 are,

$$U_a = 219V, U_b = 118V, U_c = 125V$$

The phase-angle jumps at MP2 are,

$$\Delta\phi_a = -2.2^\circ, \Delta\phi_b = 4.6^\circ, \Delta\phi_c = -5.8^\circ$$

The magnitudes of characteristic voltage and PN factor at MP2 are,

$$U = 126V, F = 181V$$

The phase-angle jump of characteristic voltage at MP2 is,

$$\Delta\phi = -1.1^\circ$$

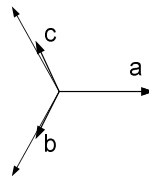
The magnitudes of positive-sequence voltage at MP2 is,

$$U_{MP2} = 154V$$

The phase-angle jump of positive-sequence voltage at MP2 is,

$$\Delta\phi_{MP2} = -2.0^\circ$$

The phasor diagram of the three phase voltages is,



Thus, according to Table 2.2, it is classified as sag type E.

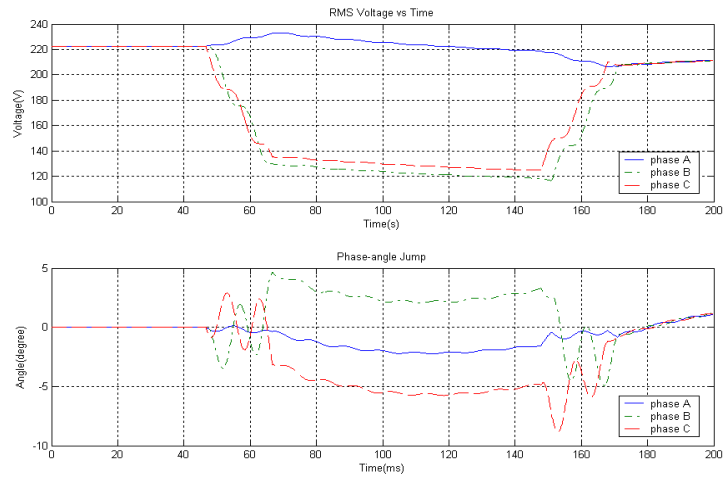
The sequence voltages calculated from the three phasors at MP2 are,

$$\overline{U}_1 = 154\angle -1.4^\circ V, \overline{U}_2 = 26.6\angle -9.1^\circ V$$

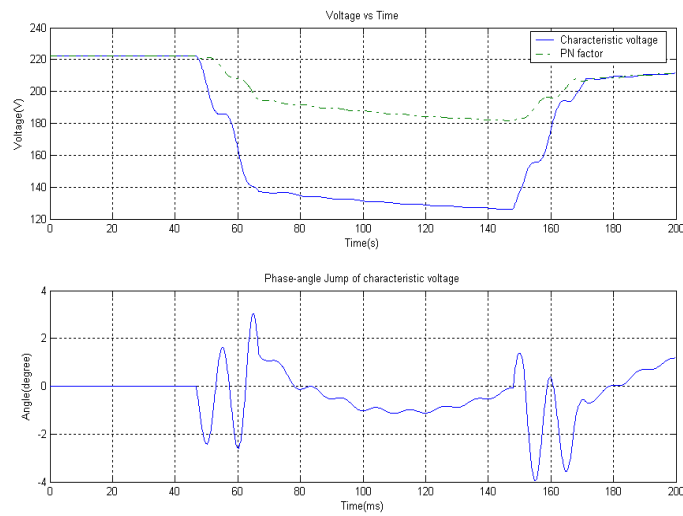
The sag index T is,

$$T = \frac{1}{60^0} \times \arg\left(\frac{26.6 \angle -9.1^0}{222 \angle 0 - 154 \angle -1.4^0}\right) = 0.20 \cong 0$$

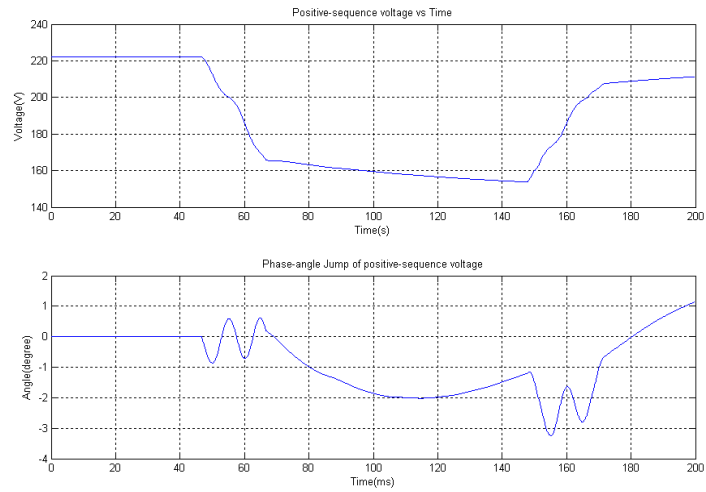
Thus, according to Table 2.3, it is classified as sag type Ca.



(a) Three-phase voltages



(b) Characteristic voltage and PN factor



(c) Positive-sequence voltage

Fig. 4.8 Double-phase-to-ground fault (MP2, fault-line with two resistive loads and IM, simulation)

C.3 Measurements on the analog network model

The experimental results for the four different circuits are obtained from the analog network model. PQ monitor is used to measure the three-phase voltages at the PCC bus. The voltage waveforms are transferred and analyzed using MATLAB. Several algorithms are used in order to obtain fundamental rms voltage, phase-angle jump and voltage sag type. Fundamental rms voltages and phase-angle jumps for basic circuit, voltage-divider circuit, open-line circuit and fault-line circuit are shown in the following figures, respectively.

In the “**Fault-line circuit**”, two measurement equipments are used to monitor two different locations. At monitoring point 1 (MP1), “Phasor measurement unit (PMU)” is used to record the voltages at the source side when faults happen at one of the parallel transmission lines. At monitoring point 2 (MP2), both PMU and PQ monitor are used to record the voltages at the load side.

PMU is a device for synchronized measurement of AC voltages and currents, with a common time (angle) reference. The reference of the time or phase angle is the Global Positioning System (GPS), which has a highly precise time and date. The precise time of measurements taken at different geographical locations makes it possible to derive the phasor quantities, i.e. magnitude and phase angle of a complex voltage (current). PMU has mainly been used for recording and on-line supervision, wide area measurement system (WAMS) applications. The phasor data is normally sent from the PMU to the database at a speed of 50/60 samples per second (50 samples in our case). The phasor data can be understood as the magnitude and the phase angle (or real part and imaginary part) of the **positive-sequence** voltage or current.

As the sampling frequency of the PMU is once per cycle, so the PMU only gives the values shown as stars in the following figures. The connected lines are interpolated as assuming linear relation between the two adjacent data.

C.3.1 Basic circuit

- **Three-phase-to-ground fault**

As shown in Fig.C.37, the three-phase retained voltages at PCC are,

$$U_a = 93.4V, U_b = 93.8V, U_c = 93.4V$$

The phase-angle jumps at PCC are,

$$\Delta\phi_a = 0.3^\circ, \Delta\phi_b = 0.3^\circ, \Delta\phi_c = 0.2^\circ$$

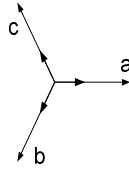
The magnitudes of characteristic voltage and PN factor at PCC are,

$$U = 93.5V, F = 93.5V$$

The phase-angle jump of characteristic voltage at PCC is,

$$\Delta\phi = 0.3^\circ$$

The phasor diagram of the three phase voltages is,



Thus, according to Table 2.2, it is classified as sag type A.

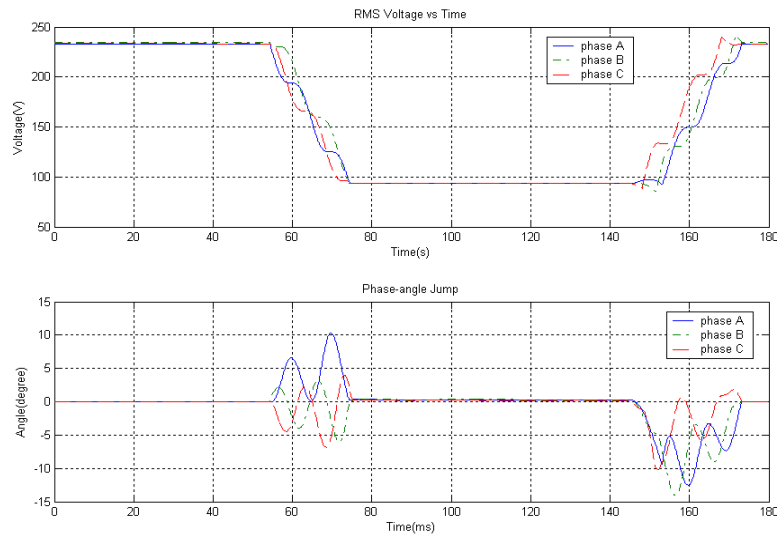
The sequence voltages calculated from the three phasors at PCC are,

$$\overline{U}_1 = 93.5 \angle 0.3^\circ V, \quad \overline{U}_2 = 0.182 \angle 12.9^\circ V$$

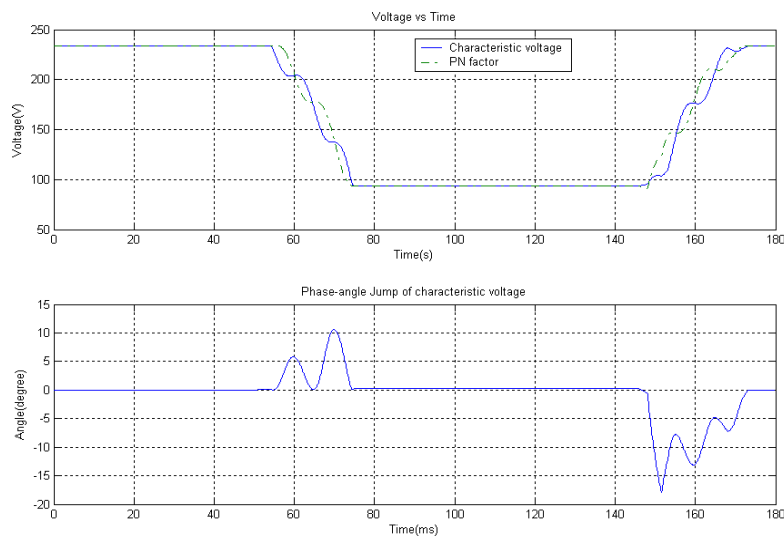
According to equation (45), the sag index T is,

$$T = \frac{1}{60^\circ} \times \arg\left(\frac{0.182 \angle 12.9^\circ}{230 \angle 0 - 93.5 \angle 0.3^\circ}\right) = 2.15 \cong 2$$

Thus, according to Table 2.3, it is classified as sag type Cb.



(a) Three-phase voltages



(b) Characteristic voltage and PN factor

Fig. C.37 Three-phase-to-ground fault (basic circuit, measurement)

● **Single-phase-to-ground fault**

As shown in Fig.C.38, the three-phase retained voltages at PCC are,

$$U_a = 93.5V, U_b = 264V, U_c = 260V$$

The phase-angle jumps at PCC are,

$$\Delta\phi_a = -0.4^\circ, \Delta\phi_b = -9.6^\circ, \Delta\phi_c = 9.1^\circ$$

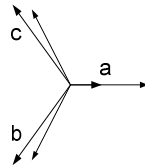
The magnitudes of characteristic voltage and PN factor at PCC are,

$$U = 170V, F = 238V$$

The phase-angle jump of characteristic voltage at PCC is,

$$\Delta\phi = -0.5^\circ$$

The phasor diagram of the three phase voltages is,



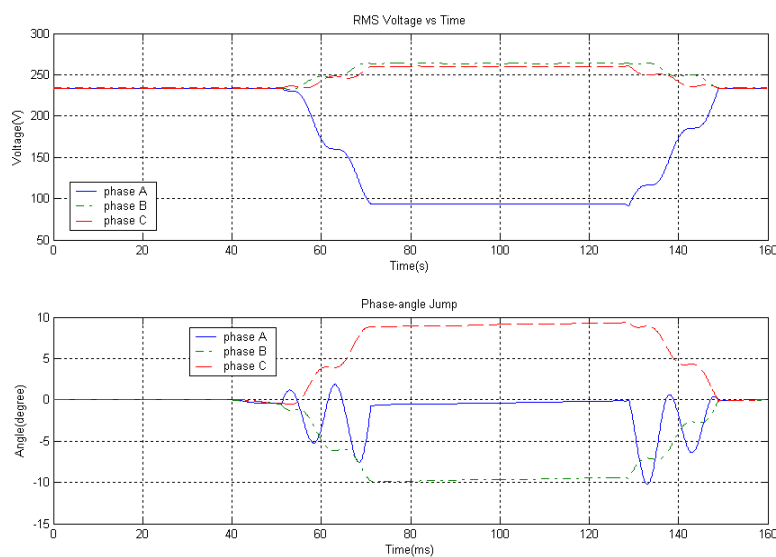
The sequence voltages calculated from the three phasors at PCC are,

$$\overline{U}_1 = 204\angle -0.3^\circ V, \overline{U}_2 = 30.5\angle 177.6^\circ V$$

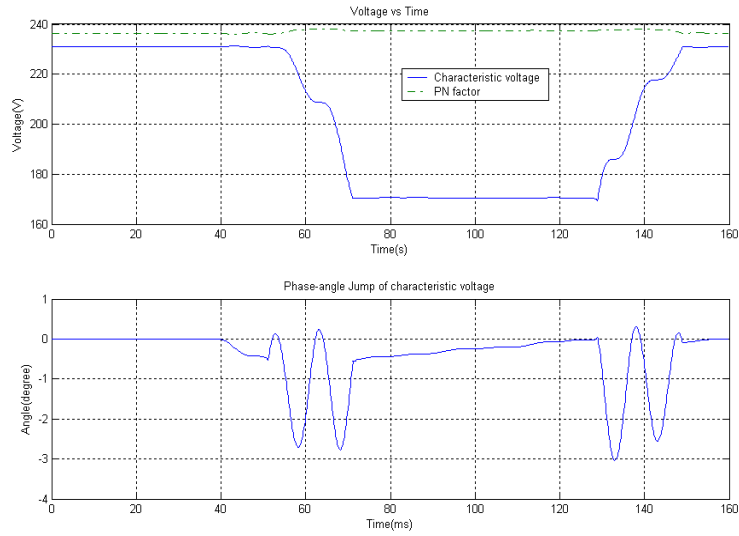
The sag index T is,

$$T = \frac{1}{60^\circ} \times \arg\left(\frac{30.5\angle 177.6^\circ}{230\angle 0^\circ - 204\angle -0.3^\circ}\right) = 2.92 \cong 3$$

Thus, according to Table 2.3, it is classified as sag type Da.



(a) Three-phase voltages



(b) Characteristic voltage and PN factor

Fig. C.38 Single-phase-to-ground fault (basic circuit, measurement)

● **Double-phase fault**

As shown in Fig.C.39, the three-phase retained voltages at PCC are,

$$U_a = 233V, U_b = 142V, U_c = 142V$$

The phase-angle jumps at PCC are,

$$\Delta\phi_a = -0.3^\circ, \Delta\phi_b = -25.2^\circ, \Delta\phi_c = 25.2^\circ$$

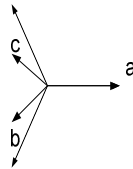
The magnitudes of characteristic voltage and PN factor at PCC are,

$$U = 96.0V, F = 232V$$

The phase-angle jump of characteristic voltage at PCC is,

$$\Delta\phi = -0.1^\circ$$

The phasor diagram of the three phase voltages is,



Thus, according to Table 2.2, it is classified as sag type C.

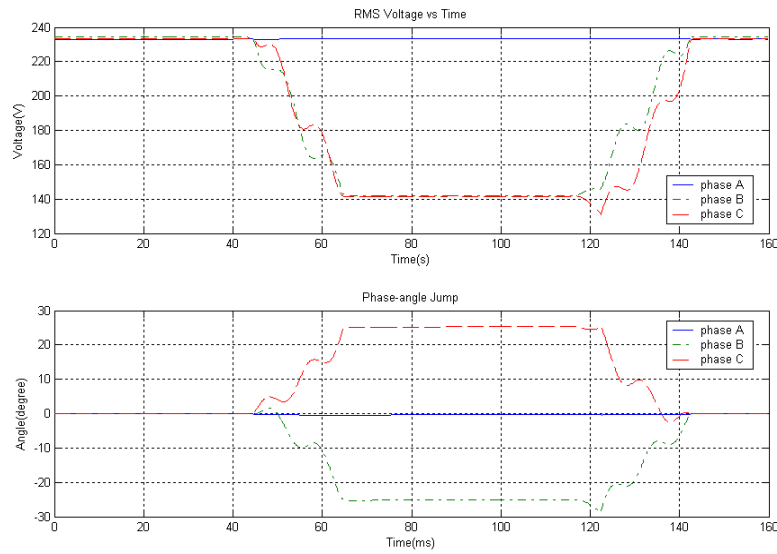
The sequence voltages calculated from the three phasors at PCC are,

$$\overline{U}_1 = 163\angle -0.1^\circ V, \overline{U}_2 = 69.7\angle -0.3^\circ V$$

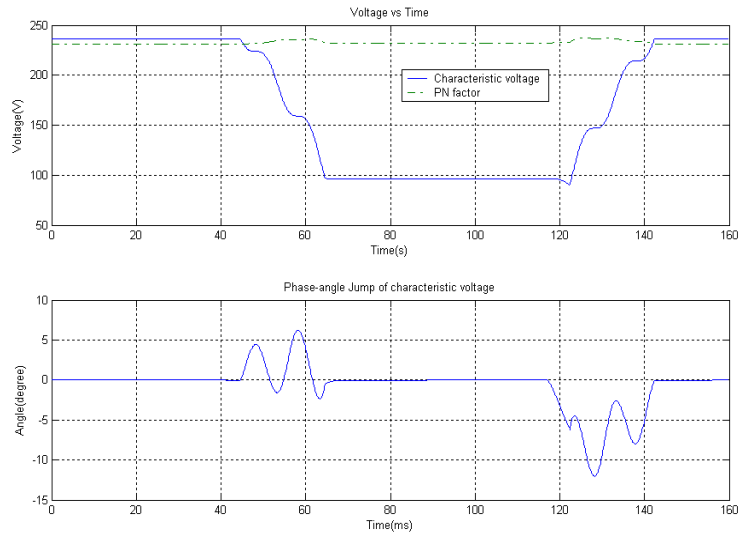
The sag index T is,

$$T = \frac{1}{60^\circ} \times \arg\left(\frac{69.7\angle -0.3^\circ}{230\angle 0^\circ - 163\angle -0.1^\circ}\right) = 0.01 \cong 0$$

Thus, according to Table 2.3, it is classified as sag type Ca.



(a) Three-phase voltages



(b) Characteristic voltage

Fig. C.39 Double-phase fault (basic circuit, measurement)

● Double-phase-to-ground fault

As shown in Fig.C.40, the three-phase retained voltages at PCC are,

$$U_a = 270V, U_b = 93.8V, U_c = 93.5V$$

The phase-angle jumps at PCC are,

$$\Delta\phi_a = 0^{\circ}, \Delta\phi_b = 0.1^{\circ}, \Delta\phi_c = 0.1^{\circ}$$

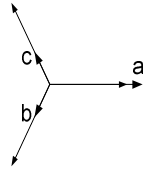
The magnitudes of characteristic voltage and PN factor at PCC are,

$$U = 94.7V, F = 210V$$

The phase-angle jump of characteristic voltage at PCC is,

$$\Delta\phi = 0.1^{\circ}$$

The phasor diagram of the three phase voltages is,



Thus, according to Table 2.2, it is classified as sag type E.

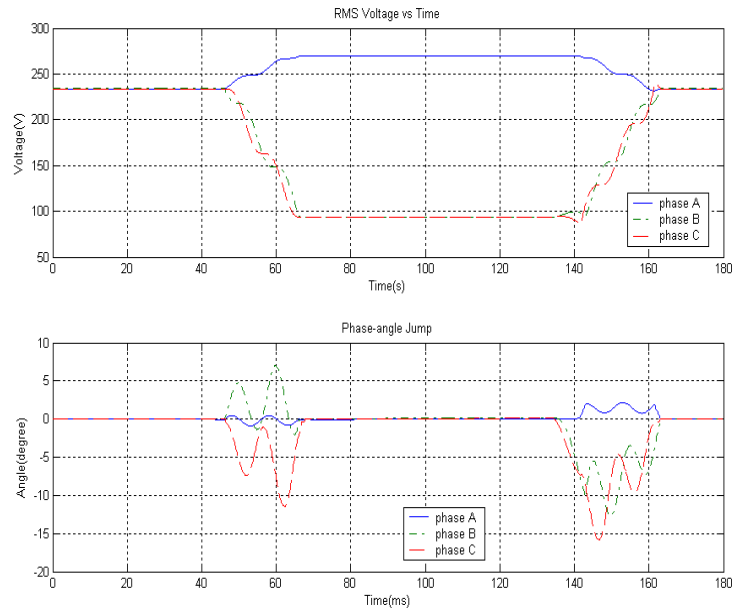
The sequence voltages calculated from the three phasors at PCC are,

$$\overline{U}_1 = 152\angle 0V, \quad \overline{U}_2 = 58.8\angle 0V$$

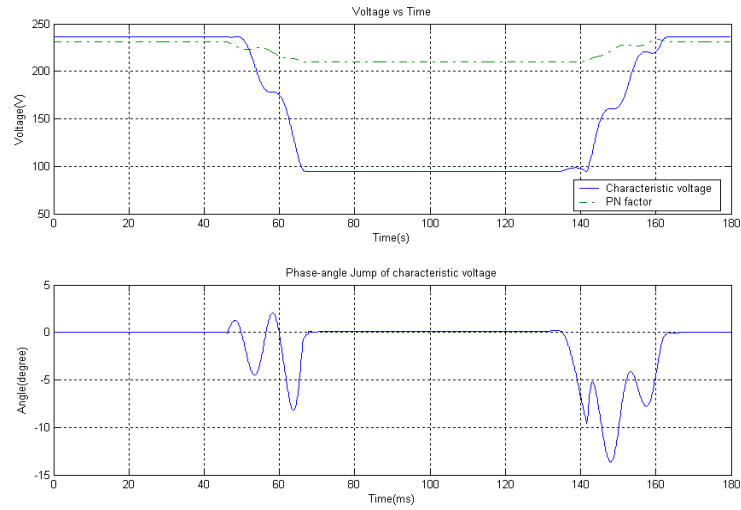
The sag index T is,

$$T = \frac{1}{60^\circ} \times \arg\left(\frac{58.8\angle 0}{230\angle 0 - 152\angle 0}\right) = 0$$

Thus, according to Table 2.3, it is classified as sag type Ca.



(a) Three-phase voltages



(b) Characteristic voltage and PN factor

Fig. C.40 Double-phase-to-ground fault (basic circuit, measurement)

C.3.2 Voltage-divider circuit

✧ NO LOAD CONDITION

● Three-phase-to-ground fault

As shown in Fig.C.41, the three-phase retained voltages at PCC are,

$$U_a = 154V, U_b = 155V, U_c = 154V.$$

The phase-angle jumps at PCC are,

$$\Delta\phi_a = -0.4^\circ, \Delta\phi_b = -0.3^\circ, \Delta\phi_c = -0.4^\circ$$

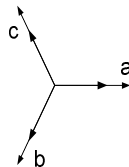
The magnitudes of characteristic voltage and PN factor at PCC are,

$$U = 155V, F = 155V$$

The phase-angle jump of characteristic voltage at PCC is,

$$\Delta\phi = -0.9^\circ$$

The phasor diagram of the three phase voltages is,



Thus, according to Table 2.2, it is classified as sag type A.

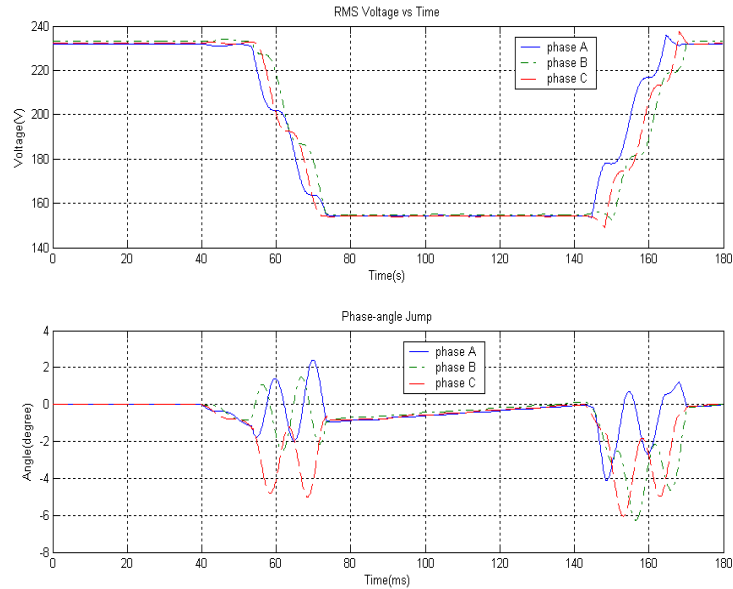
The sequence voltages calculated from the three phasors at PCC are,

$$\overline{U}_1 = 154\angle -0.4^\circ V, \overline{U}_2 = 0.345\angle 134.7^\circ V$$

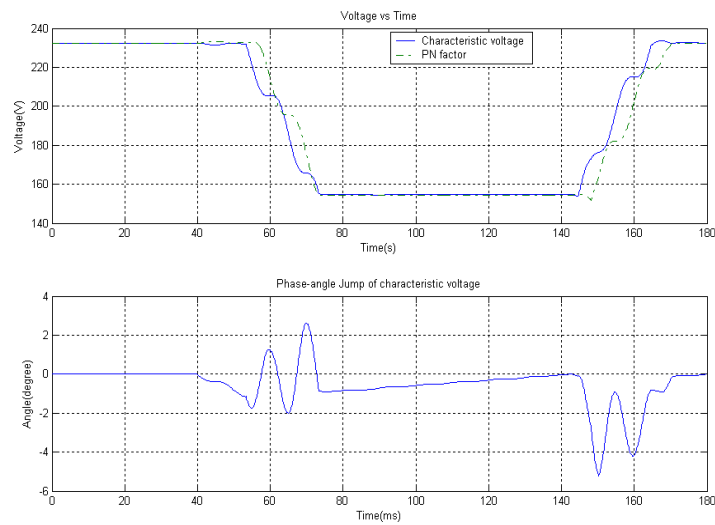
According to equation (45), the sag index T is,

$$T = \frac{1}{60^0} \times \arg\left(\frac{0.345 \angle 134.7^0}{230 \angle 0 - 154 \angle -0.4^0}\right) = 2.23 \cong 2$$

Thus, according to Table 2.3, it is classified as sag type Cb.



(a) Three-phase voltages



(b) Characteristic voltage and PN factor

Fig. C.41 Three-phase-to-ground fault (voltage-divider, measurement)

● Single-phase-to-ground fault

As shown in Fig.C.42, the three-phase retained voltages at PCC are,

$$U_a = 154V, U_b = 249V, U_c = 246V$$

The phase-angle jumps at PCC are,

$$\Delta\phi_a = 2.5^0, \Delta\phi_b = -3.3^0, \Delta\phi_c = 7.8^0$$

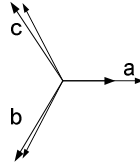
The magnitudes of characteristic voltage and PN factor at PCC are,

$$U = 199V, F = 232V$$

The phase-angle jump of characteristic voltage at PCC is,

$$\Delta\phi = 2.4^\circ$$

The phasor diagram of the three phase voltages is,



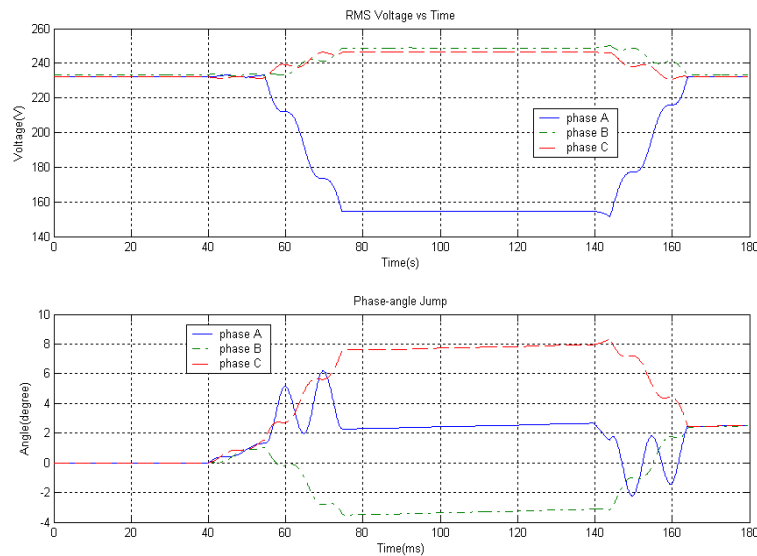
The sequence voltages calculated from the three phasors at PCC are,

$$\overline{U}_1 = 216\angle 1.6^\circ V, \overline{U}_2 = 17.1\angle -172.8^\circ V$$

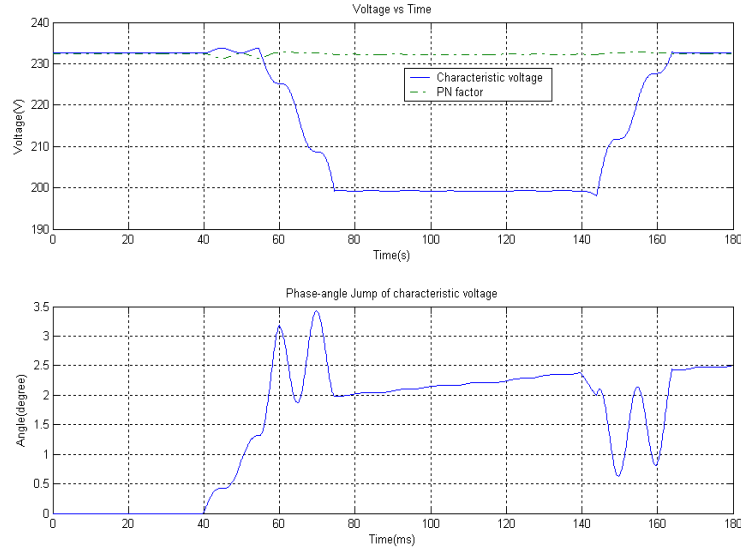
The sag index T is,

$$T = \frac{1}{60^\circ} \times \arg\left(\frac{17.1\angle -172.8^\circ}{230\angle 0 - 216\angle 1.6^\circ}\right) = 3.49 \cong 3$$

Thus, according to Table 2.3, it is classified as sag type Da.



(a) Three-phase voltages



(b) Characteristic voltage and PN factor

Fig. C.42 Single-phase-to-ground fault (voltage-divider, measurement)

● Double-phase fault

As shown in Fig.C.43, the three-phase retained voltages at PCC are,

$$U_a = 232V, U_b = 177V, U_c = 178V$$

The phase-angle jumps at PCC are,

$$\Delta\phi_a = -0.5^\circ, \Delta\phi_b = -11.0^\circ, \Delta\phi_c = 11.0^\circ$$

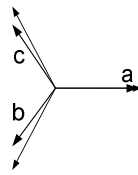
The magnitudes of characteristic voltage and PN factor at PCC are,

$$U = 154V, F = 233V$$

The phase-angle jump of characteristic voltage at PCC is,

$$\Delta\phi = 0.4^\circ$$

The phasor diagram of the three phase voltages is,



Thus, according to Table 2.2, it is classified as sag type C.

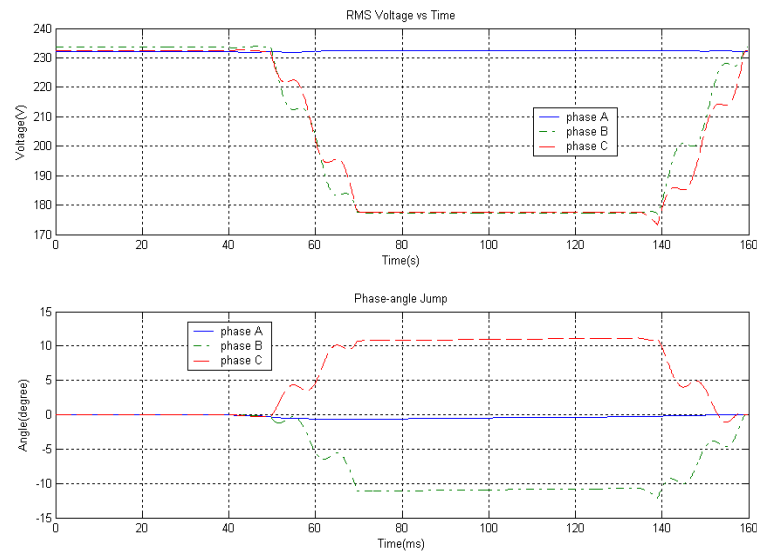
The sequence voltages calculated from the three phasors at PCC are,

$$\overline{U}_1 = 193\angle -0.2^\circ V, \overline{U}_2 = 38.8\angle -1.5^\circ V$$

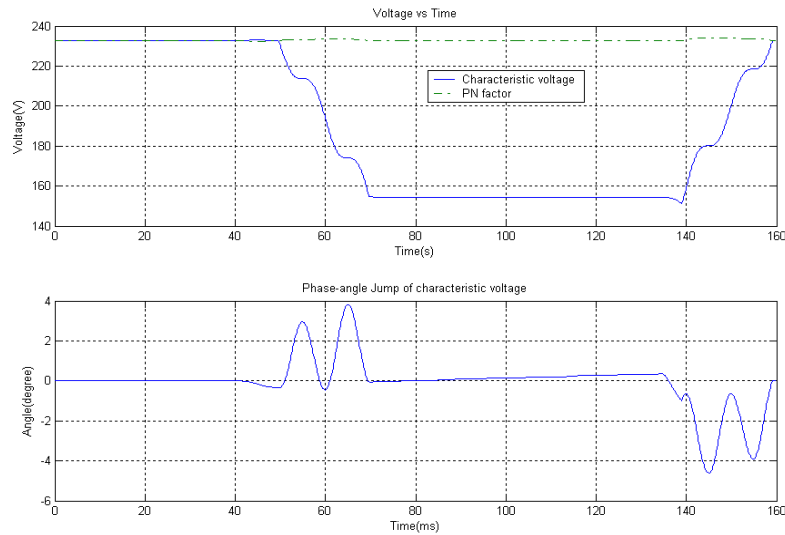
The sag index T is,

$$T = \frac{1}{60^\circ} \times \arg\left(\frac{38.8\angle -1.5^\circ}{230\angle 0 - 193\angle -0.2^\circ}\right) = 0.1 \cong 0$$

Thus, according to Table 2.3, it is classified as sag type Ca.



(a) Three-phase voltages



(b) Characteristic voltage and PN factor

Fig. C.43 Double-phase fault (voltage-divider, measurement)

● Double-phase-to-ground fault

As shown in Fig.C.44, the three-phase retained voltages at PCC are,

$$U_a = 253V, U_b = 155V, U_c = 154V$$

The phase-angle jumps at PCC are,

$$\Delta\phi_a = 0.7^\circ, \Delta\phi_b = 1.2^\circ, \Delta\phi_c = 1.1^\circ$$

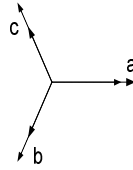
The magnitudes of characteristic voltage and PN factor at PCC are,

$$U = 155V, F = 220V$$

The phase-angle jump of characteristic voltage at PCC is,

$$\Delta\phi = 2.0^\circ$$

The phasor diagram of the three phase voltages is,



Thus, according to Table 2.2, it is classified as sag type E.

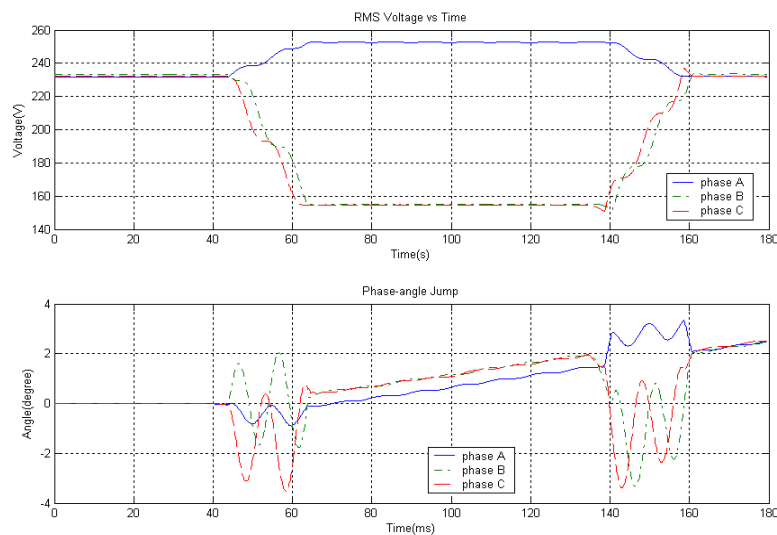
The sequence voltages calculated from the three phasors at PCC are,

$$\overline{U}_1 = 187 \angle 0.9^\circ V, \quad \overline{U}_2 = 32.8 \angle 0.5^\circ V$$

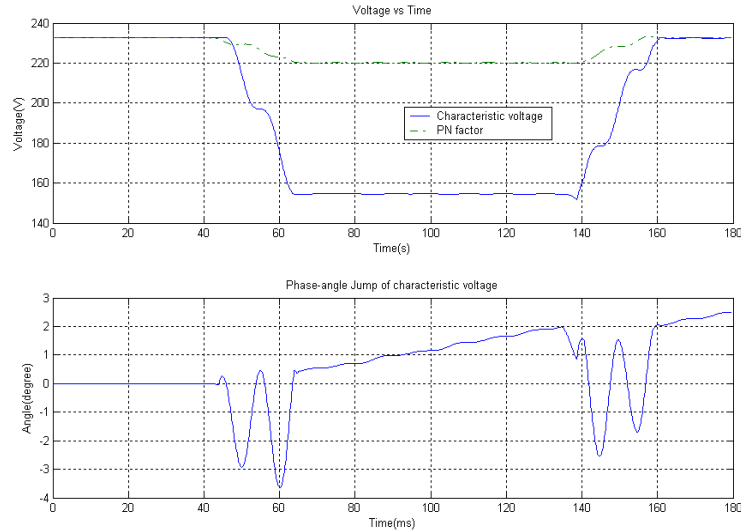
The sag index T is,

$$T = \frac{1}{60^\circ} \times \arg\left(\frac{32.8 \angle 0.5^\circ}{230 \angle 0 - 187 \angle 0.9^\circ}\right) = 0.08 \cong 0$$

Thus, according to Table 2.3, it is classified as sag type Ca.



(a) Three-phase voltages



(b) Characteristic voltage and PN factor

Fig. C.44 Double-phase-to-ground fault (voltage-divider, measurement)

◇ INDUCTION MACHINE LOADED

● Three-phase-to-ground fault

As shown in Fig.C.45, the three-phase retained voltages at PCC are,

$$U_a = 154V, U_b = 154V, U_c = 154V$$

The phase-angle jumps at PCC are,

$$\Delta\phi_a = 1.4^\circ, \Delta\phi_b = 1.4^\circ, \Delta\phi_c = 1.3^\circ$$

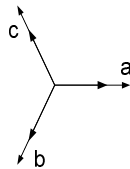
The magnitudes of characteristic voltage and PN factor at PCC are,

$$U = 153V, F = 153V$$

The phase-angle jump of characteristic voltage at PCC is,

$$\Delta\phi = 1.6^\circ$$

The phasor diagram of the three phase voltages is,



Thus, according to Table 2.2, it is classified as sag type A.

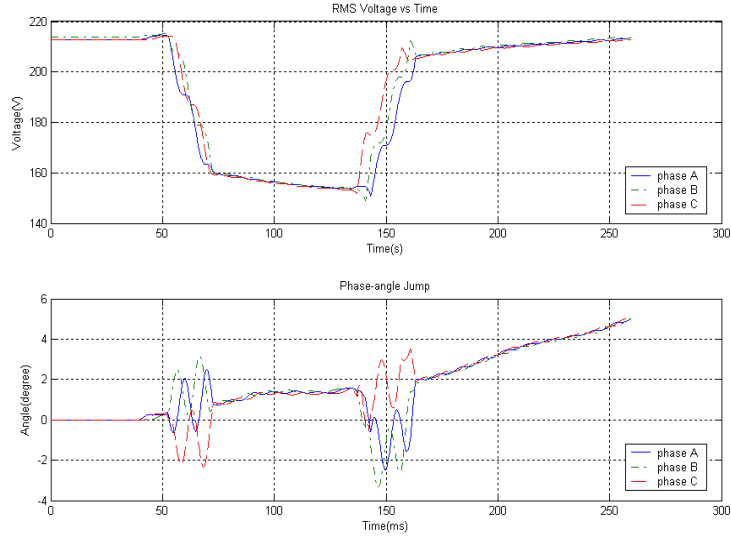
The sequence voltages calculated from the three phasors at PCC are,

$$\overline{U}_1 = 154\angle 1.4^\circ V, \overline{U}_2 = 0.09\angle 151.4^\circ V$$

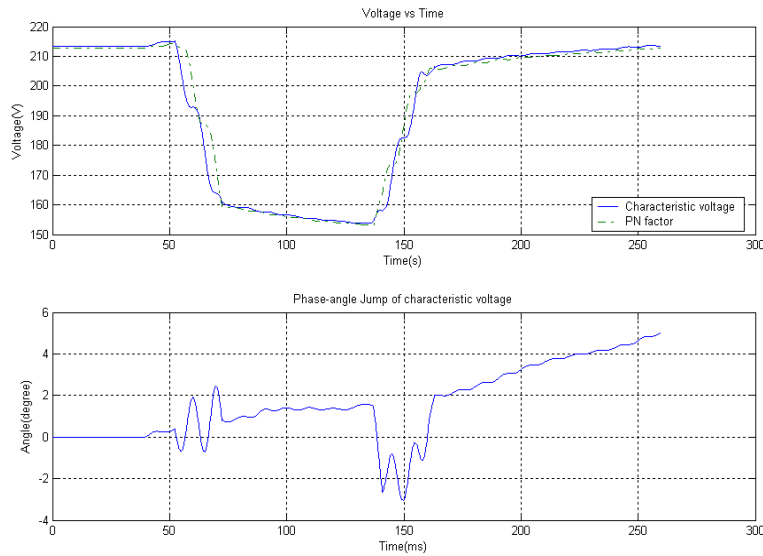
If we assume the pre-fault voltage at PCC is $215\angle 0V$, according to equation (45), the sag index T is,

$$T = \frac{1}{60^0} \times \arg\left(\frac{0.09 \angle 151.4^0}{215 \angle 0 - 154 \angle 1.4^0}\right) = 2.58 \approx 3$$

Thus, according to Table 2.3, it is classified as sag type Da.



(a) Three-phase voltages



(b) Characteristic voltage and PN factor

Fig. C.45 Three-phase-to-ground fault (voltage-divider with IM, measurement)

● Single-phase-to-ground fault

As shown in Fig.C.46, the three-phase retained voltages at PCC are,

$$U_a = 149V, U_b = 233V, U_c = 230V$$

The phase-angle jumps at PCC are,

$$\Delta\phi_a = 0, \Delta\phi_b = -7.4^0, \Delta\phi_c = 6.5^0$$

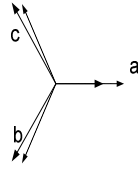
The magnitudes of characteristic voltage and PN factor at PCC are,

$$U = 192V, F = 215V$$

The phase-angle jump of characteristic voltage at PCC is,

$$\Delta\phi = -0.2^\circ$$

The phasor diagram of the three phase voltages is,



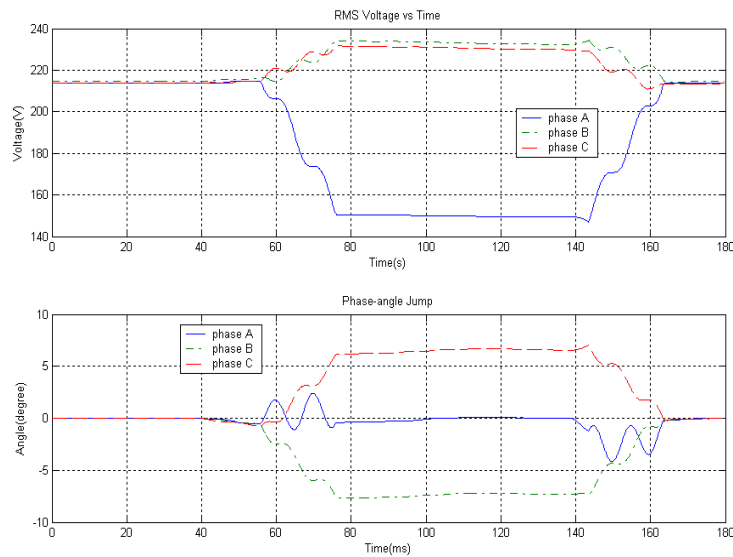
The sequence voltages calculated from the three phasors at PCC are,

$$\overline{U}_1 = 203\angle 0V, \overline{U}_2 = 11.1\angle 166.4V$$

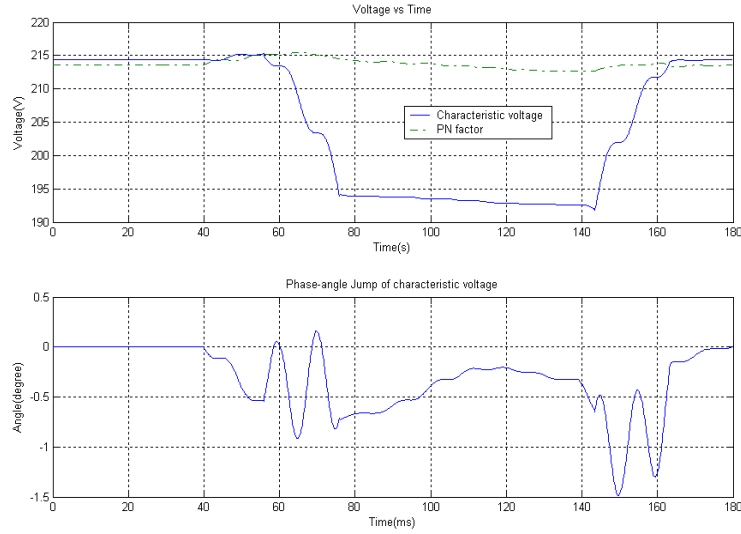
The sag index T is,

$$T = \frac{1}{60^\circ} \times \arg\left(\frac{11.1\angle 166.4}{215\angle 0 - 203\angle 0}\right) = 2.76 \approx 3$$

Thus, according to Table 2.3, it is classified as sag type Da.



(a) Three-phase voltages



(b) Characteristic voltage and PN factor

Fig. C.46 Single-phase-to-ground fault (voltage-divider with IM, measurement)

● Double-phase fault

As shown in Fig.C.47, the three-phase retained voltages at PCC are,

$$U_a = 210V, U_b = 172V, U_c = 174V$$

The phase-angle jumps at PCC are,

$$\Delta\phi_a = 1.8^\circ, \Delta\phi_b = -5.0^\circ, \Delta\phi_c = 10.0^\circ$$

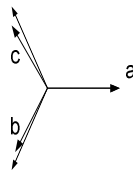
The magnitudes of characteristic voltage and PN factor at PCC are,

$$U = 154V, F = 216V$$

The phase-angle jump of characteristic voltage at PCC is,

$$\Delta\phi = 2.9^\circ$$

The phasor diagram of the three phase voltages is,



Thus, according to Table 2.2, it is classified as sag type C.

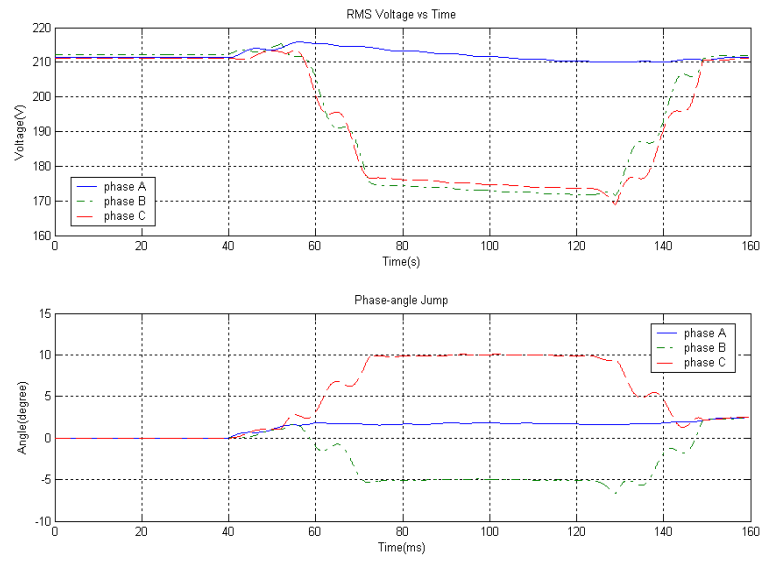
The sequence voltages calculated from the three phasors at PCC are,

$$\overline{U}_1 = 184\angle 2.3^\circ V, \overline{U}_2 = 25.9\angle -0.8^\circ V$$

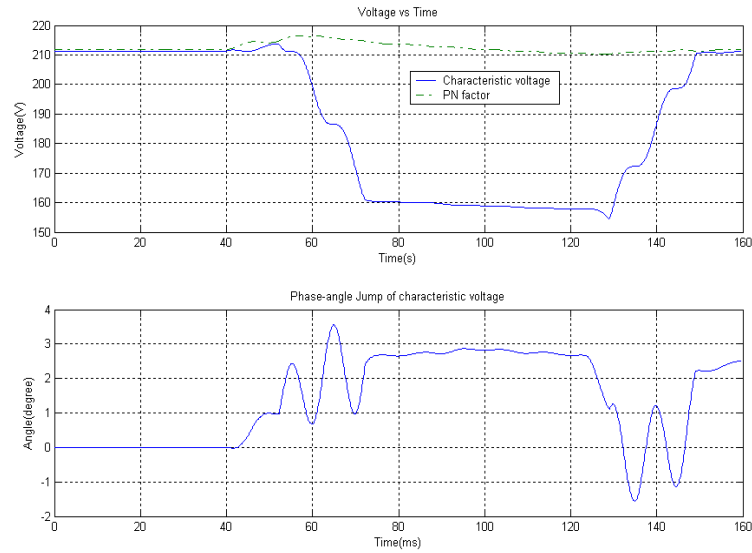
The sag index T is,

$$T = \frac{1}{60^\circ} \times \arg\left(\frac{25.9\angle -0.8^\circ}{215\angle 0 - 184\angle 2.3^\circ}\right) = 0.21 \cong 0$$

Thus, according to Table 2.3, it is classified as sag type Ca.



(a) Three-phase voltages



(b) Characteristic voltage and PN factor

Fig. C.47 Double-phase fault (voltage-divider with IM, measurement)

● **Double-phase-to-ground fault**

As shown in Fig.C.48, the three-phase retained voltages at PCC are,

$$U_a = 236V, U_b = 153V, U_c = 154V$$

The phase-angle jumps at PCC are,

$$\Delta\phi_a = 1.3^0, \Delta\phi_b = 4.5^0, \Delta\phi_c = -1.3^0$$

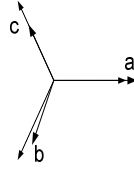
The magnitudes of characteristic voltage and PN factor at PCC are,

$$U = 155V, F = 206V$$

The phase-angle jump of characteristic voltage at PCC is,

$$\Delta\phi = 2.1^\circ$$

The phasor diagram of the three phase voltages is,



Thus, according to Table 2.2, it is classified as sag type E.

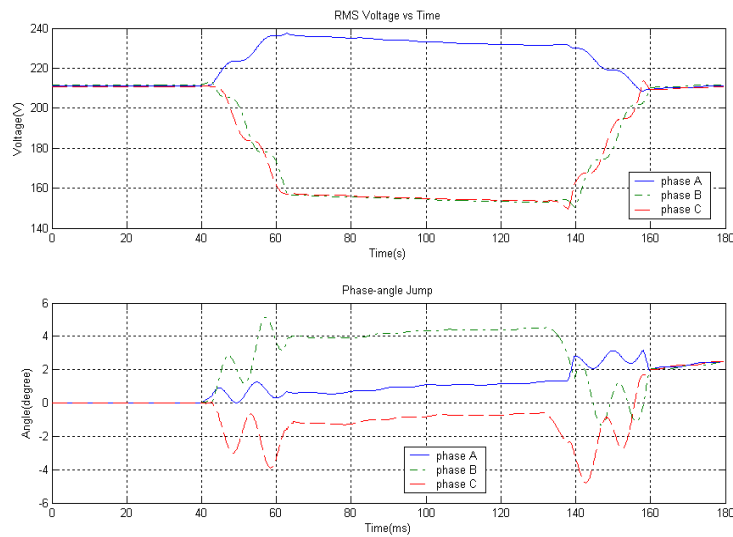
The sequence voltages calculated from the three phasors at PCC are,

$$\bar{U}_1 = 181\angle 1.5^\circ V, \quad \bar{U}_2 = 23.1\angle -0.1^\circ V$$

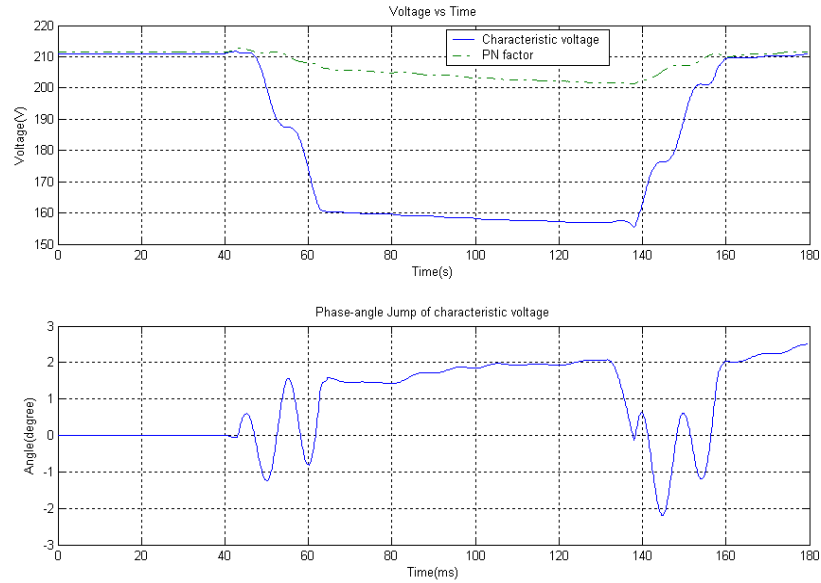
The sag index T is,

$$T = \frac{1}{60^\circ} \times \arg\left(\frac{23.1\angle -0.1^\circ}{215\angle 0 - 181\angle 1.5^\circ}\right) = 0.13 \cong 0$$

Thus, according to Table 2.3, it is classified as sag type Ca.



(a) Three-phase voltages



(b) Characteristic voltage and PN factor

Fig. C.48 Double-phase-to-ground fault (voltage-divider with IM, measurement)

C.3.3 Fault-load circuit

✧ TWO RESISTIVE LOADS

● Three-phase-to-ground fault

As shown in Fig.C.49, the three-phase retained voltages at the monitoring point (MP) are,

$$U_a = 1.63V, \quad U_b = 1.75V, \quad U_c = 1.69V$$

The phase-angle jumps at MP are not applicable in this case, because the monitoring point is the fault point and magnitudes of the phase voltages decrease to almost zero.

The magnitudes of characteristic voltage and PN factor at MP are,

$$U = 1.76V, \quad F = 1.76V$$

The phase-angle jump of characteristic voltage at MP is also not applicable,

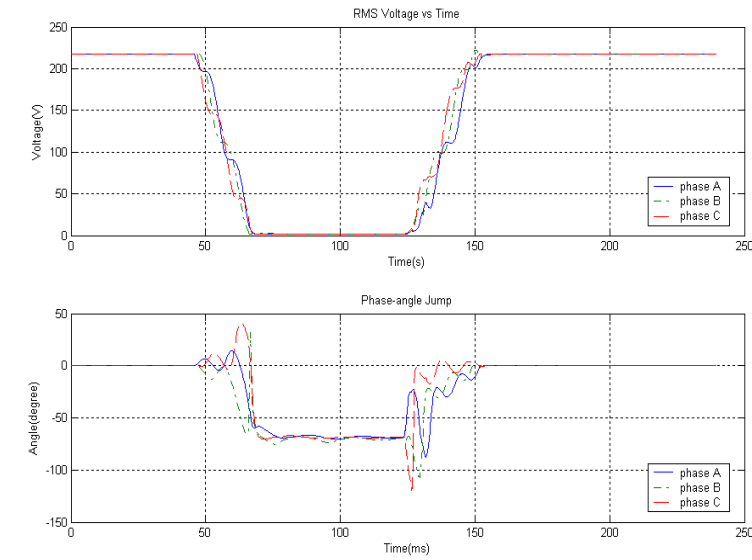
There is no phasor diagram of the three phase voltages.

Thus, according to Table 2.2, it can be classified as any sag type, i.e. sag type A.

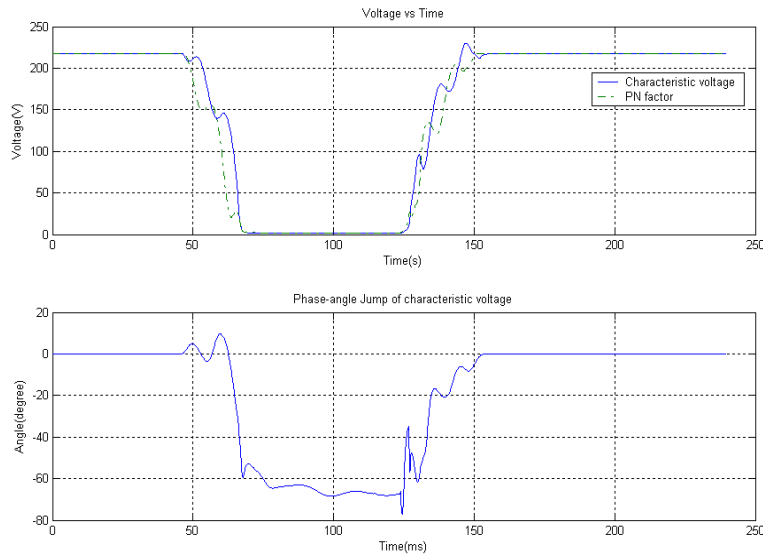
If assume the pre-fault voltage at MP2 to be $220\angle 0V$, according to equation (45), the sag index T is,

$$T = \frac{1}{60^\circ} \times \arg\left(\frac{0.03\angle 80.0^\circ}{220\angle 0 - 1.69\angle -70.0^\circ}\right) = 1.32 \cong 1$$

Thus, according to Table 2.3, it is classified as sag type Dc.



(a) Three-phase voltages



(b) Characteristic voltage and PN factor

Fig. C.49 Three-phase-to-ground fault (fault-load with two resistive loads, measurement)

● Single-phase-to-ground fault

As shown in Fig.C.50, the three-phase retained voltages at MP are,

$$U_a = 26.3V, U_b = 295V, U_c = 244V$$

The phase-angle jumps at MP are,

$$\Delta\phi_a = -88.4^{\circ}, \Delta\phi_b = -10.2^{\circ}, \Delta\phi_c = 21.3^{\circ}$$

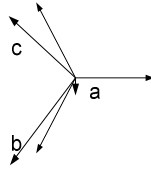
The magnitudes of characteristic voltage and PN factor at MP are,

$$U = 128V, F = 217V$$

The phase-angle jump of characteristic voltage at MP is,

$$\Delta\phi = 2.1^\circ$$

The phasor diagram of the three phase voltages is,



Thus, according to Table 2.2, it is classified as sag type B.

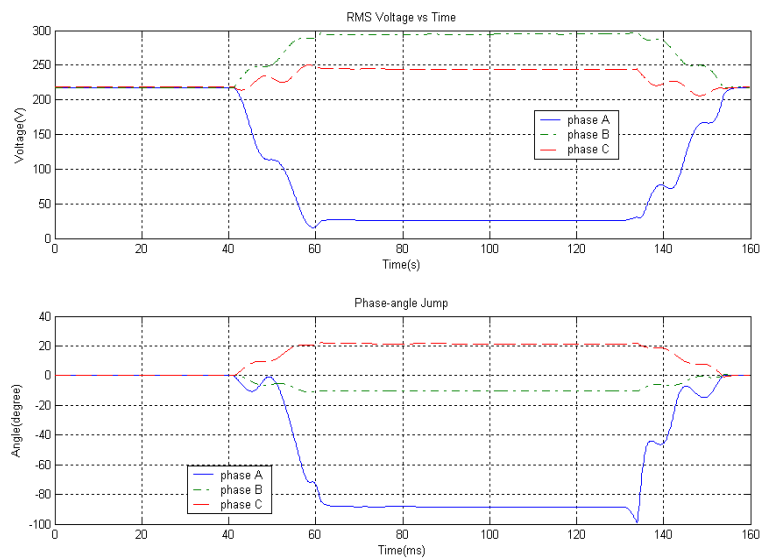
The sequence voltages calculated from the three phasors at MP2 are,

$$\bar{U}_1 = 173\angle 1.1^\circ V, \quad \bar{U}_2 = 45.5\angle 175.8^\circ V$$

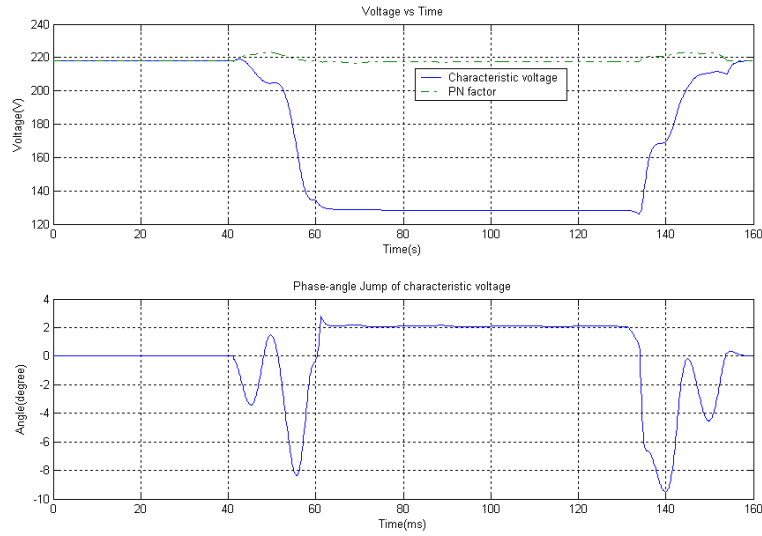
The sag index T is,

$$T = \frac{1}{60^\circ} \times \arg\left(\frac{45.5\angle 175.8^\circ}{220\angle 0 - 173\angle 1.1^\circ}\right) = 3.0 \cong 3$$

Thus, according to Table 2.3, it is classified as sag type Da.



(a) Three-phase voltages



(b) Characteristic voltage and PN factor

Fig. C.50 Single-phase-to-ground fault (fault-load with two resistive loads, measurement)

- **Double-phase fault**

As shown in Fig.C.51, the three-phase retained voltages at MP are,

$$U_a = 216V, U_b = 110V, U_c = 108V$$

The phase-angle jumps at MP are,

$$\Delta\phi_a = 3.2^\circ, \Delta\phi_b = -59.5^\circ, \Delta\phi_c = 61.0^\circ$$

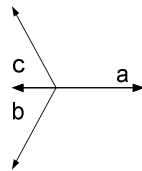
The magnitudes of characteristic voltage and PN factor at MP are,

$$U = 1.35V, F = 217V$$

The phase-angle jump of characteristic voltage at MP is,

$$\Delta\phi = -112.4^\circ$$

The phasor diagram of the three phase voltages is,



Thus, according to Table 2.2, it is classified as sag type C.

The sequence voltages calculated from the three phasors at MP2 are,

$$\overline{U}_1 = 108\angle 2.1^\circ V, \overline{U}_2 = 109\angle 2.7^\circ V$$

The sag index T is,

$$T = \frac{1}{60^\circ} \times \arg\left(\frac{109\angle 2.7^\circ}{220\angle 0^\circ - 108\angle 2.1^\circ}\right) = 0.08 \cong 0$$

Thus, according to Table 2.3, it is classified as sag type Ca.

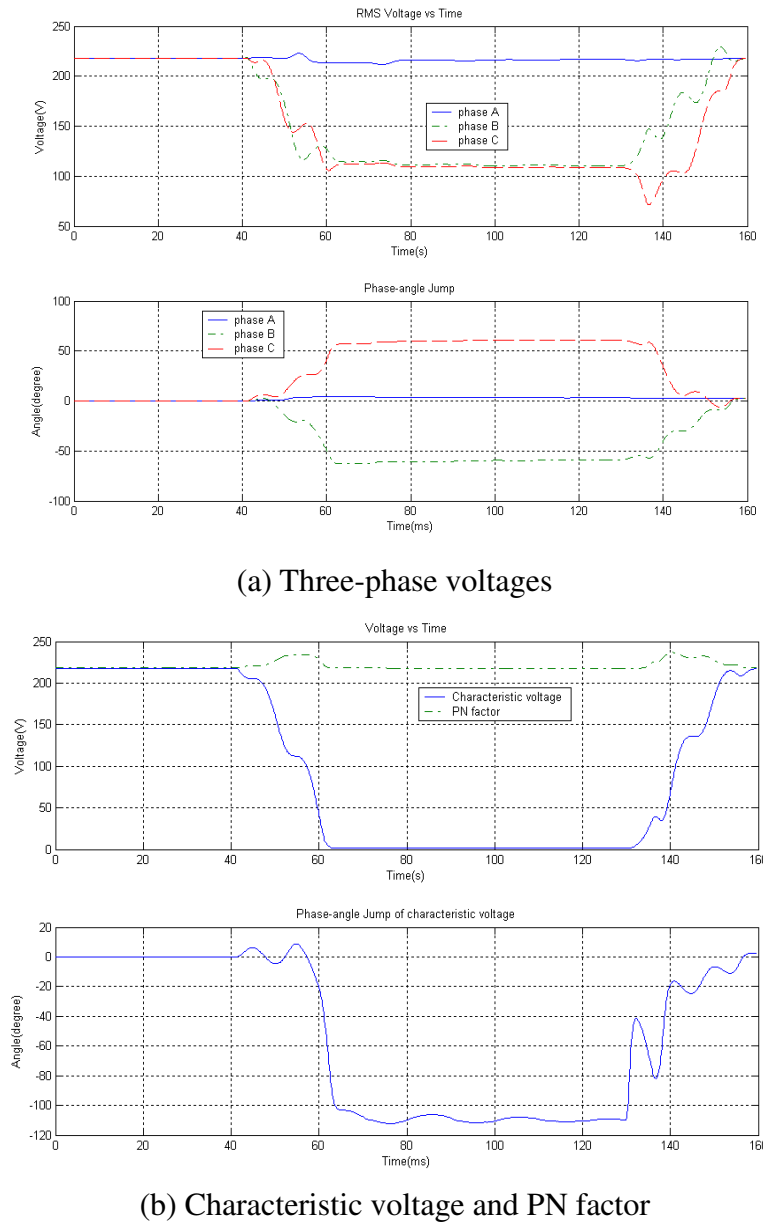


Fig. C.51 Double-phase fault (fault-load with two resistive loads, measurement)

● Double-phase-to-ground fault

As shown in Fig.C.52, the three-phase retained voltages at MP are,

$$U_a = 278V, U_b = 18.0V, U_c = 18.8V$$

The phase-angle jumps at MP are,

$$\Delta\phi_a = 6.2^\circ, \Delta\phi_b = -147.5^\circ, \Delta\phi_c = -35.5^\circ$$

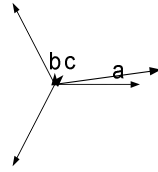
The magnitudes of characteristic voltage and PN factor at MP are,

$$U = 1.4V, F = 179V$$

The phase-angle jump of characteristic voltage at MP is,

$$\Delta\phi = -80.3^\circ$$

The phasor diagram of the three phase voltages is,



Thus, according to Table 2.2, it is classified as sag type E.

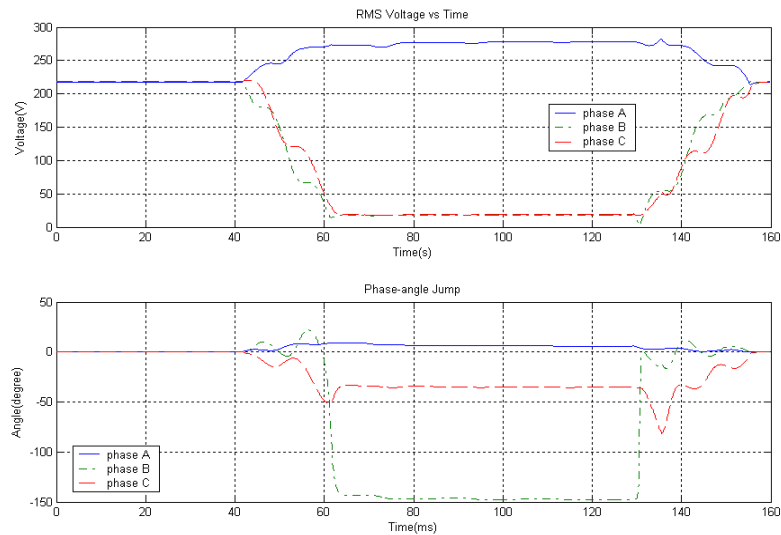
The sequence voltages calculated from the three phasors at MP2 are,

$$\overline{U}_1 = 92.2 \angle 2.0^\circ V, \quad \overline{U}_2 = 91.9 \angle 2.9^\circ V$$

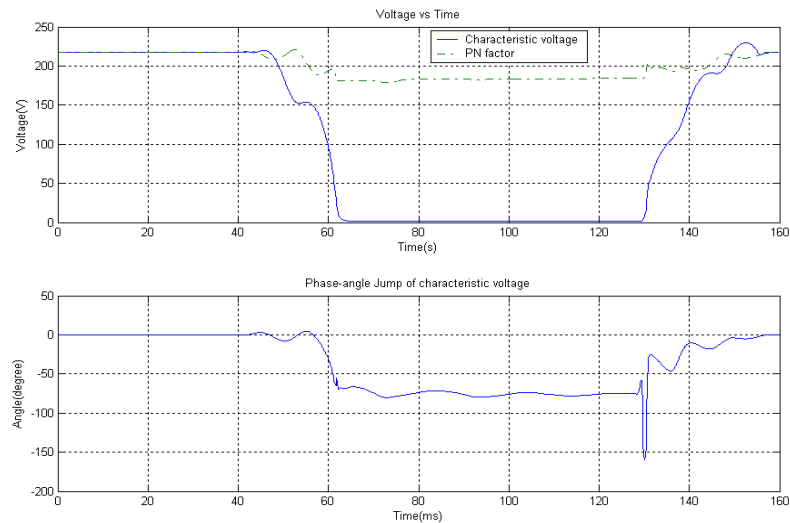
The sag index T is,

$$T = \frac{1}{60^\circ} \times \arg\left(\frac{91.9 \angle 2.9^\circ}{220 \angle 0 - 92.2 \angle 2.0^\circ}\right) = 0.07 \cong 0$$

Thus, according to Table 2.3, it is classified as sag type Ca.



(a) Three-phase voltages



(b) Characteristic voltage and PN factor

Fig. C.52 Double-phase-to-ground fault (fault-load with two resistive loads, measurement)

✧ **TWO RESISTIVE LOADS AND INDUCTION MACHINE (IM)**

● **Three-phase-to-ground fault**

As shown in Fig.C.53, the three-phase retained voltages at MP are,

$$U_a = 41.9V, U_b = 40.8V, U_c = 40.9V$$

The phase-angle jumps at MP are,

$$\Delta\phi_a = -46.0^\circ, \Delta\phi_b = -48.0^\circ, \Delta\phi_c = -46.3^\circ$$

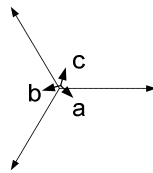
The magnitudes of characteristic voltage and PN factor at MP are,

$$U = 40.6V, F = 40.6V$$

The phase-angle jump of characteristic voltage at MP is,

$$\Delta\phi = -46.3^\circ$$

The phasor diagram of the three phase voltages is,



Thus, according to Table 2.2, it is classified as sag type B.

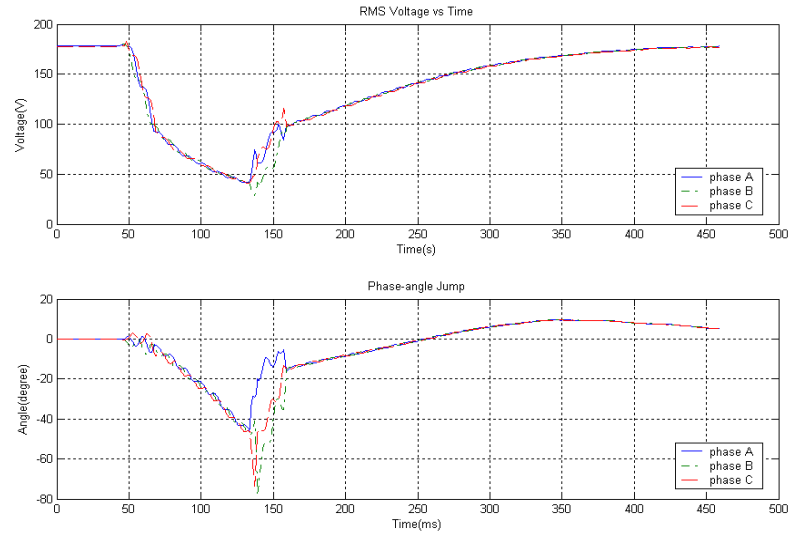
The sequence voltages calculated from the three phasors at MP2 are,

$$\bar{U}_1 = 41.2\angle -46.7^\circ V, \bar{U}_2 = 0.742\angle -27.4^\circ V$$

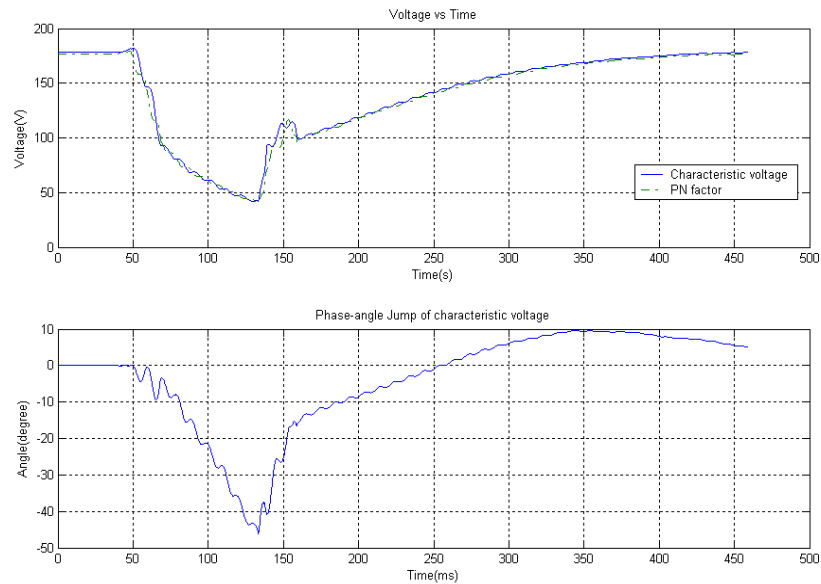
The sag index T is,

$$T = \frac{1}{60^\circ} \times \arg\left(\frac{0.742\angle -27.4^\circ}{222\angle 0 - 41.2\angle -46.7^\circ}\right) = 5.40 \cong 5$$

Thus, according to Table 2.3, it is classified as sag type Db.



(a) Three-phase voltages



(b) Characteristic voltage and PN factor

Fig. C.53 Three-phase-to-ground fault (fault-load with two resistive loads and IM, measurement)

● **Single-phase-to-ground fault**

As shown in Fig.C.54, the three-phase retained voltages at MP are,

$$U_a = 31.9V, U_b = 282V, U_c = 244V$$

The phase-angle jumps at MP are,

$$\Delta\phi_a = -72.1^{\circ}, \Delta\phi_b = -20.4^{\circ}, \Delta\phi_c = 28.5^{\circ}$$

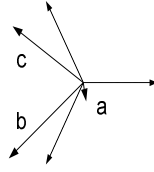
The magnitudes of characteristic voltage and PN factor at MP are,

$$U = 144V, F = 168V$$

The phase-angle jump of characteristic voltage at MP is,

$$\Delta\phi = -2.5^{\circ}$$

The phasor diagram of the three phase voltages is,



Thus, according to Table 2.2, it is classified as sag type B.

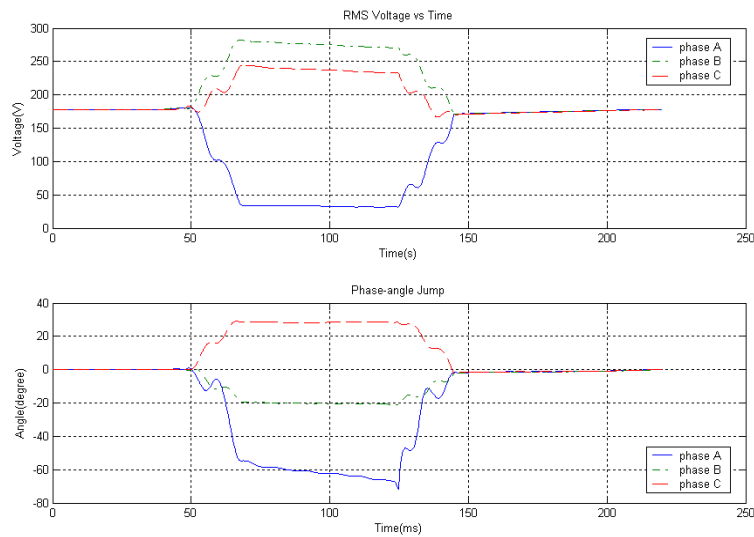
The sequence voltages calculated from the three phasors at MP2 are,

$$\overline{U}_1 = 163 \angle -1.4^{\circ} V, \quad \overline{U}_2 = 14.6 \angle 175.0^{\circ} V$$

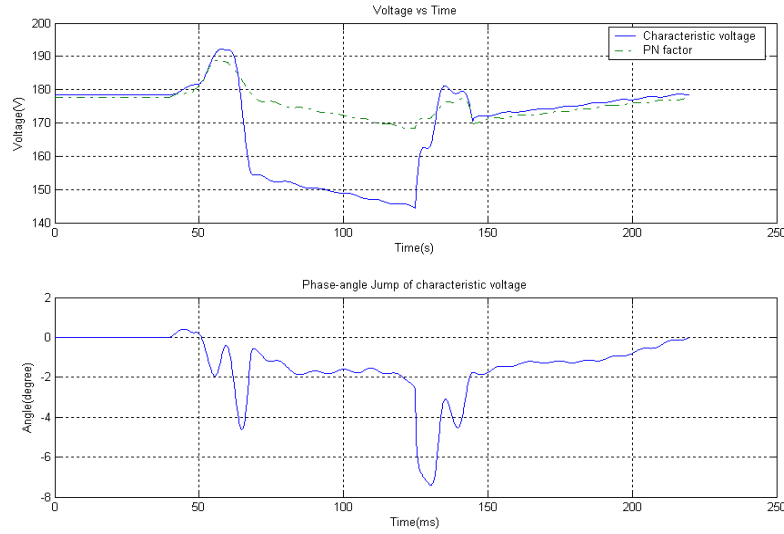
The sag index T is,

$$T = \frac{1}{60^{\circ}} \times \arg\left(\frac{14.6 \angle 175.0^{\circ}}{220 \angle 0 - 163 \angle -1.4^{\circ}}\right) = 2.85 \cong 3$$

Thus, according to Table 2.3, it is classified as sag type Da.



(a) Three-phase voltages



(b) Characteristic voltage and PN factor

Fig. C.54 Single-phase-to-ground fault (fault-load with two resistive loads and IM, measurement)

● Double-phase fault

As shown in Fig.C.55, the three-phase retained voltages at MP are,

$$U_a = 141V, U_b = 98.0V, U_c = 89.5V$$

The phase-angle jumps at MP are,

$$\Delta\phi_a = -8.2^\circ, \Delta\phi_b = -32.1^\circ, \Delta\phi_c = 12.9^\circ$$

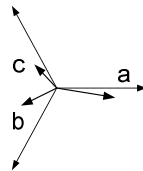
The magnitudes of characteristic voltage and PN factor at MP are,

$$U = 92.8V, F = 143V$$

The phase-angle jump of characteristic voltage at MP is,

$$\Delta\phi = -17.4^\circ$$

The phasor diagram of the three phase voltages is,



Thus, according to Table 2.2, it is classified as sag type C.

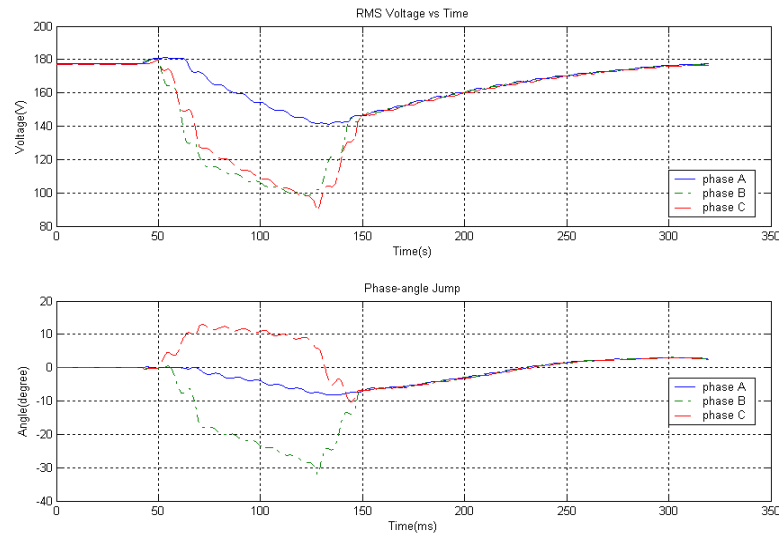
The sequence voltages calculated from the three phasors at MP2 are,

$$\overline{U}_1 = 105\angle -9.6^\circ V, \overline{U}_2 = 39.0\angle -3.8^\circ V$$

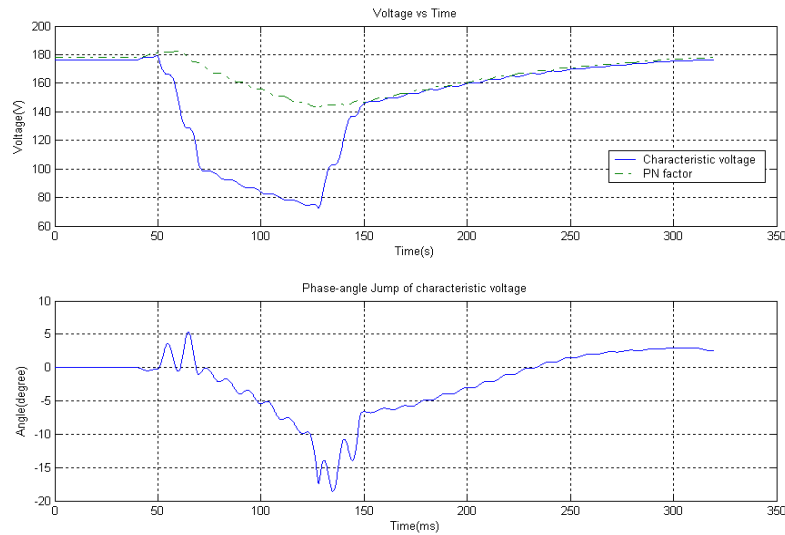
The sag index T is,

$$T = \frac{1}{60^\circ} \times \arg\left(\frac{39.0\angle -3.8^\circ}{220\angle 0 - 105\angle -9.6^\circ}\right) = 0.20 \cong 0$$

Thus, according to Table 2.3, it is classified as sag type Ca.



(a) Three-phase voltages



(b) Characteristic voltage and PN factor

Fig. C.55 Double-phase fault (fault-load with two resistive loads and IM, measurement)

● Double-phase-to-ground fault

As shown in Fig.C.56, the three-phase retained voltages at MP are,

$$U_a = 251V, U_b = 29.8V, U_c = 89.1V$$

The phase-angle jumps at MP are,

$$\Delta\phi_a = 2.6^{\circ}, \Delta\phi_b = 44.7^{\circ}, \Delta\phi_c = -55.3^{\circ}$$

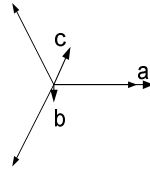
The magnitudes of characteristic voltage and PN factor at MP are,

$$U = 67.1V, F = 125V$$

The phase-angle jump of characteristic voltage at MP is,

$$\Delta\phi = -11.6^\circ$$

The phasor diagram of the three phase voltages is,



Thus, according to Table 2.2, it is classified as sag type E.

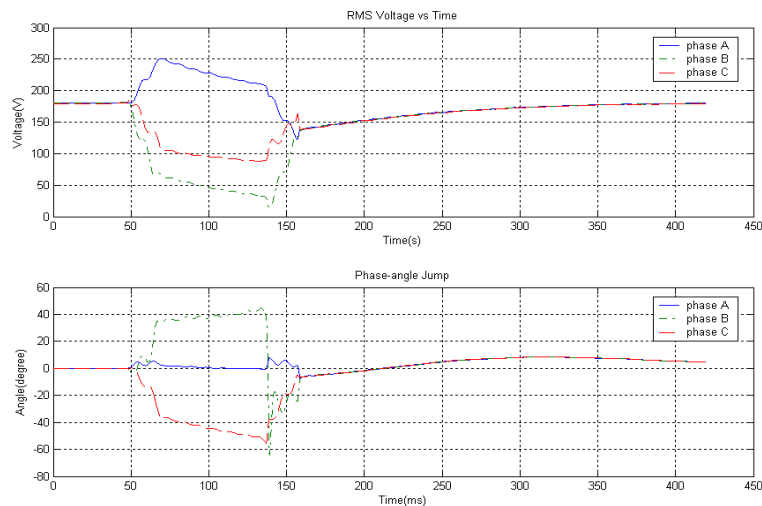
The sequence voltages calculated from the three phasors at MP2 are,

$$\overline{U}_1 = 108 \angle -7.2^\circ V, \quad \overline{U}_2 = 44.6 \angle 5.1^\circ V$$

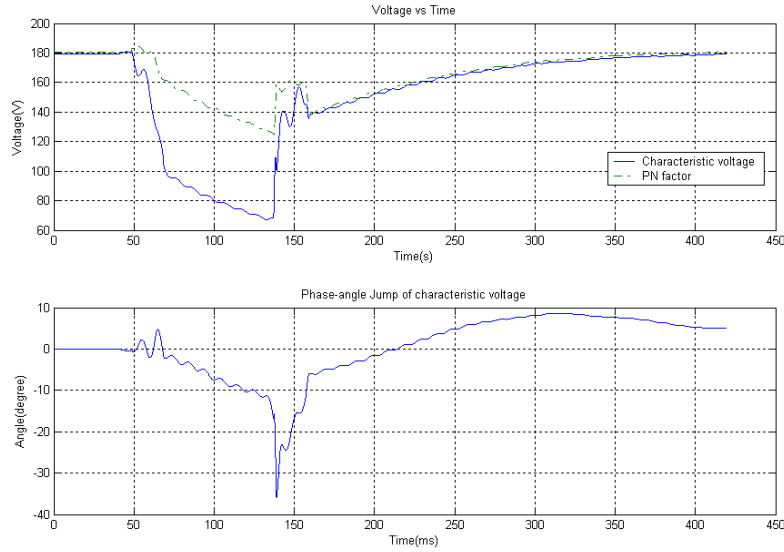
The sag index T is,

$$T = \frac{1}{60^\circ} \times \arg\left(\frac{44.6 \angle 5.1^\circ}{220 \angle 0 - 108 \angle -7.2^\circ}\right) = 0.03 \cong 0$$

Thus, according to Table 2.3, it is classified as sag type Ca.



(a) Three-phase voltages



(b) Characteristic voltage and PN factor

Fig. C.56 Double-phase-to-ground fault (fault-load with two resistive loads and IM, measurement)

C3.4 Fault-line circuit

◇ TWO RESISTIVE LOADS

● Three-phase-to-ground fault

As shown in Fig. 4.9., the retained positive-sequence voltages at MP1 and MP2 by PMU are,

$$U_{MP1} = 222V, \quad U_{MP2} = 110V$$

The phase-angle jumps at MP1, MP2, and the difference of them by PMU are,

$$\Delta\phi_{MP1} = 4.4^{\circ}, \quad \Delta\phi_{MP2} = 4.4^{\circ}, \quad \Delta\phi_{MP21} = 0.1^{\circ}$$

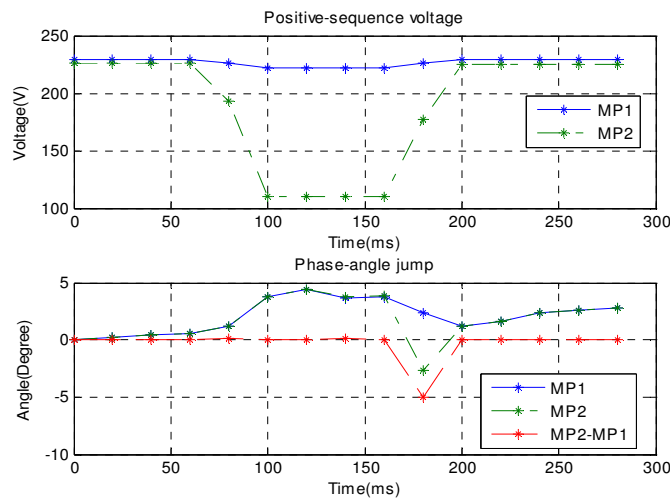


Fig. 4.9 Three-phase-to-ground fault (PMU, Fault-line with two resistive loads)

As shown in Fig.4.10, the three-phase retained voltages at MP2 by PQ monitor are,

$$U_a = 112V, U_b = 113V, U_c = 113V$$

The phase-angle jumps at MP2 are,

$$\Delta\phi_a = 1.7^\circ, \Delta\phi_b = 1.4^\circ, \Delta\phi_c = 1.5^\circ$$

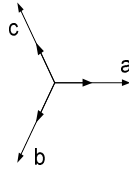
The magnitudes of characteristic voltage and PN factor at MP2 are,

$$U = 113V, F = 113V$$

The phase-angle jump of characteristic voltage at MP2 is,

$$\Delta\phi = 1.5^\circ$$

The phasor diagram of the three phase voltages is,



Thus, according to Table 2.2, it is classified as sag type A.

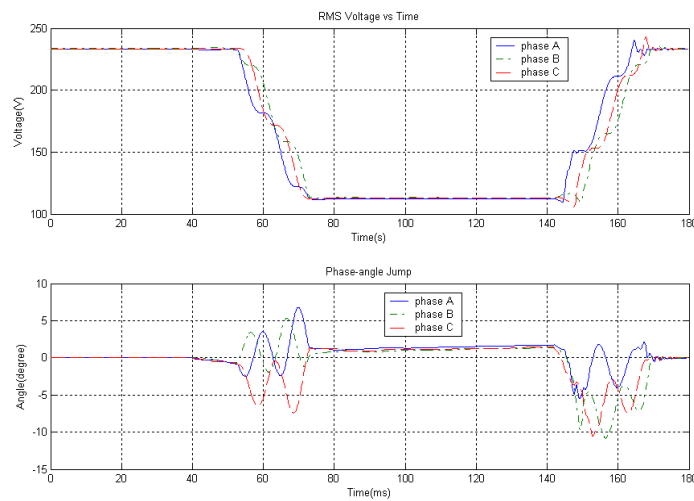
If we assume the pre-fault voltage at MP2 is $233\angle 0V$, the sequence voltages calculated from the three phasors at MP2 are,

$$\overline{U}_1 = 113\angle 1.5^\circ V, \overline{U}_2 = 0.321\angle 151.0^\circ V$$

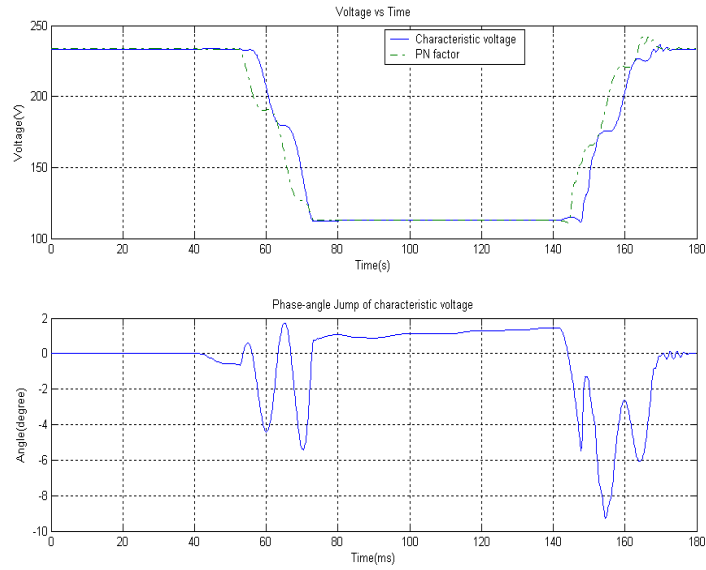
The sag index T is,

$$T = \frac{1}{60^\circ} \times \arg\left(\frac{0.321\angle 151.0^\circ}{233\angle 0 - 113\angle 1.5^\circ}\right) = 2.54 \cong 3$$

Thus, according to Table 2.3, it is classified as sag type Da.



(a) Three-phase voltages



(b) Characteristic voltage and PN factor

Fig. 4.10 Three-phase-to-ground fault (MP2, Fault-line with two resistive loads, measurement)

● Single-phase-to-ground fault

As shown in Fig. 4.11, the retained positive-sequence voltages at MP1 and MP2 by PMU are,

$$U_{MP1} = 227V, U_{MP2} = 197V$$

The phase-angle jumps at MP1, MP2, and the difference of them by PMU are,

$$\Delta\phi_{MP1} = 2.5^{\circ}, \Delta\phi_{MP2} = 2.8^{\circ}, \Delta\phi_{MP21} = 0.2^{\circ}$$

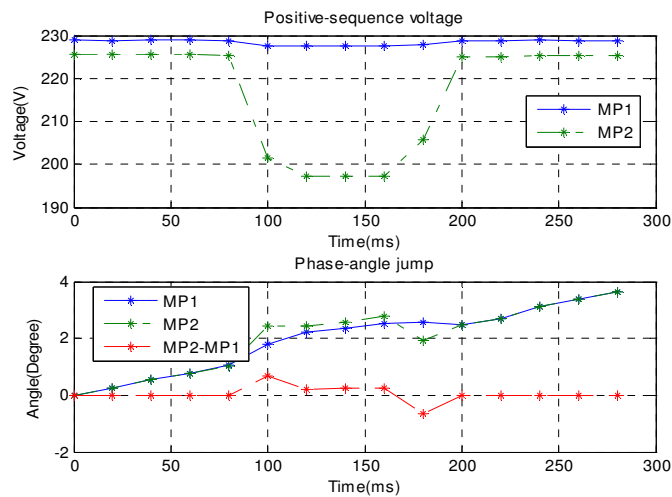


Fig. 4.11 Single-phase-to-ground fault (PMU, Fault-line with two resistive loads)

As shown in Fig. 4.12, the three-phase retained voltages at MP2 by PQ monitor are,

$$U_a = 111V, U_b = 262V, U_c = 255V$$

Phase-angle jumps at MP2 are,

$$\Delta\phi_a = -2.5^\circ, \quad \Delta\phi_b = -7.0^\circ, \quad \Delta\phi_c = 11.0^\circ$$

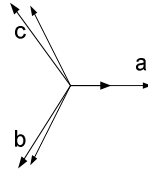
The magnitudes of characteristic voltage and PN factor at MP2 are,

$$U = 182V, \quad F = 233V$$

The phase-angle jump of characteristic voltage at MP2 is,

$$\Delta\phi = 2.5^\circ$$

The phasor diagram of the three phase voltages is,



Thus, according to Table 2.2, it is classified as sag type B.

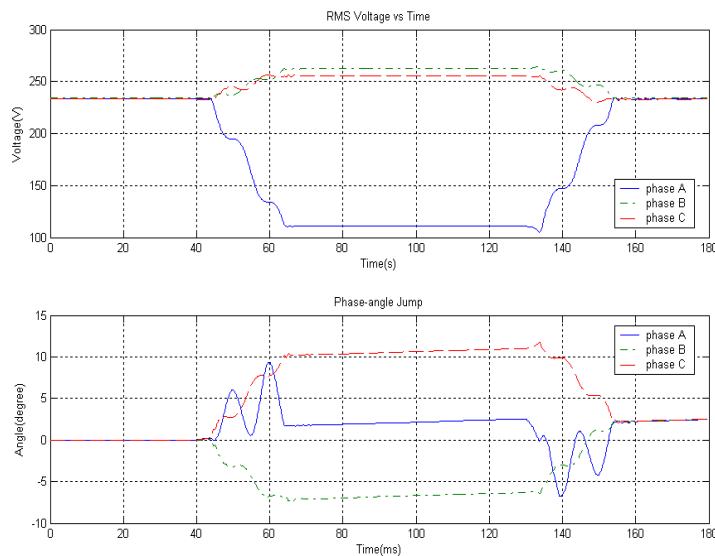
The sequence voltages calculated from the three phasors at MP2 are,

$$\overline{U}_1 = 207 \angle 1.1^\circ V, \quad \overline{U}_2 = 24.9 \angle -176.3^\circ V$$

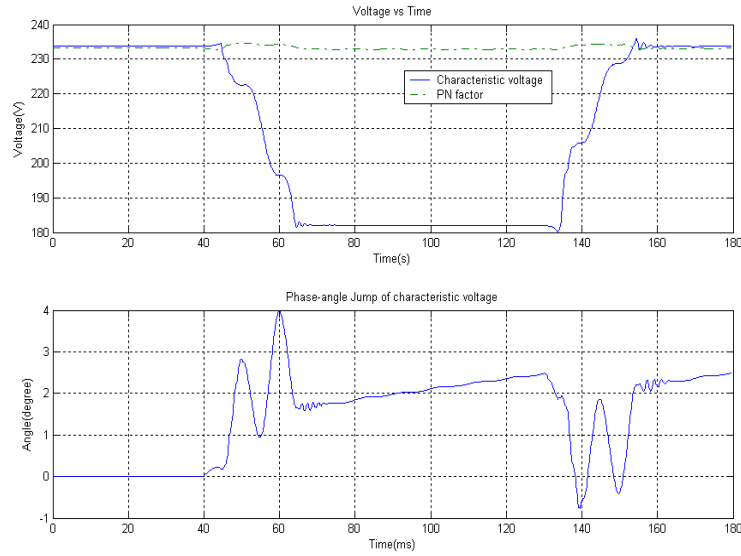
The sag index T is,

$$T = \frac{1}{60^\circ} \times \arg\left(\frac{24.9 \angle -176.3^\circ}{233 \angle 0 - 207 \angle 1.1^\circ}\right) = 3.23 \approx 3$$

Thus, according to Table 2.3, it is classified as sag type Da.



(a) Three-phase voltages



(b) Characteristic voltage and PN factor

Fig. 4.12 Single-phase-to-ground fault (MP2, Fault-line with two resistive loads, measurement)

● Double-phase fault

As shown in Fig. 4.13, the retained positive-sequence voltages at MP1 and MP2 by PMU are,

$$U_{MP1} = 225V, \quad U_{MP2} = 169V$$

The phase-angle jumps at MP1, MP2, and the difference of them by PMU are,

$$\Delta\phi_{MP1} = 3.0^{\circ}, \quad \Delta\phi_{MP2} = 2.7^{\circ}, \quad \Delta\phi_{MP21} = -0.3^{\circ}$$

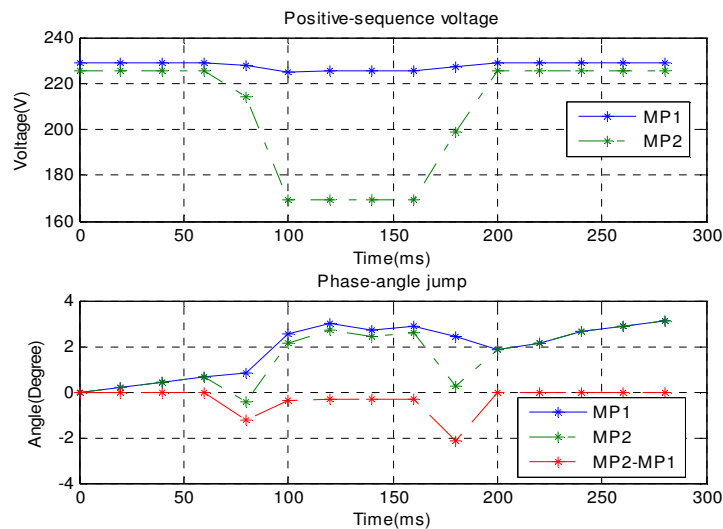


Fig. 4.13 Double-phase fault (PMU, Fault-line with two resistive loads)

As shown in Fig. 4.14, the three-phase retained voltages at MP2 by PQ monitor are,

$$U_a = 233V, \quad U_b = 149V, \quad U_c = 155V$$

Phase-angle jumps at MP2 are,

$$\Delta\phi_a = 2.2^\circ, \quad \Delta\phi_b = -18.4^\circ, \quad \Delta\phi_c = 22.7^\circ$$

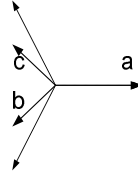
The magnitudes of characteristic voltage and PN factor at MP2 are,

$$U = 113V, \quad F = 233V$$

The phase-angle jump of characteristic voltage at MP2 is,

$$\Delta\phi = 4.1^\circ$$

The phasor diagram of the three phase voltages is,



Thus, according to Table 2.2, it is classified as sag type C.

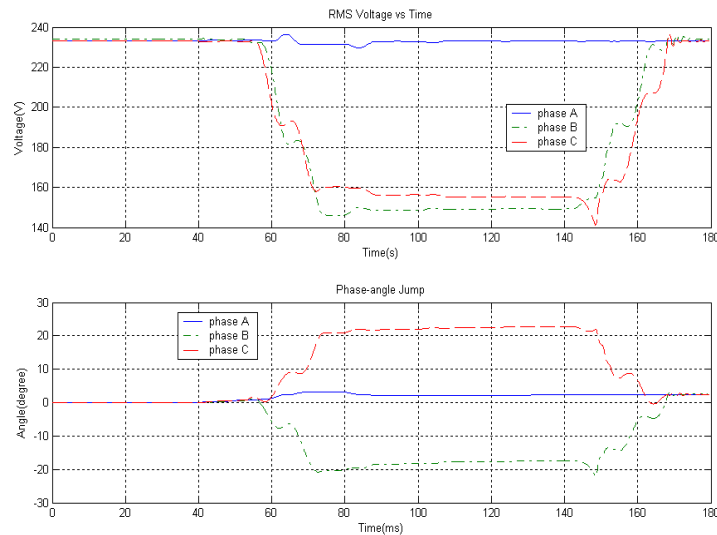
The sequence voltages calculated from the three phasors at MP2 are,

$$\overline{U}_1 = 173\angle 2.4^\circ V, \quad \overline{U}_2 = 61.1\angle 0.4^\circ V$$

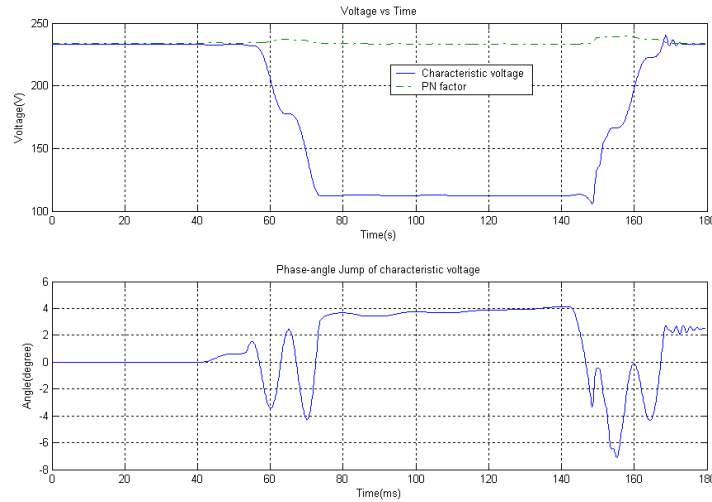
The sag index T is,

$$T = \frac{1}{60^\circ} \times \arg\left(\frac{61.1\angle 0.4^\circ}{233\angle 0 - 173\angle 2.4^\circ}\right) = 0.13 \cong 0$$

Thus, according to Table 2.3, it is classified as sag type Ca.



(a) Three-phase voltages



(b) Characteristic voltage and PN factor

Fig. 4.14 Double-phase fault (MP2, Fault-line with two resistive loads, measurement)

● Double-phase-to-ground fault

As shown in Fig. 4.15, the retained positive-sequence voltages at MP1 and MP2 by PMU are,

$$U_{MP1} = 224V, \quad U_{MP2} = 160V$$

The phase-angle jumps at MP1, MP2, and the difference of them by PMU are,

$$\Delta\phi_{MP1} = 1.7^{\circ}, \quad \Delta\phi_{MP2} = 1.7^{\circ}, \quad \Delta\phi_{MP21} = 0.1^{\circ}$$

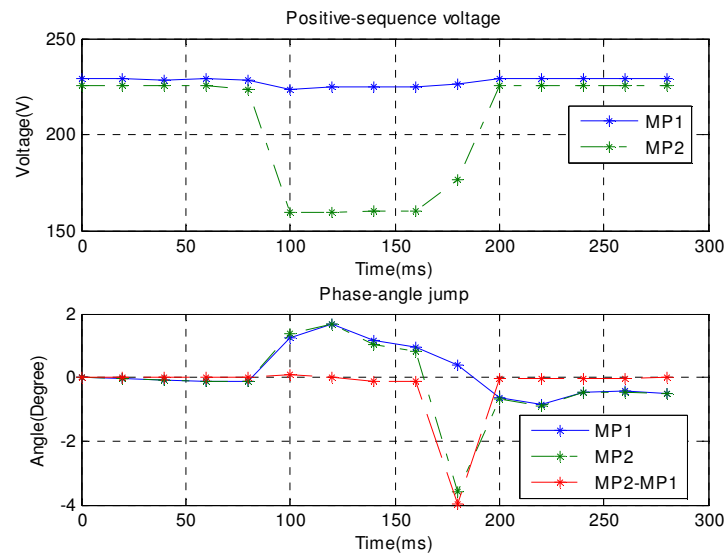


Fig. 4.15 Double-phase-to-ground fault (PMU, Fault-line with two resistive loads)
As shown in Fig. 4.16, the three-phase retained voltages at MP2 by PQ monitor are,

$$U_a = 266V, \quad U_b = 111V, \quad U_c = 114V$$

Phase-angle jumps at MP2 are,

$$\Delta\phi_a = 0.9^{\circ}, \quad \Delta\phi_b = 2.3^{\circ}, \quad \Delta\phi_c = 1.1^{\circ}$$

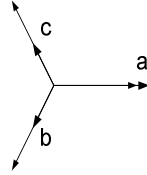
The magnitudes of characteristic voltage and PN factor at MP2 are,

$$U = 113V, F = 214V$$

The phase-angle jump of characteristic voltage at MP2 is,

$$\Delta\phi = 2.4^\circ$$

The phasor diagram of the three phase voltages is,



Thus, according to Table 2.2, it is classified as sag type E.

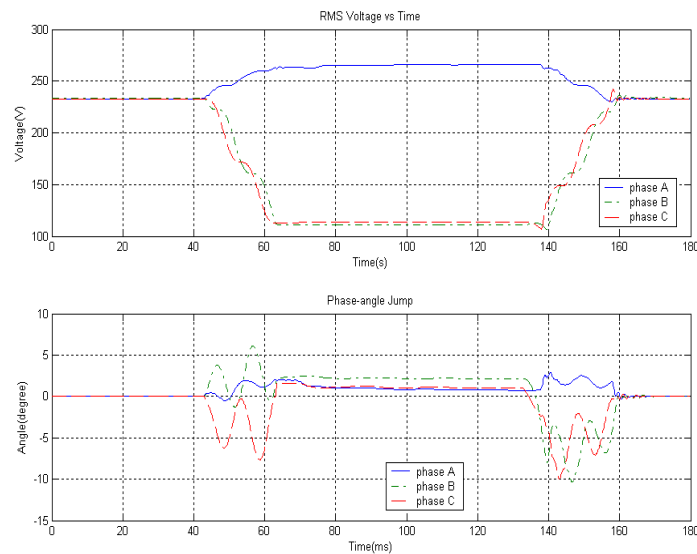
The sequence voltages calculated from the three phasors at MP2 are,

$$\overline{U}_1 = 164\angle 1.3^\circ V, \overline{U}_2 = 50.5\angle -0.7^\circ V$$

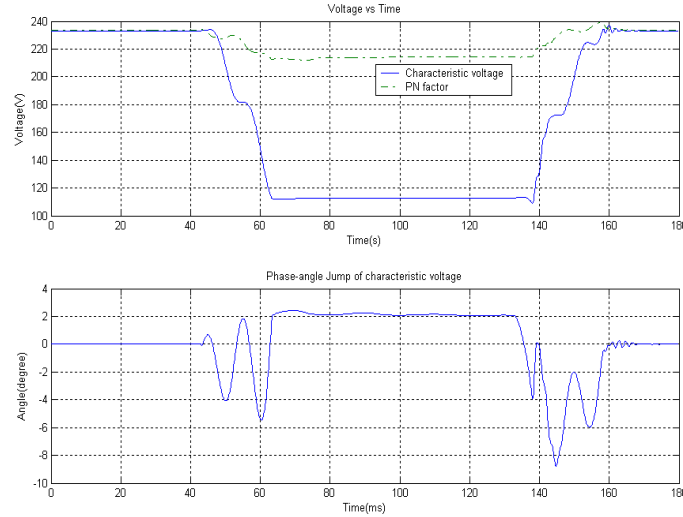
The sag index T is,

$$T = \frac{1}{60^\circ} \times \arg\left(\frac{50.5\angle -0.7^\circ}{233\angle 0 - 164\angle 1.3^\circ}\right) = 0.04 \cong 0$$

Thus, according to Table 2.3, it is classified as sag type Ca.



(a) Three-phase voltages



(b) Characteristic voltage and PN factor

Fig. 4.16 Double-phase-to-ground fault (MP2, Fault-line with two resistive loads, measurement)

◇ **TWO RESISTIVE LOADS AND INDUCTION MACHINE**

● **Three-phase-to-ground fault**

As shown in Fig. 4.17, the retained positive-sequence voltages at MP1 and MP2 by PMU are,

$$U_{MP1} = 222V, U_{MP2} = 113V$$

The phase-angle jumps at MP1, MP2, and the difference of them by PMU are,

$$\Delta\phi_{MP1} = 3.9^{\circ}, \Delta\phi_{MP2} = 1.8^{\circ}, \Delta\phi_{MP21} = -3.9^{\circ}$$

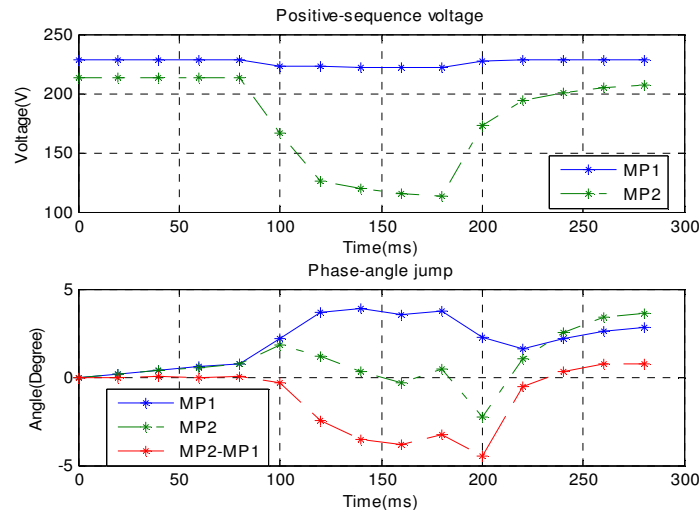


Fig. 4.17 Three-phase-to-ground fault (PMU, Fault-line with two resistive loads and IM)

As shown in Fig. 4.18., the three-phase retained voltages at MP2 by PQ monitor are,

$$U_a = 115V, U_b = 115V, U_c = 115V$$

Phase-angle jumps at MP2 are,

$$\Delta\phi_a = -3.7^\circ, \Delta\phi_b = -4.1^\circ, \Delta\phi_c = -4.0^\circ$$

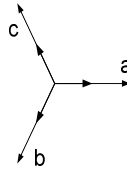
The magnitudes of characteristic voltage and PN factor at MP2 are,

$$U = 115V, F = 115V$$

The phase-angle jump of characteristic voltage at MP2 is,

$$\Delta\phi = -3.8^\circ$$

The phasor diagram of the three phase voltages is,



Thus, according to Table 2.2, it is classified as sag type A.

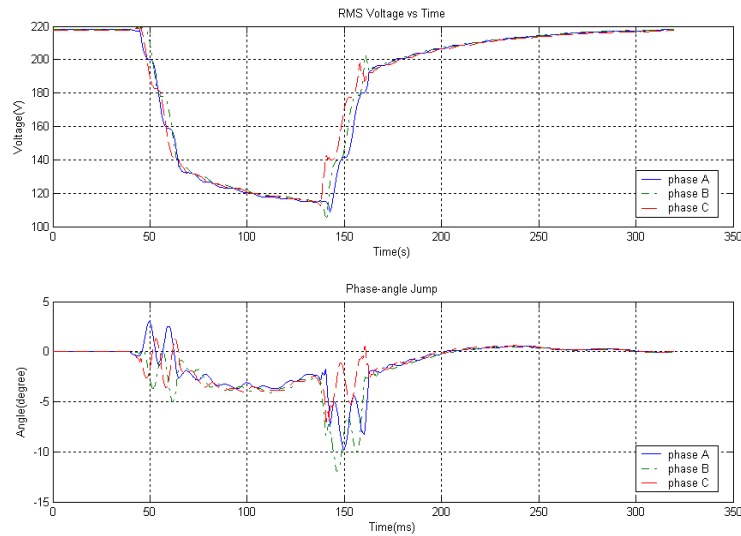
If we assume the pre-fault voltage at MP2 is $218\angle 0^\circ V$, the sequence voltages calculated from the three phasors at MP2 are,

$$\overline{U}_1 = 115\angle -3.9^\circ V, \overline{U}_2 = 0.241\angle 72.2^\circ V$$

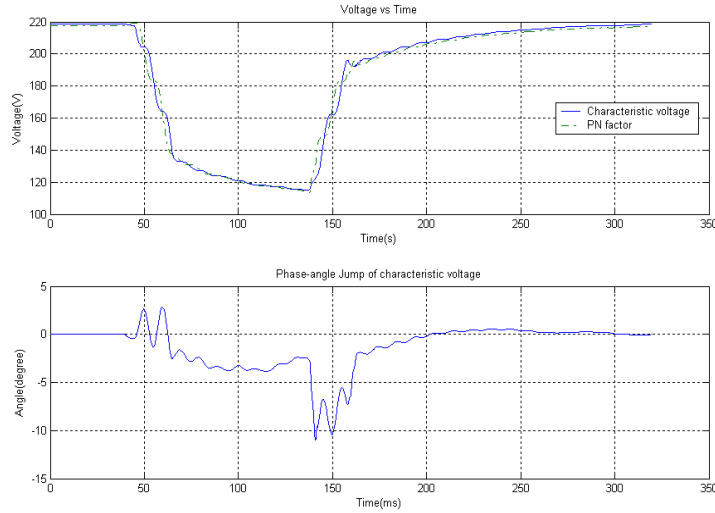
The sag index T is,

$$T = \frac{1}{60^\circ} \times \arg\left(\frac{0.241\angle 72.2^\circ}{218\angle 0^\circ - 115\angle -3.9^\circ}\right) = 1.13 \cong 1$$

Thus, according to Table 2.3, it is classified as sag type Dc.



(a) Three-phase voltages



(b) Characteristic voltage and PN factor

Fig. 4.18 Three-phase-to-ground fault (MP2, Fault-line with two resistive loads and IM, measurement)

● **Single-phase-to-ground fault**

As shown in Fig. 4.19, the retained positive-sequence voltages at MP1 and MP2 by PMU are,

$$U_{MP1} = 227V, \quad U_{MP2} = 190V$$

The phase-angle jumps at MP1, MP2, and the difference of them by PMU are,

$$\Delta\phi_{MP1} = -0.2^{\circ}, \quad \Delta\phi_{MP2} = -0.3^{\circ}, \quad \Delta\phi_{MP21} = -0.1^{\circ}$$

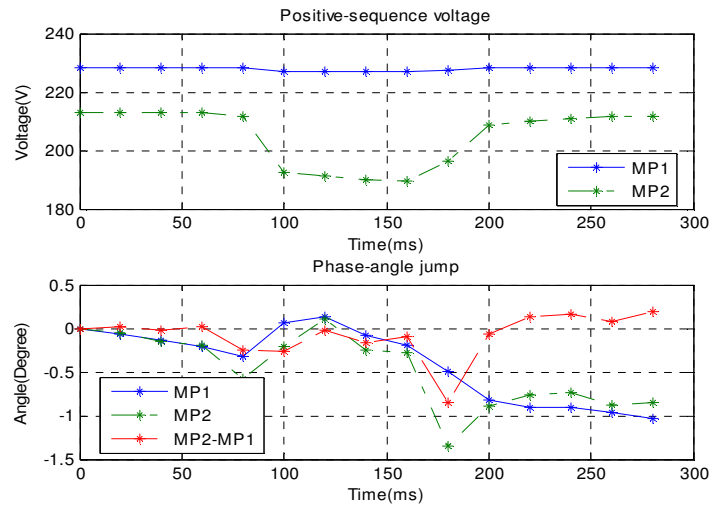


Fig. 4.19 Single-phase-to-ground fault (PMU, Fault-line with two resistive loads and IM)

As shown in Fig. 4.20, the three-phase retained voltages at MP2 by PQ monitor are,

$$U_a = 113V, \quad U_b = 254V, \quad U_c = 244V$$

Phase-angle jumps at MP2 are,

$$\Delta\phi_a = -1.9^0, \quad \Delta\phi_b = -13.8^0, \quad \Delta\phi_c = 9.5^0$$

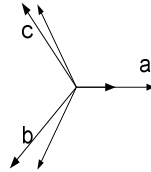
The magnitudes of characteristic voltage and PN factor at MP2 are,

$$U = 184V, \quad F = 212V$$

The phase-angle jump of characteristic voltage at MP2 is,

$$\Delta\phi = -2.0^0$$

The phasor diagram of the three phase voltages is,



Thus, according to Table 2.2, it is classified as sag type B.

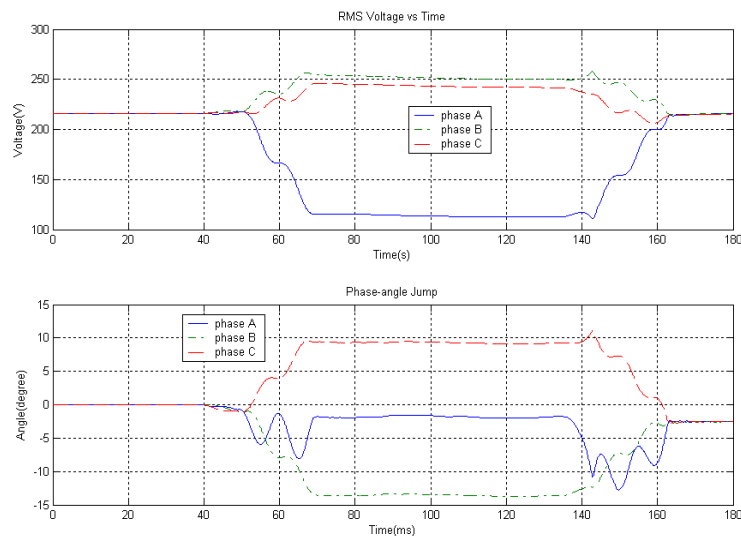
The sequence voltages calculated from the three phasors at MP2 are,

$$\overline{U}_1 = 200\angle -2.3^0V, \quad \overline{U}_2 = 15.0\angle 165.0^0V$$

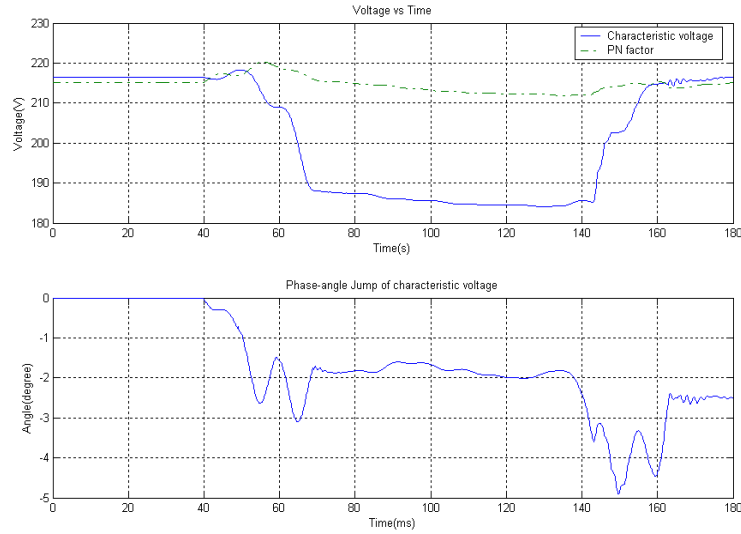
The sag index T is,

$$T = \frac{1}{60^0} \times \arg\left(\frac{15.0\angle 165.0^0}{218\angle 0 - 200\angle -2.3^0}\right) = 2.35 \cong 2$$

Thus, according to Table 2.3, it is classified as sag type Ca. **Note** that the symmetrical component algorithm gives an erroneous result of sag type.



(a) Three-phase voltages



(b) Characteristic voltage and PN factor

Fig. 4.20 Single-phase-to-ground fault (MP2, Fault-line with two resistive loads and IM, measurement)

● Double-phase fault

As shown in Fig. 4.21, the retained positive-sequence voltages at MP1 and MP2 by PMU are,

$$U_{MP1} = 225V, U_{MP2} = 164V$$

The phase-angle jumps at MP1, MP2, and the difference of them by PMU are,

$$\Delta\phi_{MP1} = 1.8^{\circ}, \Delta\phi_{MP2} = -1.4^{\circ}, \Delta\phi_{MP21} = -2.6^{\circ}$$

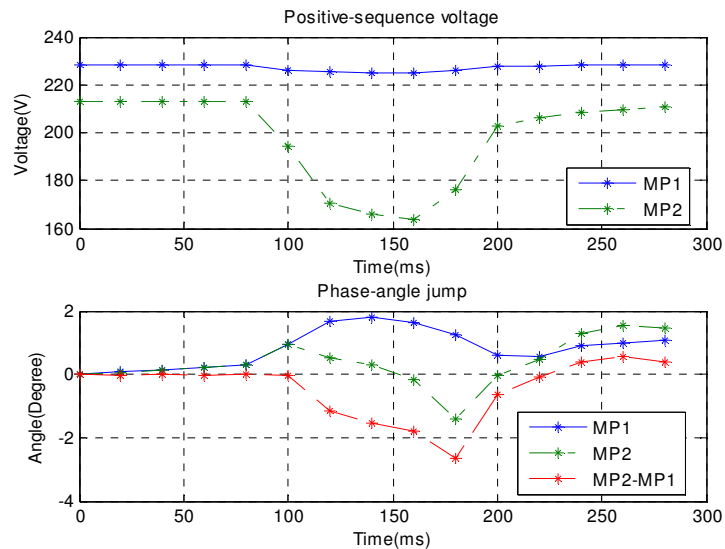


Fig. 4.21 Double-phase fault (PMU, Fault-line with two resistive loads and IM)

As shown in Fig. 4.22, the three-phase retained voltages at MP2 by PQ monitor are,

$$U_a = 202V, U_b = 146V, U_c = 157V$$

Phase-angle jumps at MP2 are,

$$\Delta\phi_a = -3.0^\circ, \Delta\phi_b = -13.4^\circ, \Delta\phi_c = 10.6^\circ$$

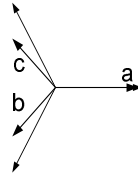
The magnitudes of characteristic voltage and PN factor at MP2 are,

$$U = 130V, F = 203V$$

The phase-angle jump of characteristic voltage at MP2 is,

$$\Delta\phi = 1.1^\circ$$

The phasor diagram of the three phase voltages is,



Thus, according to Table 2.2, it is classified as sag type C.

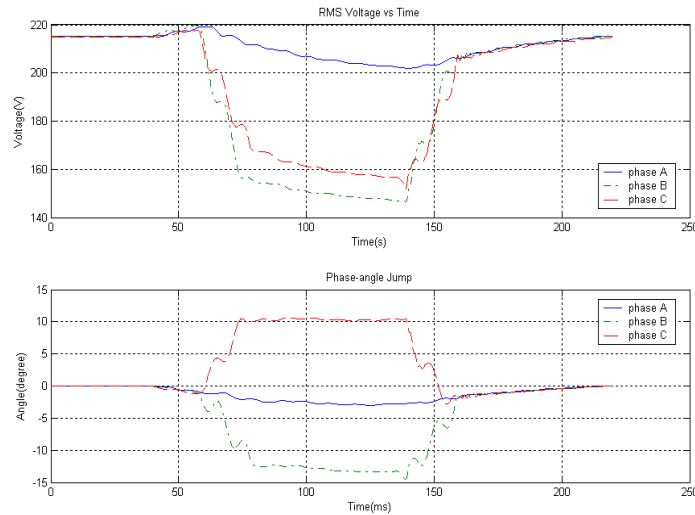
The sequence voltages calculated from the three phasors at MP2 are,

$$\overline{U}_1 = 166\angle -1.8^\circ V, \overline{U}_2 = 36.5\angle -9.9^\circ V$$

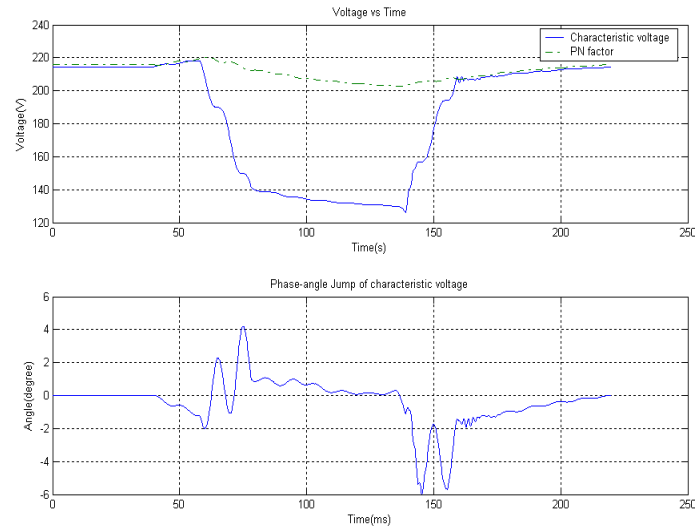
The sag index T is,

$$T = \frac{1}{60^\circ} \times \arg\left(\frac{36.5\angle -9.9^\circ}{218\angle 0 - 166\angle -1.8^\circ}\right) = 0.26 \cong 0$$

Thus, according to Table 2.3, it is classified as sag type Ca.



(a) Three-phase voltages



(b) Characteristic voltage and PN factor

Fig. 4.22 Double-phase fault (MP2, Fault-line with two resistive loads and IM, measurement)

● Double-phase-to-ground fault

As shown in Fig. 4.23, the retained positive-sequence voltages at MP1 and MP2 by PMU are,

$$U_{MP1} = 225V, \quad U_{MP2} = 156V$$

The phase-angle jumps at MP1, MP2, and the difference of them by PMU are,

$$\Delta\phi_{MP1} = 1.5^{\circ}, \quad \Delta\phi_{MP2} = -1.9^{\circ}, \quad \Delta\phi_{MP21} = -2.0^{\circ}$$

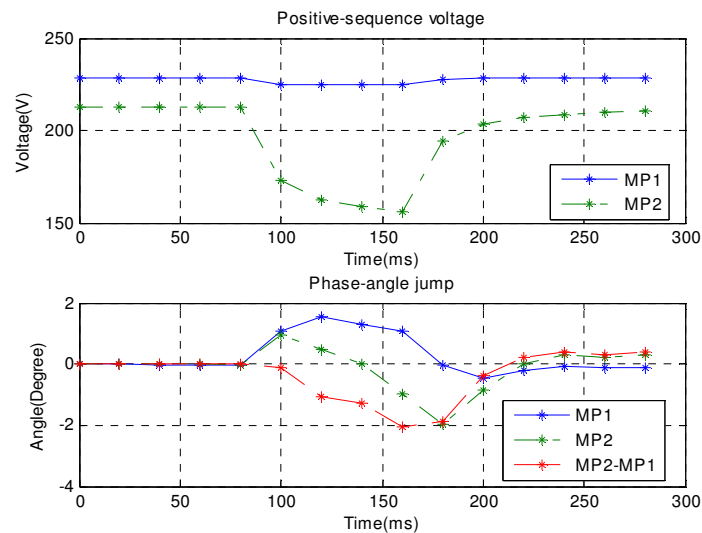


Fig. 4.23 Double-phase-to-ground fault (PMU, Fault-line with two resistive loads and IM)

As shown in Fig. 4.24, the three-phase retained voltages at MP2 by PQ monitor are,

$$U_a = 25V, \quad U_b = 116V, \quad U_c = 123V$$

Phase-angle jumps at MP2 are,

$$\Delta\phi_a = -1.8^\circ, \quad \Delta\phi_b = 9.4^\circ, \quad \Delta\phi_c = -7.9^\circ$$

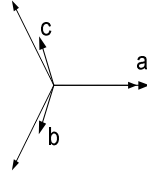
The magnitudes of characteristic voltage and PN factor at MP2 are,

$$U = 127V, \quad F = 189V$$

The phase-angle jump of characteristic voltage at MP2 is,

$$\Delta\phi = 2.1^\circ$$

The phasor diagram of the three phase voltages is,



Thus, according to Table 2.2, it is classified as sag type E.

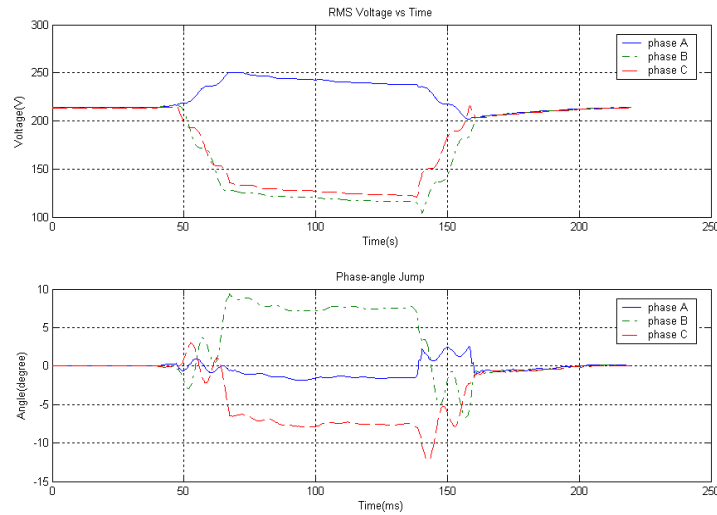
The sequence voltages calculated from the three phasors at MP2 are,

$$\overline{U}_1 = 162\angle -0.7^\circ V, \quad \overline{U}_2 = 34.3\angle -8.6^\circ V$$

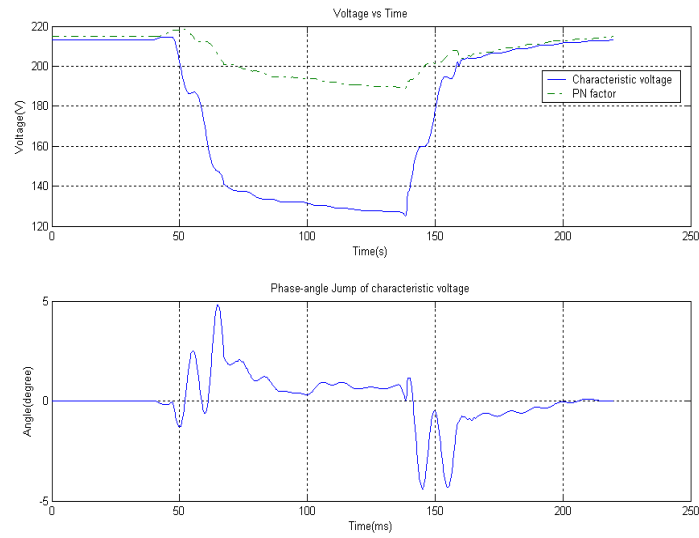
The sag index T is,

$$T = \frac{1}{60^\circ} \times \arg\left(\frac{34.3\angle -8.6^\circ}{218\angle 0 - 162\angle -0.7^\circ}\right) = 0.18 \cong 0$$

Thus, according to Table 2.3, it is classified as sag type Ca.



(a) Three-phase voltages



(b) Characteristic voltage and PN factor

Fig. 4.24 Double-phase-to-ground fault (MP2, Fault-line with two resistive loads and IM, measurement)